U.S.NRC
United States Nuclear Regulatory Commission
Protecting People and the Environment

NUREG/CR-7119

Experimental Studies of Reinforced Concrete Structures Under Multi-Directional Earthquakes and Design Implications

Office of Nuclear Regulatory Research

AVAILABILITY OF REFERENCE MATERIALS IN NRC PUBLICATIONS

NRC Reference Material

As of November 1999, you may electronically access NUREG-series publications and other NRC records at NRC's Public Electronic Reading Room at http://www.nrc.gov/reading-rm.html. Publicly released records include, to name a few, NUREG-series publications; *Federal Register* notices; applicant, licensee, and vendor documents and correspondence; NRC correspondence and internal memoranda; bulletins and information notices; inspection and investigative reports; licensee event reports; and Commission papers and their attachments.

NRC publications in the NUREG series, NRC regulations, and Title 10, "Energy," in the *Code of Federal Regulations* may also be purchased from one of these two sources.

1. The Superintendent of Documents
   U.S. Government Printing Office Mail Stop SSOP
   Washington, DC 20402–0001
   Internet: bookstore.gpo.gov
   Telephone: 202-512-1800
   Fax: 202-512-2250
2. The National Technical Information Service
   Springfield, VA 22161–0002
   www.ntis.gov
   1–800–553–6847 or, locally, 703–605–6000

A single copy of each NRC draft report for comment is available free, to the extent of supply, upon written request as follows:

Address: U.S. Nuclear Regulatory Commission
Office of Administration
Publications Branch
Washington, DC 20555-0001
E-mail: DISTRIBUTION.RESOURCE@NRC.GOV
Facsimile: 301–415–2289

Some publications in the NUREG series that are posted at NRC's Web site address http://www.nrc.gov/reading-rm/doc-collections/nuregs are updated periodically and may differ from the last printed version. Although references to material found on a Web site bear the date the material was accessed, the material available on the date cited may subsequently be removed from the site.

Non-NRC Reference Material

Documents available from public and special technical libraries include all open literature items, such as books, journal articles, transactions, *Federal Register* notices, Federal and State legislation, and congressional reports. Such documents as theses, dissertations, foreign reports and translations, and non-NRC conference proceedings may be purchased from their sponsoring organization.

Copies of industry codes and standards used in a substantive manner in the NRC regulatory process are maintained at—

The NRC Technical Library
Two White Flint North
11545 Rockville Pike
Rockville, MD 20852–2738

These standards are available in the library for reference use by the public. Codes and standards are usually copyrighted and may be purchased from the originating organization or, if they are American National Standards, from—

American National Standards Institute
11 West 42nd Street
New York, NY 10036–8002
www.ansi.org
212–642–4900

Legally binding regulatory requirements are stated only in laws; NRC regulations; licenses, including technical specifications; or orders, not in NUREG-series publications. The views expressed in contractor-prepared publications in this series are not necessarily those of the NRC.

The NUREG series comprises (1) technical and administrative reports and books prepared by the staff (NUREG–XXXX) or agency contractors (NUREG/CR–XXXX), (2) proceedings of conferences (NUREG/CP–XXXX), (3) reports resulting from international agreements (NUREG/IA–XXXX), (4) brochures (NUREG/BR–XXXX), and (5) compilations of legal decisions and orders of the Commission and Atomic and Safety Licensing Boards and of Directors' decisions under Section 2.206 of NRC's regulations (NUREG–0750).

U.S.NRC
United States Nuclear Regulatory Commission
Protecting People and the Environment

NUREG/CR-7119

Experimental Studies of Reinforced Concrete Structures Under Multi-Directional Earthquakes and Design Implications

Manuscript Completed: September 2011
Date Published: July 2013

Prepared by
N. Simos and C. H. Hofmayer

Brookhaven National Laboratory
P.O. Box 5000
Upton, NY 11973-5000

A. Murphy, NRC Program Manager

Job Code N6510

Office of Nuclear Regulatory Research

ABSTRACT

This report describes the results of a multi-phase study focusing on the SMART2008 (***S***eismic design and best-estimate **M**ethods **A**ssessment for **R**einforced concrete buildings subjected to **T**orsion and non-linear effects) shaking table experiment. The aim of the project was to enable an international benchmarking study to take place where different methodologies, modeling, and numerical approaches are used to study and predict the non-linear behavior and damage of reinforced concrete structures. Specifically, a 1/4th scale model of a nuclear reinforced concrete structure designed according to the French nuclear practices was tested on the shaking table at Commissart a' l'Energie Atomique Saclay, France using thirteen multi-dimensional earthquakes ranging from low seismic intensities to five times the design level. Three numerical prediction phases were executed which included (a) a "blind" prediction phase based on using best-estimate data for the structural properties and the induced seismic loads, (b) an "updated" prediction phase where best estimates were improved using some of the initial shaking table test results enabling the studies of higher loadings, and (c) a sensitivity and vulnerability analysis phase based on the SMART2008 specimen numerical model used in the prediction phase enabling the generation of damage fragility curves for the structure.

The report provides a detailed description of the SMART2008 experiments, an assessment of the test results, the structural response predictions using modeling and numerical techniques, and a damage fragility assessment. The report also discusses potential design implications of addressing the non-linear structural behavior during seismic events exceeding the design values or Design Basis Earthquake (DBE). The design implications are derived primarily from the ability of the numerical approaches adopted in this effort to predict highly non-linear structural behavior under seismic loading.

While the 1/4th scale SMART2008 test structure was designed and constructed following the French nuclear design code, the observations and assessments stemming from the test results should not be considered directly applicable to the seismic behavior of US nuclear structures due to differences in the details in the two national codes. However, this report summarizes the various aspects of the benchmark and the findings that were drawn from the shaking table tests and the numerical analyses. Based on this study, the following specific observations were noted and may warrant further consideration, as consensus codes are updated and the NRC revises regulatory guidance:

1. For the model used in the SMART2008 experiment, the capacity of the model, built per the French code, was higher that the design capacity, i.e., the model was designed for a 0.2g peak ground acceleration and withstood shaking table induced ground motions of about 1.1 g with only concrete cracking and minor localized steel reinforcement yielding.
2. The observed reductions in stiffness at lower seismic intensities are attributed to micro-cracking within the concrete.

3. The use of non-linear treatment of real concrete structures should be considered by regulatory authorities and it may be appropriate to allow it to influence the design through consensus codes.

TABLE OF CONTENTS

LIST OF FIGURES

LIST OF TABLES

EXECUTIVE SUMMARY

This report presents the results of a comprehensive study of reinforced concrete structures exhibiting three-dimensional effects as well as non-linear response under multi-directional earthquakes. The study was started in 2008 and it consists of (a) shaking table tests and response results of a 1/4th scale structure, (b) numerical prediction results based on the test structure design and the shaking table multi-directional excitations, and (c) sensitivity and structural vulnerability assessments of the test structure leading to fragility curves for pre-defined limit states based on different metrics.

The primary goal of this multi-faceted effort was to understand, based on both the experimental results and the benchmarked numerical models, the implications of three-dimensional effects in reinforced concrete nuclear structures. These effects manifest themselves in the ability of these structures to withstand multi-directional seismic loads and the generation of more realistic response spectra or critical equipment loadings at elevations within the structure. Further, by utilizing the shaking table test results and those of a comprehensive sensitivity and vulnerability analysis performed on the test structure, another goal was to identify the most appropriate metric that captures the damageability of the overall structure and the establishment of limit states.

The US Nuclear Regulatory Commission participated in this international effort through contractor support from the Brookhaven National Laboratory. The raw information that may influence the nuclear design code evolution as a result of this effort stems from:

- the quantification of torsion effects,
- the performance of a structure designed according to a nuclear code (in this case the French code) when subjected to seismic loads that far exceed the design basis earthquake,
- the ability of the much advanced numerical modelling and analysis to predict the non-linear response of a complex reinforced concrete structure,
- qualitatively addressing various metrics for establishing limit states for a complex structure and their implementation into performance-based design approaches.

The SMART2008 project was initiated in 2008 as an international benchmark study and was opened to teams within the practicing nuclear engineering community as well as the earthquake engineering research community. It was supported by the Commissariat à l'Energie Atomique (CEA), Electricité de France (EDF), the Organization for Economic Cooperation and Development of the Nuclear Energy Agency (OECD/NEA) and the International Atomic Energy Agency (IAEA) Extra Budgetary Program on Seismic Safety. The primary focus was the response of reinforced concrete nuclear structures exhibiting torsion effects as well as non-linear response. Of interest was the generation of more realistic floor response spectra to be used in the design of critical equipment. The experimental effort used a 1/4th scale 3-story structure tested on the shaking table capable of 100 ton capacity and 1g maximum acceleration. By accompanying the series of shaking table tests with a benchmark study by the international practicing community, the goal was expanded to enable the quantification of margins in different design methods accepted around the world, identify the more relevant methods in quantifying seismic analysis variability due to uncertainties in structural properties and seismic input, and generating appropriate fragility data for such structures. To accomplish the benchmark aspect of the SMART2008 study, two distinct phases were introduced. The first phase consisted of a blind prediction of a subset of the actual test results based on best

estimates of the structural properties and the intended shaking table accelerations. The blind prediction covered both “under design” and “over design” levels. The objectives were to (a) assess the different design methods for spectra generation, for both dynamic response and floor response, and (b) compare best-estimate methods ranging from linear to non-linear approaches and different levels of complexity in numerically representing the structure. During the second prediction phase, preliminary test results for some of the actual shaking tests were shared with the participants. This enabled a more realistic numerical representation of the structure in place of the best-estimate representation of the first phase, as well as the prediction of the response based on achieved shaking table excitations rather than desired load levels and earthquake content. Lastly, following the prediction phases and by utilizing the more realistic representation of the structure, sensitivity and vulnerability studies were conducted leading to fragility curves for pre-conceived limit states of the test structure. The primary objectives of the sensitivity/vulnerability phase of the SMART2008 benchmark were to (a) quantify the variability in the structural seismic response and identify contributions stemming from uncertainties in structural properties, and (b) assess and compare different methods leading to the generation of fragility curves associated with defined limit states and qualify the different metrics that were used.

While the 1/4th scale test structure was designed and constructed following the French nuclear design code, the observations and assessments stemming from the test results should not be generalized to the seismic behavior of other nuclear structures due to significant deviation of the tested structure from actual reinforced concrete nuclear structures especially at foundation conditions. However, the lessons learned from this study are very useful for numerical modeling and analysis of reinforced concrete structures subjected to multi-directional loading in the linear and nonlinear ranges.

A principal lesson to be taken away from this benchmark is that the non-linear techniques utilized is this benchmark indicate that non-linear techniques available for structural engineering models are or are becoming mature enough to warrant consideration in future editions of consensus codes and then in regulatory guidance, i.e., code developers should be considering the implementation of some of these techniques for future editions.

The report is organized in sections each of which describes in detail a particular aspect of the multi-faceted study. The introductory section provides a description of the background including the objectives and the scope of this undertaking, as well as a summary of the SMART2008 experimental study and the accompanying numerical prediction phases. Also included in the introductory section is a discussion of the aims and results of the SMART2008 project on design approaches.

In Section 2, the SMART2008 shaking table tests, which represent the core subject of this effort, are described in detail. Specifically, the design specifics of the test structure and of the AZALEE shaking table used in the test are described along with the properties of the family of multi-directional earthquakes that form the seismic demand array. Shaking table results of Phase I, which included modal characteristics of the test structure as well as response to low level earthquakes, and thus mostly linear response, are presented and discussed. The results of the entire series of thirteen three-directional earthquakes that were used in the shaking table test ranging from under-design levels to as much as five times the code design level are discussed. Specifically, the measurements of the test structure response provided by CEA along with the damage progression which resulted from applying the earthquake loads in tandem are evaluated and discussed. Finally, in Section 2 an overall assessment of the shaking table results is presented including (a) the global behavior of the structure including torsional effects, (b) the evolution of floor response spectra with increasing input loads and (c) the damage onset and its evolution and damping characteristics of the structure.

Section 3 depicts the description of the numerical modeling and dynamic analysis formulation used to simulate the shaking table tests. Discussed in this section are the results of the “blind

prediction" and "best estimate" phases which formed the initial approach to prediction of the actual test. Adjusted response predictions triggered by data provided as a result of low-intensity shaking table tests that reflected the actual test structure and the achieved shaking table excitation are presented, along with a discussion on the influence of uncertainties in the best-estimate phase. The overall performance of the prediction model against the actual shaking table tests at different earthquake intensity levels is discussed in detail. Discussed in Section 3 is the observed damping of the system during the shaking table tests, its impact on the numerical analyses performed, and its relevance to the general design practice. Included also in Section 3 is a discussion on the torsional effects exhibited during the tests and captured in the numerical evaluation.

The sensitivity and vulnerability studies that were undertaken using the finalized prediction model described in Section 3 are presented in Section 4 of the report. In particular, the objectives and the expected value of these studies are discussed along with the results of the numerical studies encompassing both the sensitivity or uncertainty in structural capacity and the fragility analysis. Discussed in detail is the vulnerability assessment based on the generated fragility curves using different approaches and metrics and their connection to the structural limit states.

In Section 5 a discussion on the lessons learned as a result of both the shaking table tests, the numerical predictions of the test structure response, and the "non linear" floor response spectra derived from both the tests and the simulations is presented while focusing on the torsion effects induced on three dimensional structures. Further, based on the results of the sensitivity and vulnerability analyses with emphasis on the fragility curve generation, the concept of the limit state is discussed. Most importantly in this section, the connection of the information manifested in (a) the 3D effects, (b) the non-linear floor response spectra, and (c) the fragility assessment methodology tested against actual data of the SMART2008 structure subjected to several times the design level is explored and discussed.

This report summarizes the various aspects of the benchmark and the findings that were drawn from the shaking table tests and the numerical analyses. Based on this study, the following specific observations were noted and may warrant further consideration, as consensus codes are updated and the NRC revises regulatory guidance:

1. For the model used in the SMART2008 experiment, the capacity of the model, built per the French code, was higher that the design capacity, i.e., the model was designed for a 0.2g peak ground acceleration and withstood shaking table induced ground motions of about 1.1g with only concrete cracking and minor localized steel reinforcement yielding.
2. The observed reductions in stiffness at lower seismic intensities are attributed to micro-cracking within the concrete.
3. The use of non-linear treatment of real concrete structures should be considered by regulatory authorities and it may be appropriate to allow it to influence the design through consensus codes.

ACKNOWLEDGMENTS

The work described in this report was sponsored by the Office of Nuclear Regulatory Research of the U.S. Nuclear Regulatory Commission. The authors would like to express their gratitude to Dr. A.J. Murphy (NRC Project Manager on this research program) for appreciating the importance of the involvement in the two international seismic benchmark studies whose results and findings are reported herein.

The authors would like to also extend their gratitude to the organizers and sponsors of the SMART2008 benchmark (CEA, EDF, OECD/NEA and IAEA) and in particular P. Labbe of EDF and C. Thierry and S. Juster-Lermitte of CEA for their invaluable contributions towards the organization and execution of the SMART2008 project.

1. INTRODUCTION

1.1. Background

The seismic response of reinforced concrete (RC) structures exhibiting three-dimensional or primarily torsional effects as well as non-linear behavior is a concern within the earthquake engineering community and more so within the regulatory agencies overseeing nuclear facilities. The need to understand the behavior of such structures is not only the vulnerability or seismic capacity of the structure itself but also the proper evaluation of floor response spectra based on which critical equipment are designed. Traditionally, simplified approaches have been adopted for the seismic design of the structures (i.e., stick model representations) where the torsional effects are forced out of the estimation. In these simplified approaches the multi-directional nature of the earthquake and its effect on the structure as well as non-linearities in the structural response are accounted for through response combination schemes, i.e., Square Root Sum of the Squares method, and equivalent linearization.

In order for these effects to be quantified, a dedicated seismic test was proposed where both the nuclear design codes in above-design level situations and the ability of the earthquake community to predict the complex response of an equally complex structure were evaluated. A seismic test accompanied by a benchmark study was initiated by the Commissariat à l'Energie Atomique (CEA) and Electricité de France (EDF). The project was endorsed by the Organization for Economic Cooperation and Development (OECD)/Nuclear Energy Agency (NEA) and the International Atomic Energy Agency (IAEA). The project termed SMART-2008 project (**S**eismic design and best-estimate **M**ethods **A**ssessment for **R**einforced concrete buildings subjected to **T**orsion and non-linear effects) was started in 2008 as an international benchmark study by inviting participation by research teams from both the practicing nuclear engineering and the earthquake engineering research communities.

The US NRC's Office of Nuclear Regulatory Research, in collaboration with Brookhaven National Lab (BNL) joined this proposed international benchmark on seismic design of nuclear structures. The primary goals were to study in detail, through the assessment of the shaking table test results and the results of the numerical analyses employed to predict the response, (a) the torsional effects on 3-D structures, (b) the generation of "non-linear" floor response spectra, and (c) fragility assessment methodologies based on the SMART structure. Utilizing the wealth of new information relating to the seismic response of 3D structures, collectively as a group of participating research teams in the benchmark, and individually as a BNL team, a subsequent goal was to assess the potential impact on design provisions relevant to the US nuclear design practices.

1.2. Objective

The objective of the study was to independently evaluate and interpret the SMART2008 shaking table tests and to develop a state-of-the-art numerical prediction model to be used in the various phases of the benchmark study. The tests consisted of blind test predictions based on best-estimate structural data and actual predictions aided by structural data revealed by low-intensity tests performed on the test structure. Through the benchmarking simulations and the test results, the aim was to assess the non-linear response of the reinforced concrete structure exhibiting torsional effects and in the process to evaluate the evolution of non-linear floor response spectra.

A key part of the overall objective was the study of structural and seismic input uncertainties on 3D structures by conducting sensitivity studies around key structural properties and evaluating the seismic fragility curves of such structures using a large family of earthquakes.

Further, upon the completion of the tests and simulations and their analysis, the important objective was the identification of areas that are expected to influence the acceptable design practices. .

1.3. Seismic Tests and Response Predictions

In order to study and validate approaches that can be used in dynamic analysis and response of reinforced concrete structures which may exhibit three dimensional effects (typical of a nuclear structure) as well as non-linear behavior, a 3-story test structure was built according to the French seismic code and was seismically tested on the AZALEE shaking table at the CEA Saclay, France. The test structure shown in Figure 1.1 reproduced a nuclear building at 1/4th scale and was designed according to the RCC-G nuclear code (Regles de Conception et de Construction du Genie civil). Its seismic design was based on a 5% damped design spectrum anchored at 0.2g acceleration. The test structure was a three story trapezoid made of reinforced concrete and consisted of 4 walls supported on a continuous footing and mounted on the AZALEE shaking table via a steel plate. The design of the structure enabled the mass centre and the effective torsion centre to be along different axis and thus amplify the torsional effects resulting from the seismic loads.

The shaking table supporting the SMART structure is shown in Figure 1.2. It has a capacity of 100 ton and can produce1.0 g maximum acceleration. It has a total mass of 25 tons and is fixed to eight hydraulic jacks (4 in the horizontal directions and 4 in the vertical direction) which are controlled during the experiment. A more detailed description of the SMART structure, the shaking table and their interface is provided later in the report.

The 5% damping design spectrum anchored to 0.2g peak ground acceleration used in designing the test structure is shown in Figure 1.3.

Figure 1-1 SMART2008 test structure on the Azalee shaking table at CEA Saclay, France

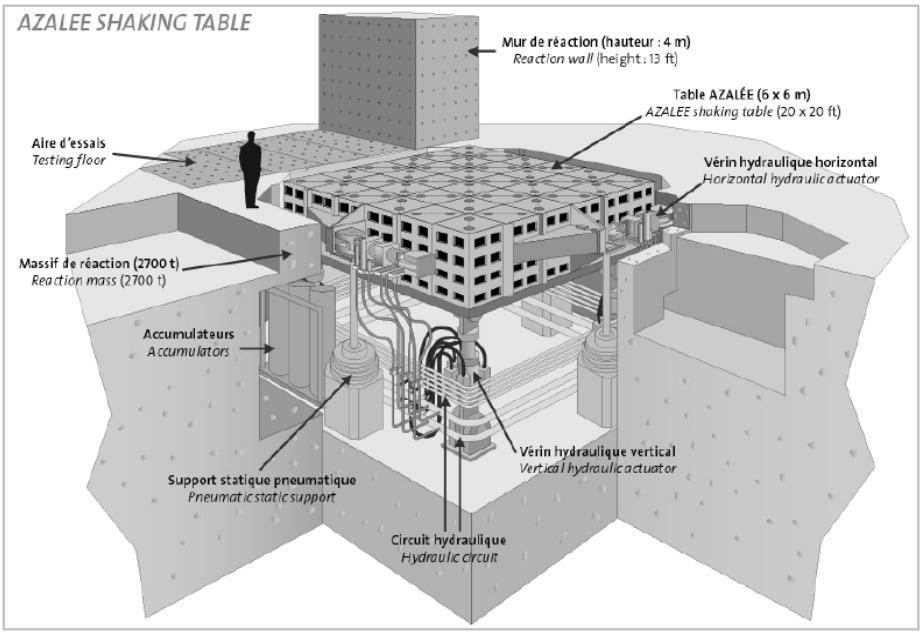

Figure 1-2 Details of Azalee shaking table used in the SMART2008 tests

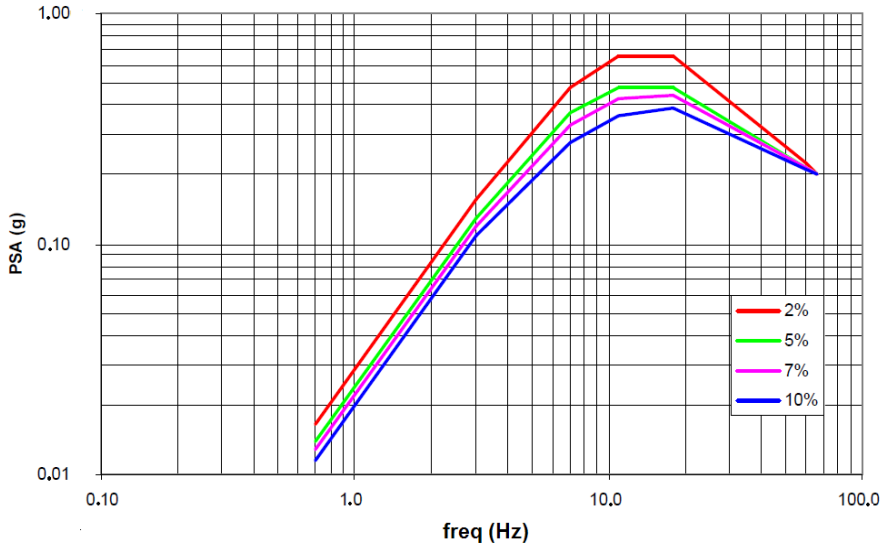

Figure 1-3 SMART2008 test structure design response spectrum

A total of thirteen (13) pairs of earthquakes (termed RUN1 thru RUN13) acting in the two horizontal directions simultaneously formed the basis of the seismic tests. Three of the earthquake pairs (RUN1, RUN2 and RUN3) were real, low-intensity records while the remaining ten (RUN4 through RUN13) were synthetic and were derived from the design spectrum starting at 0.1g and increasing to 1.0g for RUN13. The shaking table testing during which the thirteen pairs were applied in sequence thus ensuring the progression of damage consisted of two phases. In the first phase, the structure was subjected to earthquakes that represented the under-design, the design, and the over design levels (RUN1 to RUN8). Since it was intended by the designers that the test structure remains within the elastic regime during the design basis earthquake (RUN4), it can be assumed that this level earthquake would be equal to or less than an Operational Basis Earthquake (OBE) in the US.

These tests helped reveal uncertainties in the structural properties of the specimen as well as the controllability of the actuators in transferring the desired acceleration record to the shaking

table. Following these initial set of tests, the entire suite of thirteen earthquake pairs was completed. During the first phase, the over-design level, designated as RUN8 table accelerations of 0.41g in the x-direction and 0.55g in the y-direction, were recorded and the onset of non-linear structural response was observed.

As an integral part of the SMART2008 benchmark, an international numerical prediction contest was conducted to:

- assess the state-of-the-art of capabilities to numerically analyze non-linear structures and compare the different best-estimate methods for floor response spectra evaluation, and

- evaluate the different methodologies and regulatory guidelines on nuclear design.

By introducing the participation of the international practicing community, the aim was to enable the quantification of margins in different design methodologies accepted around the world and the identification of more relevant methods in quantifying seismic analysis variability due to uncertainties in structural properties and seismic input and generating appropriate fragility data for such structures.

The benchmark study consisted of two distinct phases. The first phase was conducted prior to the fabrication of the specimen and consisted of two stages. First, static, modal and dynamic analyses were performed on the structure using conventional methods of choice (i.e., spectral, pushover, linear and/or nonlinear time history analyses). This was followed by a "blind-prediction" of the shaking table test where two seismic pairs (0.2g and 0.4g PGA) were applied to the structure using best-estimate values of the structural properties. These studies were meant to provide a measure of the variability that results from the choice and complexity of the numerical model, the hypotheses, and the type analysis used. Following the construction of the specimen and the completion of the first phase of the shaking table tests, a best-estimate prediction was performed. This prediction phase was based on specific information that became available after the construction and initial testing of the specimen. The information pertinent to the shaking table test set-up, the as-built structure and achieved shaking table excitations enabled the updating of the numerical models that were then used for the best-estimate predictions. Specifically, information on

- experimental set-up including the mass of the structure and the actual added loads
- concrete and reinforcing steel properties deduced
- initial frequency and damping ratio prior to the tests
- seismic input accelerations observed on the table
- selected test results for a low-intensity signal and the design level

was provided and used in analyzing the thirteen earthquake pairs in series.

A comprehensive set of prediction results generated using the BNL numerical model and a fully non-linear analysis reflected in the constitutive relations of the concrete and the reinforcing steel are presented in the report. The prediction results are compared with the actual test results and are accompanied by assessment and discussion.

1.4. Sensitivity Studies and Fragility Evaluation

Following the completion of the shaking table tests and the best-estimate predictions, the variability in the response of structures stemming from (a) structural property uncertainties, (b) random character of the seismic input and (c) numerical representation of the structural system sensitivity and vulnerability analyses were conducted. The vulnerability analyses sought to develop fragility curves.

The primary objectives of the sensitivity/vulnerability phase of the benchmark were to:

(a) quantify the variability in the structure seismic response and identify the contribution stemming from uncertainties in structural properties, and
(b) assess and compare different methods leading to the generation of fragility curves associated with defined limit states and to evaluate the qualification of the different metrics that are used.

Results derived from the sensitivity and vulnerability analysis in terms of floor response spectra and fragility curves for different combinations of demand and capacity indicators are presented in Chapter 4 of the report. Also included are discussions on the methodologies used to develop fragility curves, as well as discussions on the findings and the needs for further studies.

1.5. Lessons Learned and Design Impact

The results and assessment derived from the distinct phases of the benchmark are summarized in last section of the report.

First, the shaking table tests and the recorded structural response are discussed in terms of (a) challenges in conducting such a test and in particular the ability to control the key elements comprising the test such as the shaking table and structure interaction and its influence on the observed in-structure response, (b) the evolution of the “damage” observed in the structure as a result of the sequential application of seismic loads with increasing intensity, (c) the in-structure response in terms of accelerations, inter-story drifts and most importantly floor response spectra, and (d) qualification of the overall response and exhibited structural capacity as compared to the design levels. Safety-significant observations were made regarding the overall response and the changes that occur in the concrete material, such as softening in the concrete, at much lower than design level intensity values.

The performance of the numerical model generated and implemented in the non-linear analysis and prediction of the test is summarized and the potential implications in the design practice are drawn and presented in the summary section. Specifically, based on the demonstrated ability of the computationally costly non-linear model to trace the structural response even when the structure entered the non-linear regime, arguments are presented for the potential use of these types of analyses in the design practice of reinforced concrete structures. Observations on studies that will further enhance the understanding of the nonlinearities in reinforced concrete, and subsequently the adaptation into numerical models and design analyses, are also made.

The assessments from the dedicated studies performed on the sensitivity of the structural response due to uncertainties in structural parameters and the vulnerability study which resulted in seismic fragility curves are summarized along with considerations for further study. The need for enhanced approaches or alternative methods that may lead to seismic fragility assessment with higher confidence levels is discussed.

Finally, by taking into account the results and lessons learned from the three main thrusts of the SMART2008 benchmark summarized above, design implications are drawn and presented. In particular the performance of the actual structure in terms of capacity, evolution of its dynamic characteristics at below design level and the exhibited damping are put into context with the current practice and design provisions. Further, the potential of using the non-linear type analysis in design provisions and especially in validating current practice and methodologies to account for nonlinearities in the reinforced concrete at levels which currently ensure the linear-elastic behaviour is discussed.

2. SMART2008 BENCHMARK

To address the issue of multi-directional seismic loading on nuclear structures where torsion is induced while it is influenced by the non-linear behaviour of reinforced concrete, an international benchmark study under the term SMART-2008 (Seismic design and best-estimate Methods Assessment for Reinforced concrete buildings subjected to Torsion and non-linear effects) was initiated. The benchmark that was coordinated by CEA Saclay, France and supported by Electricite de France (EDF) was established around a scaled nuclear structure that was to be tested on the Azalee shaking table at CEA under multi-directional seismic loadings. In order for the study to be relevant to the nuclear sector, the scaled structure was to be designed according to the French nuclear code RCCG and used a 5% damped design spectrum anchored at 0.2g acceleration (see Figure 1.3). Following the construction of the scaled nuclear structure, a sequence of selected multi-directional earthquake inputs consisting of real seismic records and synthetic ones derived from scaled design spectra has performed on the shaking table to assess the vulnerability of the structure and its damage progression.

Shown in Figure 2.1 is a flowchart of the various phases of the SMART2008 benchmark which addressed different aspects of the study.

In Phase-Ia, preliminary analyses were performed on the SMART2008 structure based on the per-design model and the expected structural and material properties of the structure. Static analyses for a fixed-base structure under (a) gravity loads which included the additional masses on the floor slabs and (b) horizontal loads applied at the 3rd level were performed. A series of modal analyses were also performed which included (a) the fixed-base and free-free structure without the added masses and prior to its placement on the shaking table and (b) the mass-loaded structure under fixed-base conditions and on the shaking table. The primary goal of the preliminary static and modal analyses was to assess the variability of solutions stemming from the different numerical methods the participating teams were utilizing in the SMART2008 benchmark (i.e. stick model representation, shell or solid element, rebar consideration, etc.). The dynamic analysis or blind prediction of Phase-Ia consisted of a conventional dynamic analysis and a best-estimate analysis subtask. For the conventional analysis the participating teams were provided with synthetic time histories and corresponding response spectra of a two-directional synthetic earthquake of 0.2g peak acceleration to analyse the structure using either time history analysis or response spectra analysis to predict the response of the structure which exhibits the per-design properties. Upon completion of the conventional dynamic analysis, a best-estimate prediction of the response of the structure based on shaking table inputs (thirteen pairs of horizontal accelerations consisting of real and synthetic earthquakes with increasing peak acceleration to 1.0g) was performed and a series of structural response data (resultant forces, peak displacements, peak accelerations, floor response spectra, stresses and strains in the concrete and rebar, etc.) were computed and provided to the SMART2008 organizers. The choice of analysis for the blind prediction (spectral, time-history, equivalent static, etc.) was left up to the participating teams. Non-linear time history analyses were adopted and used in the US NRC/BNL study.

Following the fabrication of the test structure and the completion of the shaking table tests, the as-built structural parameters were provided to the participants along with the actual shaking table accelerations achieved during the tests. During Phase-Ib, which followed the shaking table tests, the structural model was updated to reflect the “as-built” conditions and the series of the thirteen (13) pairs of horizontal accelerations recorded on the shaking table during the tests were used to predict the response and damage of the structure and make direct comparisons with the test results.

Upon completion of the shaking table test phase, a vulnerability study defined as Phase II of the SMART2008 benchmark was performed. The primary objectives of the study were to (a) quantify the sensitivity of the seismic response stemming from uncertainties surrounding structural properties and the random character of the seismic input and (b) assess the

vulnerability of the structure and generate fragility curves by accounting for uncertainties in the structural modelling, in concrete constitutive relations, and in damage progression. The report focuses on the evaluation of the actual test data, the numerical prediction based on the as-built structure and the actual shaking table inputs (Phase-Ib) and on the vulnerability study (Phase II).

This chapter focuses on the experimental part of the SMART-2008 benchmark and presents details relevant to the actual test. This includes (a) the description of the scaled structure and the material properties that are influential in the seismic response, (b) the description of the shaking table infrastructure and the interface conditions between the test structure and the table, (c) the description of the input earthquake suite and discussion on its dynamic characteristics, and (d) the presentation of experimental campaign results and assessment.

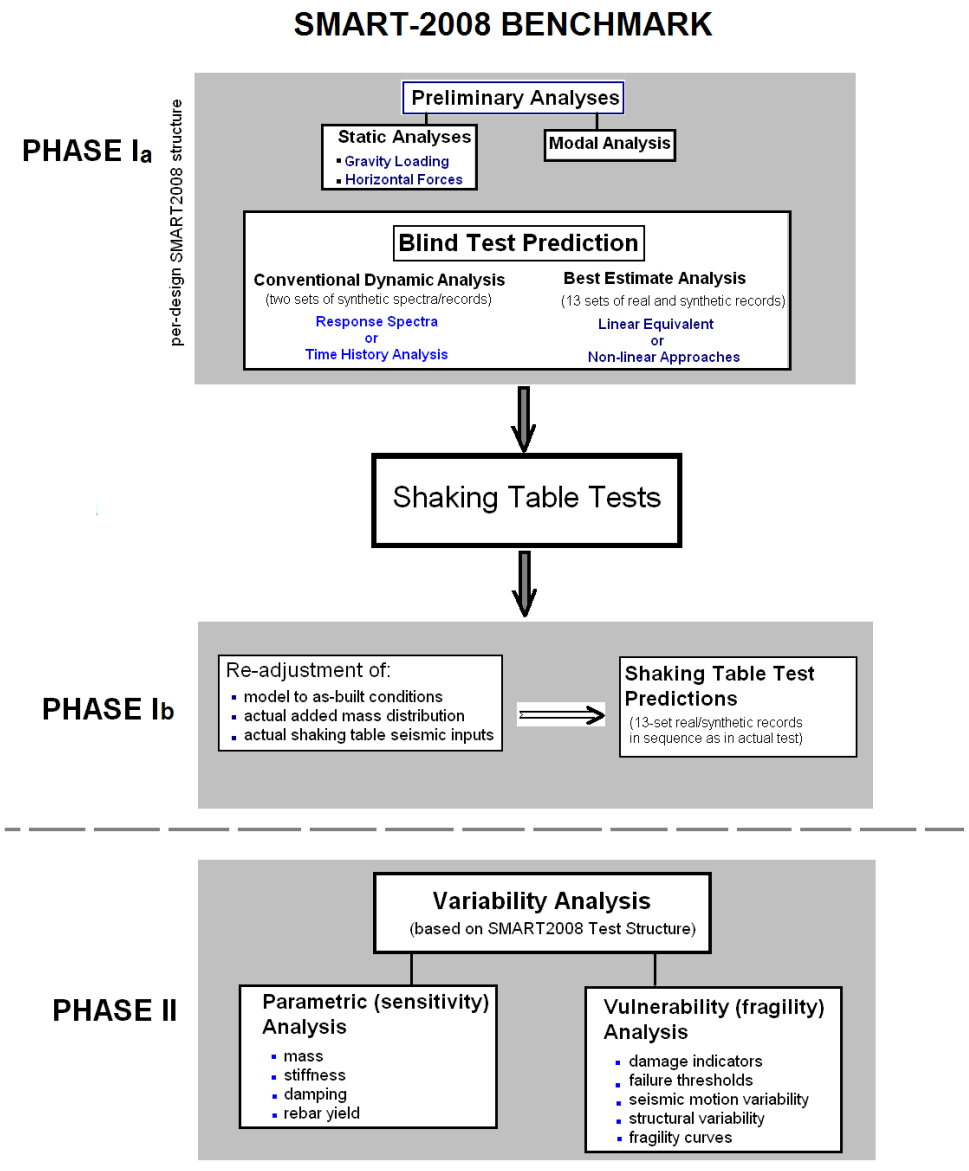

Figure 2-1 SMART2008 benchmark flowchart of the sequence of phases

2.1. SMART2008 Test Structure

The SMART2008 test structure shown schematically in Figure 2.2 is a reproduction of a nuclear building at 1/4th scale and was designed according to the French nuclear code RCCG with its seismic design based on a 5% damped design spectrum anchored at 0.2g acceleration. The test structure is a three-story trapezoid made of reinforced concrete. IT consisted of 4 walls supported on a continuous footing and mounted on the AZALEE shaking table via a steel plate. Key provision in the design of the structure is to enable for the mass centre and the effective torsion centre to be along different axis and thus accentuate the torsional effects of the seismic loads on the structure.

Figure 2.3 illustrates all the dimensional details of the test structure. The 3-story structure is a 1/4th scale trapezoidal shape model of a typical nuclear support structure consisting of three walls forming a U shape. Two of the walls have openings in all three levels to reproduce realistic design configurations of shear walls. A reinforced concrete column connected to all three level slabs and was situated in the geometrical middle of the structure. Reinforced concrete beams supporting the floor slabs span the distance between one of the walls and the column. Based on the 1/4th scale model the mass scaling is 1/16 and, therefore, the wall thicknesses were selected accordingly. All three walls are 20 cm thick. The three beams had a cross section of 15cm x 32.5 cm and the column a cross section of 20cm x 20cm. The wider of the tree walls (normal to the beams) was designated as Wall #V01 and Wall #V02 (beam mid-section representing the separating line) while the remaining two walls were designated as Wall #V03 (wall with opening) and Wall #V04.

The structure was supported on a continuous 38cm wide by 15 cm high reinforced concrete footing (see Figure 2.5) that was built on a continuous 62cm wide steel plate of 2cm thickness. The steel plate was the means by which the whole structure was mounted on the top surface of the shaking table. The reinforced concrete column, on the other hand, was directly anchored on the 62cm by 62cm steel plate which in turn was mounted on the shaking table with screws.

The centre of mass of the SMART2008 structure is at x_{cg} =1.28 m and y_{cg} = 0.98 m based on the coordinate system shown in Figure 2.3c.

The steel reinforcement in the test structure was designed according to the European design code EC2. An elaborate reinforcing scheme was implemented using a set of different bars. These include HA10 (Ø=10mm; R_m=654-661 MPa), HA8 (Ø=8mm; R_m=577-591 MPa), HA6 (Ø=6mm; R_m=617-637 MPa), HA4 (Ø=4mm; R_m=565 MPa). HA10 rebars were used in the foundation and the reinforced column. The reinforcement in the wall consisted of primarily 4mm diameter bars at 100 mm spacing which was further supplemented by HA10, HA8 and HA6 rebars near the wall openings. The nominal yield stress for the reinforcing steel was F_e = 500 MPa.

Nominal concrete properties were initially established in order for the preliminary estimates of the structural properties to be derived and also for the numerical side of the benchmark to be started. These basic concrete properties are listed below.

f_c	=	30 MPa *Compressive strength*
f_t	=	2.4 MPa *Tensile strength*
E	=	32,000 MPa Concrete *Young modulus*
ν	=	0.20 *Poisson's ratio*

Following the initial estimates, results of concrete cylinder tests from actual casts used to construct the structure became available. The cylinder tests showed that the actual concrete modulus was lower than the best estimate listed above and varied between casts. The results of seven (7) different casts are listed in Table 2.1. Listed in the table are both concrete tangent

and secant modules with the latter derived from the first point on the stress-strain curve and the 1/3rd of the ultimate (failure) loading.

The concrete density, based on the test cylinders was approximately 2372 kg/m^3. The average density of the reinforced concrete of the structure was approximately 2460 kg/m^3.

Since gravity loads and stresses do not undergo scaling, to reproduce the state of stress in the structure walls and column anticipated in typical nuclear structures, additional loads were applied on each level using lead and steel blocks placed directly on each slab. The total weight of the structure, following the addition of floor masses, was estimated at about 46.81 T and is distributed as follows:

- *weight of structure* ~ 9.31 T
- *weight of foundations* ~ 2.11 T
- *added load at level 1* ~ 12.06 T
- *added load at level 2* ~ 12.70 T
- *added load at level 3* ~ 10.63 T

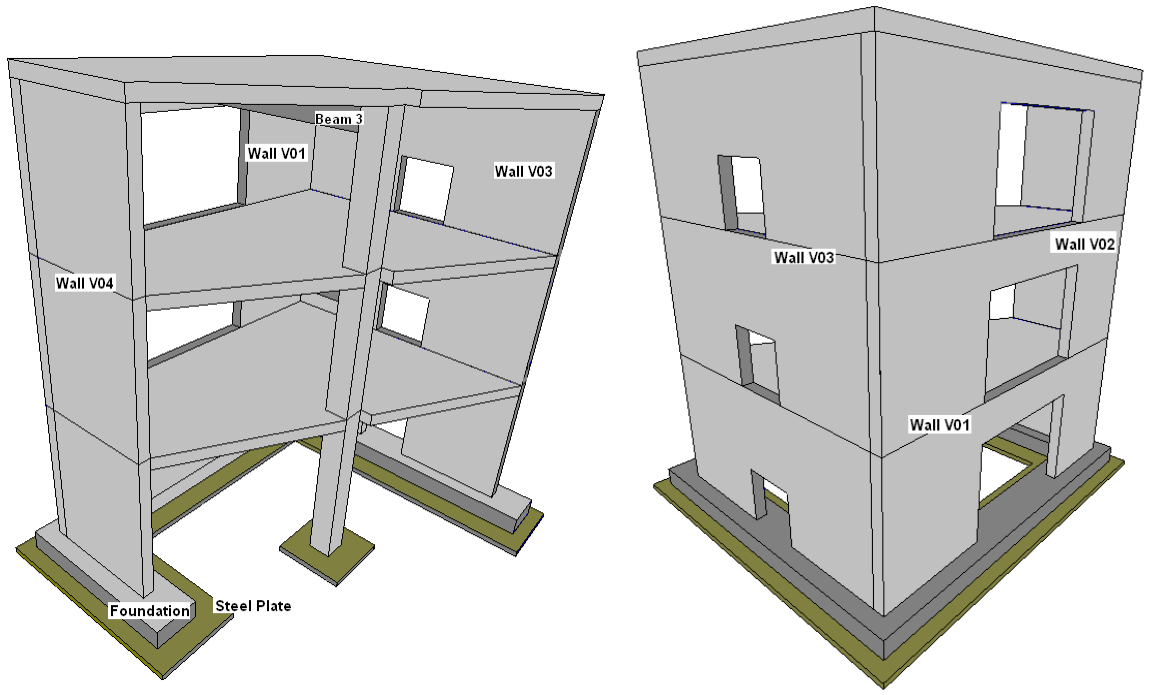

Figure 2-2 SMART2008 test structure schematic

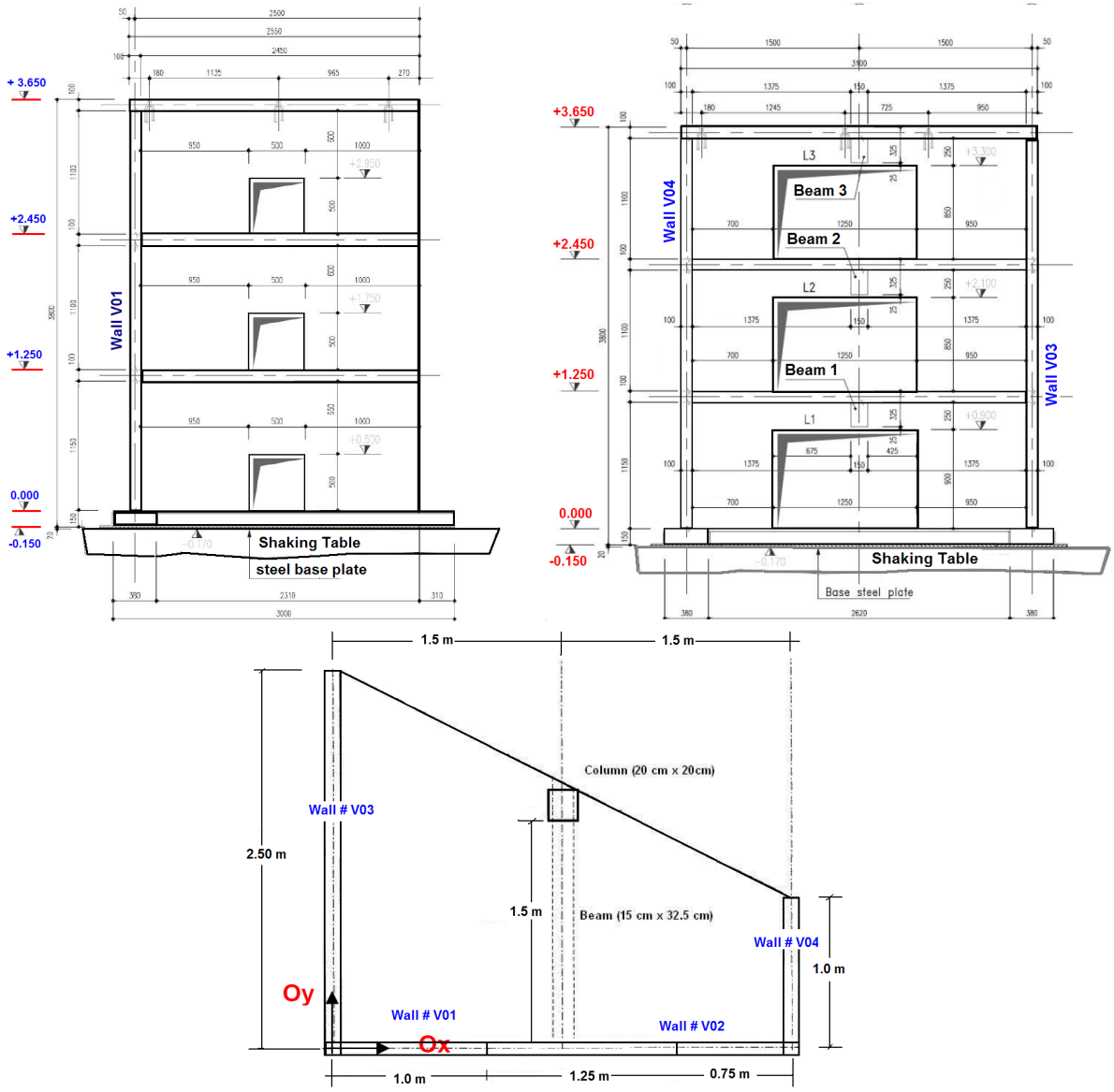

Figure 2-3 Geometric description of the SMART2008 structure

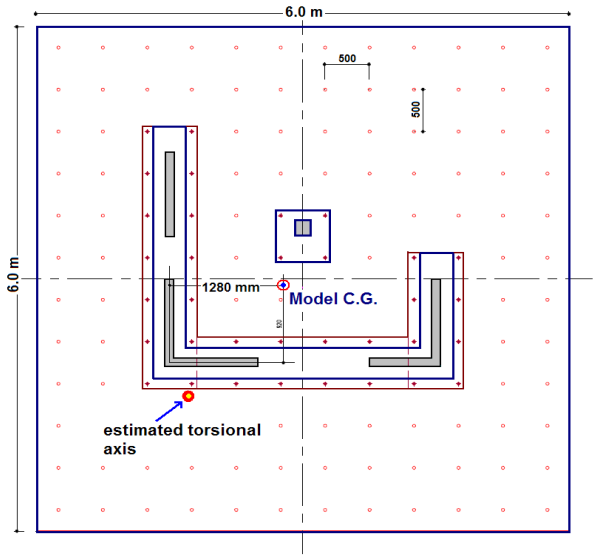

Figure 2-4 Footprint of the SMART2008 structure with CG and torsion axes

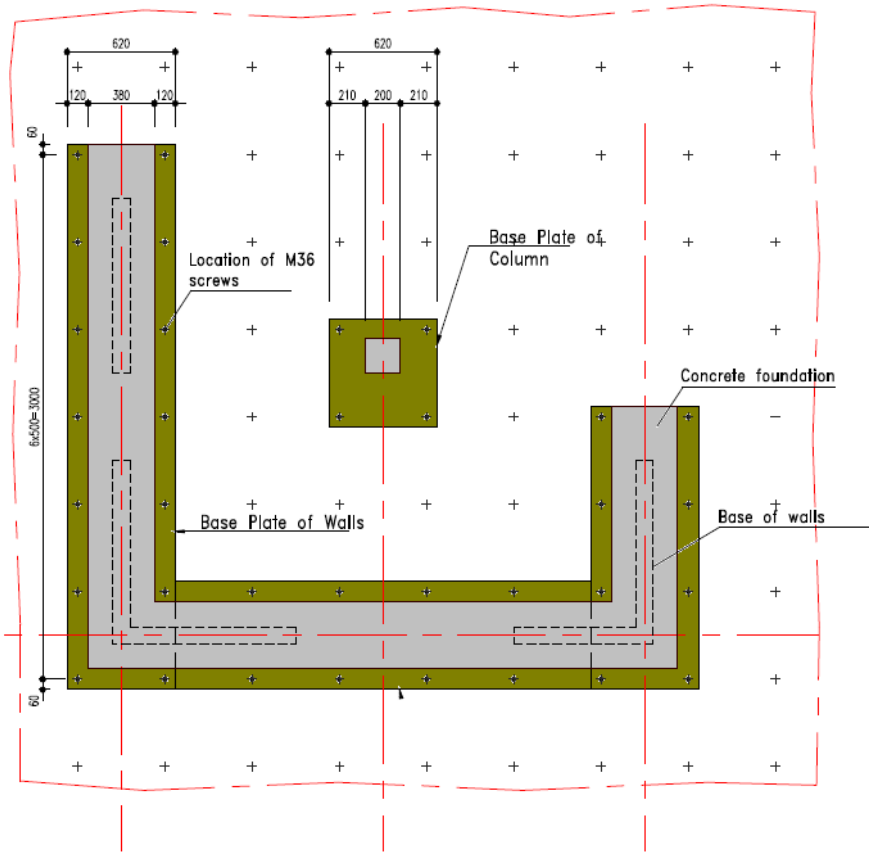

Figure 2-5 **Geometric description of the base plate and foundation**

Table 2.1 **Concrete properties derived from actual casts of the SMART2008 structure.**

	E tangent (MPa)	E secant (MPa)
Foundation	31 500	30 000
Walls and column 1st level	30 500	29 000
Slab and beam 1st level	29 000	26 500
Walls and column 2nd level	26 500	25 000
Slab and beam 2nd level	31 500	30 000
Walls and column 3rd level	33 500	30 000
Slab and beam 3rd level	29 500	28 000

2.2. Shaking Table Characteristics

The Azalée shaking table, shown in Figure 2.6 with the schematic of the SMART2008 structure placed on it for reference, has a total mass of 25 tons and for simplicity it may be considered as a rigid block. It is fixed to eight hydraulic jacks (4 in the horizontal direction and 4 in the vertical direction) with their orientation shown in Figure 2.7. As indicated in Figure 2.7, the distance between two vertical actuators is 4 meters. The actuators controlling the horizontal motion of the table are located at ~1.02 m below the upper face of the shaking table (where the SMART2008 structure is mounted via the steel base plate), while the centre of gravity is 0.60 m below the table top. All the jacks can be described as active systems, meaning that they are controlled during the experiment. The implication, however is that it is extremely difficult to extract dynamic properties which are expected to influence the dynamic response of the shaking table system that in turn will affect the response of the supported structure.

Given the geometry of the test model, rocking motions may be experienced at the shaking table's level during the seismic tests. Due to gaps in the understanding of the dynamic behavior of the overall table system stemming from the active nature of the actuators, the structure/table interaction is very difficult to predict. Approximate data regarding the effective stiffness of the vertical actuators have been used in past shaking table tests where the vertical actuators were represented by 215 MN/m springs. Based on the position of the test structure on the shaking table and the coordinate system used, the table center of mass is estimated to be at X_{CG}^{TABLE} = 1.50 m and Y_{CG}^{TABLE} = 0.92 m (1.28 m and 0.92m respectively for the test structure).

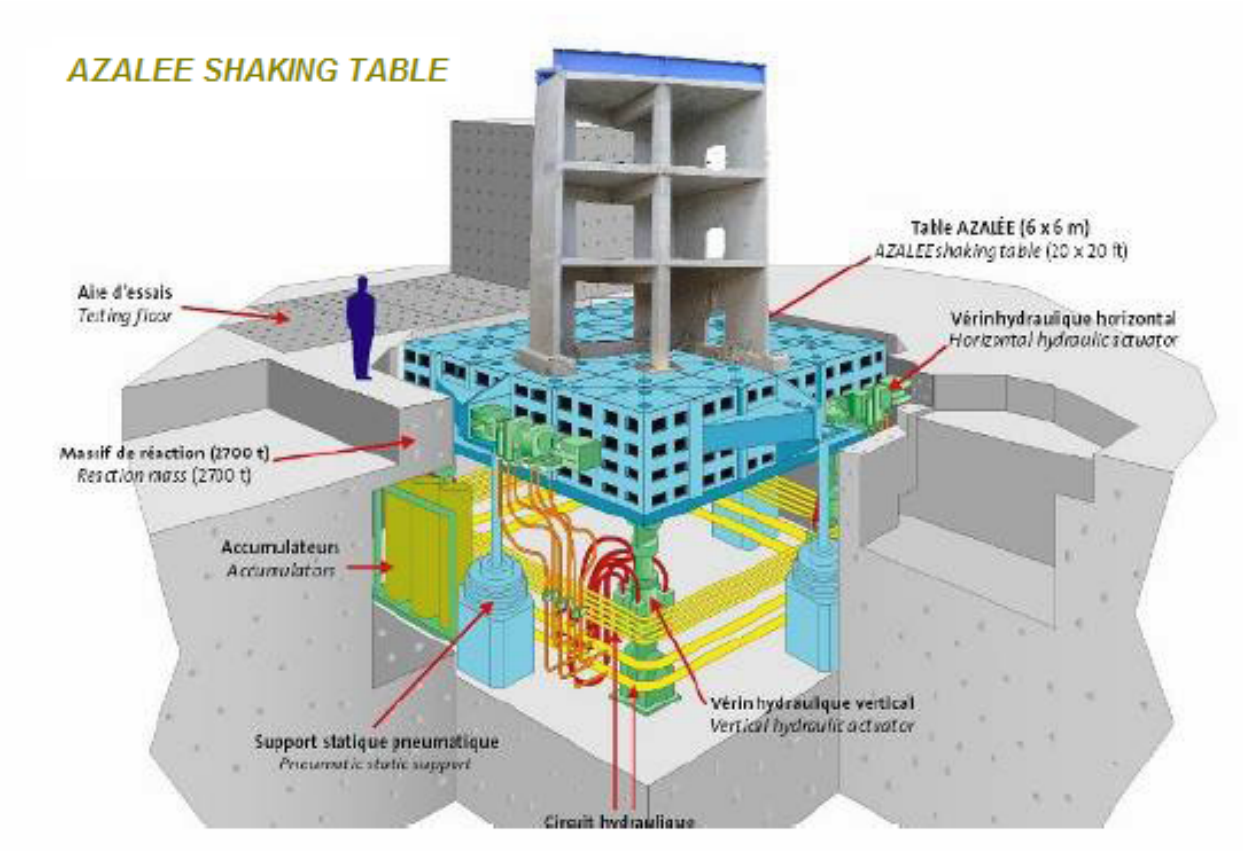

Figure 2-6 Geometric description of the AZALEE shaking table

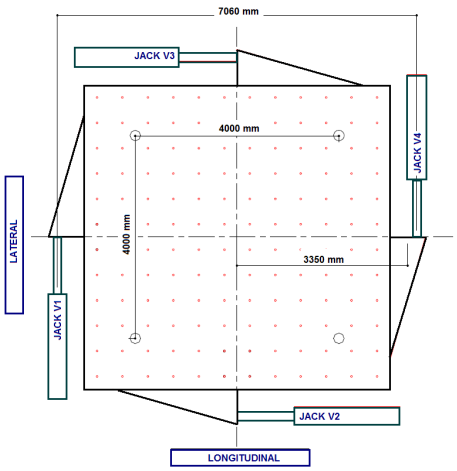

Figure 2-7 Shaking table hydraulic jacks/actuators orientation

2.3. Instrumentation

An extensive array of 3-D accelerometers, displacement transducers and rebar strain gauges were introduced onto the test structure in an effort to monitor and capture the complex response. As shown in Figure 2.8, accelerometers capturing the horizontal components of the shaking table accelerations (AXTAB and AYTAB) were installed on the top surface at table mass centre. Four vertical accelerometers (AZTAB1-4) placed at each corner were to monitor the vertical motion and thus rocking of the table. Shown also in Figure 2.8a are a series of accelerometers capturing the horizontal and vertical components of acceleration at foundation level (i.e. Ac00xA, Ac00yA, Ac00zA). The distribution of accelerometers over the three levels of the structure and of the displacement transducers for Wall 3 and 4 respectively are shown in Figure 2.9. Displacements were measured by cable extension sensors with precision potentiometers.

Strain gauges were placed on several extreme locations of the structure and in particular on the reinforcing steel (as shown in Figure 2.10) near the foundation and the first story walls to monitor steel non-linear behaviour. Figure 2.10b depicts an actual strain gauge placed on one of the rebars of Wall 4. Shown in Figure 2.11 is the constructed SMART2008 structure on the shaking table with the added floor masses and the instrumentation on key locations of its walls.

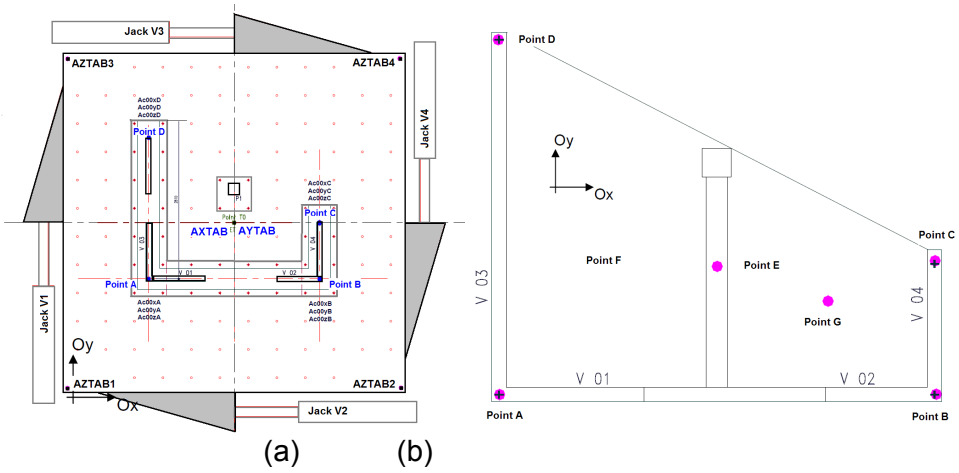

(b)

Figure 2-8 Layout of accelerometer distribution on the shaking table, the foundation of the structure, and the floor slab locations

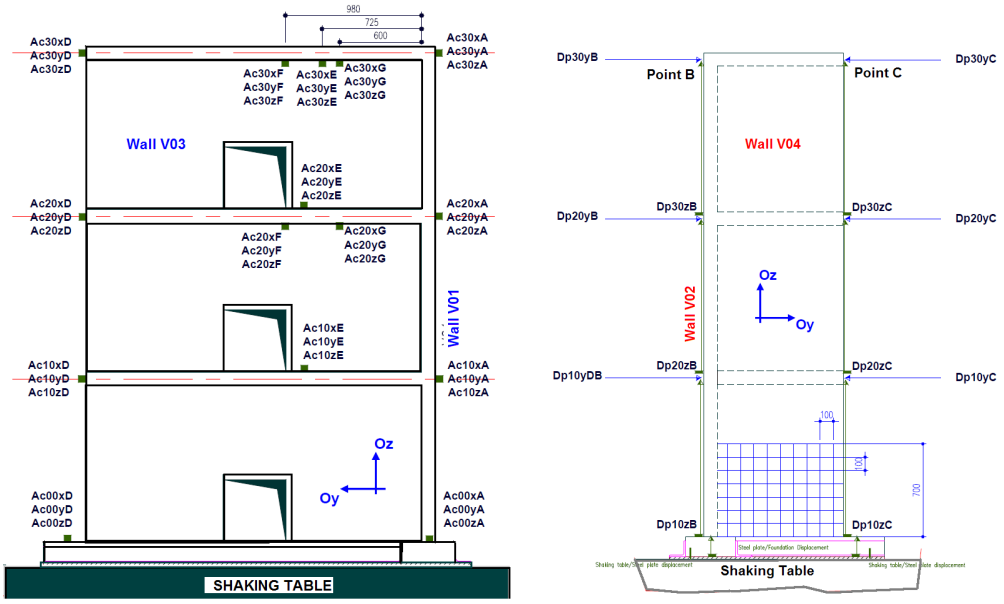

Figure 2-9 Acceleration sensor locations on Wall #3 and displacement transducers on Wall #4

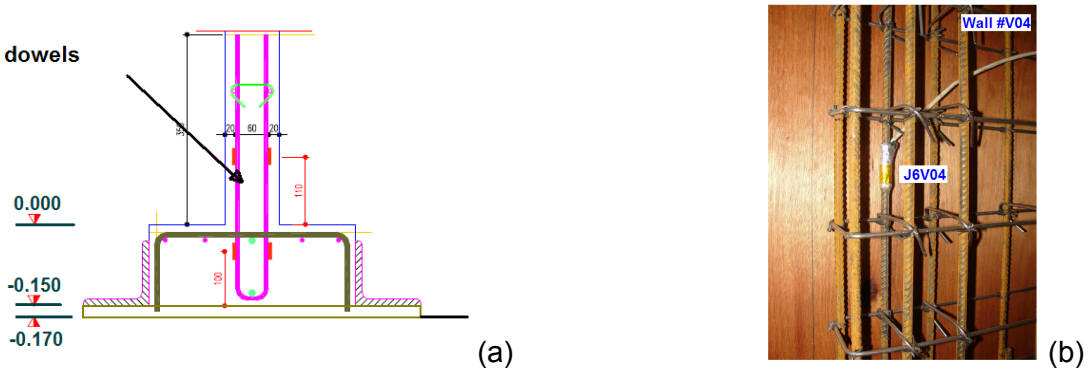

Figure 2-10 Schematic and actual configuration of rebar strain gauges

Figure 2-11 Instrumented and loaded SMART2008 structure on shaking table prior to the seismic tests

2.4. Shaking Table Seismic Tests

Following the construction, instrumentation, and placement of the test structure on the Azalee shaking table, a suite of bi-directional horizontal earthquakes were applied and the response of the structure was monitored and recorded. The shaking table tests began in July of 2008 and were completed in the Spring of 2009.

Seismic Input Suite

The SMART2008 benchmark consisted of thirteen pairs of seismic table excitations which were applied in sequence in an effort to observe the structural degradation and non-linear effects of the test structure. In other words damage that was induced by a given earthquake pair in the series would affect the response of the structure under the application of the next pair which was to increase in intensity. Low-intensity white noise excitations were applied between runs in an effort to extract key dynamic properties of the progressively damaged structure (i.e., eigenfrequencies).

It was understood early in the benchmark effort that the effect of the shaking table on the dynamic response of the test structure may be dominant. Specifically, the eigenmodes of the structure will be directly linked to the dynamic properties of the table/structure system. It is to be expected that participation of the shaking table in the system, because of its large mass, will reduce the eigenfrequencies of the structure considerably. Since the response of the structure is the result of the convolution of its dynamic properties with the frequency content of the seismic excitation, it is thus expected that the structural response will differ depending on where its eigenfrequencies lie. Therefore, it is crucial that the dynamic properties of the system, as a whole, are well understood. As noted earlier, however, knowledge gaps exist regarding the dynamic characteristics of the shaking table stemming primarily from the active nature of the actuators. Recognizing the importance of this information, both the benchmark organizers and the participating research teams conducted sensitivity studies prior to the shaking table tests to quantify the effect. Based on numerical best-estimates the first three important modes (two flexural modes and twisting mode) differed significantly between the fixed-base configuration of the structure (where no shaking table is present) and the case of shaking table participation under best estimate dynamic property values for the table system. For example, the first flexural mode identified in the fixed base at frequency ~9 Hz under table participation was reduced to ~7 Hz. The second flexural mode from ~16 Hz in the fixed-base configuration was reduced to ~9 Hz and the twisting mode from ~28 Hz to 16 Hz. Hammer-induced white noise tests on the SMART2008 structure prior to the series of seismic loads generally confirmed the effect of the shaking table. Figure 2.12 depicts the numerical estimates of the eigenfrequencies prior to the test and the progressive damage of the structure. As a result, monitoring of the modal degradation of the structure was undertaken during the series of tests utilizing both white noise inputs between the tests or estimating structural frequencies from the tail-ends of the response transients.

The thirteen horizontal pairs used in sequence in the test consisted of both real and synthetic records. Three real records of lower intensity than the design level of 0.2g where applied first. The input accelerograms of these real earthquake records are depicted in Figure 2.13. These were scaled from the actual records by a factor between 1.03 and 1.58 in order to arrive at a PGA = 0.05g, a minimum level at which the shaking table can be controlled. Depicted in Figure 2.14 are acceleration time histories recorded on the top surface of the shaking table during the application of the three real records along with the corresponding response spectra.

The ten synthetic earthquake pairs were generated from the design spectrum shown in Figure 2.1 anchored at 0.1 g and scaled to 1.0 g in order to generate pairs with 0.1g incremental increase in intensity. Figure 2.15 depicts the shaking table horizontal accelerations recorded during the RUN4 test. Figure 2.16 shows the response spectra of the shaking table

acceleration which needs to be compared to the one in Figure 2.1. Clearly seen in the actual table spectra are the two peaks corresponding to the first two flexural modes of the table/structure system.

Test Observations

Following the completion of the sequence of the thirteen horizontal acceleration pairs introduced on the table through the actuators and the recording of (a) accelerations on the table top and throughout the structure, (b) absolute displacements (measured with respect to the facility floor surrounding the moving table), (c) reinforcing rebar strains, and (d) damage progression through monitoring of the concrete crack development, the following major observations were made:

Shaking Table – Structure Interaction

Of primary interest in the course of the 13-run test was the qualification and quantification of the influence of the shaking table on the response of the SMART structure under study. As noted earlier in the report, controlling the shaking table and especially in the vertical direction was a challenge. Compounded onto the controllability of the table is the epistemic uncertainty surrounding its effective dynamic properties. As a result, there has been a significant variability between the intended motions on the shaking table and the recorded motions on the table top surface during the tests. Table 2.2 depicts peak ground acceleration comparisons between the input goals and the actual recorded motions on the table. The difference observed is assessed to be the combined result of both the inability to control the vertical and rocking motion of the table and of the structure-table interaction. As noted in Figure 2.16 where the table spectra during the synthetic seismic pairs for RUN4 are shown, the eigenmodes of the structure are influencing the shaking table response. This is clearly depicted by the appearance of two distinct peaks at 7 Hz and 16 Hz which in turn correspond to the fist two modes of the SMART2008 structure. Further, as shown in Figure 2.17 for RUN4 and RUN13 pairs, the vertical acceleration measured on the table (geometric corners) is approximately equal in PGA to the horizontal components.

Table 2.2 Shaking table recorded horizontal accelerations observed during tests.

	Acceleration A_{xx} (g)		**Acceleration A_{yy} (g)**	
	Goal	**Test**	**Goal**	**Test**
Run 1	0.05	0.08	0.05	0.03
Run 2	0.05	0.08	0.05	0.05
Run3	0.05	0.19	0.05	0.15
Run 4	0.1	0.20	0.1	0.24
Run 5	0.2	0.19	0.2	0.20
Run 6	0.3	0.23	0.3	0.32
Run 7	0.4	0.33	0.4	0.35
Run 8	0.5	0.41	0.5	0.55
Run 9	0.6	0.41	0.6	0.56
Run 10	0.7	0.53	0.7	0.67
Run 11	0.8	0.58	0.8	0.77
Run 12	0.9	0.70	0.9	1.06
Run 13	1.0	0.75	1.0	1.13

Evolution of Eigenfrequencies

To assess the progression of damage in the reinforced concrete structure resulting from the sequence of seismic excitations, special attention was paid in estimating the evolution of eigenfrequencies as a key indicator of damage. Between some of the successive tests, white noise low-level excitations were applied on the structure in order to arrive at an estimate of the condition of its dynamic properties. Estimates of the updated frequencies were derived from displacement response spectra that resulted from the white noise input. In addition, by utilizing the free-vibration of the structure that followed the end of the strong motion part of the input record, similar estimates were made. The two approaches resulted in similar estimates of eigenfrequencies. The main objective and impact of such estimation on both the shaking table tests assessment and the numerical evaluation of the response is a better understanding of the actual degradation that takes place and its influence on the floor response spectra of the "damaged" structure. Shifting of the frequencies due to concrete damage or rebar yield will indicate change in the stiffness of the structure and potential shifting away or towards frequency bands of the input excitation containing the bulk of its energy.

Table 2.3 lists the estimates of the first three structural eigenfrequencies (f_1 = flexural along x-axis, f_2 = flexural along y-axis, and f_3 = twisting) upon completion of the corresponding input record. It should be noted that the modes identified as flexural modes are not purely flexural but have twisting contribution due to the asymmetry in the SMART structure. Shown in Figure 2.12 are numerical estimates of the modes prior to the application of the thirteen seismic tests.

Based on the eigenfrequency evolution listed in Table 2.3 the following important observations are made:

- A drop in eigenfrequencies is observed even after the application of very low intensity excitations (i.e. real records in RUN1 through RUN3) where no cracking in concrete or yielding in the reinforcement is expected. This has been attributed to damage in concrete due to micro-cracking. Similar observations have been made during similar shaking table tests on the seismic response of shear walls. This is significant in nuclear design due to the fact that the structural eigenfrequencies may experience shifting even at levels far below the design basis earthquake.

- A significant drop in frequency is observed following RUN5 even though the intensities of the input accelerations are at the level of the design basis earthquake for the structure. As will be discussed in more detail in the next section, this has been attributed to the fact that the structure during the application of the real, low intensity earthquakes exhibited low levels damping and as a result it experienced a significant number of stress cycles following the end of the strong motion input part of the RUN3 test.

- Eigenfrequency shifts of ~50% are observed for the 1st structural mode following the thirteen shaking table tests. Smaller shifting is observed for the next two modes. These observations are critical both in quantifying damage evolution but also in evaluating floor response spectra in structures that experience earthquakes below the design basis level.

Table 2.3 **Observed degradation of SMART200 test structure eigenfrequencies.**

seismic test	f_1 (Hz)	f_2 (Hz)	f_3 (Hz)
RUN 1	6.10	7.96	15
RUN 2	6.13	7.96	14.70
RUN 3	5.69	7.33	14.24
RUN 4	5.66	6.94	14.18
RUN 5	5.14	6.91	14.13
RUN 6	5.02	6.78	11.44
RUN 7	4.56	6.81	11.63
RUN 8	4.16	6.11	11.61
RUN 9	4.06	5.98	11.56
RUN 10	3.98	5.95	11.56
RUN 11	3.95	5.82	11.48
RUN 12	3.87	5.71	11.40
RUN 13	3.49	5.65	11.15

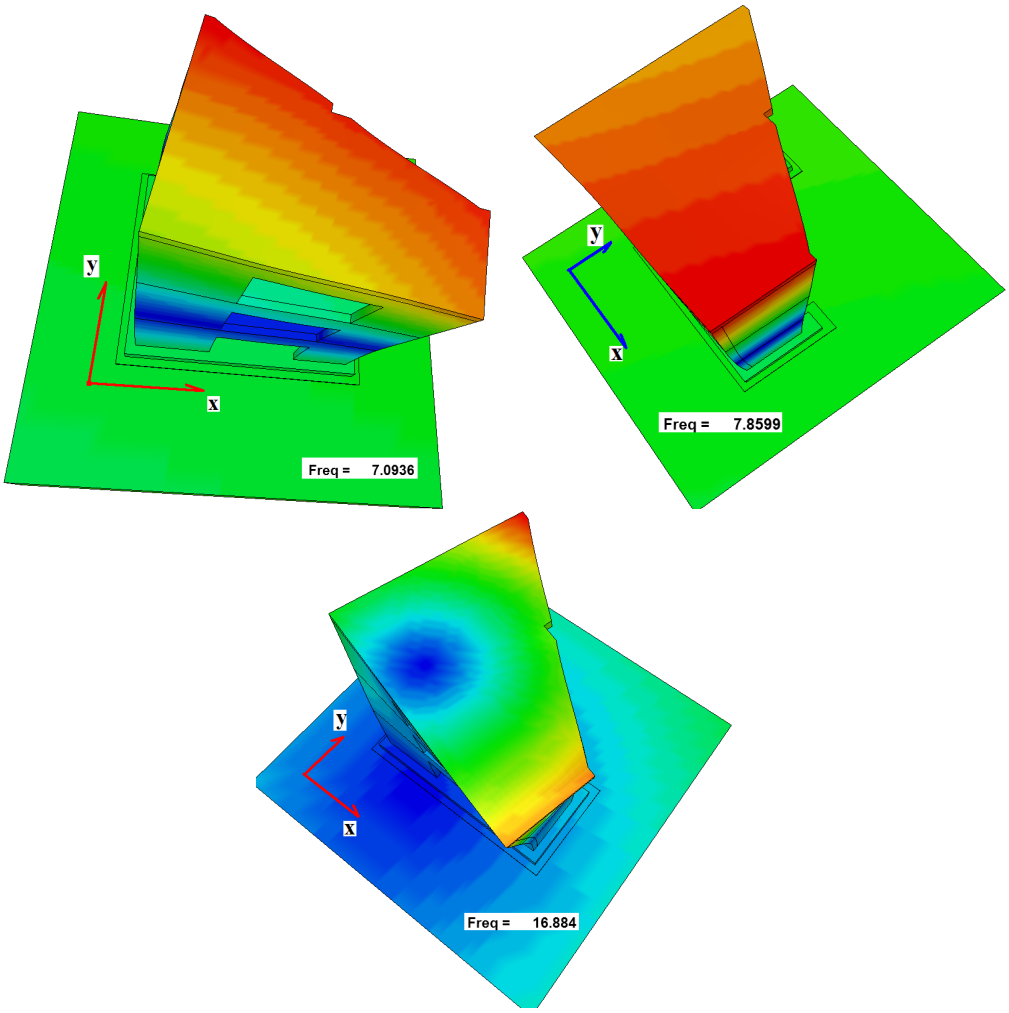

Figure 2-12 **Numerical estimates of the first three eigenfrequencies and modes of the SMART structure on the shaking table prior to the application of the thirteen seismic tests**

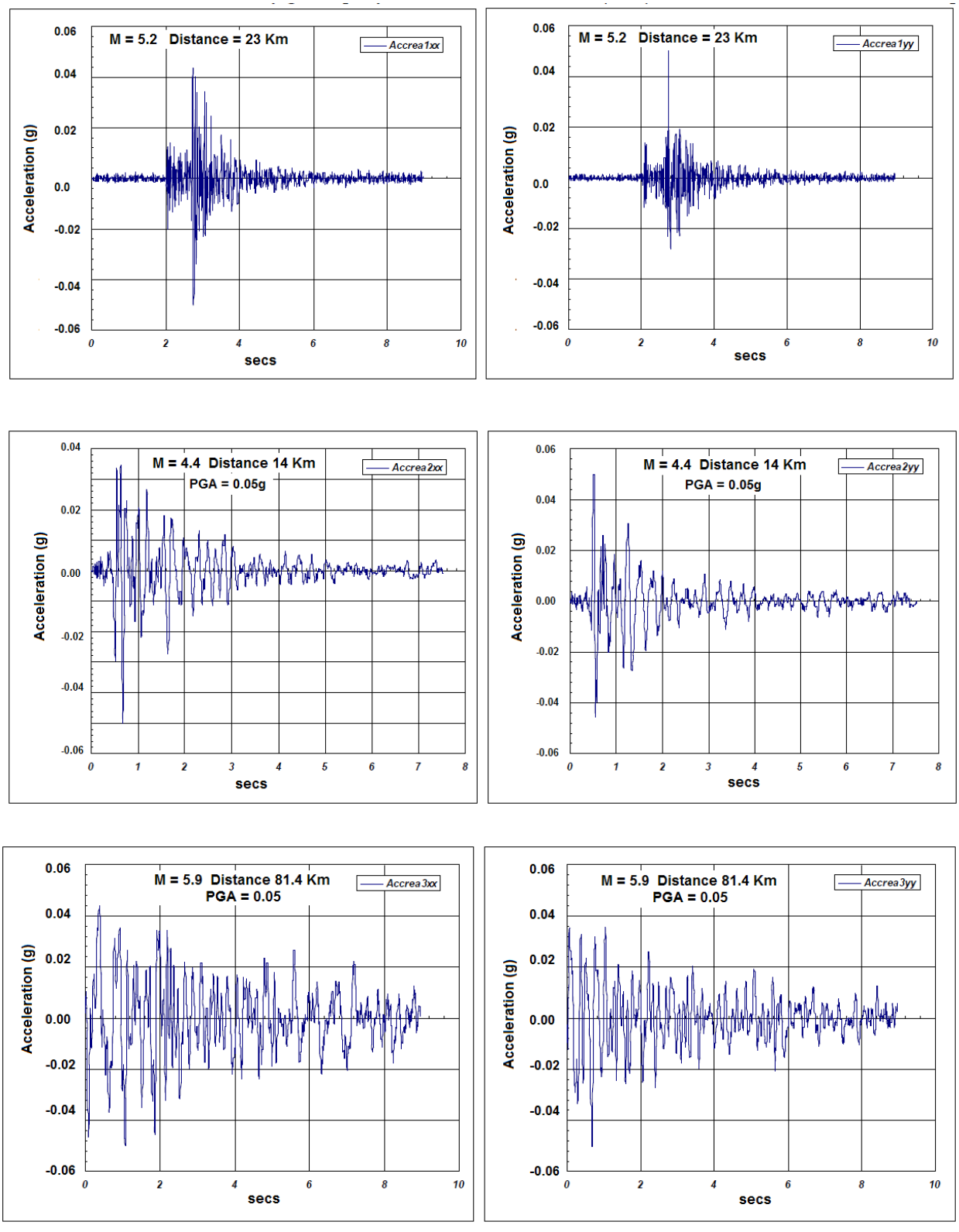

Figure 2-13 Acceleration time histories of the three real earthquake records used in the SMART2008 shaking table experiment

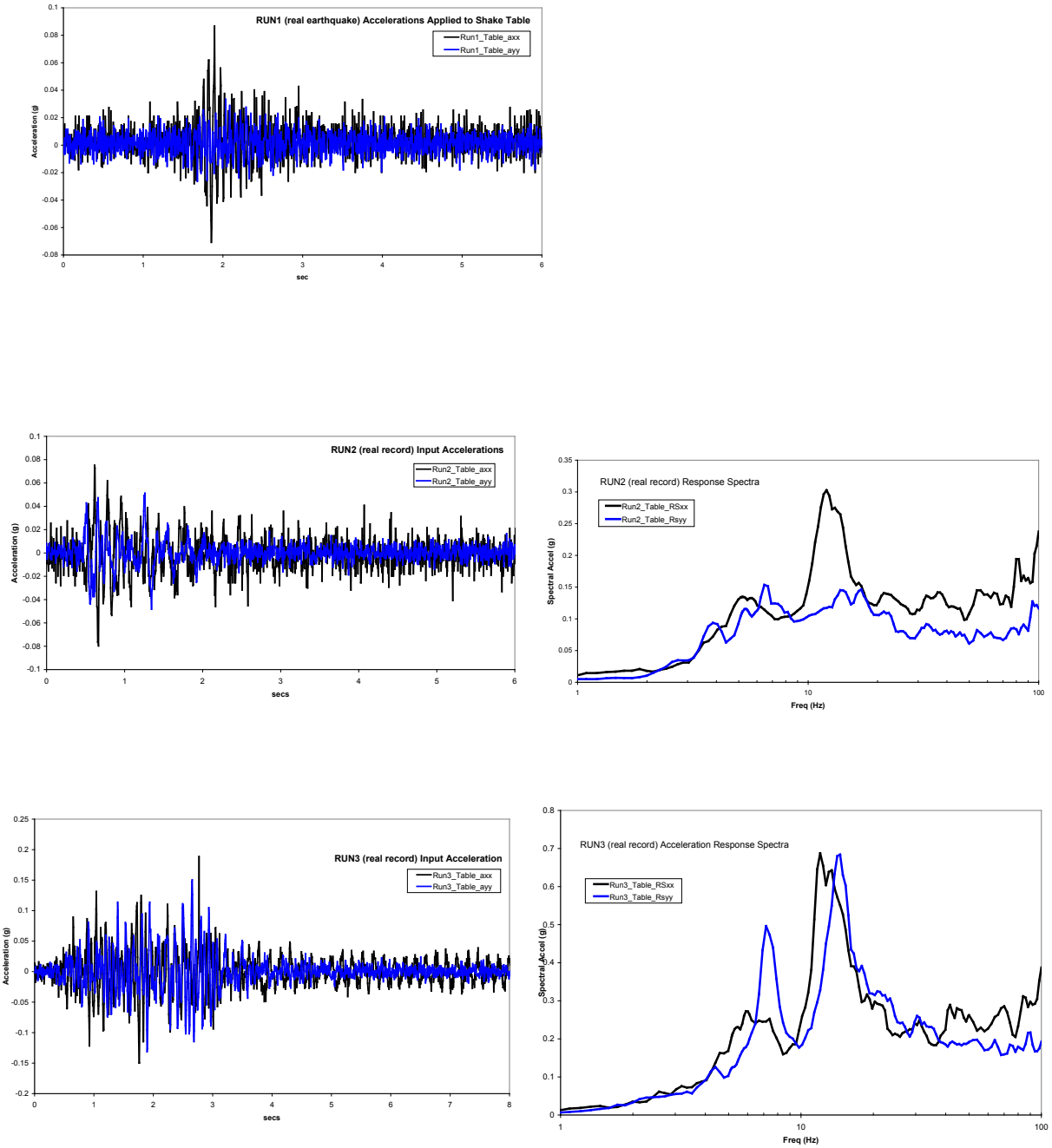

Figure 2-14 Acceleration time histories recorded on the shaking table during the SMART2008 tests RUN1, RUN2 and RUN3 and the corresponding response spectra

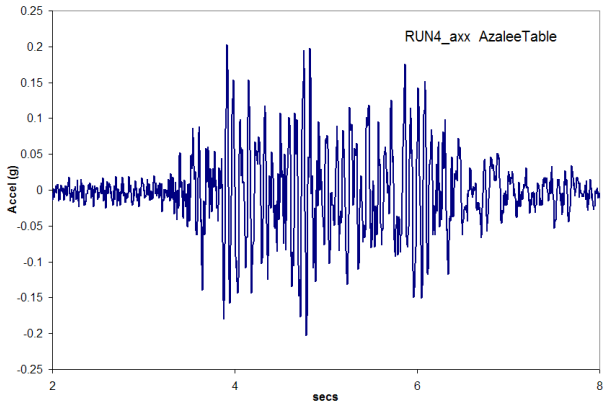

Figure 2-15 Acceleration time histories recorded on the shaking table during the SMART2008 RUN4 test for the two horizontal directions x and y

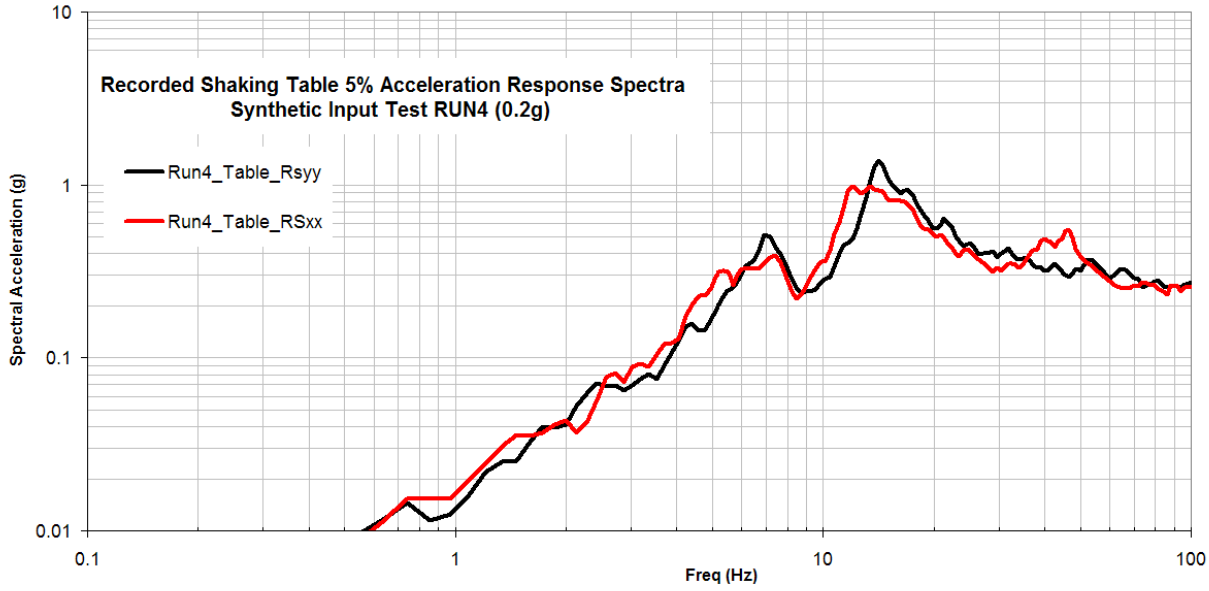

Figure 2-16 Acceleration response spectra on the shaking table during the SMART2008 test RUN4 indicating deviation from the design spectrum of Figure 2.1 near the structural modes at 7 Hz and 16 Hz

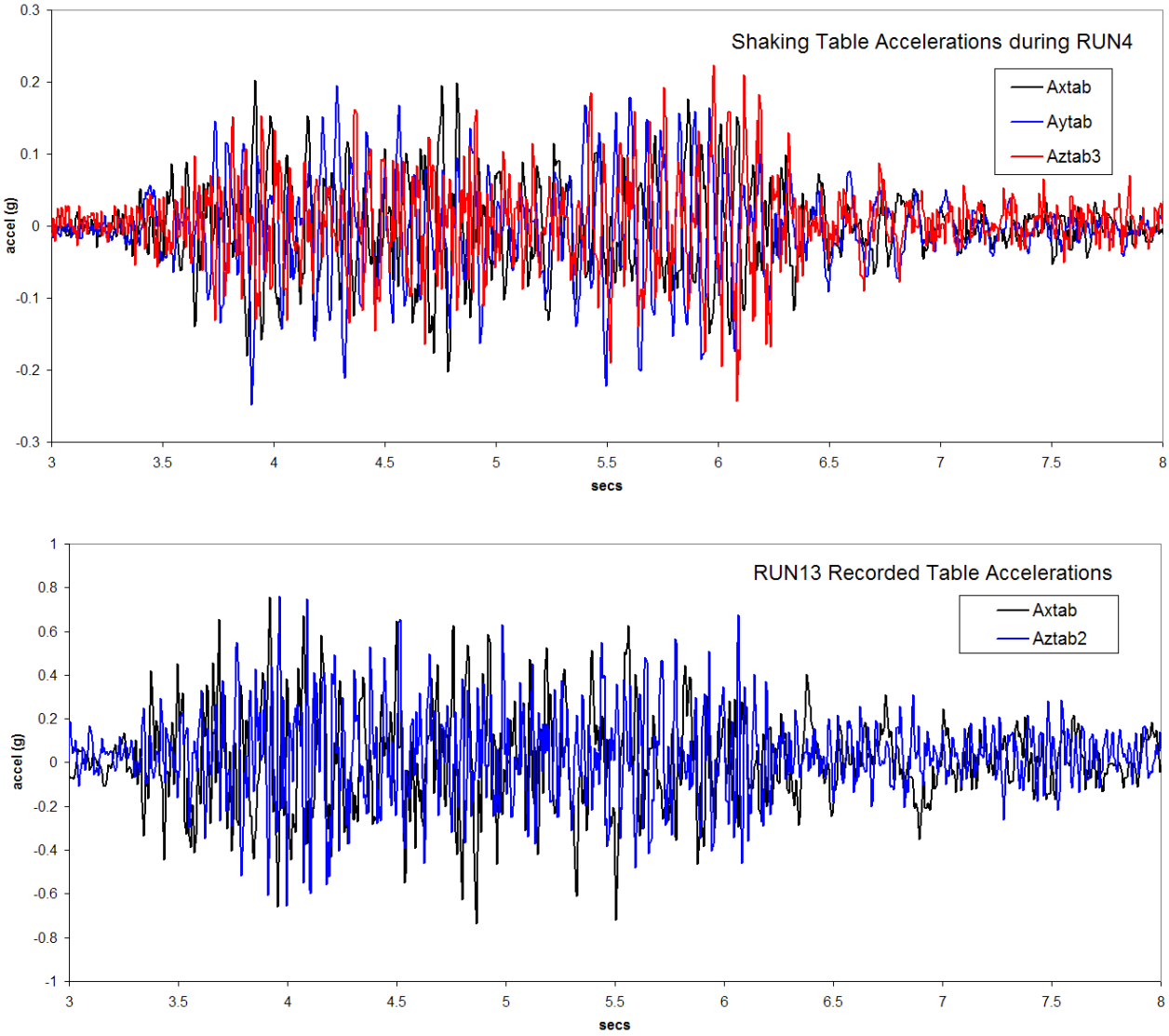

Figure 2-17 Comparison of horizontal and vertical acceleration components recorded on the shaking table during the test

Shaking Table Test Results

In this section, selected results from the extensive matrix of recorded data are presented and discussed. Shown in Figure 2.18 are the coordinate system for acceleration and displacement records and the designation of the key locations. Also shown are the designations and position of the strain gauges where rebar strains were monitored and reported herein.

Real Earthquake Records

The real earthquake records designated as RUN1, RUN2 and RUN3 were applied in the first phase of the shaking table tests. Of interest was to observe the response of the structure to realistic earthquake signals. While RUN1 and RUN2 achieved relatively low intensities (even though degradation in terms of eigenfrequencies was observed), RUN3 represented a more realistic case for analysis since it approached intensities close to design basis. Figure 2.19 depicts the recorded horizontal table accelerations. As seen from the figure, the strong motion portion is approximately 3 seconds. Examining, however, the recorded acceleration data shown in Figure 2.20 (along the x-axis at location D and y-axis at location C) it is evident that the structure experiences a long-lasting free vibration. The implication of such response is that the structure resonated with the input, (more detailed discussion on this point is provided in Section 3.4.2) and that the damping of the combined system (structure and shaking table) is very low for this low intensity seismic excitation (measured during the test as ~1%). The multitude of stress cycles experienced by the structure may well explain the shifting of the eigenfrequencies due to micro-cracking caused by the cyclic load.

Figures 2.21 and 2.22 depict acceleration response spectra for all three real signals used in the test. Relative displacements and rebar strains shown in Figures 2.23 and 2.24 respectively, further confirm the presence of “un-damped” free vibration of the structure during RUN3.

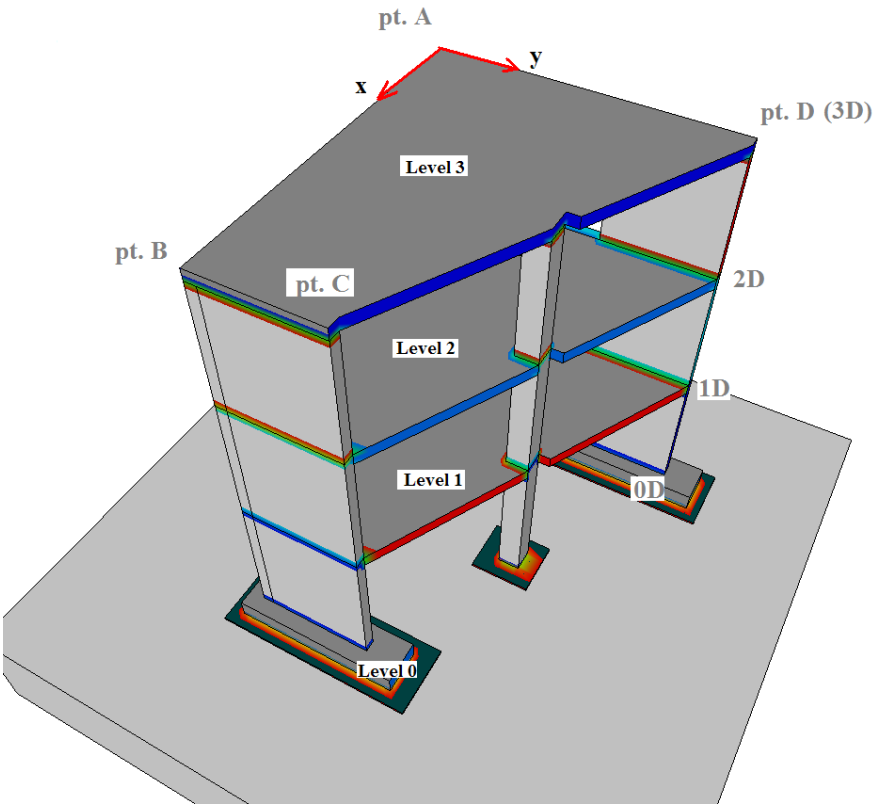

Figure 2-18 Response output locations on the SMART structure

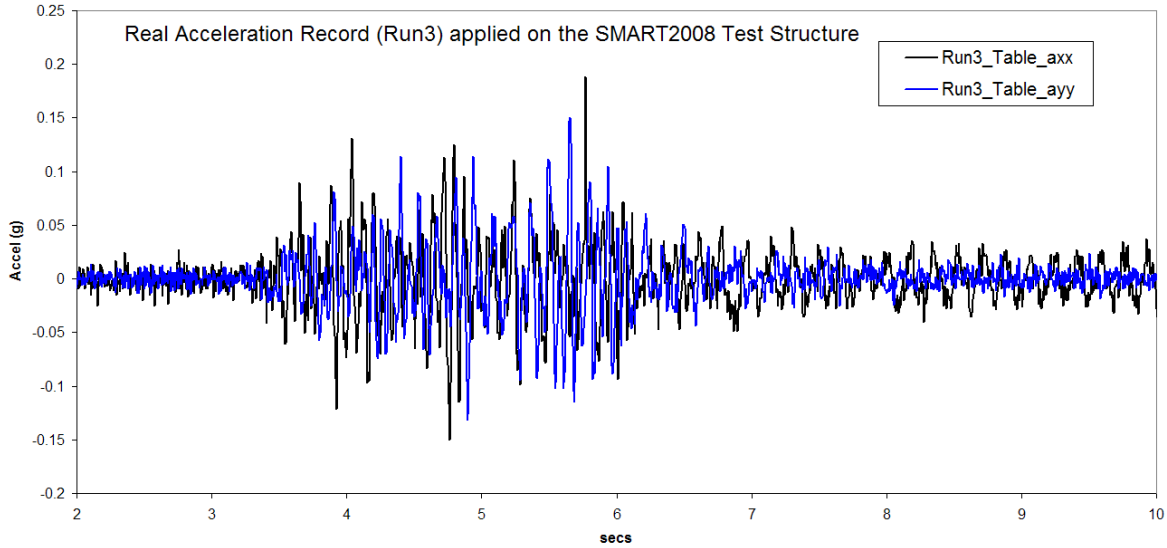

Figure 2-19 Table horizontal accelerations recorded during test RUN3

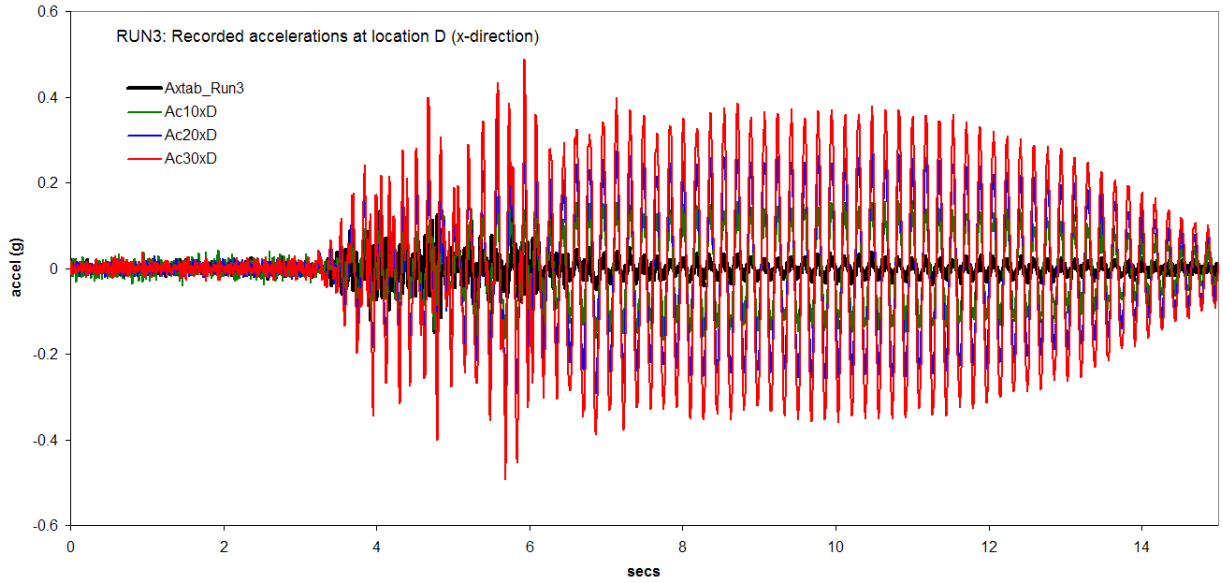

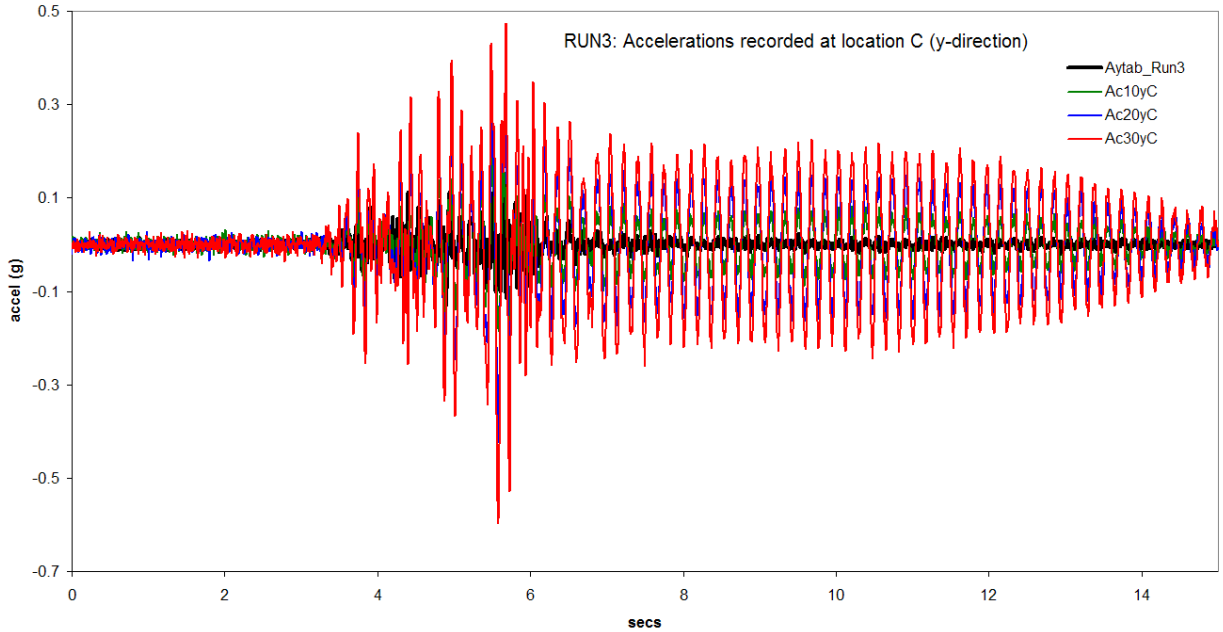

Figure 2-20 Recorded horizontal accelerations on the structure during test RUN3

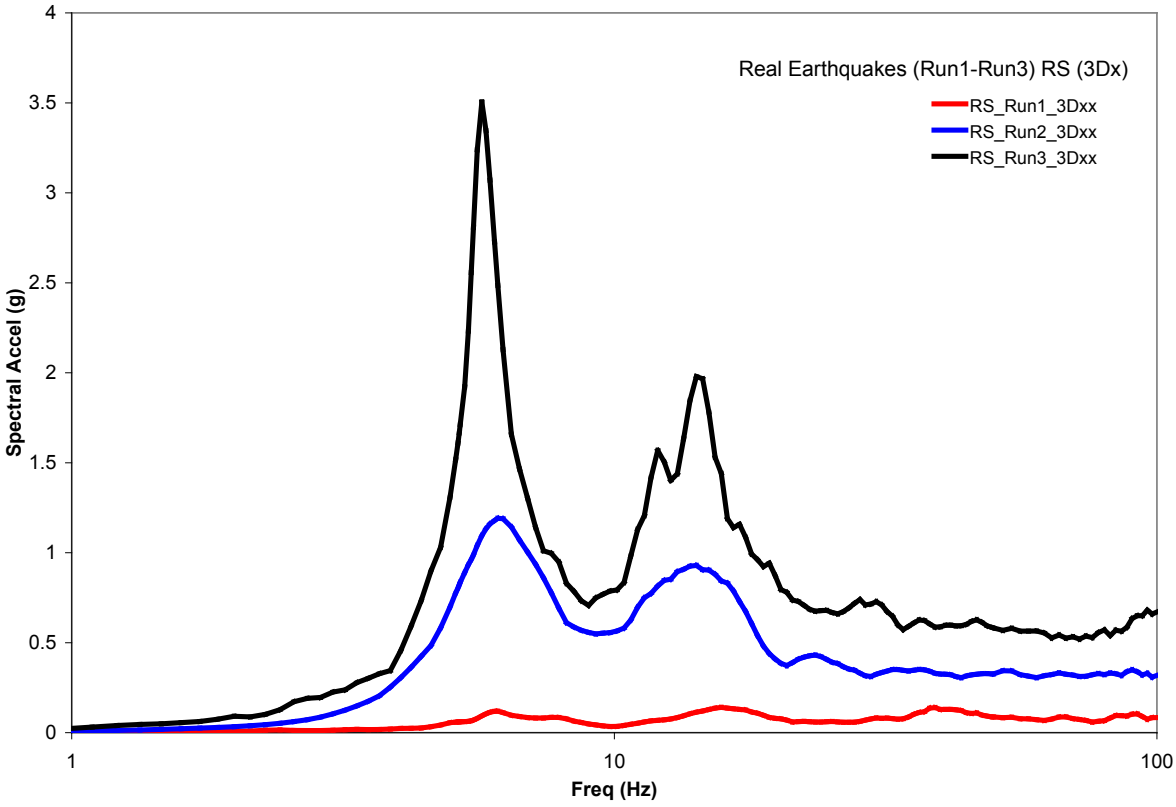

Figure 2-21 Acceleration response spectra at level 3 and location D recorded during the application of the three real earthquake records (RUN1, RUN2 and RUN3)

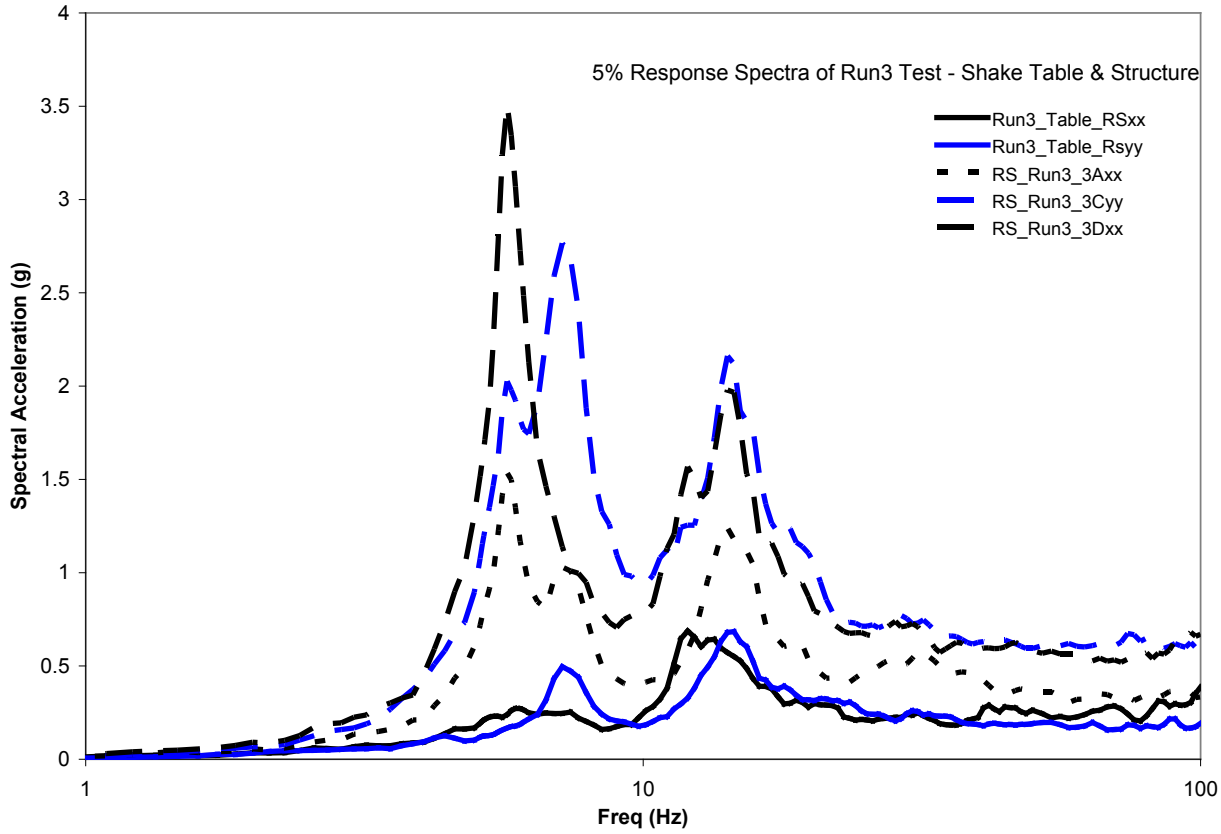

Figure 2-22 Table and structure acceleration response spectra comparison for RUN3 test

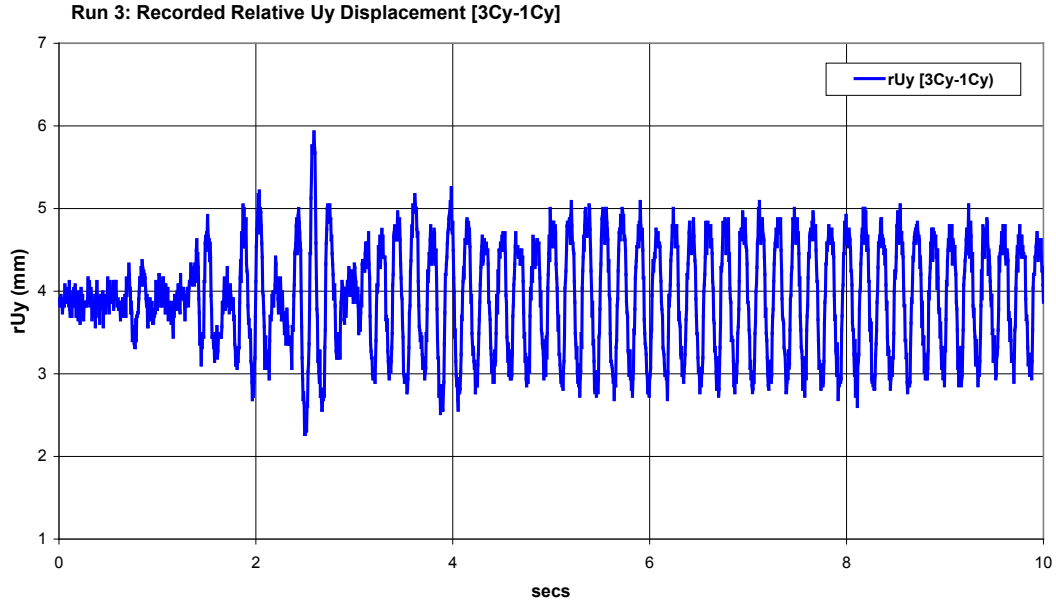

Figure 2-23 Relative displacement rUy between level 3 and table recorded during RUN3 test

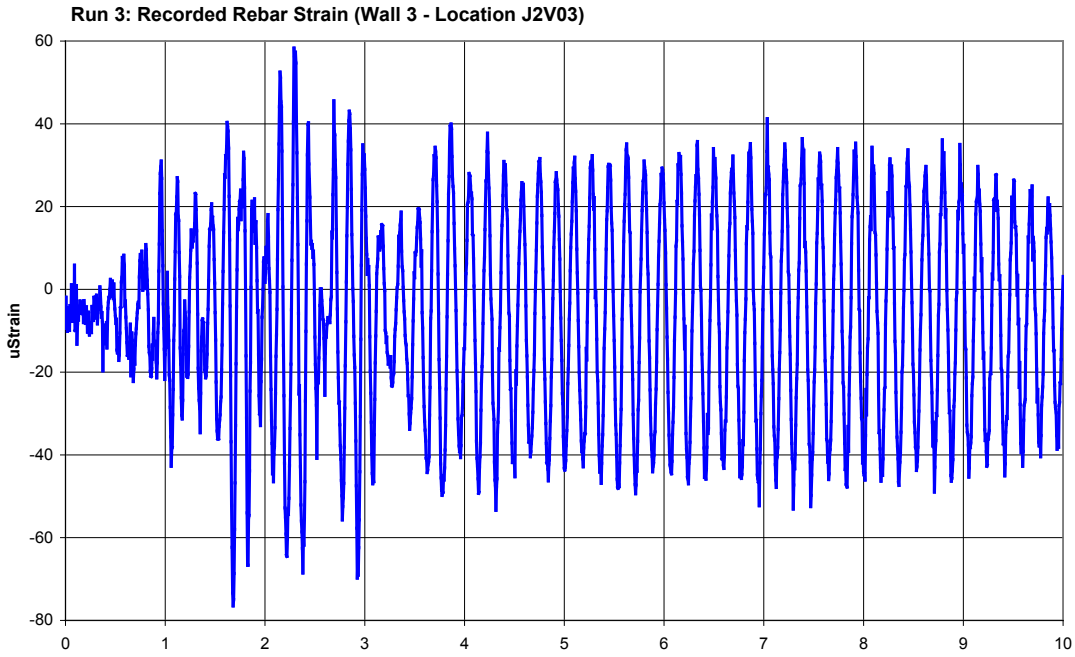

Figure 2-24 Rebar strain on Wall 3 recorded during RUN3 test

Synthetic Records

The synthetic records, designated as RUN4 through RUN13, were applied following the three real signals of the seismic input suite. As noted previously these synthetic records were generated from the design spectrum of Figure 2.1 aiming to progressively reach 1.0 g intensity in the input acceleration. According to Table 2.2 which lists the acceleration intensities achieved at the table level, RUN4 with a_{xx} = 0.2g and a_{yy} = 0.24g table accelerations ended up representing the design basis earthquake which governed the design of the test structure. In addition to the RUN4 seismic input pair, RUN8 (with a_{xx} = 0.41g and a_{yy} = 0.55g) was considered in this benchmark as the "over-design" seismic level. As a result, special attention was given in the post-analysis as well as the predictions to these two tests.

Depicted in Figure 2.25 are the table accelerations recorded during RUN4 indicating strong motion duration of about 3 seconds. Figure 26 on the other hand illustrates in-structure accelerations induced by the RUN4 pair for both horizontal directions and compares them with the table accelerations. While not as dramatic as in real earthquake RUN3, the structure undergoes free vibration indicating low damping. Accelerations recorded on the 3rd level at higher intensities (RUN8 through RUN13) are shown in Figure 2.27. It is deduced from the acceleration transients that higher levels of damping are exhibited by the structure due to the absence of free vibration in the response.

Acceleration response spectra of all the synthetic earthquakes at the table top surface are shown in Figure 2.28. It can be deduced from the spectral traces that there exist a structure-table interaction stemming from the shifting of the frequencies which originate in the degradation of the structure.

In addressing the degradation of the structure with the sequential application of the increasing seismic loads, floor response spectra were generated. Seen in Figure 2.29 are floor response spectra at the 3rd level from three tests, RUN3 (real earthquake), RUN4 (design-level) and RUN8 (over design level). The figure very clearly demonstrates the changes that occur in the stiffness of the structure which are caused by damage accumulation (through mico-cracking) in the concrete. To compare the table spectra with the shape of the design spectrum (Figure 2.1) the RUN4 and RUN13 table response spectra are compared in Figure 2.30. One notices that the interaction, which was more visible in the low intensity (RUN4) input has blended in and it is less distinguishable. In general, however, the spectra maintain the general shape of the original spectrum from which the input was generated.

More complete information regarding the damage evolution can be deduced from Figures 2.31-2.33 which depict floor response spectra at the same structural location respectively and indicate the trend and shifting of the eigenfrequencies to lower values. As is seen in Figure 2.32 the spectral acceleration associated with the first flexural mode decreases while the intensity of the input increases stemming from the fact that the structure is being progressively damaged.

Relative displacements between the 3rd and first levels of the structure are shown in Figure 2.34 for the RUN9 test. The increased level of damping in the structure due to micro-cracking is evident in that the deformations of the structure cease soon after the strong motion part is over.

Interesting results of rebar strain are depicted in Figure 2.35 which traces the strain during different tests. For RUN4 the response is linear because of the two-sided nature of the strain transient. As the intensity increased in RUN9 and beyond, it is suspected that rebars at the extremities and near the foundation are experiencing yielding.

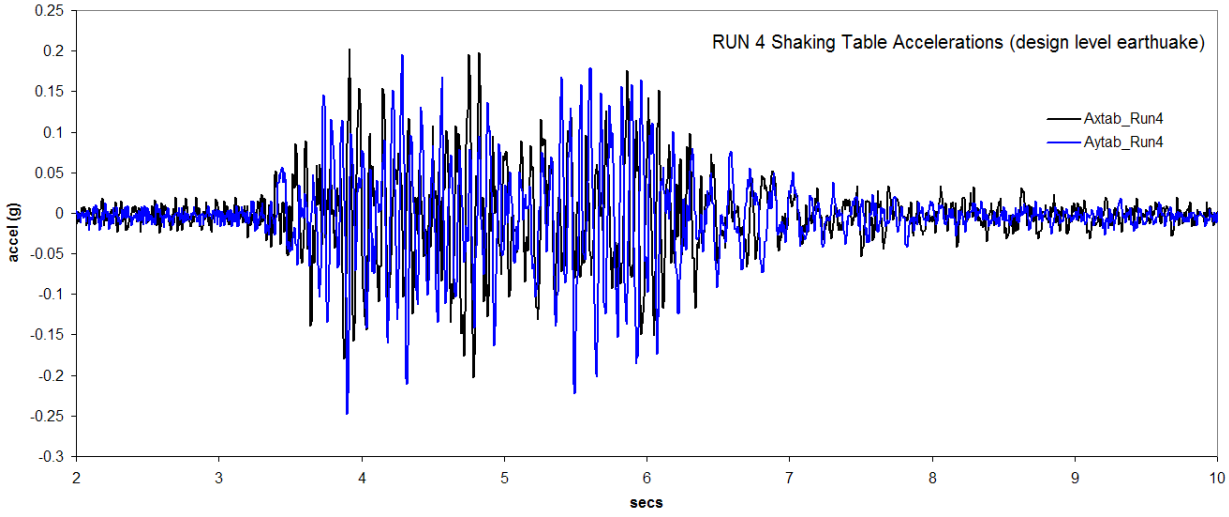

Figure 2-25 Recorded shaking table horizontal accelerations during the RUN4 test

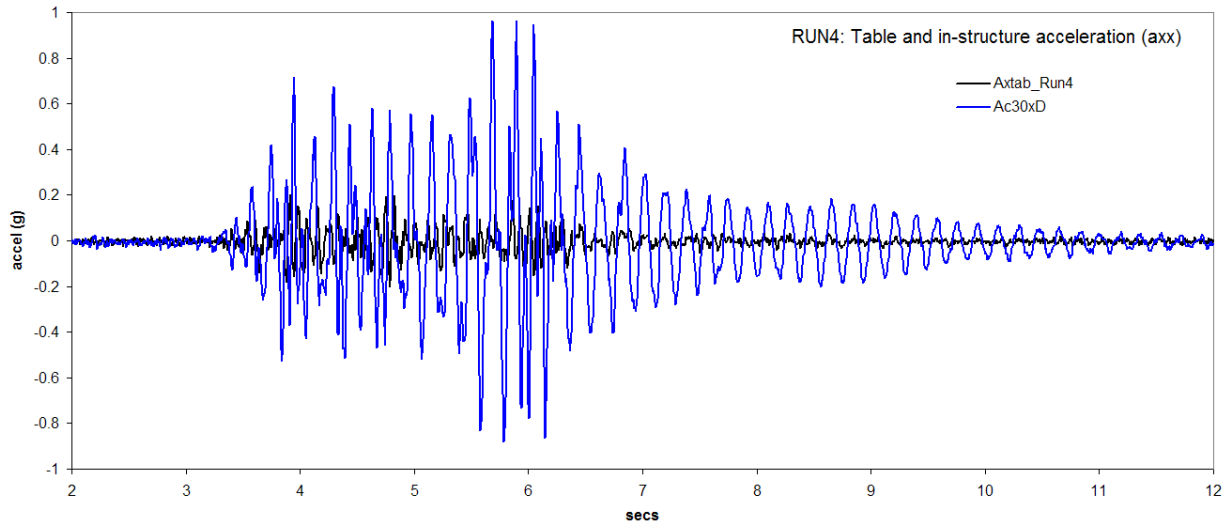

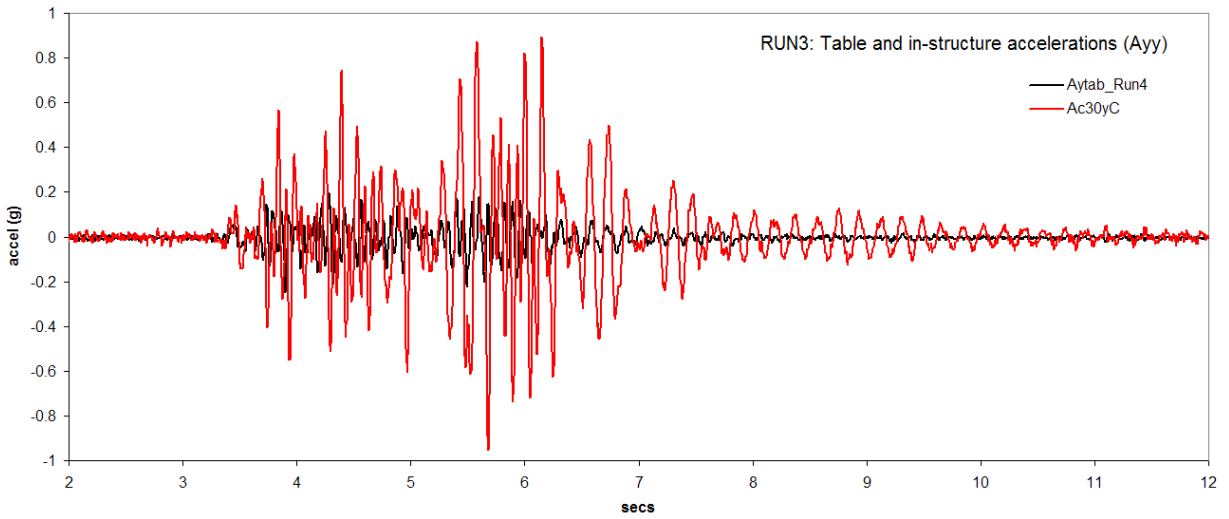

Figure 2-26 Recorded shaking table and in-structure horizontal accelerations in RUN4

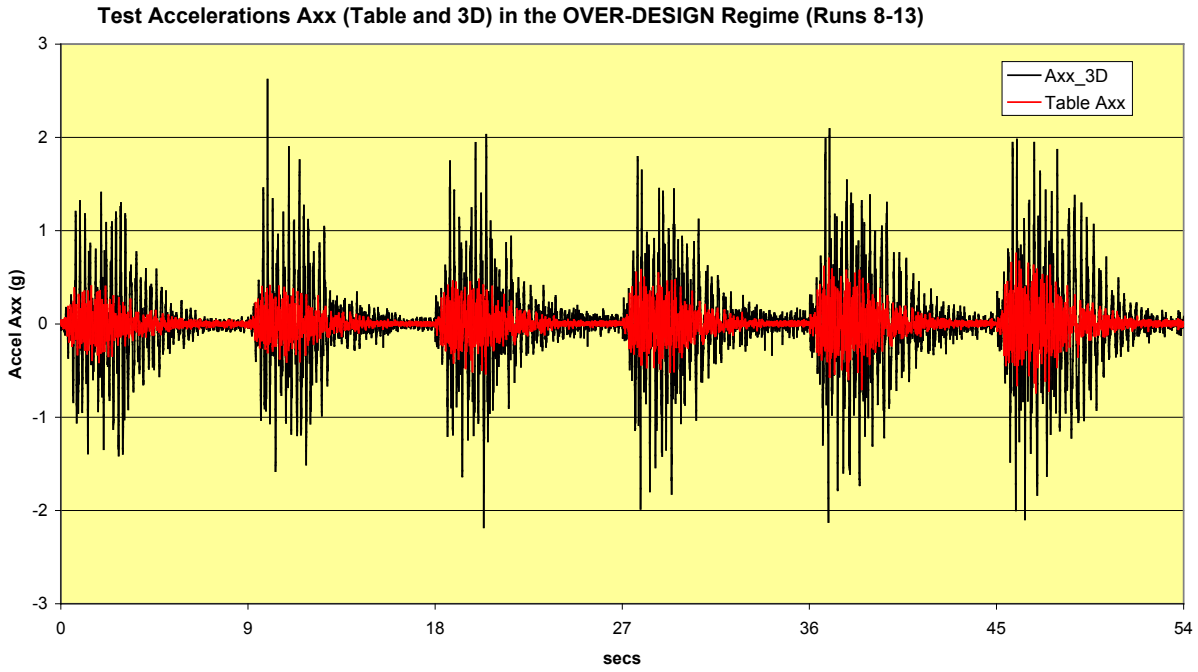

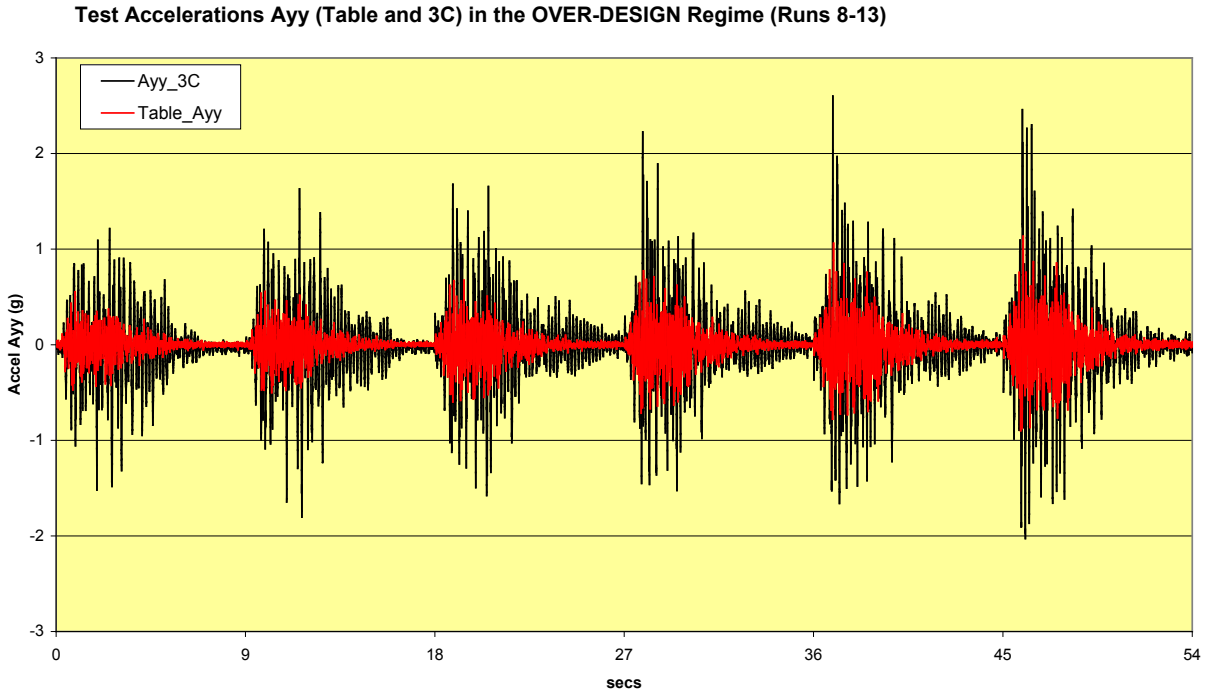

Figure 2-27 Recorded shaking table and in-structure horizontal accelerations during the sequence of RUN8 to RUN13 tests

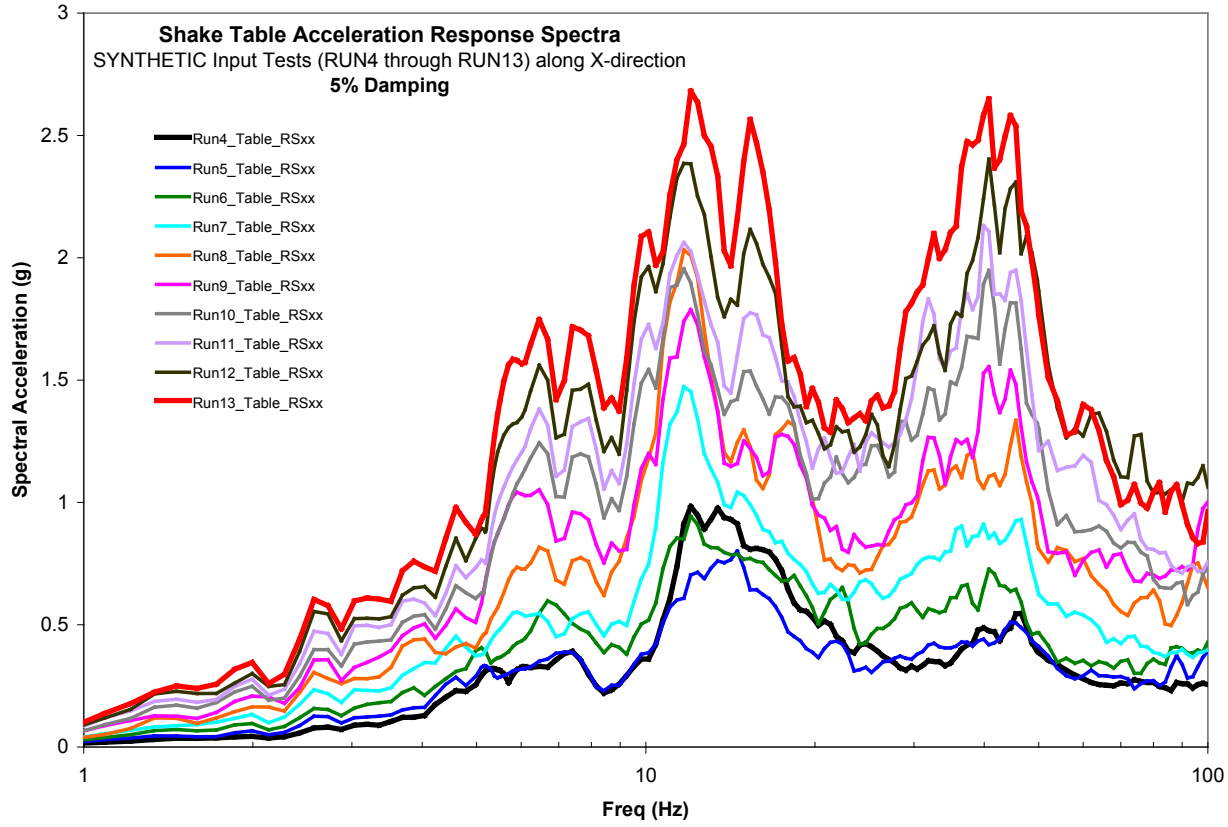

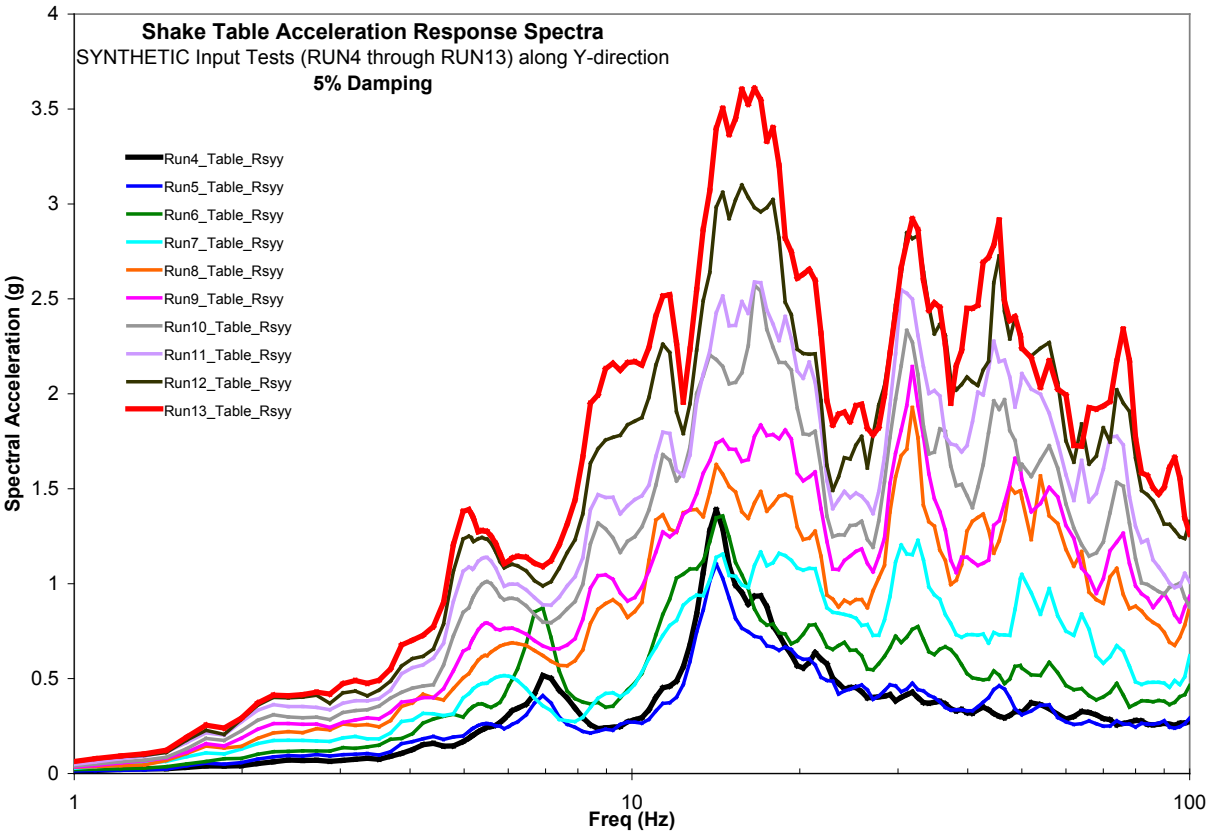

Figure 2-28 Shaking table acceleration response spectra in the two horizontal directions recorded during the synthetic earthquake tests (RUN4 through RUN13)

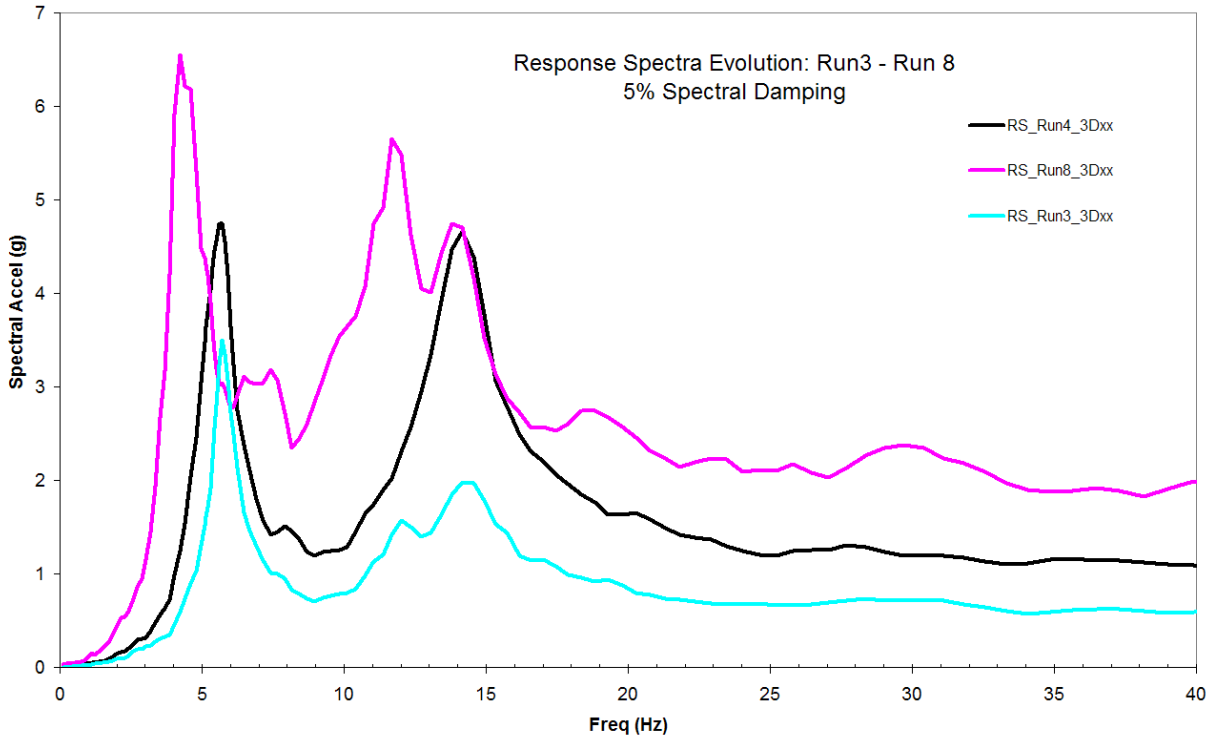

Figure 2-29 Evolution of floor spectra and comparison of real record (RUN3)spectra with the design-level (RUN4) and the over-design RUN8

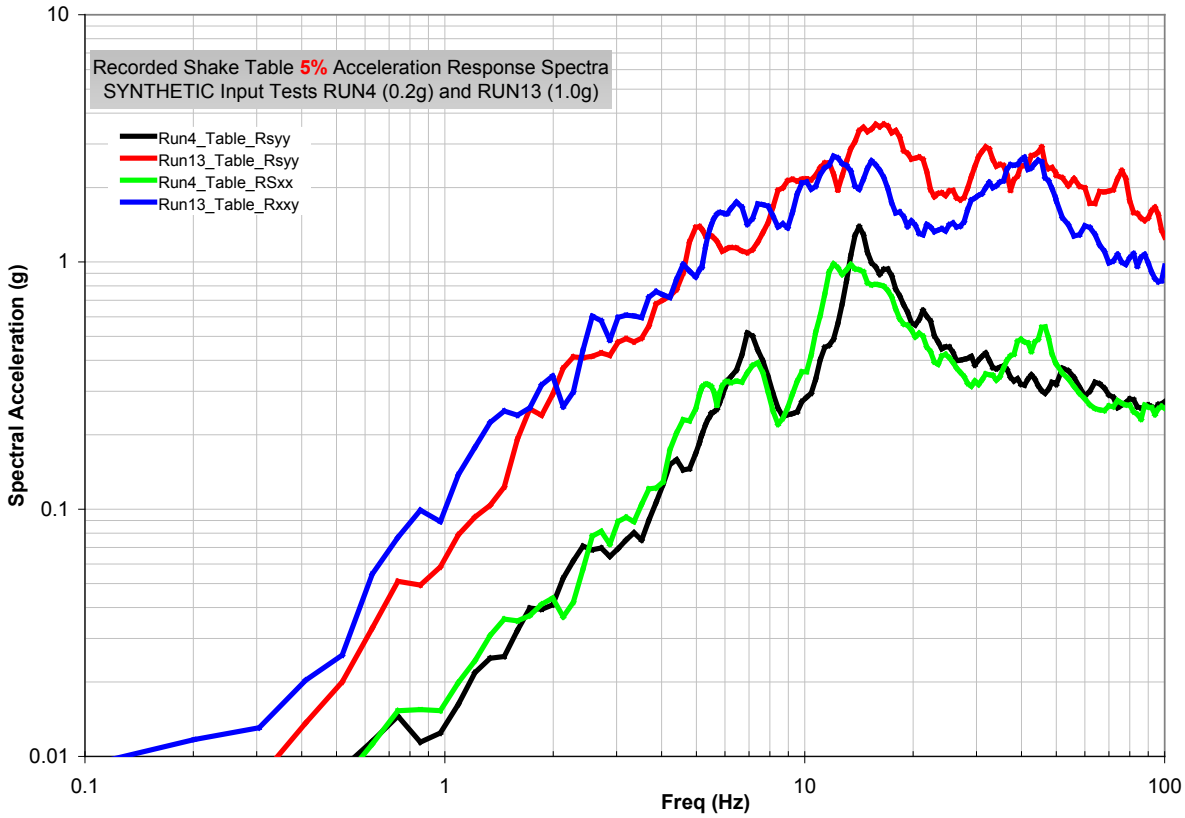

Figure 2-30 Comparison of shaking table acceleration response spectra in the two horizontal directions for design level (RUN4) and last test in sequence (RUN13) to identify structure-table interaction effects

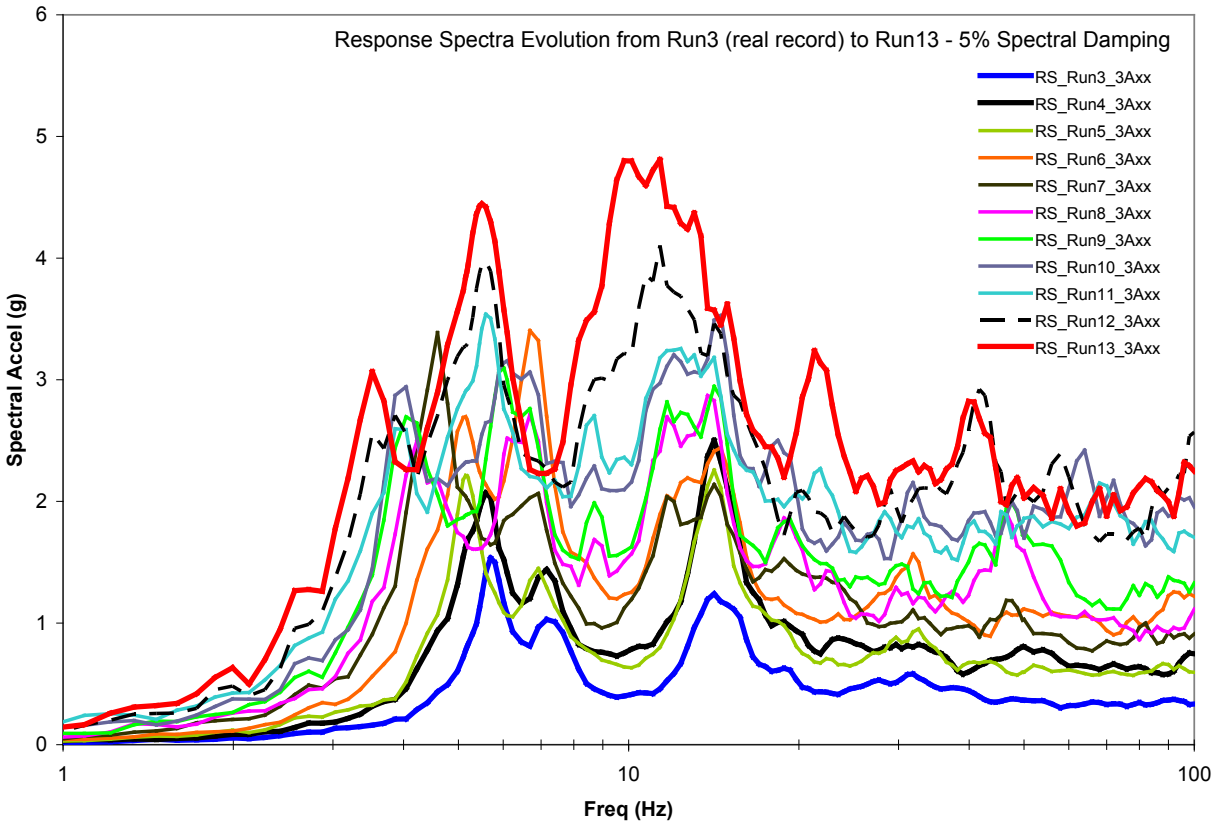

Figure 2-31 Evolution of in-structure response spectra (level 3 - location A) for tests RUN3 through RUN13. Location A is close to the stiffest section of the test structure

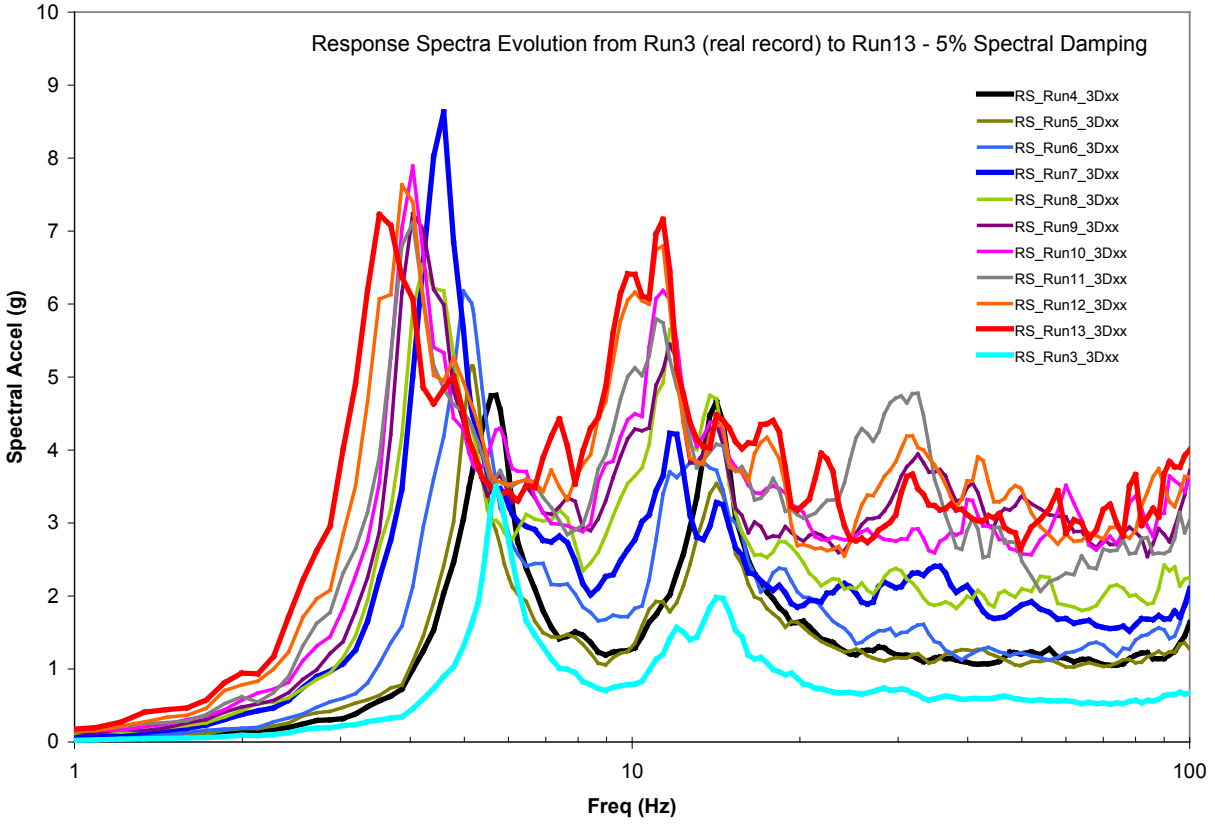

Figure 2-32 Evolution of in-structure response spectra (level 3 - location D) for tests RUN4 through RUN1

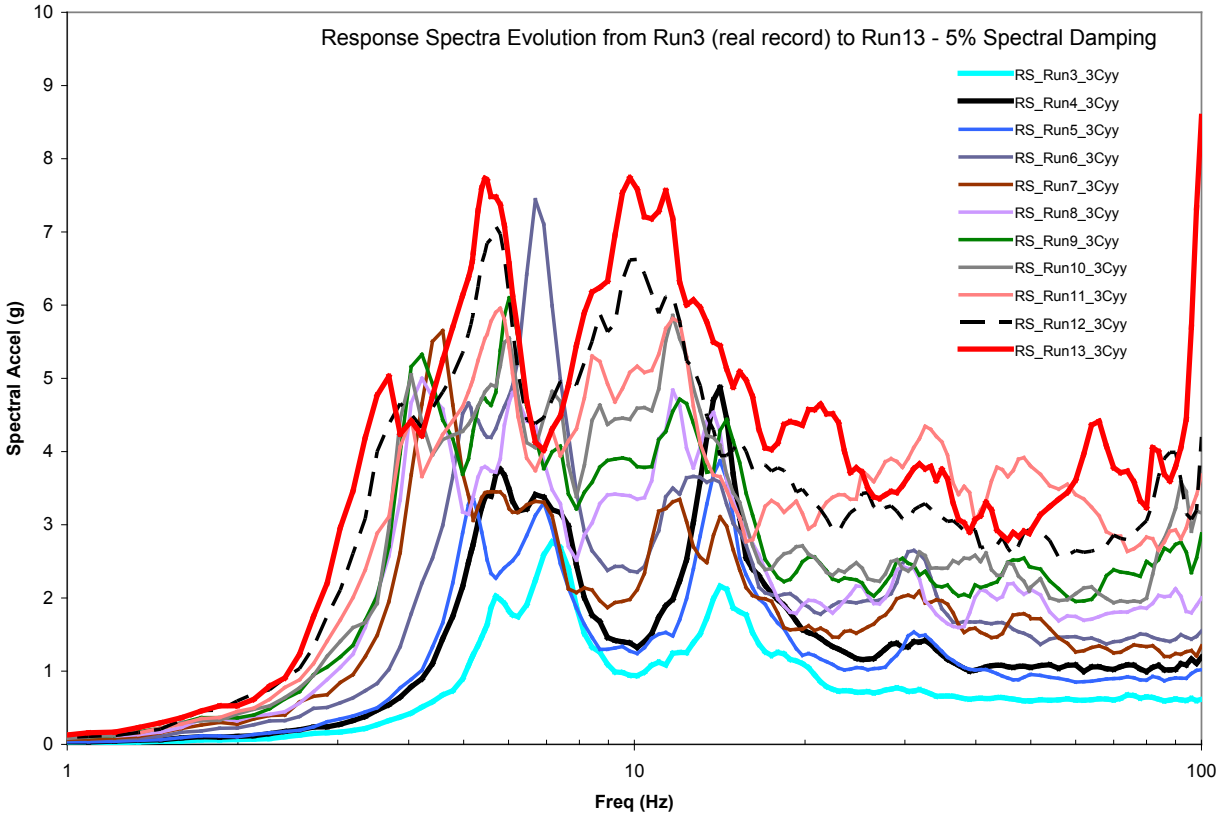

Figure 2-33 Evolution of in-structure response spectra (level 3 - location C) for tests RUN4 through RUN13

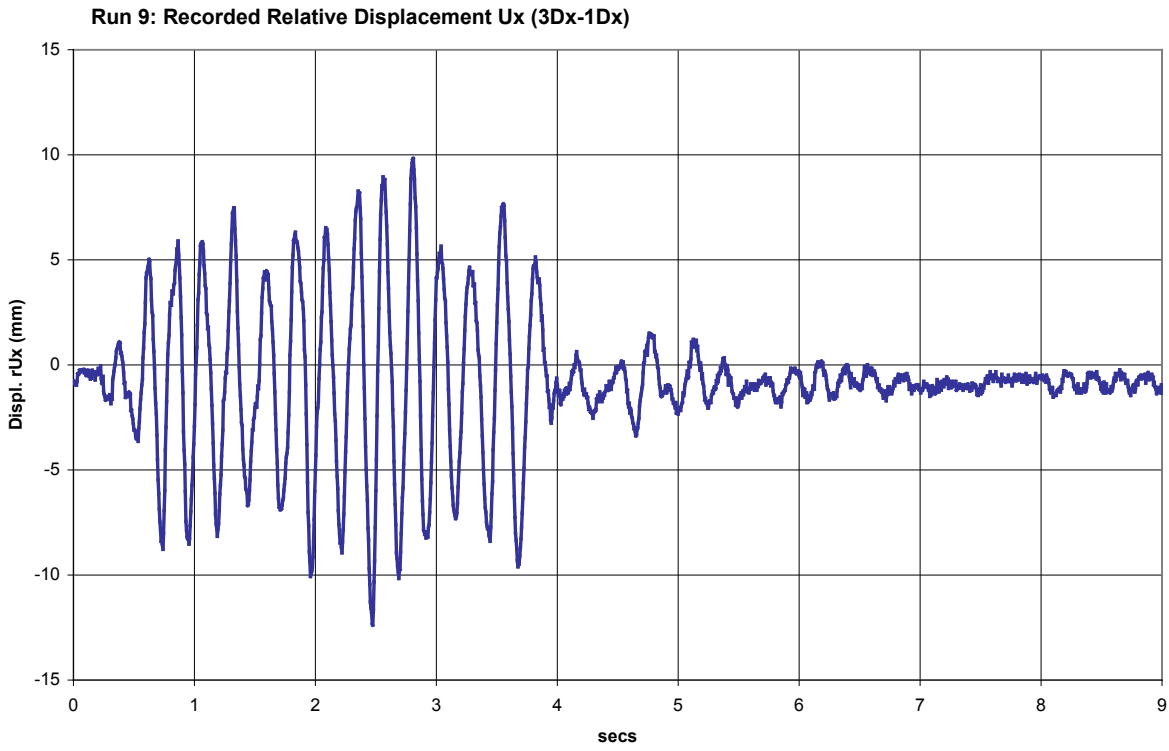

Figure 2-34 Relative displacement between 3rd and 1st level recorded during RUN9

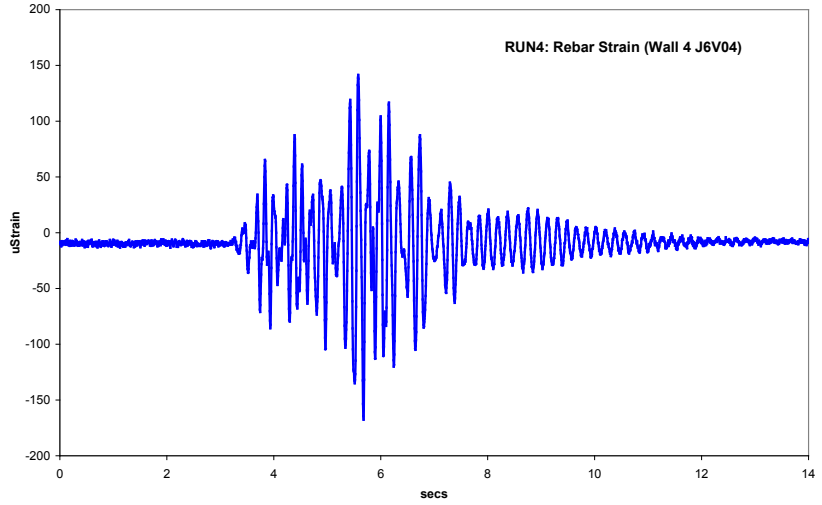

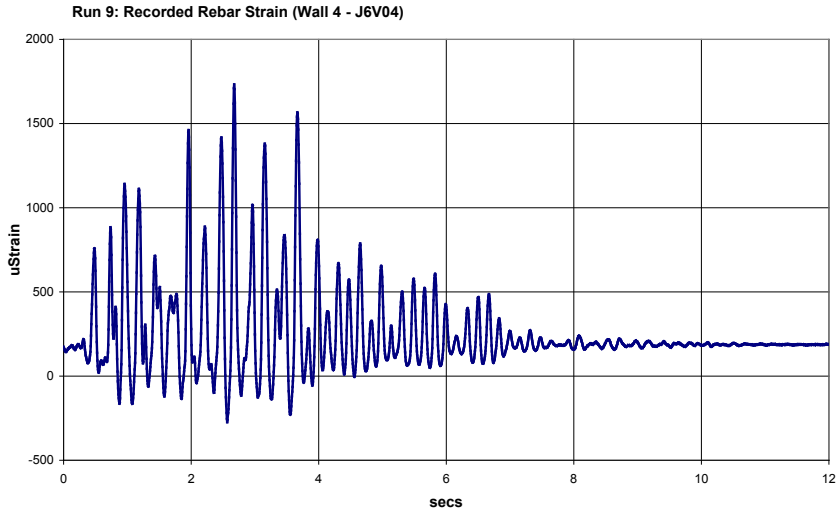

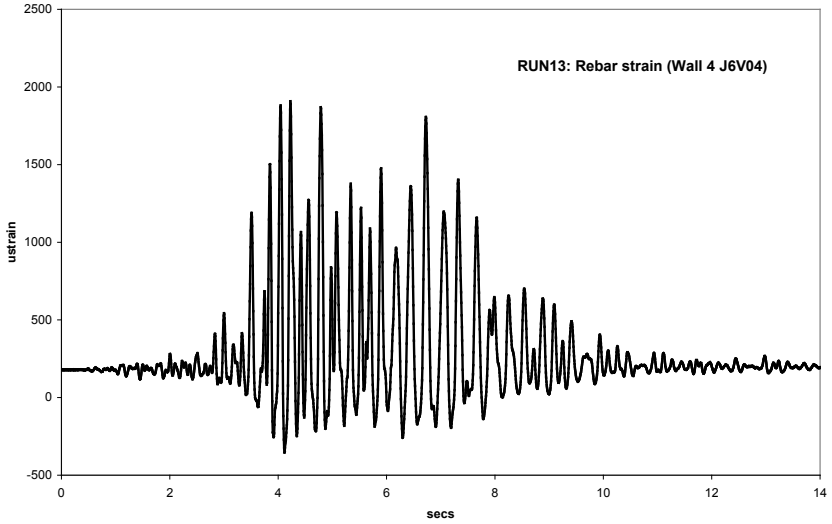

Figure 2-35 Evolution of rebar strain in Wall 4. Comparison of RUN4, RUN9, and RUN13

Observed Structural Damage

At the end of each run in the 13-run sequence the walls of the structure were thoroughly examined for developed cracks. Figure 2.36 depicts the crack pattern observed at the end of the 13-run test. They were predominantly surface cracks. Given that the structure was designed with the design level earthquake at 0.2g and during the shaking table tests it experienced seismic input in excess of 1.0 g (1.13 g during RUN13), the damage level is considered low with the structure maintaining its overall integrity.

Based on the monitoring process, no cracks appeared on the structure at design level (RUN4). The first noticeable cracks appeared during the RUN6 test near the openings of walls 1 and 2 (shown in red in Figure 2.36) (over design level). At the end of the 13-run tests, wall 4 exhibited the most damage in terms of cracking (inner and outer faces) between level 0 and level 1, while on wall 3 cracks emanated from the top corners of the wall openings. Small horizontal surface cracks could be seen in the column near the junctions with the floor slabs and the base plate. Yielding in the monitored rebars was first suspected to occur during RUN10 in the top corners of the openings in walls 1 and 2. There was no evidence of rebar rupture anywhere in the structure and in particular near the wall-foundation interface that is anticipated to first occur at loads exceeding the structural capacity. In order to shed some light on the damage progression, “pseudo” transfer functions were developed between the table and the structure based on the test records. Clearly seen in Figures 2.37 is shifting of the frequencies where the transfer function associated with the first frequency occurs and the reduction of the peak values as the structure experiences damage and exhibits non-linear behaviour (inability to transfer acceleration). Dramatic changes occur during RUN10 (where yielding occurred in rebars accompanied with cracking in all four walls) which result in the lowering of motion transfer capability of the structure in the subsequent and higher intensity seismic tests. Since the initiation of rebar yielding accompanied by concrete cracking in the US practice is associated with the Safe Shutdown Earthquake (SSE) then it may be assumed that the RUN10 earthquake of the SMART2008 test is equivalent to an SSE and therefore it can be concluded that the structure remained intact at 1.5 SSE which in the SMART2008 experiment is represented by RUN13.

One important finding, however, was the appearance of separation gaps between the foundation and the steel plate that mounts the test structure to the top of the shaking table. This may be attributed to the structure-table interaction in which the table top is not acting as a rigid plate but experiences localized deformations along its interface with the structure.

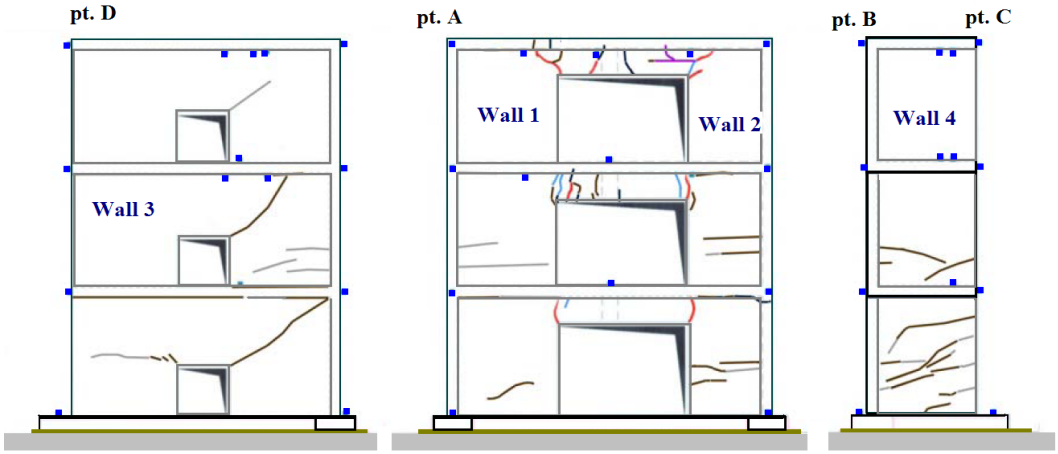

Figure 2-36 Identified cracking patterns at the end of the 13-run shaking table tests on the inside surfaces of the test structure walls

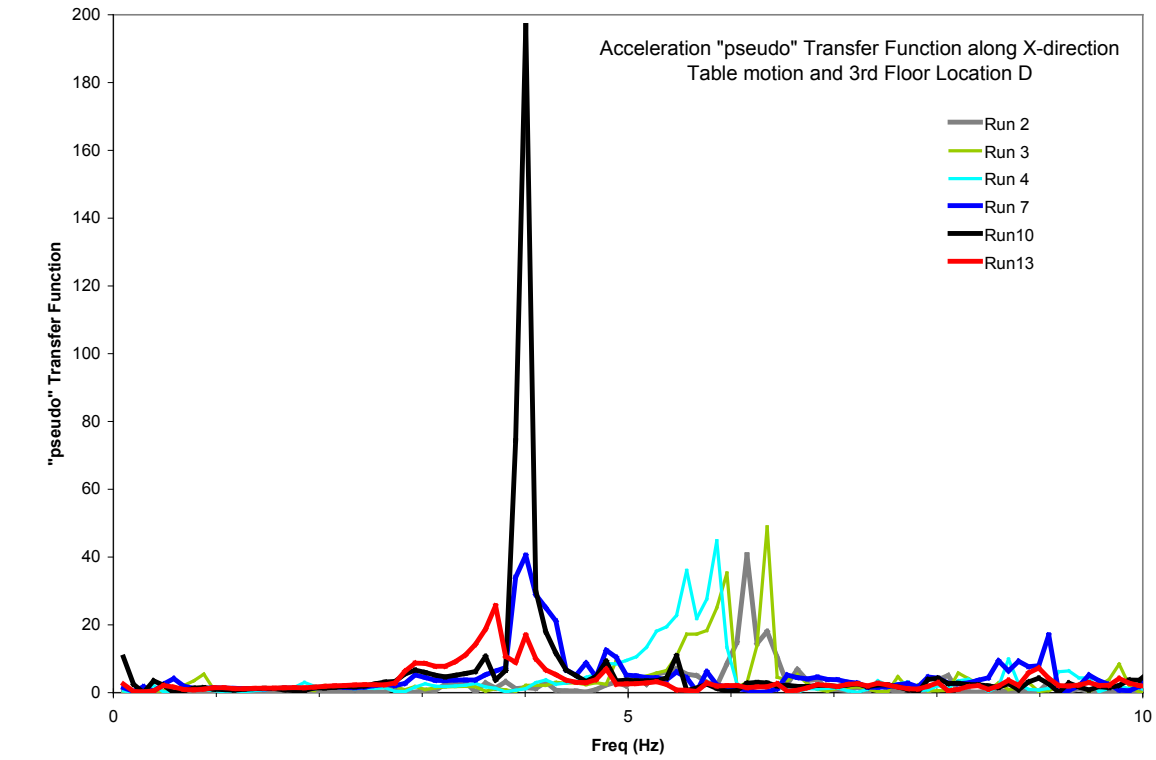

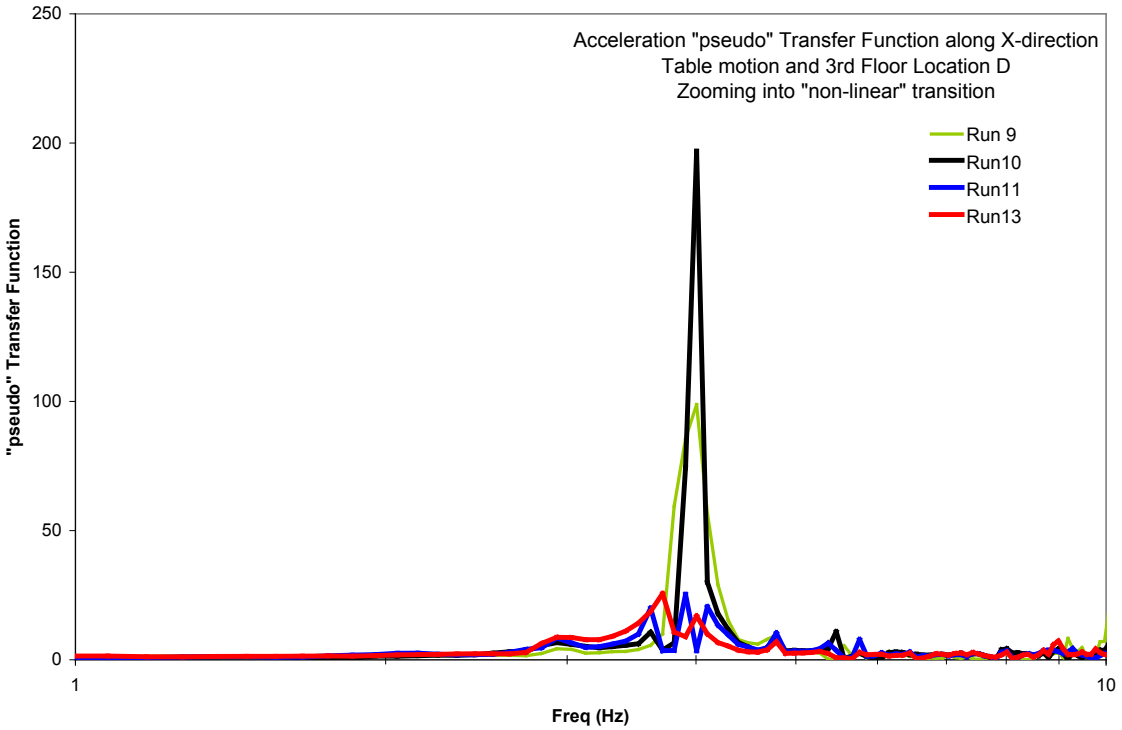

Figure 2-37 "Pseudo" transfer functions between table accelerations and 3rd level of structure identifying transitions to non-linear behaviour Measured damping values

To address the issue of real damping that is exhibited by a reinforced concrete structure during a dynamic event, shaking table test data were used to both quantify and identify the evolution of progressive damage in the structure. As noted previously, between some of the tests low-

intensity white noise excitation was applied to the structure in order to extract information on its actual dynamic properties and in particular eigenfrequencies. It was also noticed during the tests that during some of the runs the structure exhibited a long tail of free vibration. By utilizing information from both the free-vibration portion and/or response to white noise the actual damping of the structure was assessed through (a) the logarithmic decrement and (b) the power bandwidth methods. It is speculated by the authors that the energy absorption characteristics exhibited during the SMART2008 tests is the result of the combined system, reinforced concrete structure and the shaking table as well as the effect of the mounting of the structure on the shaking table.

Figure 2.38 depicts the principle governing the application of the two methods. Figure 2.39 illustrates the free-vibration tail that was observed in the structure during two of the tests (RUN3 and RUN10). As seen in RUN3 the structure exhibits very low damping demonstrated by the long duration free-vibration. On the other hand, after the strong motion part of RUN10 where significant damage to the structure was estimated to have occurred (formation of large, visible cracks and rebar yielding), the free vibration of the structure is quickly damped out indicating overall increased energy absorption of the system prompted by the contribution provided by the extensive, large cracks in the concrete.

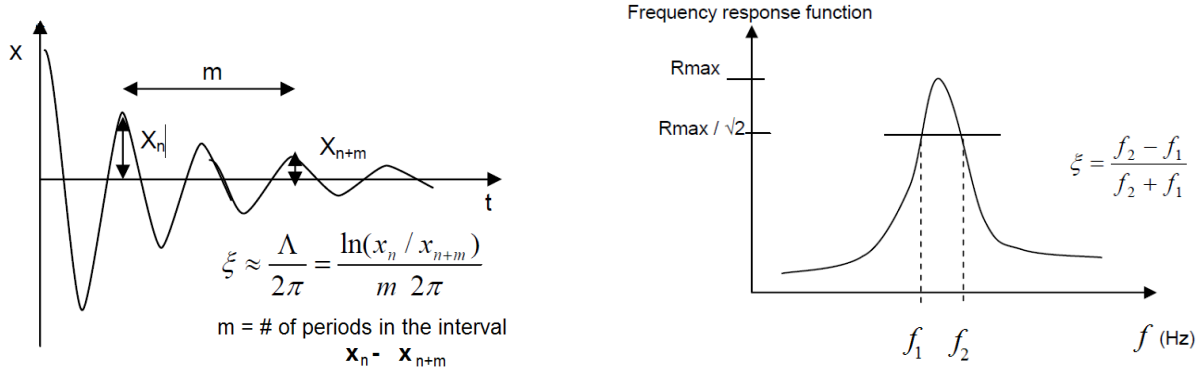

Figure 2-38 Method schematics for estimating actual damping values in the SMART structure from shaking table tests. (a) logarithmic decrement and (b) half-power bandwidth method

Based on the evaluation using the two approaches was assessed that during the low-intensity tests (below the design level of 0.2g) the damping in the overall system (structure and table) was approximately 1%. At RUN5 which was slightly over the design level the damping ratio increased to ~2% and gradually reached levels of 7% above Run 11.

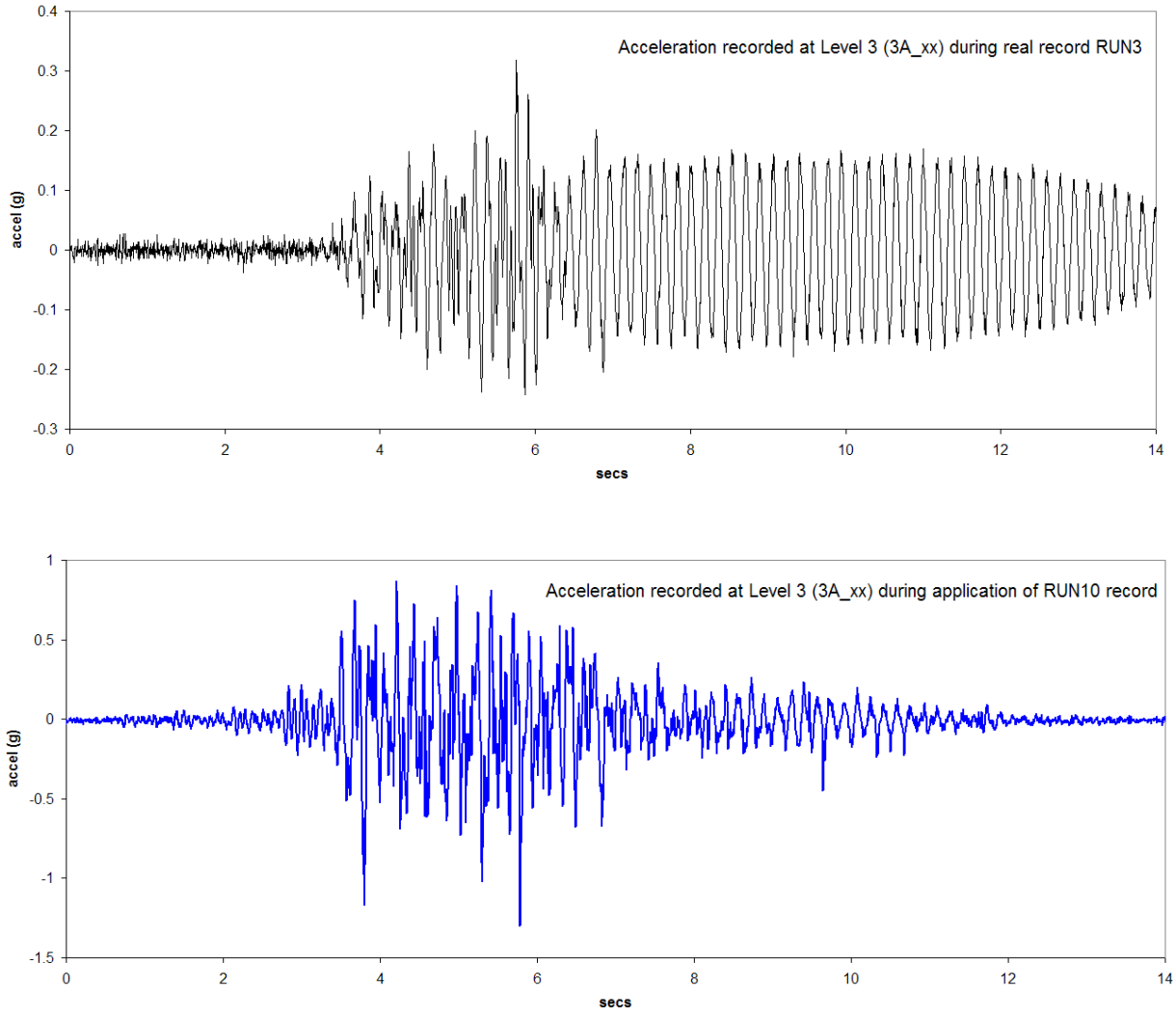

Figure 2-39 Free-vibration characteristics of structure during different tests Global Behaviour of the Structure

The SMART2008 structure was designed to accentuate the 3-D effects during multi-directional seismic inputs and in particular to assess torsion in reinforced concrete structures. As a result the trapezoidal structure had its mass and torsion centres far apart with the torsion centre located closest to the stiffest corner of the structure (point A) as shown in Figure 2.40. Based on recorded absolute displacements the trend of the general motion of the structure can be deduced. Shown in Figure 2.40 is a plot of the movement of each of the four corner points of the structure at the 3rd level. The displacement of each corner shown has been amplified by a factor of 50. The displacement trend of each corner depicted in Figure 2.40 confirms the global rotational character of the structure with respect to the rotational axis shown. Corner A being the closest to the axis exhibits the smallest movement while extremities C and D the largest.

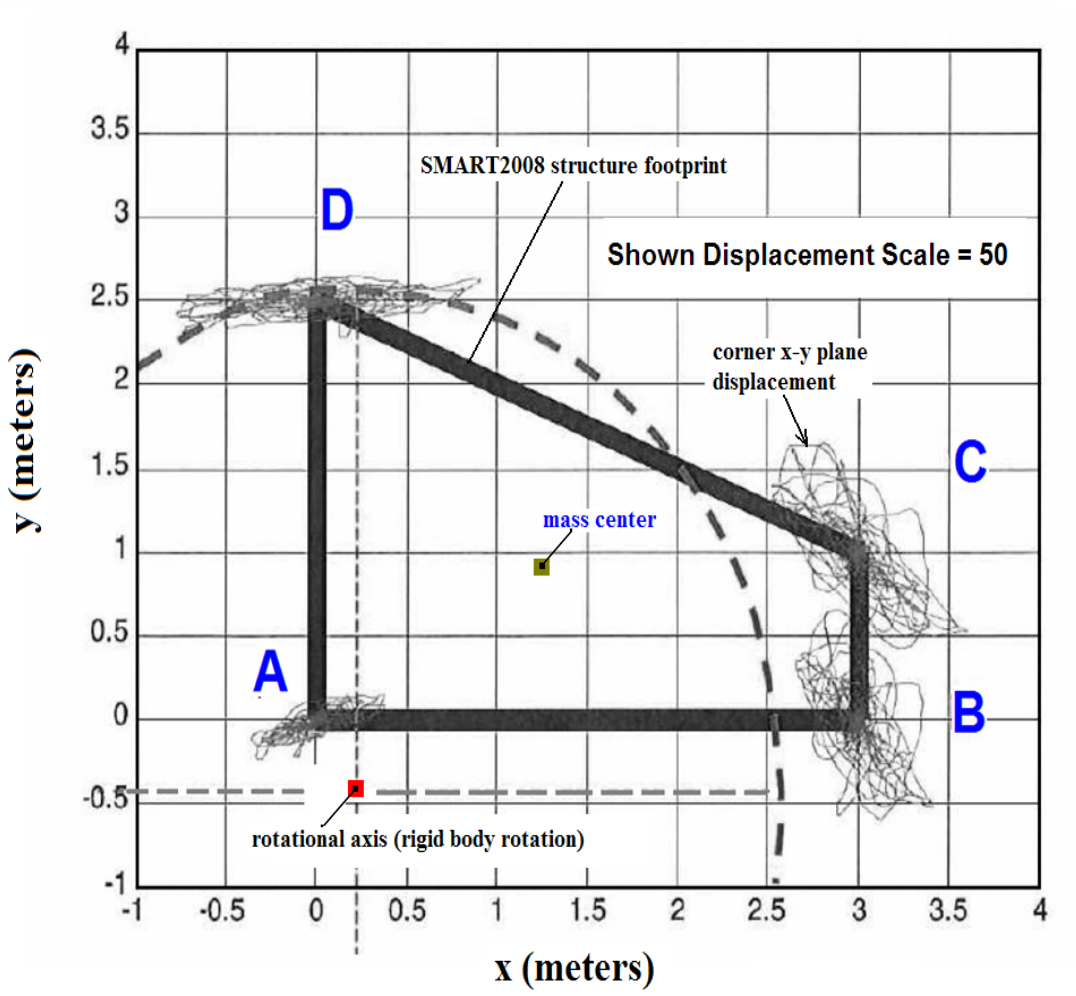

Figure 2-40 **Identification of rotational behaviour of the test structure based on the displacement patterns recorded at the corners of the 3rd level**

3. NUMERICAL ANALYSES AND TEST PREDICTIONS

The SMART2008 benchmark also included a series of numerical analyses in order to (a) assess design practices around the world and the use of analysis methods in nuclear structure design and (b) use the shaking table tests as the basis for assessing the capabilities of the different methods in predicting the response of reinforced concrete structures under multi-directional seismic inputs.

The numerical part of the benchmark consisted of two distinct phases. Phase 1 which is described in this chapter had the following objectives:

- Assessment of conventional design methods and structural dynamic analyses including floor response spectra generation
- Comparison of best-estimate methods in predicting the response of structures which will be allowed to enter the non-linear regime and the generation of corresponding "non-linear" floor response spectra

Phase 2 which is described in detail in Chapter 4 and was initiated following the completion of the actual shaking table tests and the corresponding analyses, aimed at (a) quantifying the variability in structural response resulting from uncertainties in structural properties and (b) generating fragility curves for structural vulnerability.

Phase 1 was divided into two parts namely Phase 1a and Phase 1b. Phase 1a was termed the "blind-prediction" phase where conventional and best-estimate analyses were performed to assess (a) the ability to analyze 3-D structures with non-linear behaviour using methodologies from conventional practice (which include equivalent static analysis, response spectra analysis, linear dynamic analysis, non-linear static or pushover analysis and non-linear time history analysis) and (b) the ability of an adopted best-estimate methodology using basic material and geometry information to predict the non-linear response of a structure resulting from a controlled test such as the shaking table test on the SMART structure. Phase 1a was conducted prior to any shaking table tests. The key objective of Phase 1a was to assess the variability that exists between methodologies and modelling/analysis techniques that are currently in use within the nuclear sector.

Phase 1b represented the "best-estimate" analysis where specific information regarding the shaking table test set-up, the as-built structure and the actual excitations were available. Specifically, information on:

- The actual experimental set-up of the shaking table tests including the mass of the structure, the added loads and their distribution as well as interface conditions between the structure and the table

- Concrete and reinforcing steel properties of the as-built test structure which was deduced during construction

- The estimated initial frequency of the test structure on the shaking table and damping ratio prior to performing any of the 13 tests in an effort to fill the information gap on the dynamic properties of the table itself and the structure-table interaction

- Actual seismic input accelerations observed at the table top surface and the foundation level for the initial tests (actual table accelerations differed significantly from the intended excitation derived from scaling the design response spectrum)

- Selected structural response results for the lowest seismic input (RUN1) and the design level (RUN4)

BNL participated and contributed the results of its independent studies to all phases of the benchmark listed above. Results of Phase 1a (pre-test conventional analyses) generated by the BNL studies are included in the referenced documents and not included in the body of this report. This is because the objective of Phase 1a was to primarily obtain a correlated trend between all the participating teams and the adopted methodologies and not to quantify the ability of predicting the SMART shaking table test results. This overall assessment is summarized in the summary and conclusions section. In this chapter, the results of the Phase 1b or "best-estimate" prediction analysis will be presented and compared with the corresponding shaking table test results which became available after the completion of Phase 1b and the submission of the independent results to the SMART2008 project.

3.1. Structural Model

Various numerical representations of the SMART structure were developed and used in the various phases of the SMART benchmark. These were based on a three-dimensional description of the structure very close to the actual geometry. In addition to the structure, the foundation, the base plate mounting to the table, and the table itself were modelled and integrated. In addition, the added masses were introduced in the form of solid blocks as they were described in the initial phases of the study (prior to the construction of the test structure and the final configuration of the masses).

Following the design drawings on reinforcing steel rebar layout, the steel rebars were discretely modelled into the structure. The concrete walls, floor slabs and foundation were represented by solid elements, as well as the beams, the column and steel plates.

The shaking table was modelled as a rigid block. However, sensitivity analyses were performed to observe the effect of its stiffness on the structural response. Shown in Figure 3.1 and 3.2 are global representations of the numerical model and modelling of local elements respectively.

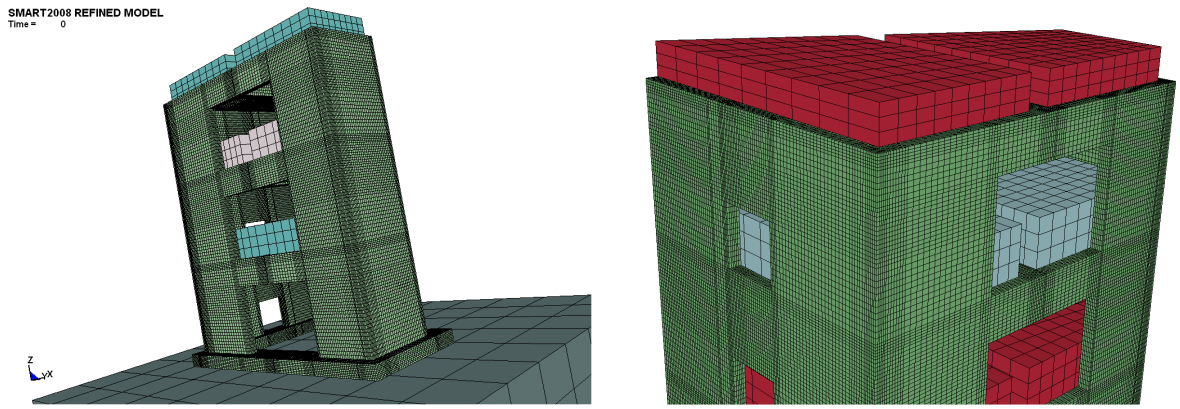

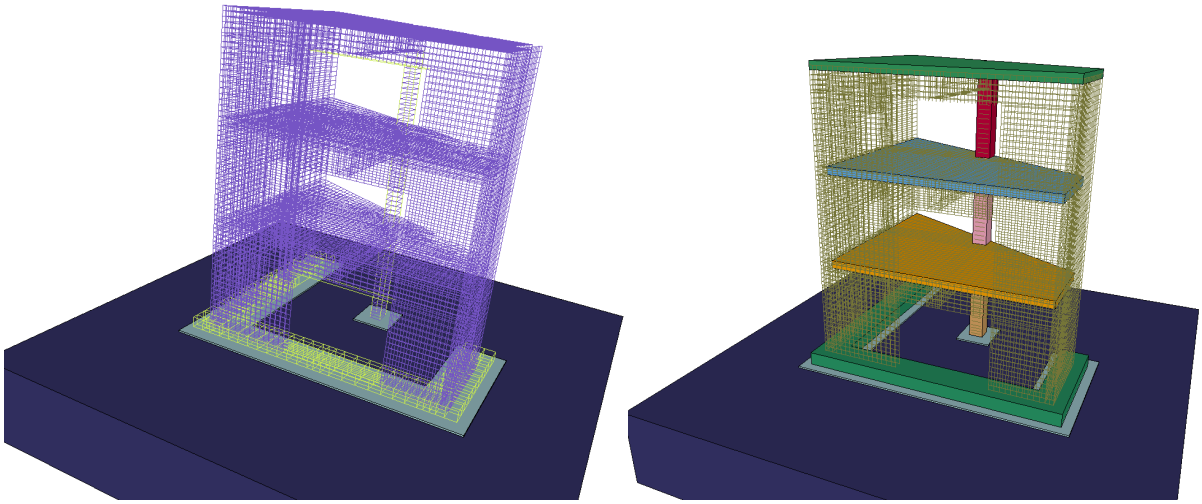

Figure 3-1 Numerical models used in the numerical analysis of the SMART structure

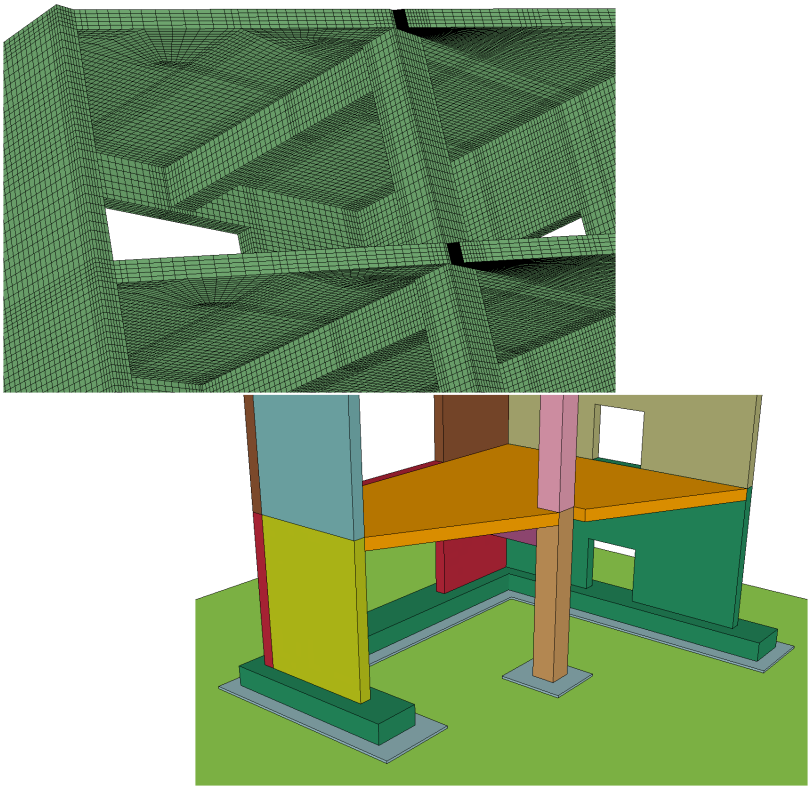

Figure 3-2 Numerical representation of structural details of the SMART structure

The SMART structure was discretized into finite elements in a way that allowed for the distribution and position of rebars using the capabilities of the TrueGrid software. That resulted in a very large numerical model which was computationally expensive (~400,000 elements in total were making up the numerical model). This model was used in Phase 1a of the benchmark which encompassed linear-static, non-linear static and modal analyses.

For the transient analyses, the discretization was “optimized” by combining some of the reinforcing bars and allowing for a smaller number of finite elements in the concrete. The optimization was done on the basis of equivalent dynamic properties (i.e., maintaining the eigenfrequencies of the structure). This resulted in a smaller numerical representation

(~260,000 finite elements total) which reduced the computational time significantly. Typical computational time for a non-linear analysis using the strong motion of the acceleration records was approximately 60 hours on a dedicated 8-CPU micro-station.

The structure was firmly connected to the top of the shaking table via the base plate. No local interaction (i.e., separation of the plate from the table between the mounting screws was allowed).

Because of the uncertainties regarding the shaking table dynamic properties and supports, different options, were explored. For the equivalent static analyses and Phase 1a dynamic analyses, the table was assumed rigid and was restricted for both cases from vertical movement. For the push-over equivalent static analyses, the table was considered fixed in all degrees of freedom. Following some additional information regarding the stiffness of the vertical jacks and eigenfrequency values for the actual SMART structure tested on the table, vertical and horizontal springs were introduced to support the rigid shaking table. This last configuration was used in the "best-estimate" response prediction phase (Phase 1b).

Input accelerations for the prediction phase were introduced at the interface of the horizontal springs (actuators) with the shaking table which was approximately at mid-height of the modelled table. The 25 ton mass of the table which is less uncertain as a parameter was introduced in the modelling of the table.

The analyses (static, modal and non-linear time history) were performed using the capabilities of the LS-DYNA finite element code.

3.2. Description of the Constitutive Relations

To perform the non-linear dynamic analyses required and to enable the capturing of the progressive damage in the concrete or the yielding or failure in the rebar, constitutive relations that are appropriate for such non-linear analysis were adopted for the concrete and the steel.

For the concrete, the constitutive relations implemented into the Winfrith Concrete Element of the LS-DYNA material library were primarily used. The volumetric compaction and yield surface for this material that are numerically implemented into the software are shown in Figure 3.3. In particular, the analysis allowed for strain rate effects in the concrete and the dissipation of energy (fracture energy) in crack opening. Cracking is formed upon exceeding the tensile (splitting) strength but was allowed to close during the shaking. Parameters such as the fracture energy of concrete are significant and they influence the generation and distribution of cracking thus causing the weakening of the structure. Also influential are concrete parameters such as aggregate size and current state of tensile and compressive strengths. Damage in this material is viewed as material cracking or crushing and its inability to carry load. By allowing for some load-carrying capability the material can be pushed beyond the uni-axial strength values. When certain thresholds are reached where the material is incapable of satisfying a combination of requirements, the material can erode from the matrix. An important parameter in establishing damage in the concrete is the fracture energy, a property that was not available for the concrete used in the SMART structure. As a result, fracture energies of 110 J-m were used for all the numerical studies. Sensitivity studies for fracture energies reaching 330 J-m were performed.

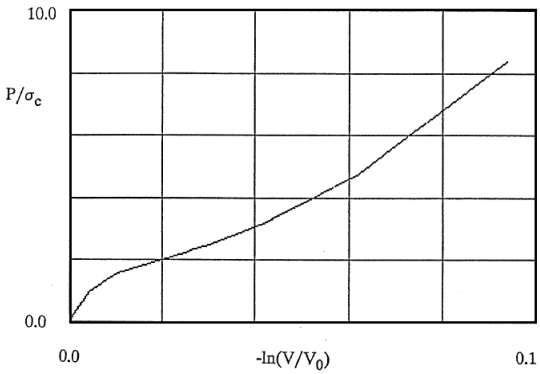

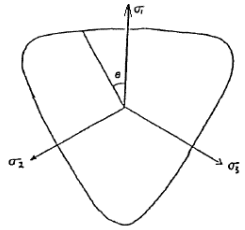

Deviatoric Section

$$\frac{A S_2}{\sigma_c^2} + \lambda\frac{\sqrt{S_2}}{\sigma_c} + B\frac{J_1}{\sigma_c} - 1 = 0$$

where $\lambda = K_1 \cos\left[\frac{1}{3}\cos^{-1}(K_2 \cos 3\theta)\right]$ for $\cos 3\theta \geq 0$

$\lambda = K_1 \cos\left[\frac{\pi}{3} - \frac{1}{3}\cos^{-1}(-K_2 \cos 3\theta)\right]$ for $\cos 3\theta \leq 0$

$\cos 3\theta = \frac{3\sqrt{3}}{2}\frac{S_3}{S_2^{1.5}}$

and A, B, K_1, K_2 are functions of $\frac{\sigma_3}{\sigma_c}$

Figure 3-3 Constitutive relations governing the Winfrith concrete element mode used in the SMART benchmark analyses

To address the progressive damage in the concrete which results in reductions of its capacity from micro-cracking, other constitutive relations were explored. An alternative concrete material model based on the research work of Holmquist, Johnson and Cook [A Computational Constitutive Model for Concrete Subjected to Large Strains and High Pressures, 14th International Symposium on Ballistics, Quebec, 1993] that is also part of the LS-DYNA library was studied and compared with the Winfrith counterpart. The constitutive and damage relations are shown in Figure 3.4. The material is formulated around an equivalent strength model, an accumulated damage model and an equation of state. Key features of this model are: (a) the accumulated damage and (b) the equation of state. In particular, the equation of state describes the relation between hydrostatic pressure and volume. The material in the impact zone is assumed to behave like a compressible fluid. The tensile pressure allowed is defined on the basis of the accumulated damage according to the relation $T^{new} = T \bullet (1\text{-}D)$, where D is the damage (shown in Figure 3.4b) and which reflects both the equivalent plastic strain and plastic volumetric strain, and T is the tensile strength.

The comparison of the two concrete constitutive and damage models is shown in Figure 3.5. The structural accelerations shown were derived by subjecting the SMART structure to the same sequence of synthetic earthquakes and implementing the different constitutive relations in the concrete.

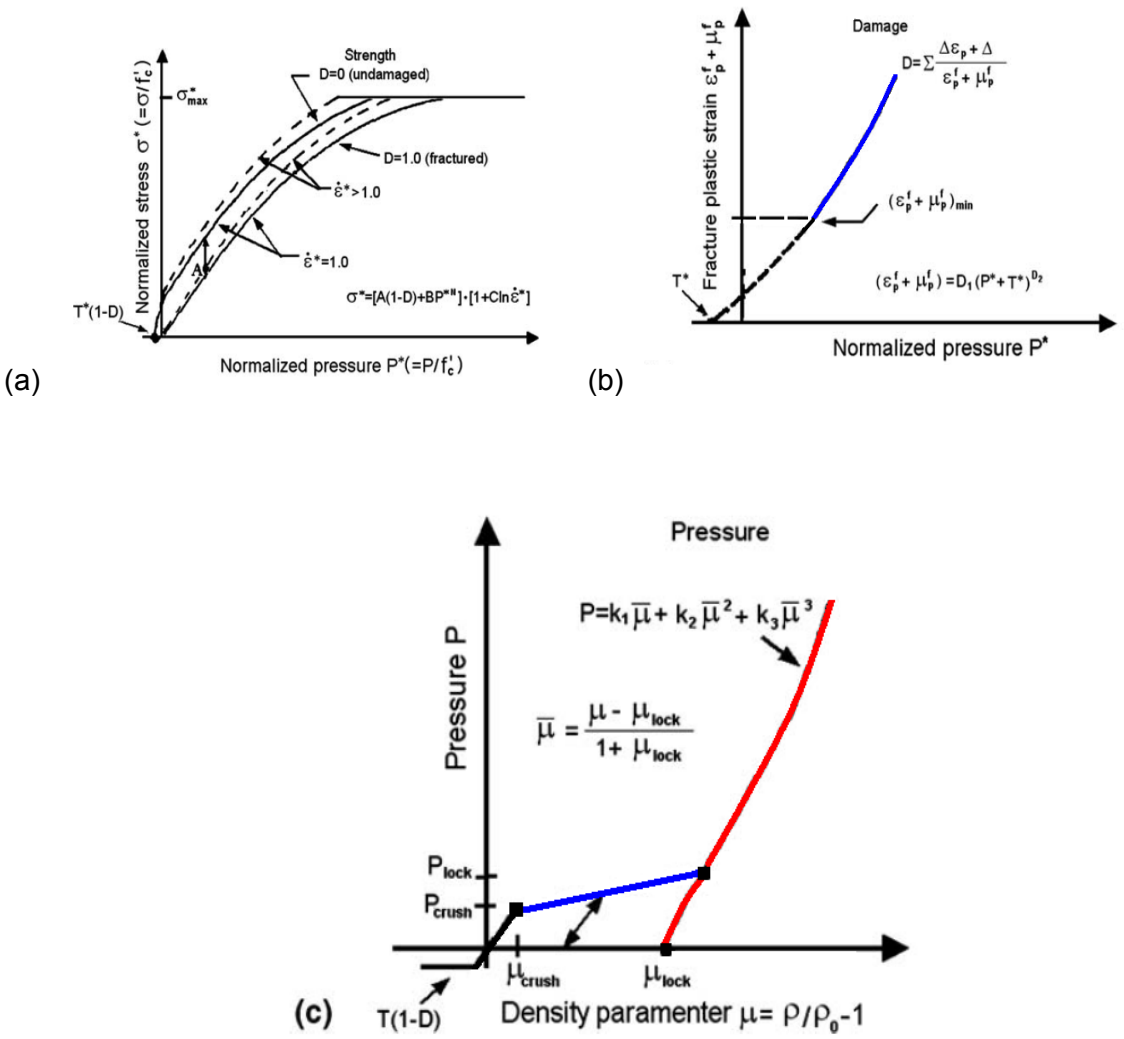

Figure 3-4 Holmquist-Johnson-Cook concrete material model

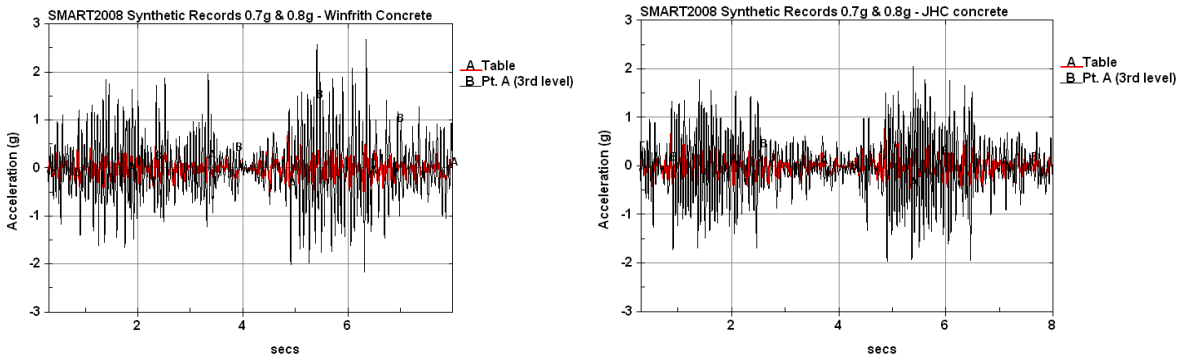

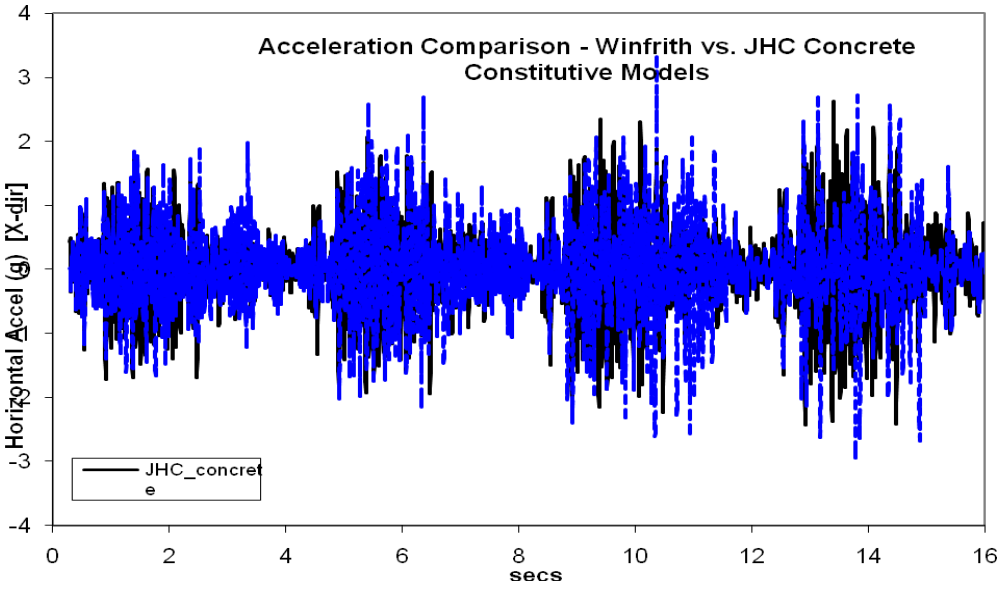

Figure 3-5 Comparison of the two concrete constitutive models in terms of the SMART structure response to synthetic accelerograms

The reinforcing steel was described using a bi-linear stress-strain model. Shown in Figure 3.6 are actual rebar stress-strain test results provided by the SMART benchmark organizers and the adopted equivalent stress strain relation.

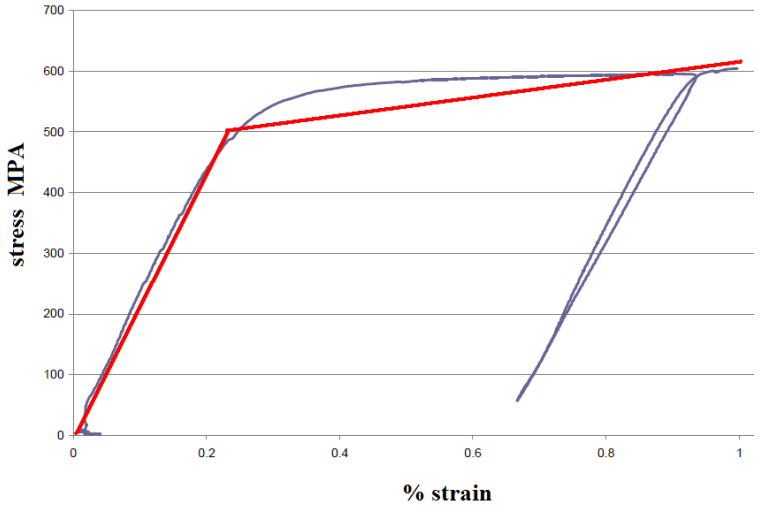

Figure 3-6 Stress-strain relation of steel used in the analysis

3.3. Shaking Table Test Predictions

Following the fabrication of the SMART specimen, the organizers provided test-specific information and actual material properties including:

- experimental set-up of the shaking table tests including the mass of the structure and final distribution of added loads
- Concrete and reinforcing steel properties of the as-built test structure which was deduced during construction

- estimated initial frequency of the test structure on the shaking table and damping ratio prior to performing any of the 13 tests

- actual seismic input accelerations observed at the table top surface and the foundation level for the initial tests

- selected structural response results for the lowest seismic input (RUN1) and the design level (RUN4)

The finite element model and its properties were re-adjusted to reflect the as-built properties and the non-linear time history analysis of the 13-run. As was described in Chapter 2, actual concrete cylinder tests on the structure concrete casts revealed a significant deviation from the nominal concrete modulus of 32,000 MPa used in the studies prior to the test. Table 2.1 which is repeated below is indicative of the variation.

Table 2.1 (Reproduced) concrete properties of as-built SMART structure.

	E tangent (MPa)	E secant (MPa)
Foundation	31 500	30 000
Walls and column 1st level	30 500	29 000
Slab and beam 1st level	29 000	26 500
Walls and column 2nd level	26 500	25 000
Slab and beam 2nd level	31 500	30 000
Walls and column 3rd level	33 500	30 000
Slab and beam 3rd level	29 500	28 000

Based on the updated material properties, the updated concrete density, and the initial eigenfrequencies of the combined system (structure plus shaking table), the modal properties of the combined system used at the start of the prediction analysis were re-assessed. Figure 3.7 depicts the first three modes of the combined table/structure exhibited by the numerical model prior to the application of seismic loads. The values of the eigenfrequencies are similar to those observed by the white noise test (7.0, 9.0 and 16.0 Hz, respectively).

In order to capture the progression of damage, the thirteen bi-directional records were applied in sequence and in a way that the information is transferred between tests. Due to the computational burden, only the strong motion portion of the provided accelerograms were used. Figure 3.8 depicts the locations and orientations where test and prediction data are compared. As in the actual test, the real earthquake records were applied first. Special attention was paid in the response of the structure to RUN3 input which is both a real earthquake record and has a PGA close to the design level. Further, as seen from the actual experimental response, the structure exhibited free-vibration that lasted very long and thus it was crucial that the prediction model was capable of replicating this interesting behaviour.

Figure 3.9 depicts acceleration time histories on three corners of the structure. As is clearly shown, the numerical model also predicts the same long-lasting free vibration while it also matches the peak acceleration values recorded during the test. It can also be observed that there exists a “structure” in the free vibration transient predicted by the numerical model attributed to the shaking table contribution for which all its dynamic properties are not available. This is more evident in the comparison of the response spectra shown in Figure 3.10 for both horizontal directions.

Comparison of relative displacements in the structure, depicted in Figures 3.11 and 3.12, reveal that the displacement range is well replicated (please note the offset of the horizontal axis in the recorded data). Examination of the recorded and predicted strains in a rebar of wall 4 shown in Figure 3.13 reveals that the simulation model is capable of capturing the strain in the rebars and that both (test and prediction) show that it is the whole structure and not the top section that undergoes free vibration with very little damping in the system.

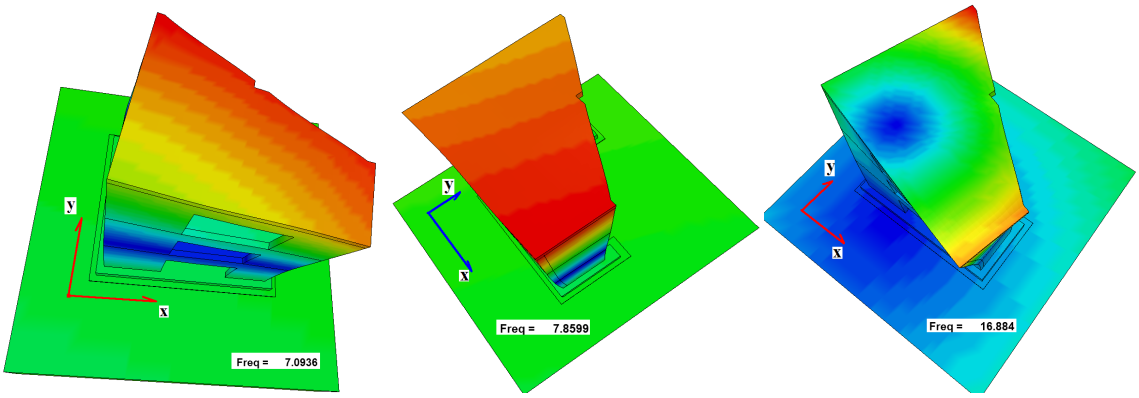

Figure 3-7 **Eigenfrequencies and modes of the final 3-D model used in the numerical predictions of the SMART2008 tests**

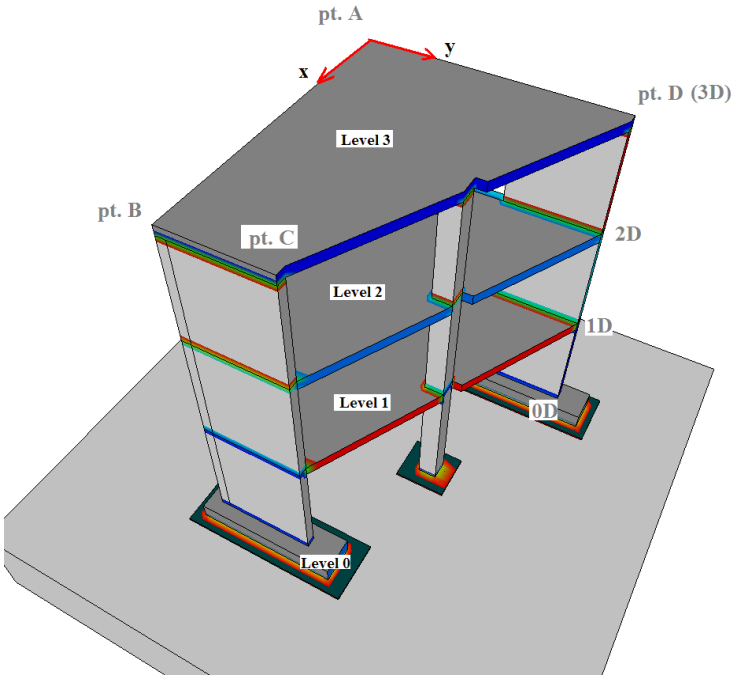

Figure 3-8 **Locations on the structure used for comparison of predictions with test data**

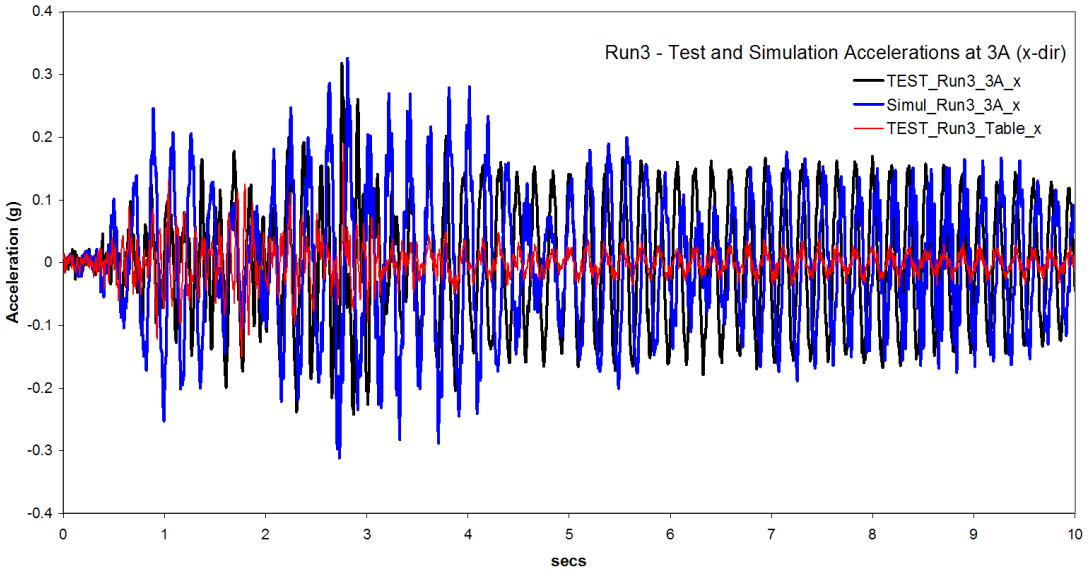

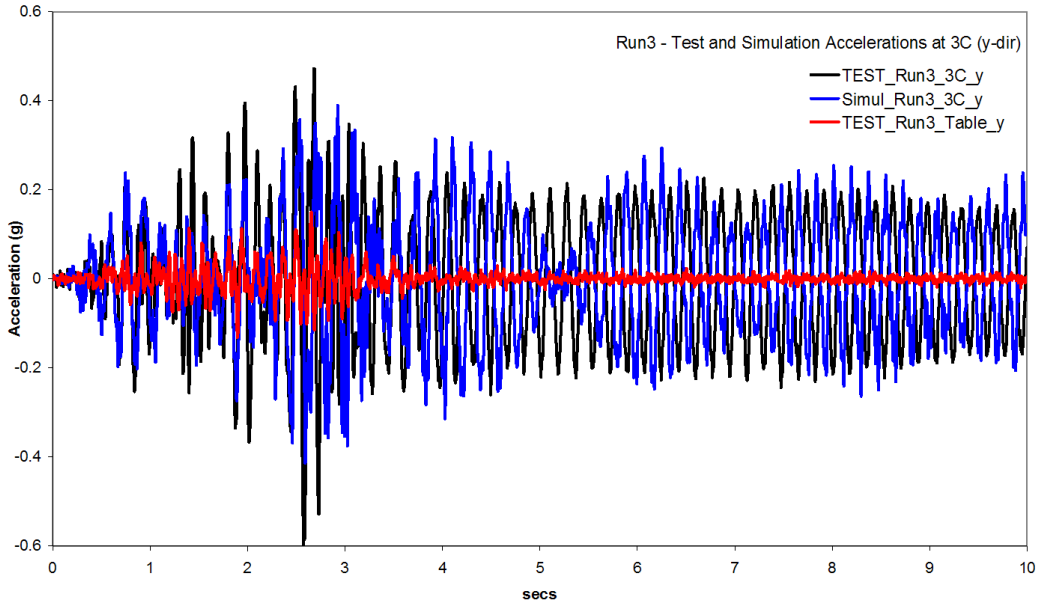

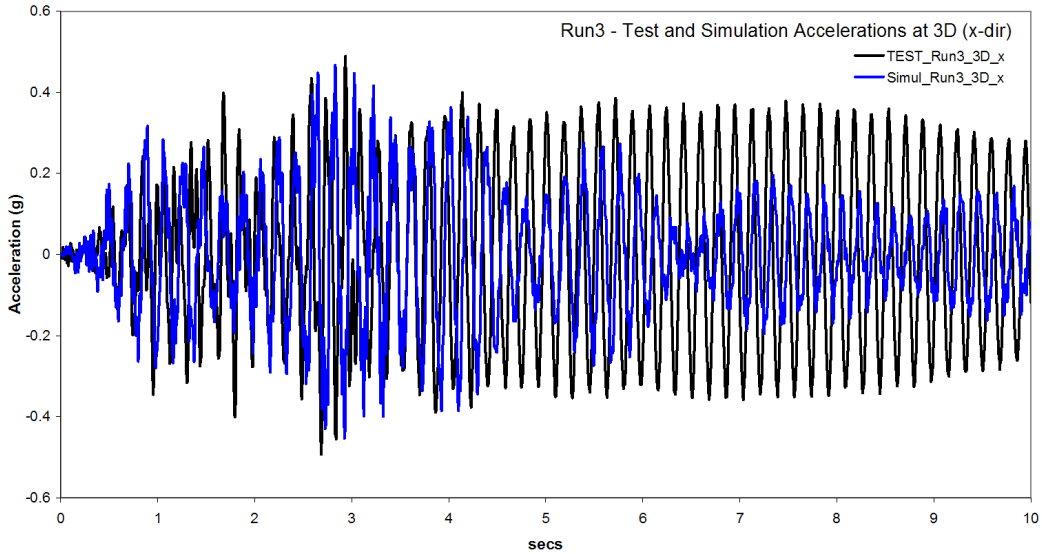

Figure 3-9 Comparison of horizontal accelerations at the corner locations of the 3rd level between recorded test data and prediction from the BNL simulation for RUN3

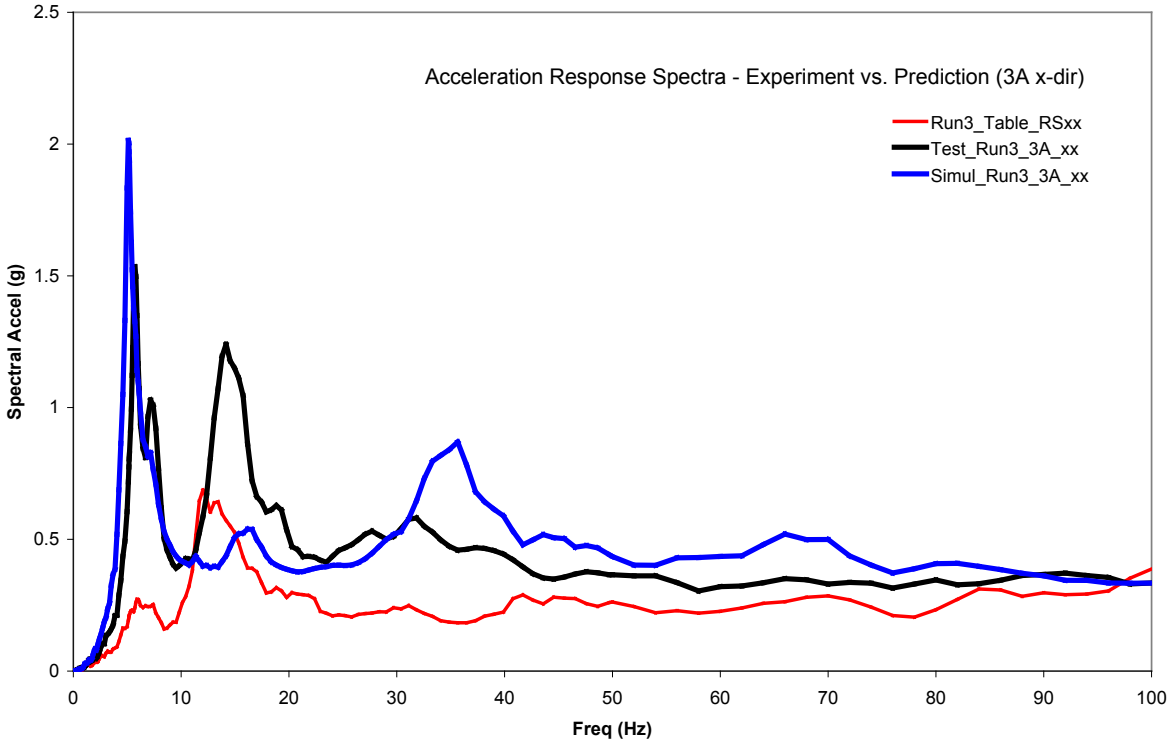

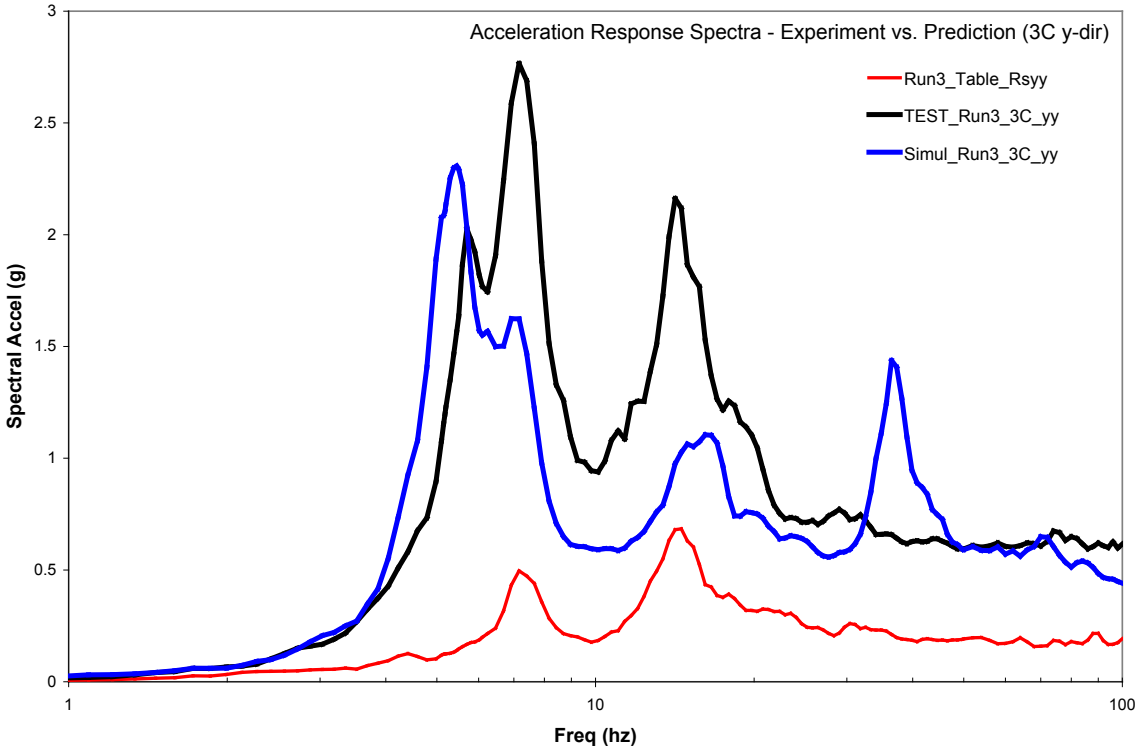

Figure 3-10 Comparison of horizontal acceleration response spectra between recorded data and predictions from BNL simulation for the real earthquake RUN3

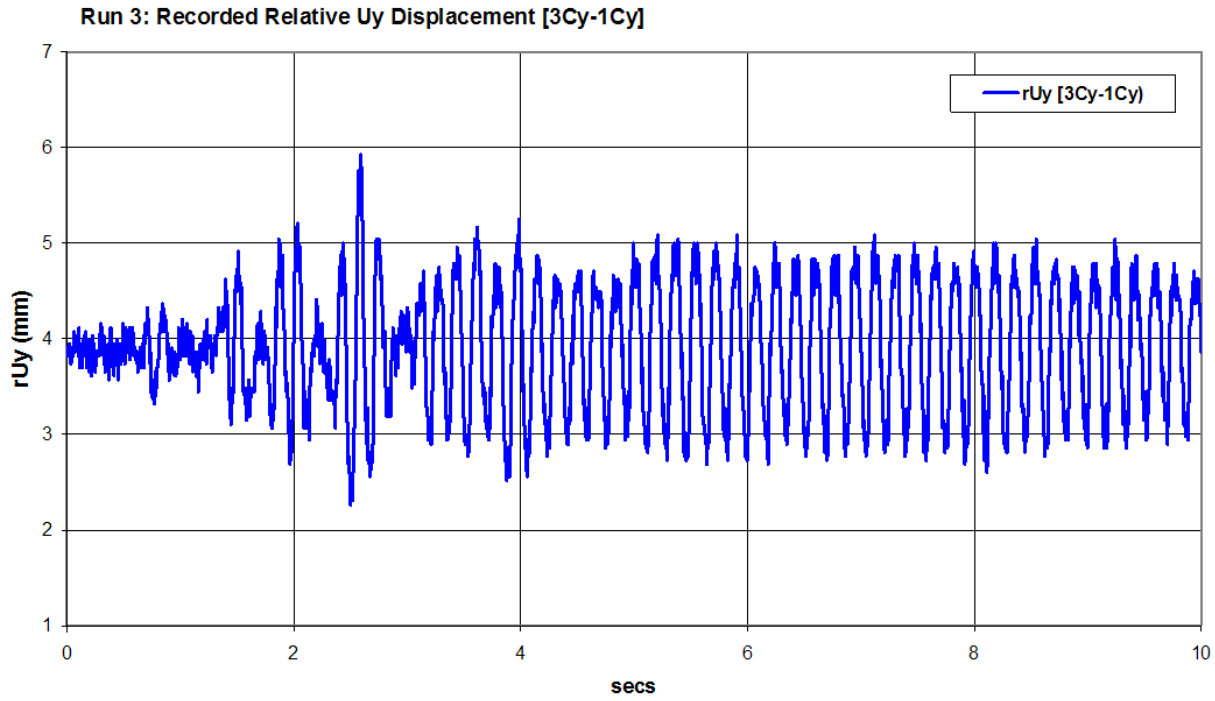

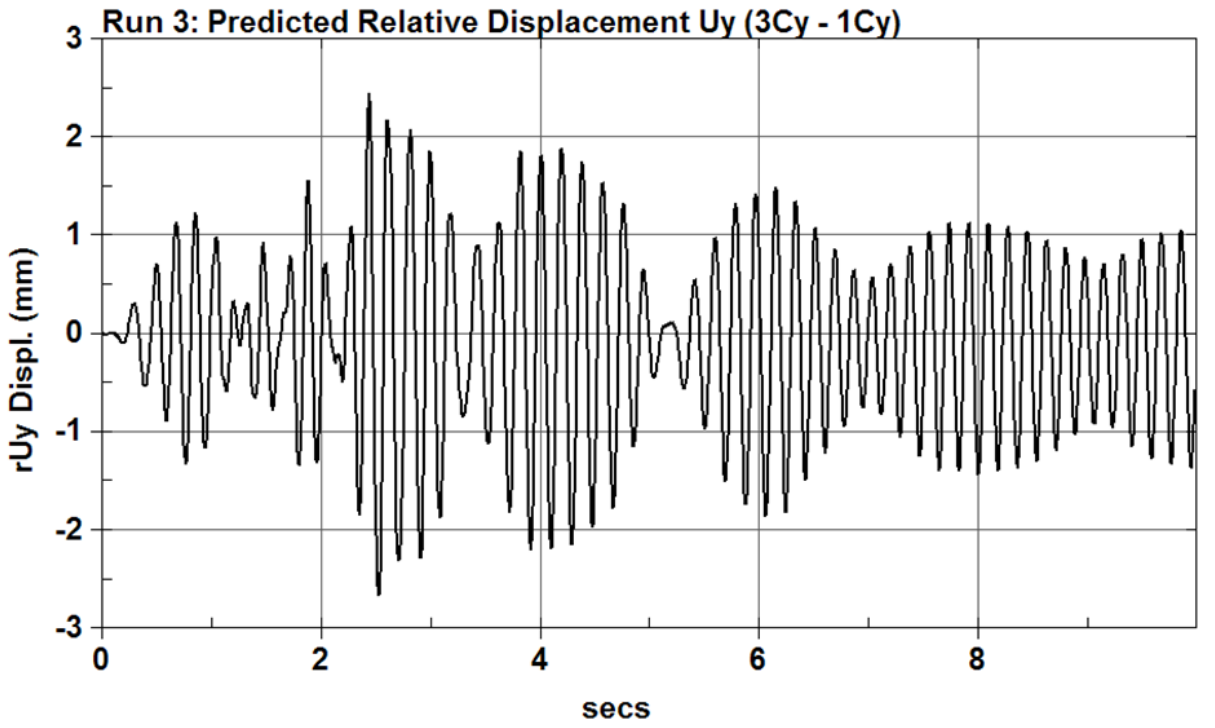

Figure 3-11 **Comparison of horizontal relative displacement Uy at location C between recorded data and predictions from BNL simulation for the real earthquake RUN3 (note the offsetting of the recorded data in the y-axis)**

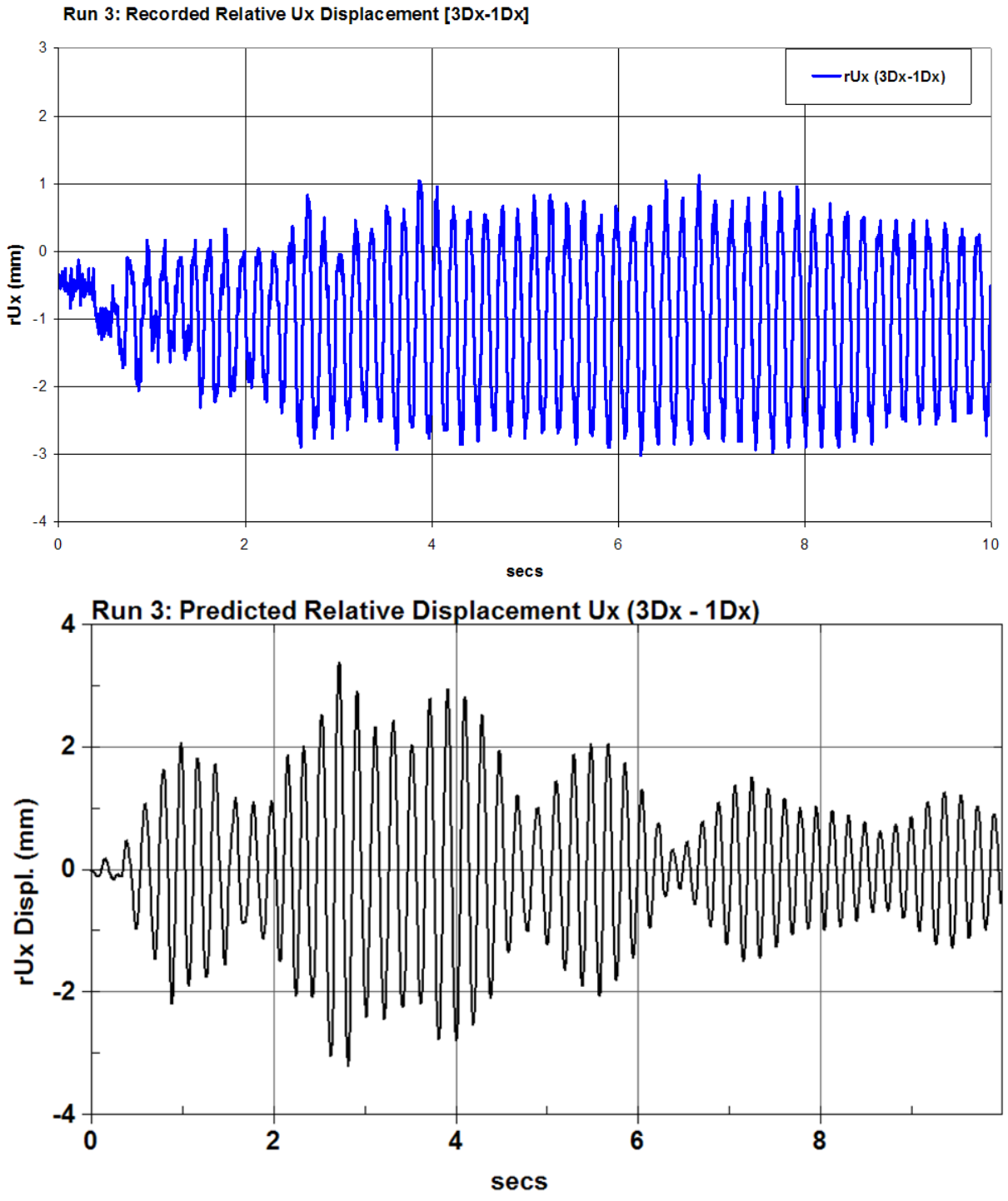

Figure 3-12 Comparison of horizontal relative displacement Ux at location D between recorded data and predictions from BNL simulation for the real earthquake RUN3

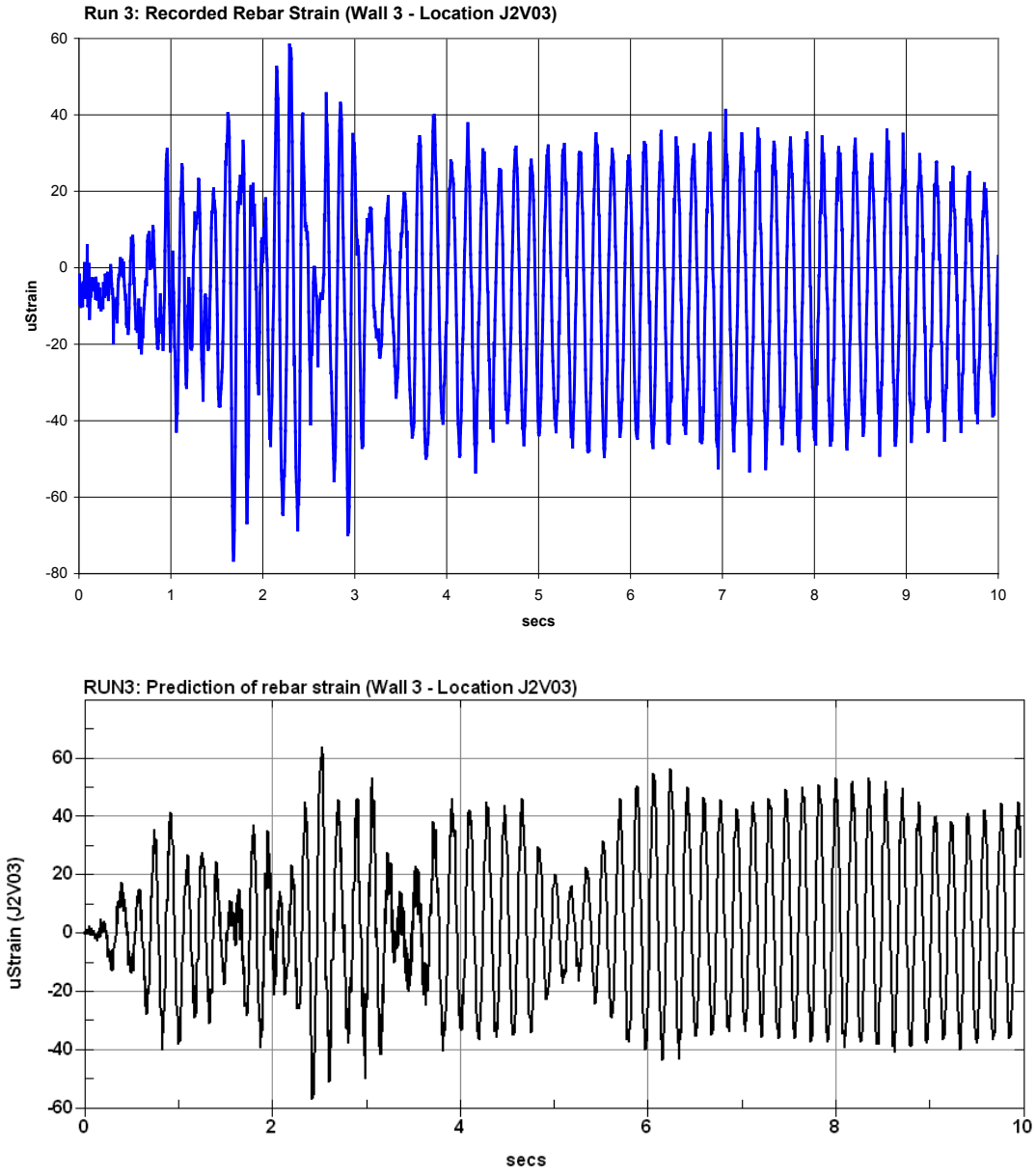

Figure 3-13 Comparison of rebar strain on Wall 3 between recorded data and predictions from BNL simulation for the real earthquake RUN3

Comparison of results for the RUN4 (design level) earthquake input

The first synthetic earthquake applied to the structure was the design level earthquake (RUN4). The analysis continued using the initial damping of 1% and completed 7 seconds of excitation. Similarly as in RUN3, response data of acceleration, relative displacement, and rebar strain in the four walls were post-processed. In addition, the appearance of cracks was monitored throughout the RUN4 simulation.

Figure 3.14 depicts the comparison of acceleration in the two horizontal directions at locations C (y-direction) and D (x-direction) at the 3rd level. While the acceleration at D is slightly underestimated, the acceleration in location C is well reproduced. As in RUN3 it is suspected that the table is playing a role as can be seen in the floor response spectra comparison shown in Figure 3.15.

Rebar strain comparison is shown in Figures 3.16-17 and relative displacements in Figure 3.18. From the strain comparison in Figure 3.17 it is concluded that the simulation is able to predict the permanent deformation or slight adjustment experienced at wall #4.

Consistent with post-test observations, the simulation showed no cracks in the concrete at the end of RUN4.

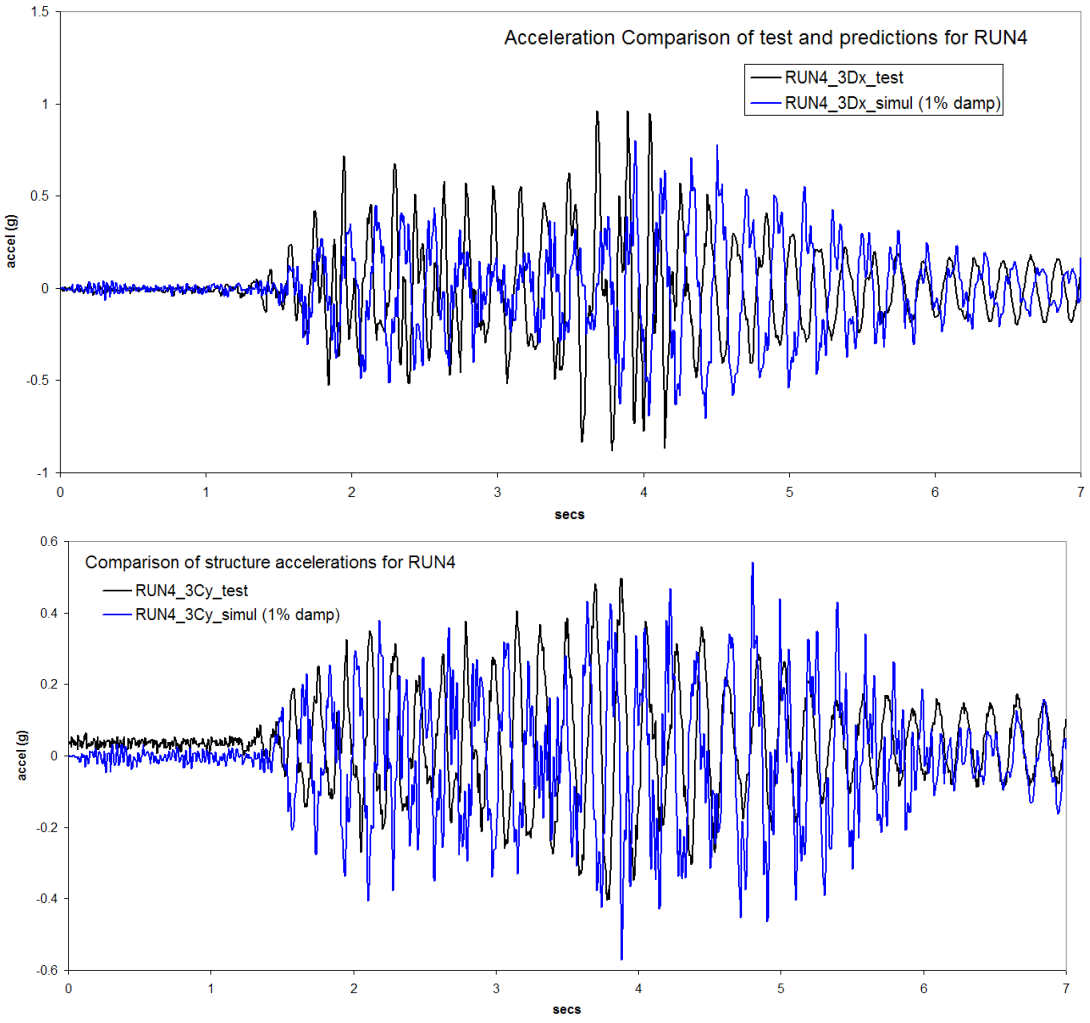

Figure 3-14 Comparison of structure accelerations for the design earthquake level (RUN4) between the experiment and the BNL simulation

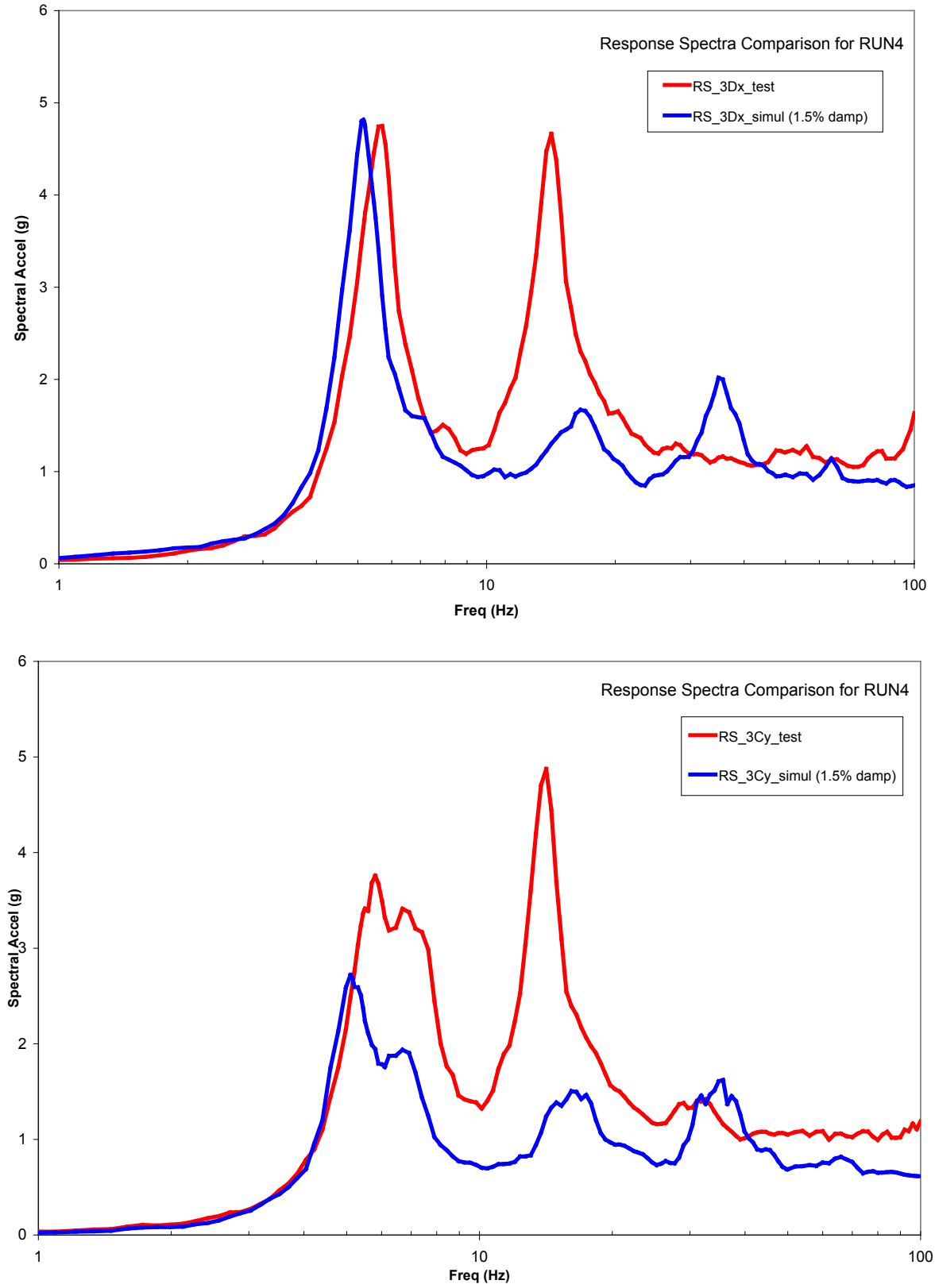

Figure 3-15 Comparison of floor response spectra for the design earthquake level (RUN4) between the experiment and the BNL simulation

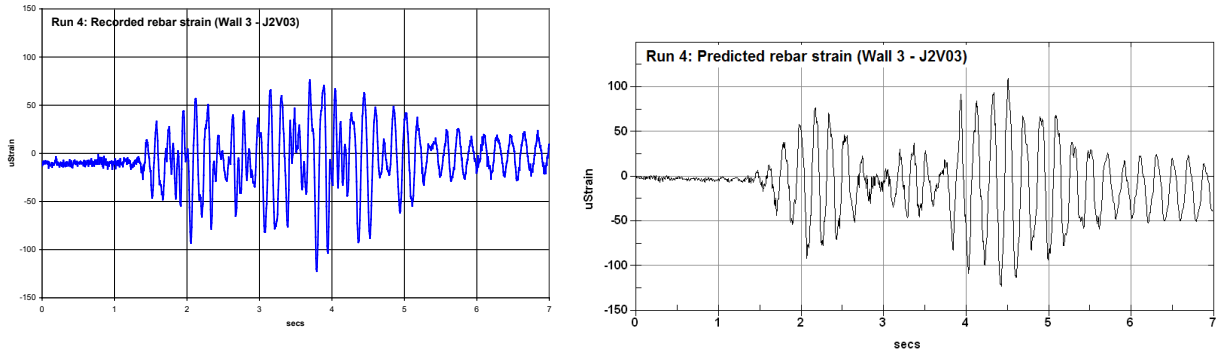

Figure 3-16 Comparison rebar strain in wall 3 for the design earthquake level (RUN4) between the experiment and the BNL simulation

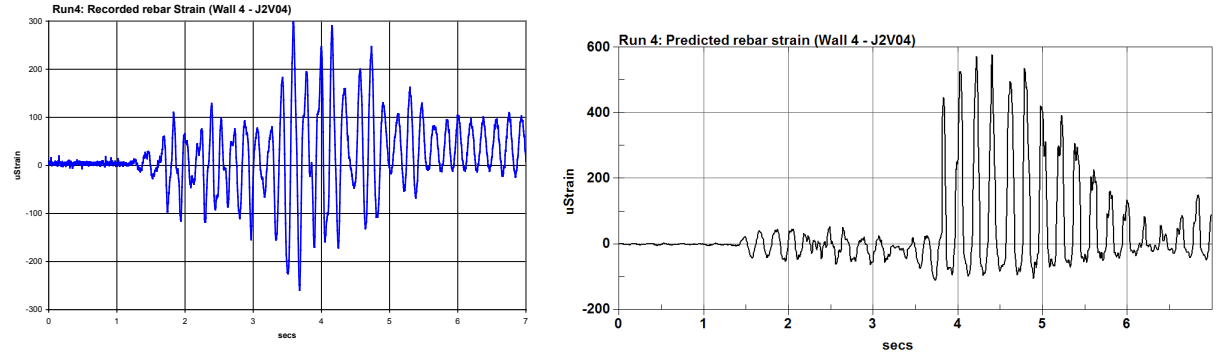

(a) (b)

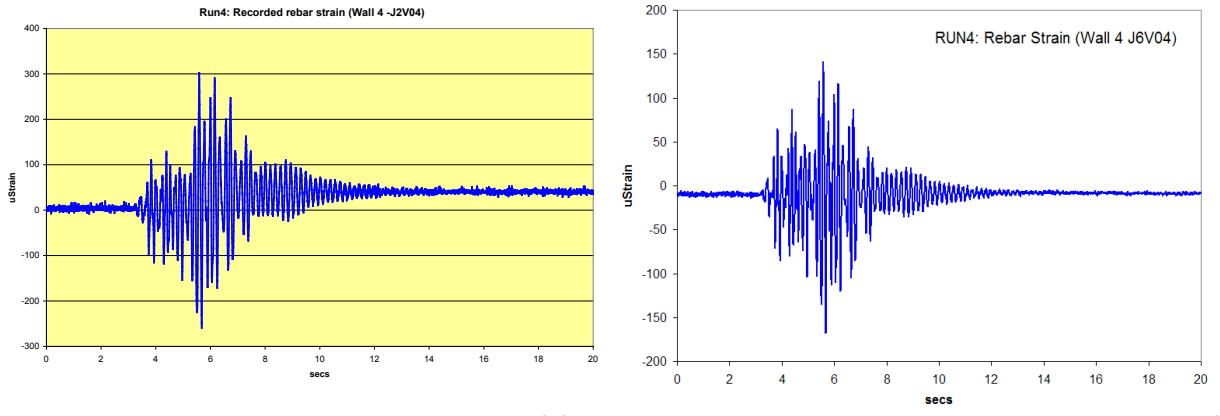

(c) (d)

Figure 3-17 Comparison of rebar strain in wall 4 for the design earthquake level(RUN4) between the experiment and the BNL simulation. Shown in (c) is the recorded strain in expanded scale depicting the "re-adjustment" or permanent deformation in the rebar at the selected location.

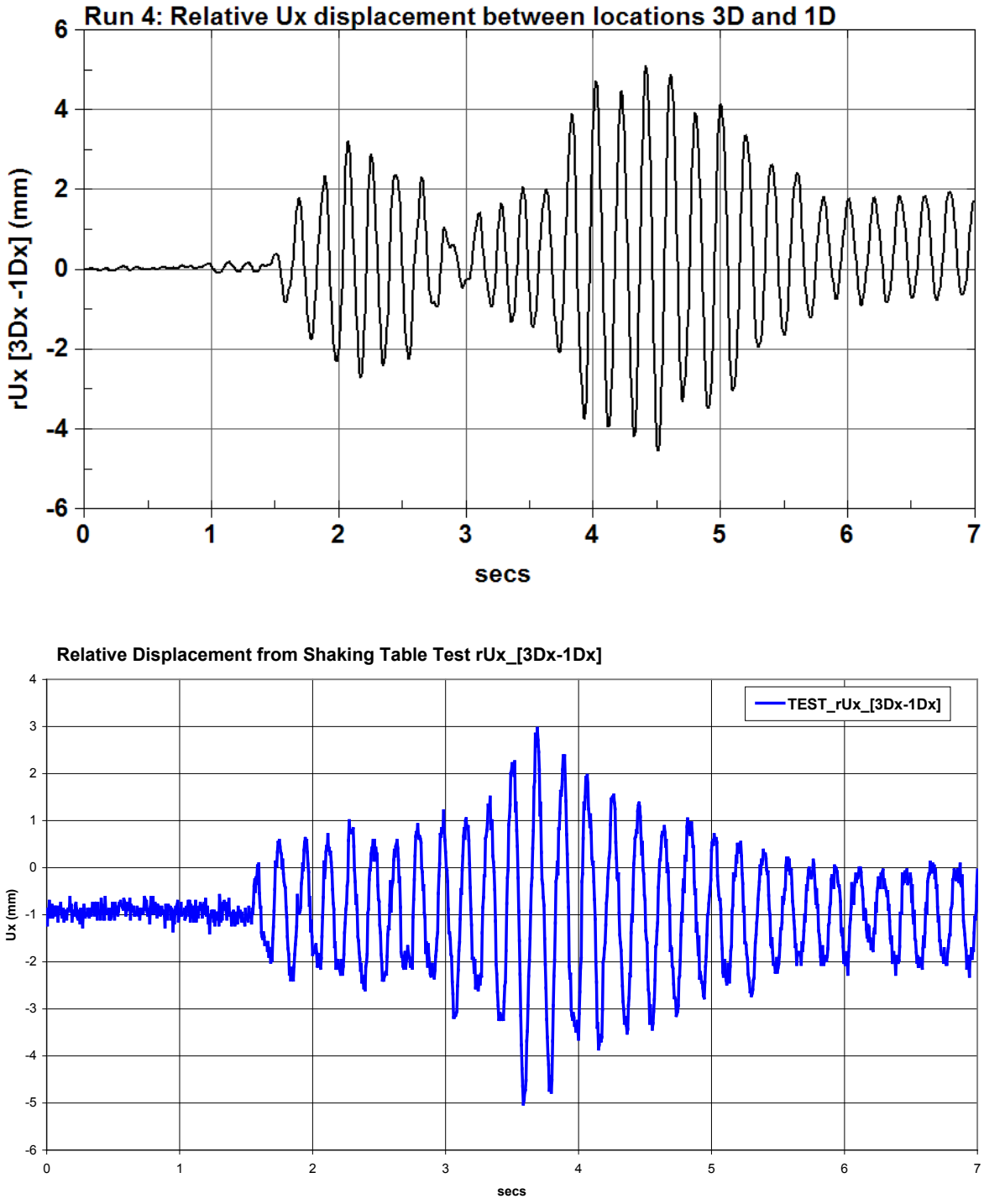

Figure 3-18 Comparison of relative displacements at location D and along the x-direction for the design earthquake level (RUN4) between the experiment and the BNL simulation

According to Table 2.3, the achieved PGA for RUN5, which was the test following the design level earthquake was lower than RUN4. As a result, the effects of tests beyond RUN5 are presented in the following figures. During the test a significant drop in the frequency associated with the torsional mode (3rd eigen mode) was measured during RUN5 without any correlation to any visible damage in the structure.

Shown in Figure 3.19 are comparisons of predicted accelerations and experimental measurements. While the predictions generally agree with the experiment, they seem to under predict the accelerations. This indicates that (a) the increased damping introduced into the analysis following the completion of RUN5 (2% damping ratio from 1.0% used in the below design level seismic intensity tests and 1.5% for RUN4) combined with (b) the effect of visible cracking on the acceleration response of the structure observed during the simulation of RUN6 (isolated small cracks) and RUN7 (permanent cracks) are the cause of the under prediction. Figure 3.20 depicts the comparison of floor response spectra. Figure 3.21 illustrates the spatial distribution of effective stress along with predicted cracking at the end of RUN6 and RUN7 tests respectively. As anticipated, elevated levels of stress are predicted near the corners of the wall openings that result from the torsional response of the structure.

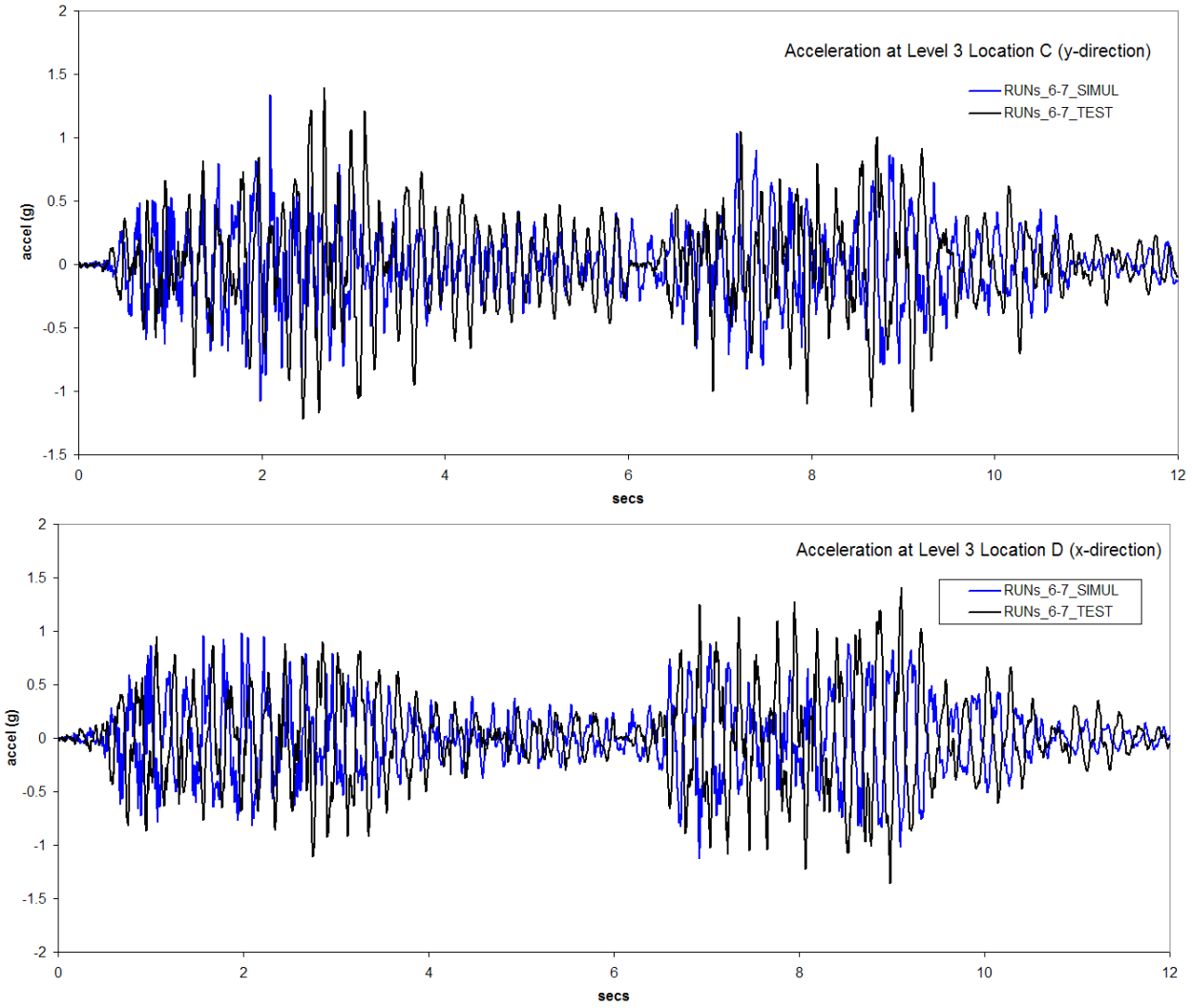

Figure 3-19 Comparison of 3rd level (locations C and D, y-direction and x-direction respectively) accelerations between test and prediction for RUN6 and RUN7 inputs

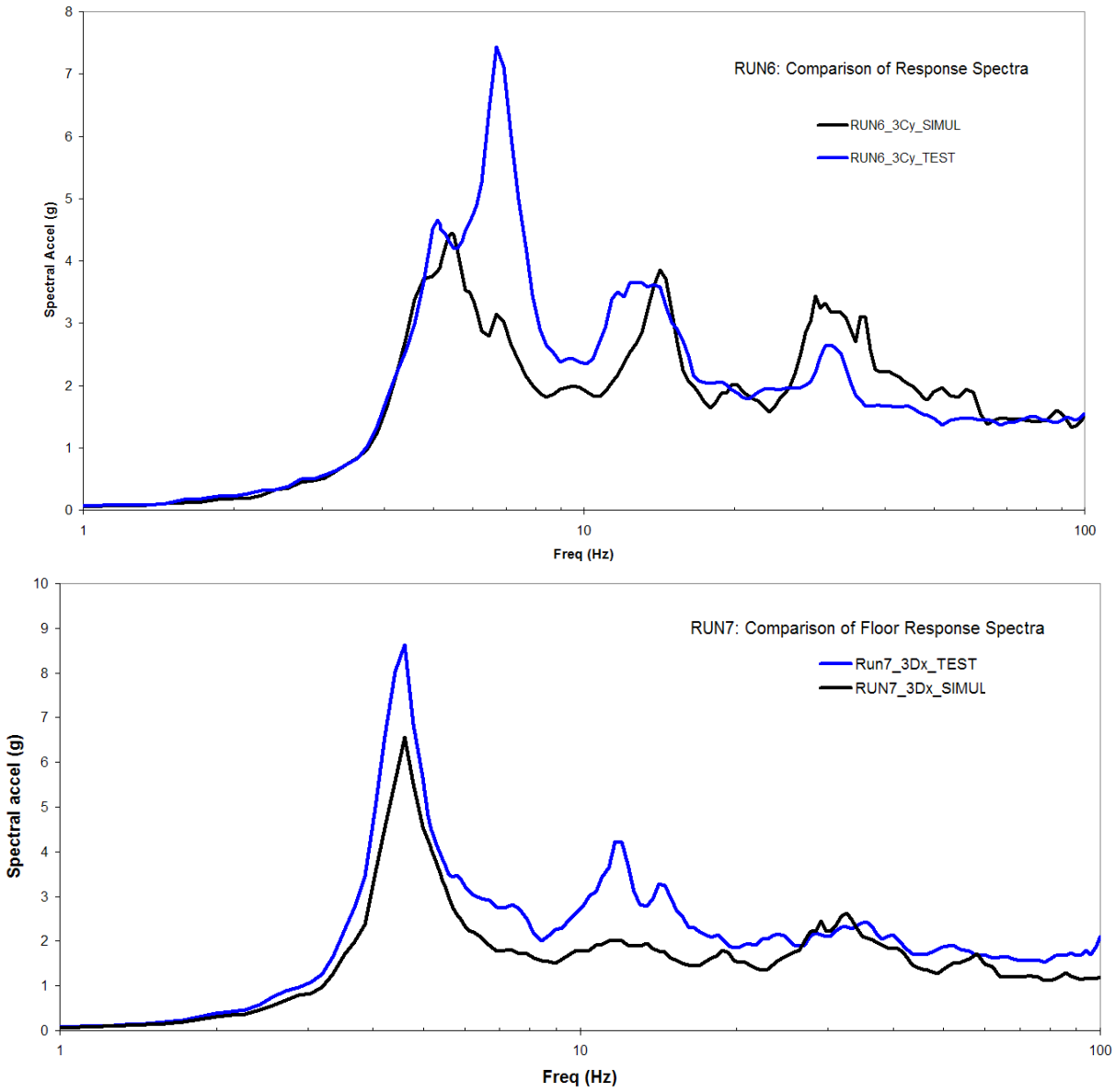

Figure 3-20 Floor response spectra comparison at the 3rd level of the structure between test and prediction for RUN6 and RUN7 inputs

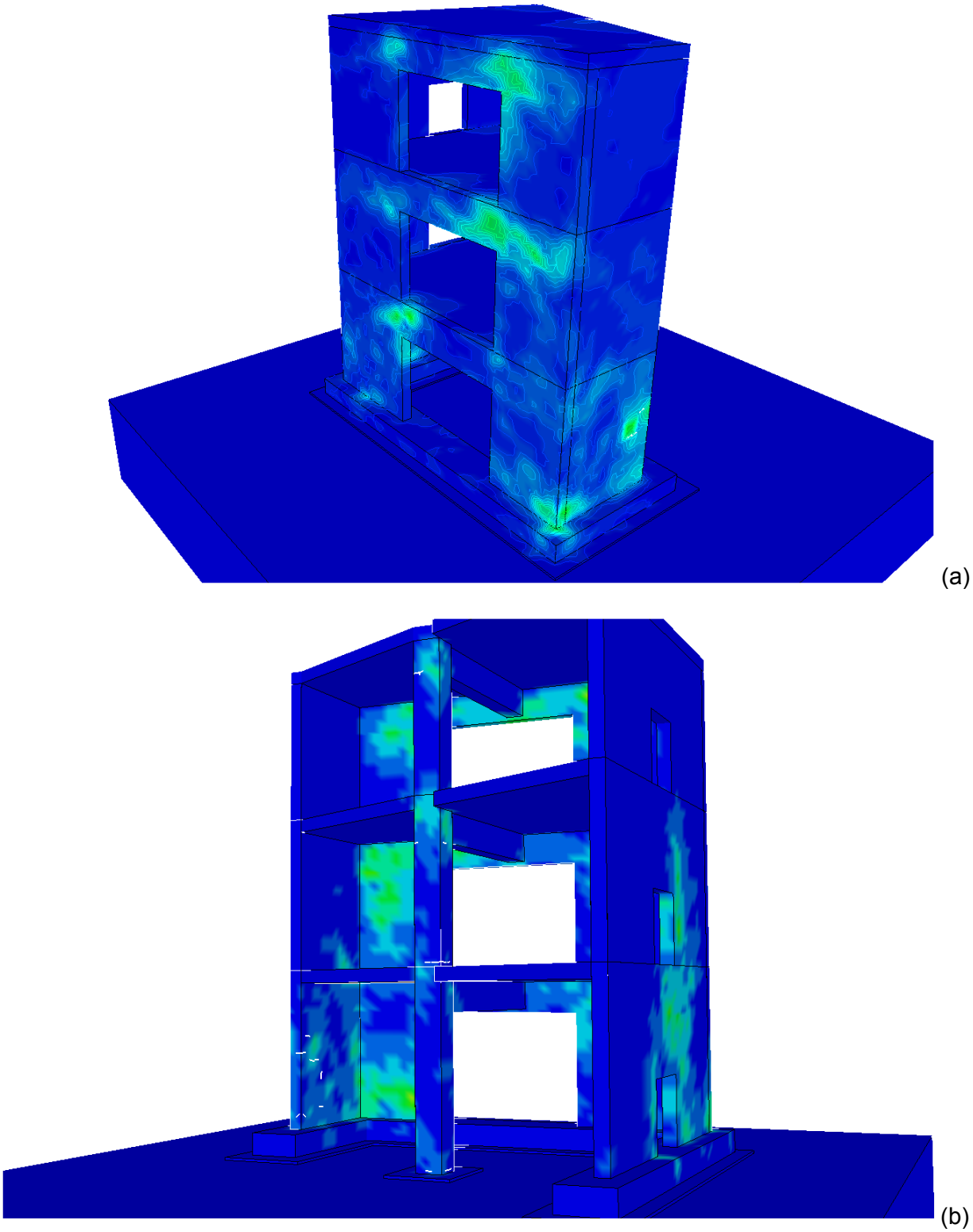

Figure 3-21 **Predicted damage in the SMART structure at the end of (a) RUN6 and (b) RUN7. Cracking of concrete is predicted to appear during the RUN7 table excitation**

The completion of RUN7 and the observation of damage that was induced indicated that the structure has entered the non-linear regime of its response. The pair of accelerograms designated as RUN8 and termed as ***over-design*** earthquake during the benchmark induced shaking table PGA values of 0.41g in the x and 0.55g in the y directions. Special attention was paid to this level anticipating that, it being double the design level earthquake, significant levels of damage could be experienced.

The analysis continued by transferring the damage information at the end of RUN7 (see Figure 3.21), maintaining the same level of 2% damping, and counting on the cracked concrete to provide additional effective damping. Figures 3.22 and 3.23 illustrate a comparison of accelerations predicted at the three corners of the structure at the 3rd level (A, C, and D) and those recorded during the test. While it slightly under predicts, the analysis reproduces the acceleration response very well throughout the strong motion part of the input earthquake even within the non-linear regime. Figure 3.24 presents the floor response spectra comparison where it is seen that the non-linear analysis is in excellent agreement for the first two eigenmodes. Figure 3.25 reflects the effective stress state of the structure during the RUN8 input earthquake and the damage in the form of concrete cracking.

Figures 3.26 and 3.27 illustrate the comparison of rebar strain in the Wall 4 (which appears to be more damaged at the end of RUN8) for the subsequent accelerograms pairs for RUN9. Similar to RUN8, RUN9 resulted in PGA values to the shaking table of 0.41g and 0.56g along x- and y-directions respectively. The non-linear analysis reproduces both the levels and the transient shape of the rebar strain. Figures 3.28 and 3.29 compare relative displacements between the 3rd level and the foundation/wall interface and demonstrate that the displacements are well matched (please note the offset in the vertical axis of the recorded data). Both the test and the prediction results show the appearance of extra damping in the structure due to the damage (rapidly dampening of the free vibration at the end of the strong motion part).

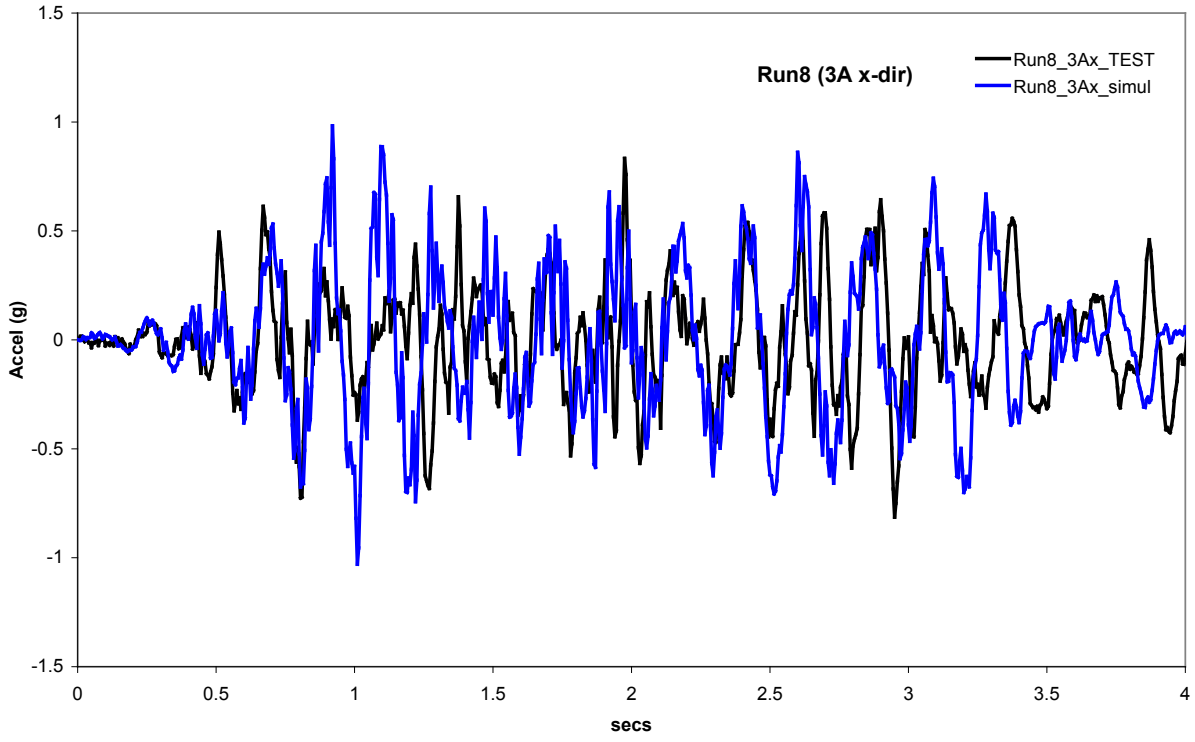

Figure 3-22 Comparison of predicted acceleration at point A of Level 3 with recorded accelerations during RUN8

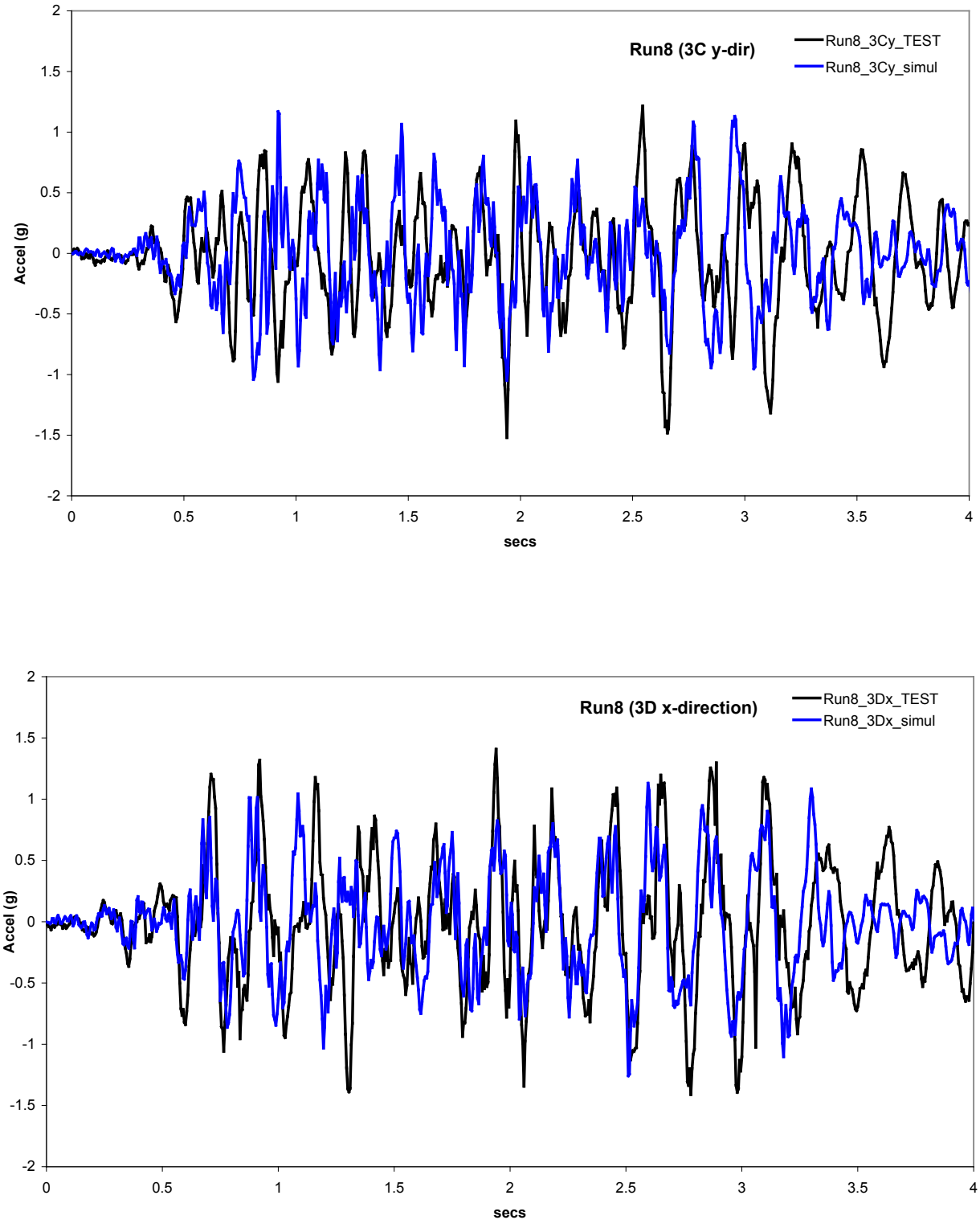

Figure 3-23 Comparison of predicted accelerations at point C (y-direction) and D (x-direction) at Level 3 of the test structure with recorded accelerations during RUN8

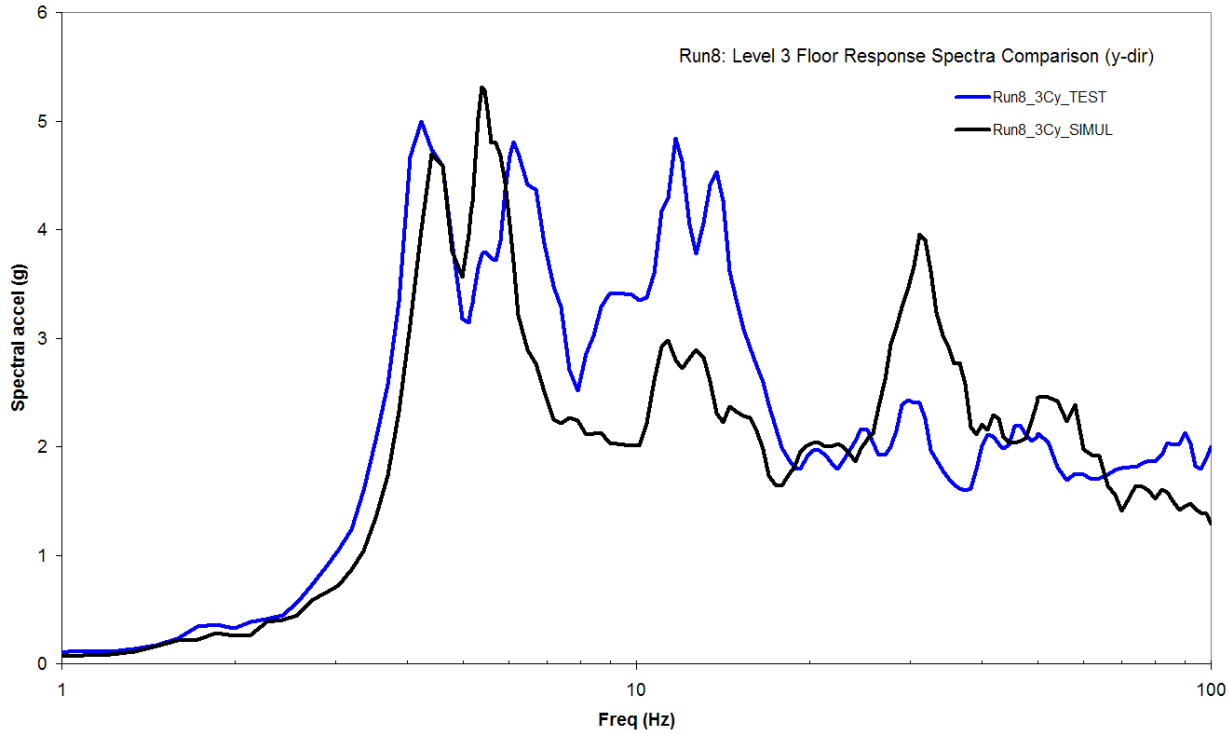

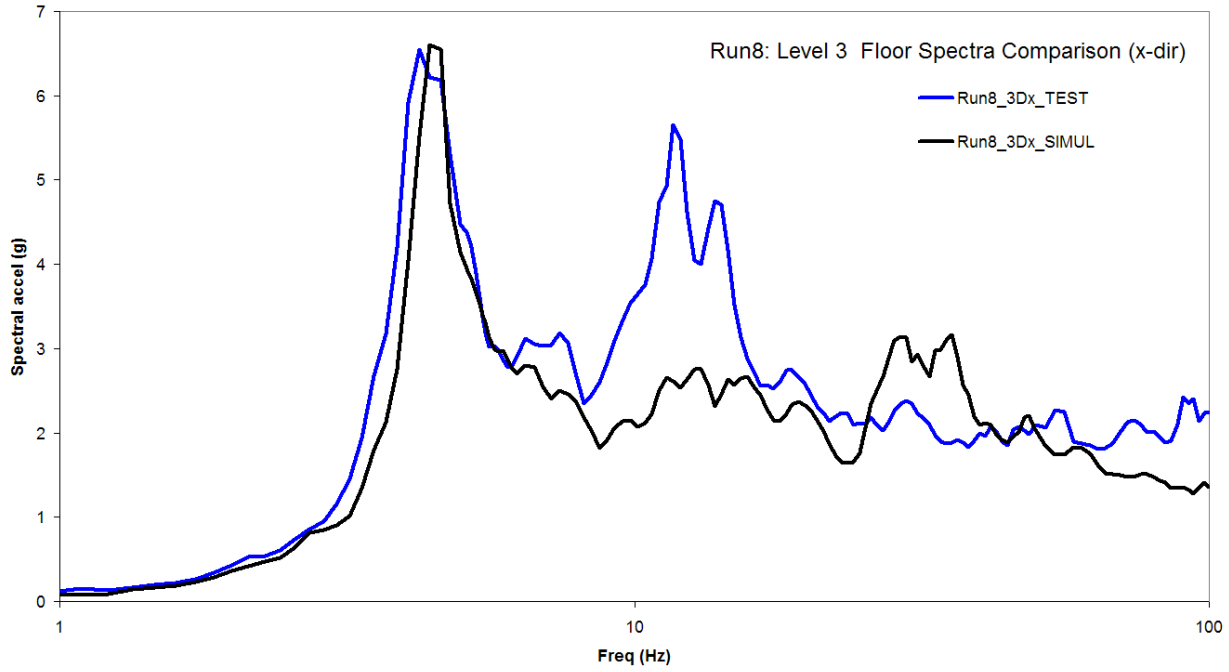

Figure 3-24 Comparison of acceleration floor response spectra at point C(y-direction) and D (x-direction) of Level 3 between recorded and predicted data

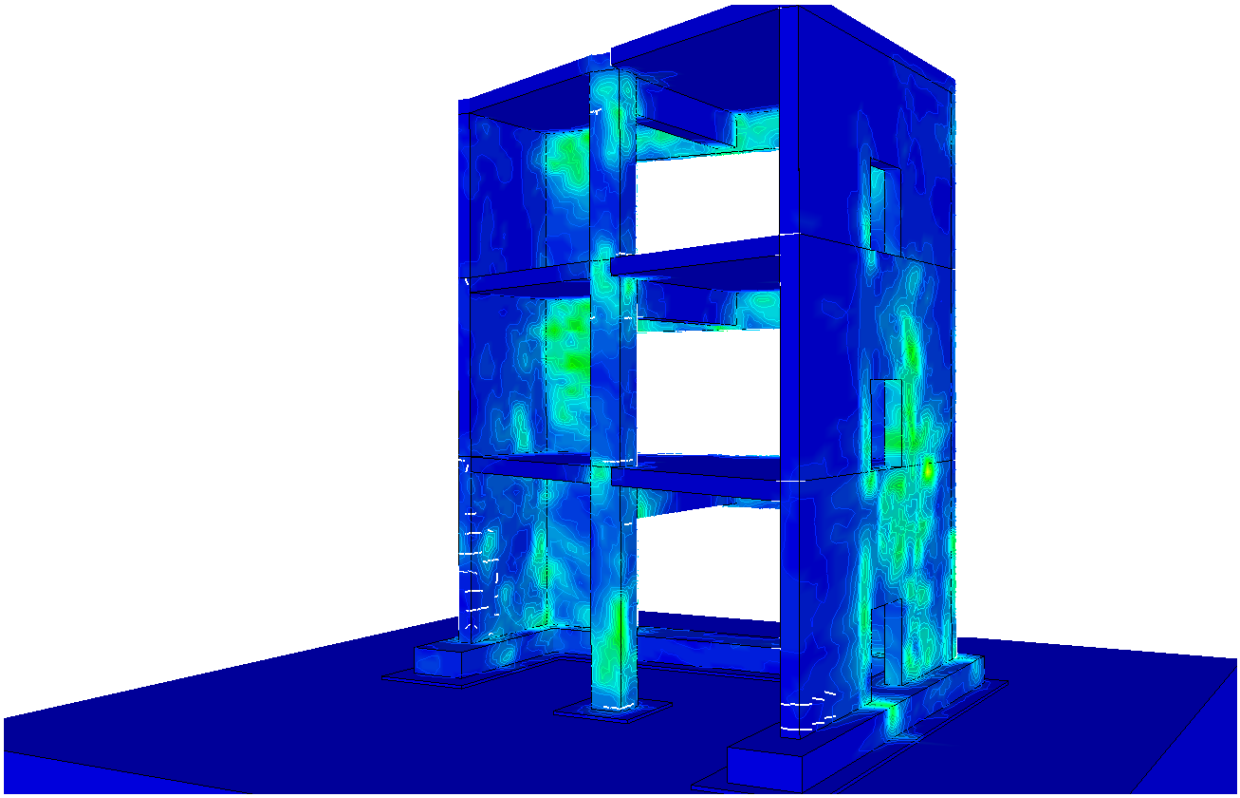

Figure 3-25 Predicted damage state of the SMART structure upon completion of the RUN8 shaking table excitation

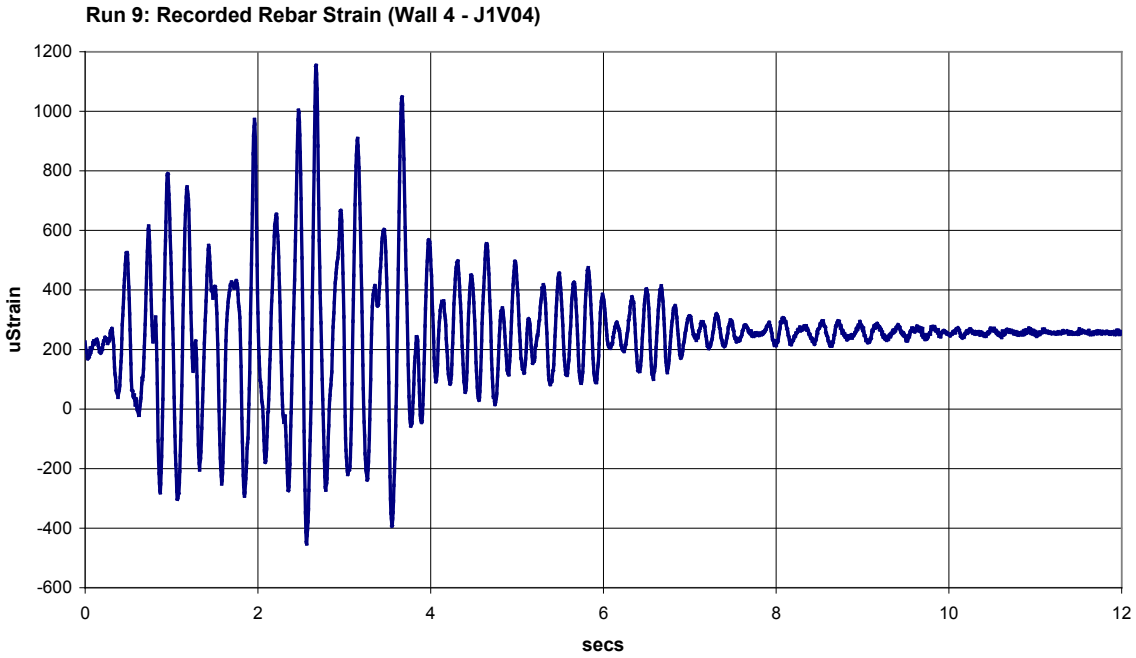

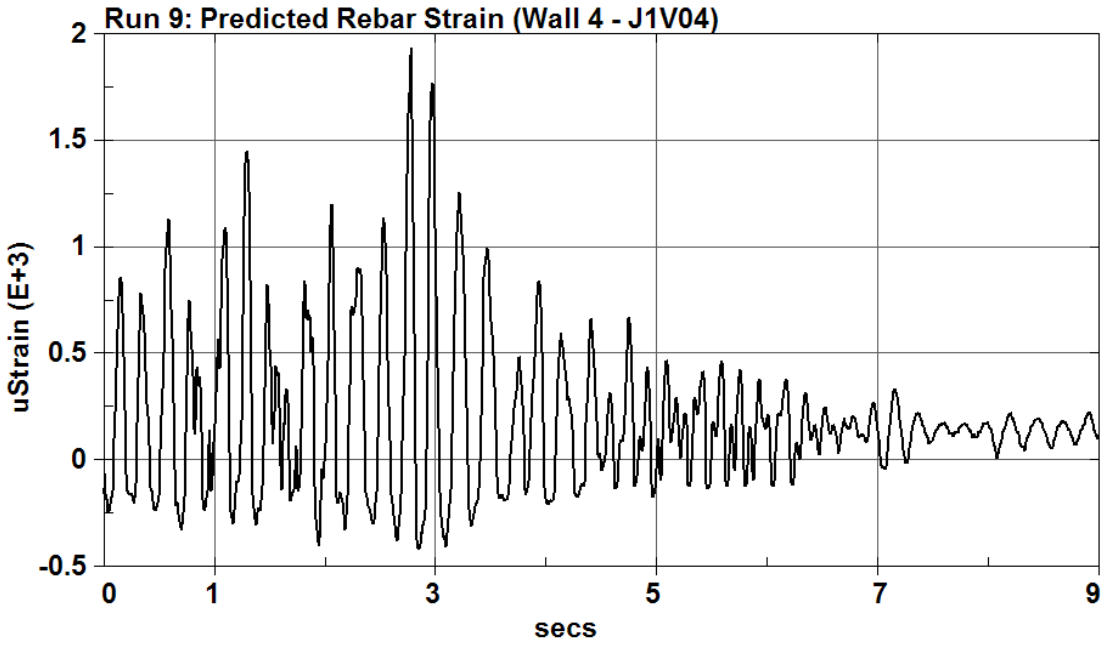

Figure 3-26 Comparison of predicted rebar strain on Wall #4 of the structure (location J1V04 near the foundation) with the one recorded by the installed strain gauge during RUN9

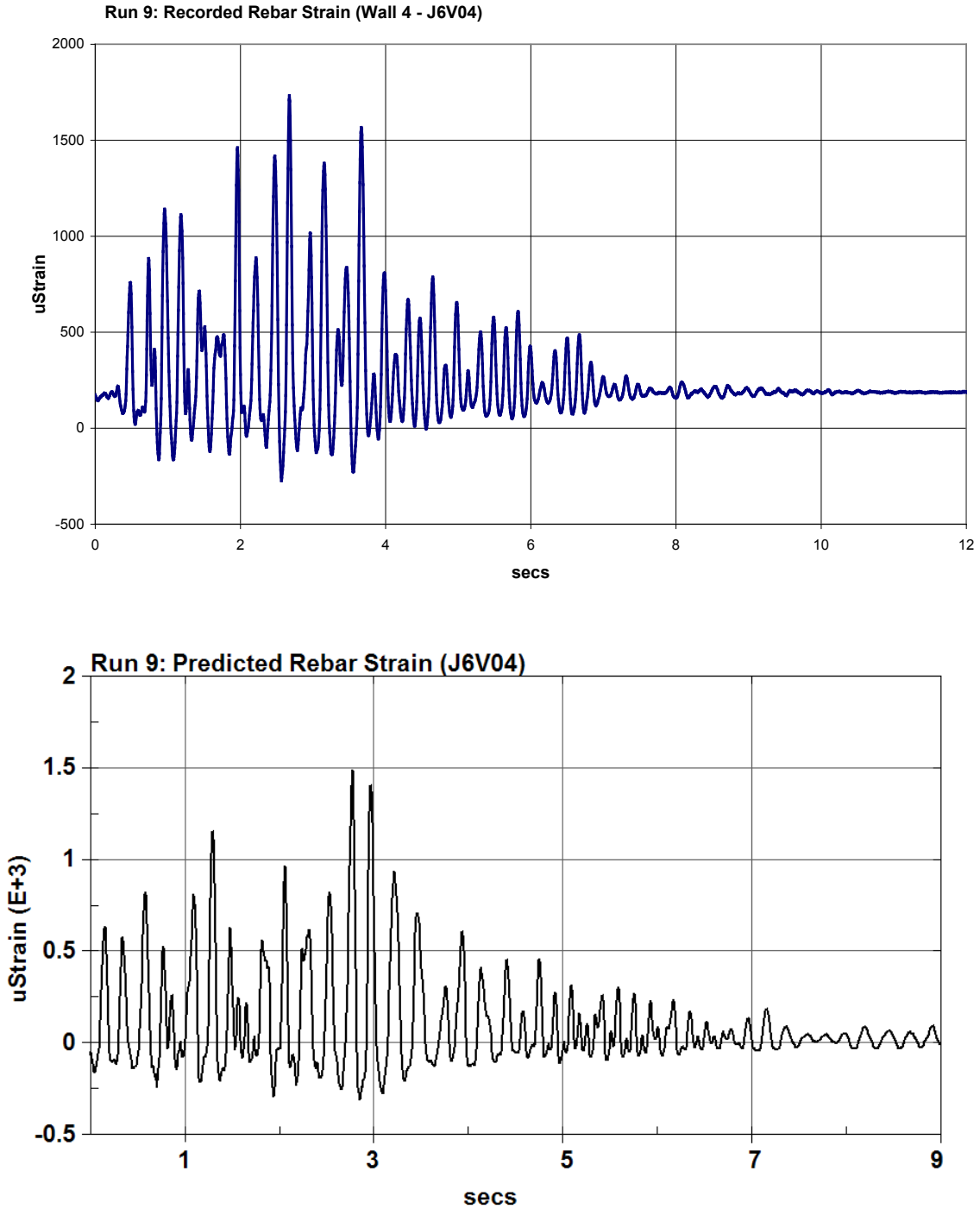

Figure 3-27 Comparison of predicted rebar strain on Wall #4 of the structure (location J6V04 mid-height between 1st and 2nd level) with recorded strain during RUN9

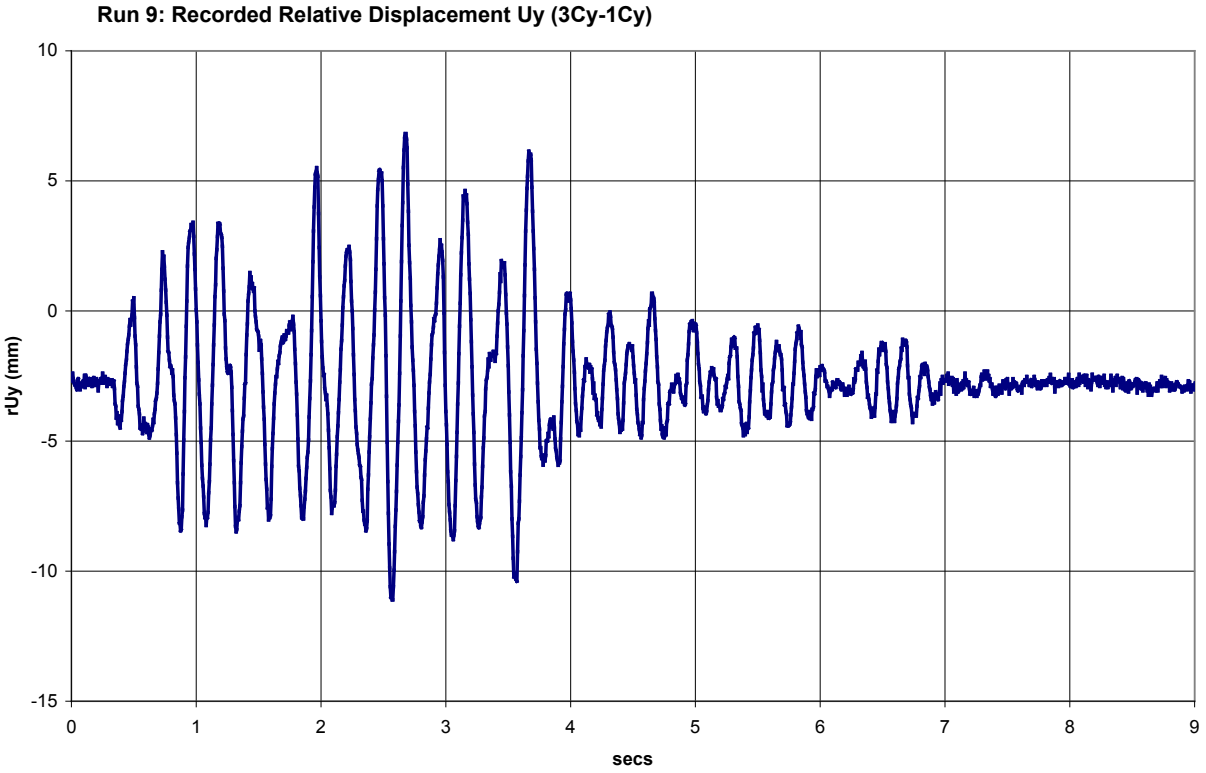

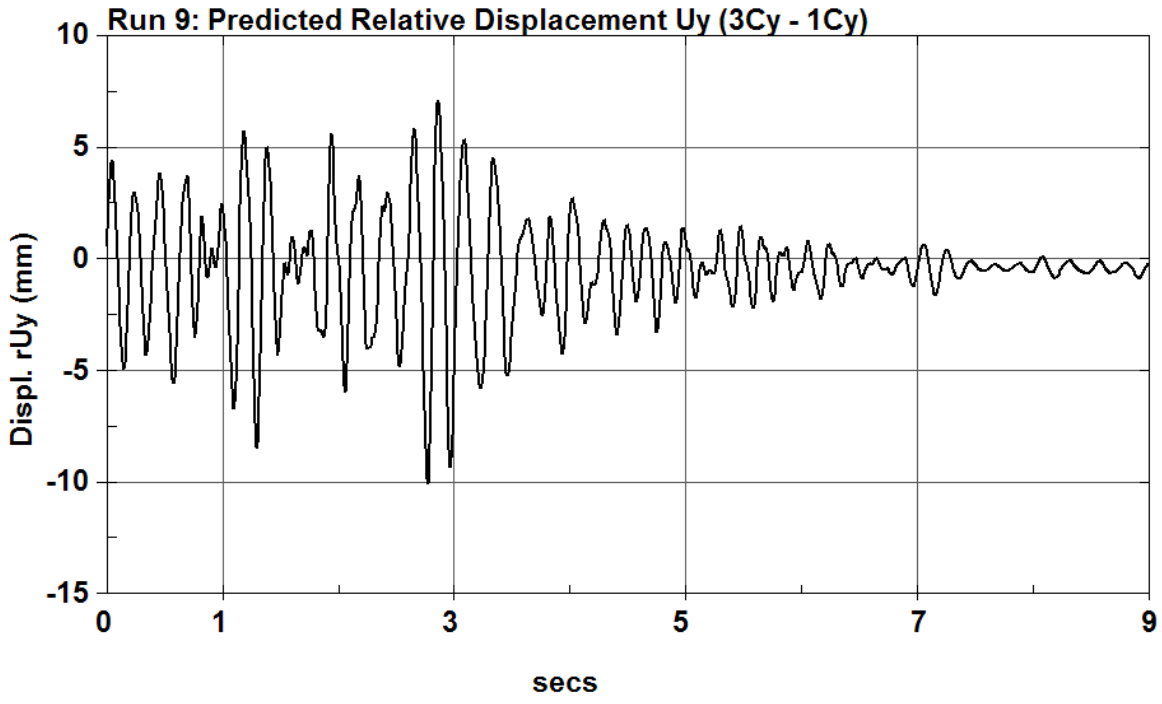

Figure 3-28 Comparison of predicted relative displacement rU_y between the 3rd level and foundation top at corner C with the recorded relative displacement during RUN9

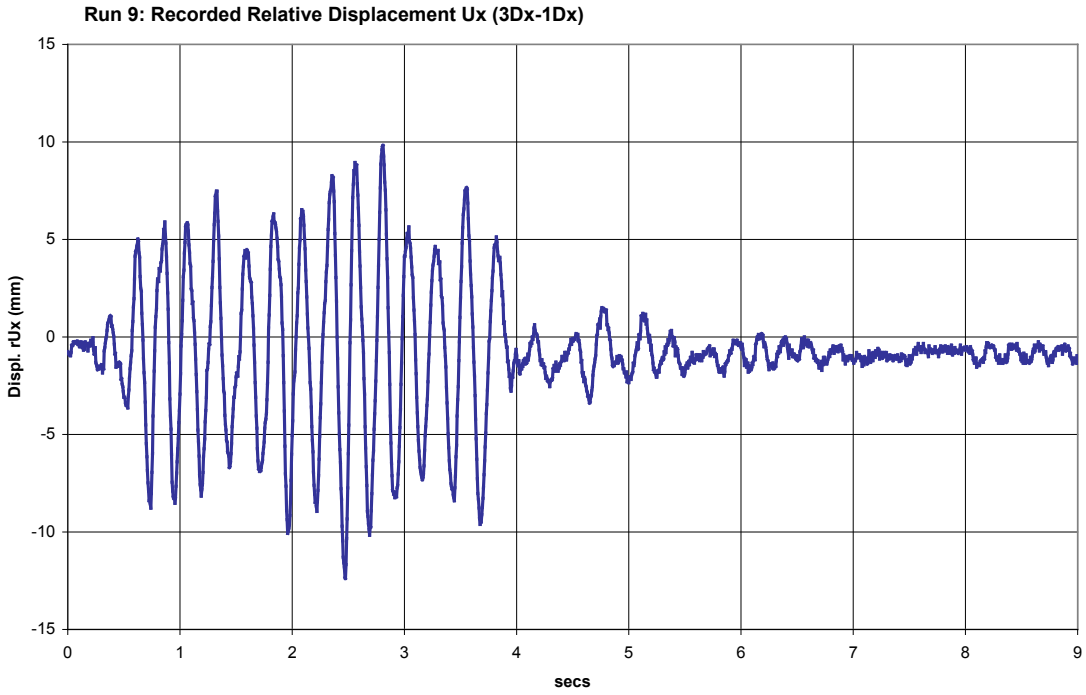

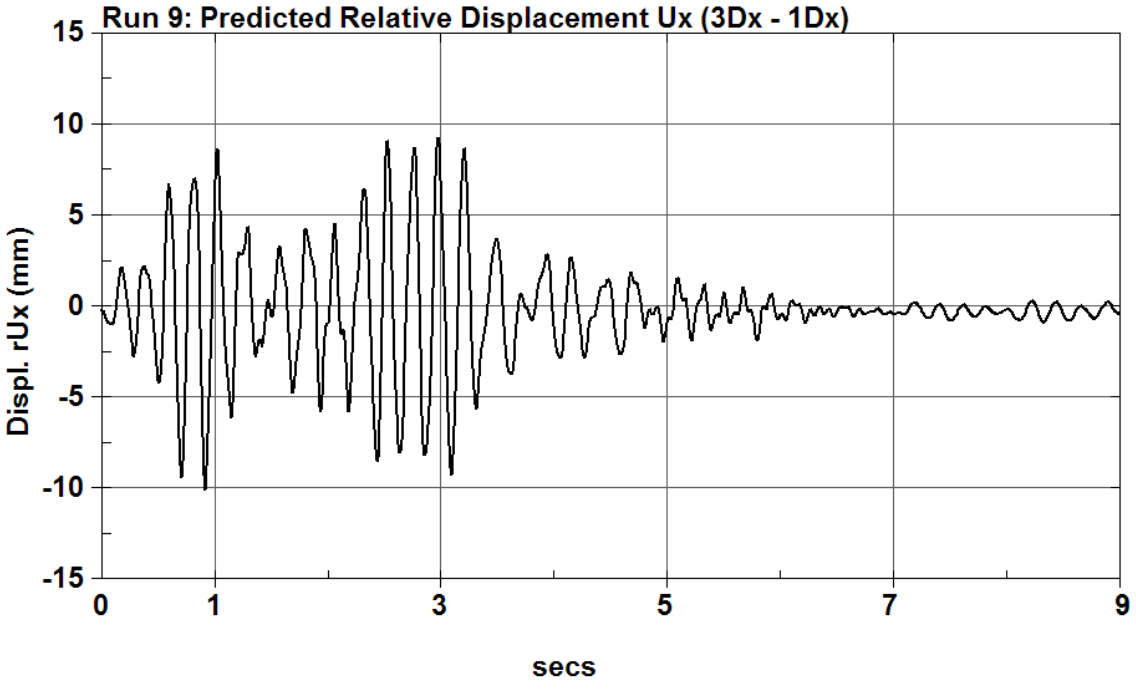

Figure 3-29 Comparison of predicted relative displacement rU_x between the 3rd level and foundation top at corner D with the recorded relative displacement during RUN9

The predicted response during RUN9 exhibited the effective damping in the damaged structure (see Figure 3.29). Originally the analysis proceeded without updating the structural damping of 2%, anticipating that the cracked concrete will introduce additional energy absorption in the system. This resulted however in solution instabilities during RUN10 indicating that the structure is being damaged as a result of the higher acceleration demand. As a result, the damping in the concrete structure was increased to 4% for the non-linear analysis for the tests beyond RUN9.

Shown in Figure 3.30 are comparisons of accelerations for the tests RUN10, RUN11 and RUN12. While the non-linear analysis model traces the floor accelerations quite well it is evident that the accelerations are under-predicted. Figure 3.31 depicts the acceleration comparison for RUN11, still showing a very good agreement between the test and the prediction results. Figure 3.32 presents the floor response spectra comparison for RUN12 at the corners C and D of the 3rd level of the structure Figure 3.33 depicts the rebar strain comparison at mid-level height (Level 0 and level 1) of Wall #4. Excellent agreement between the predicted and the recorded strains is observed.

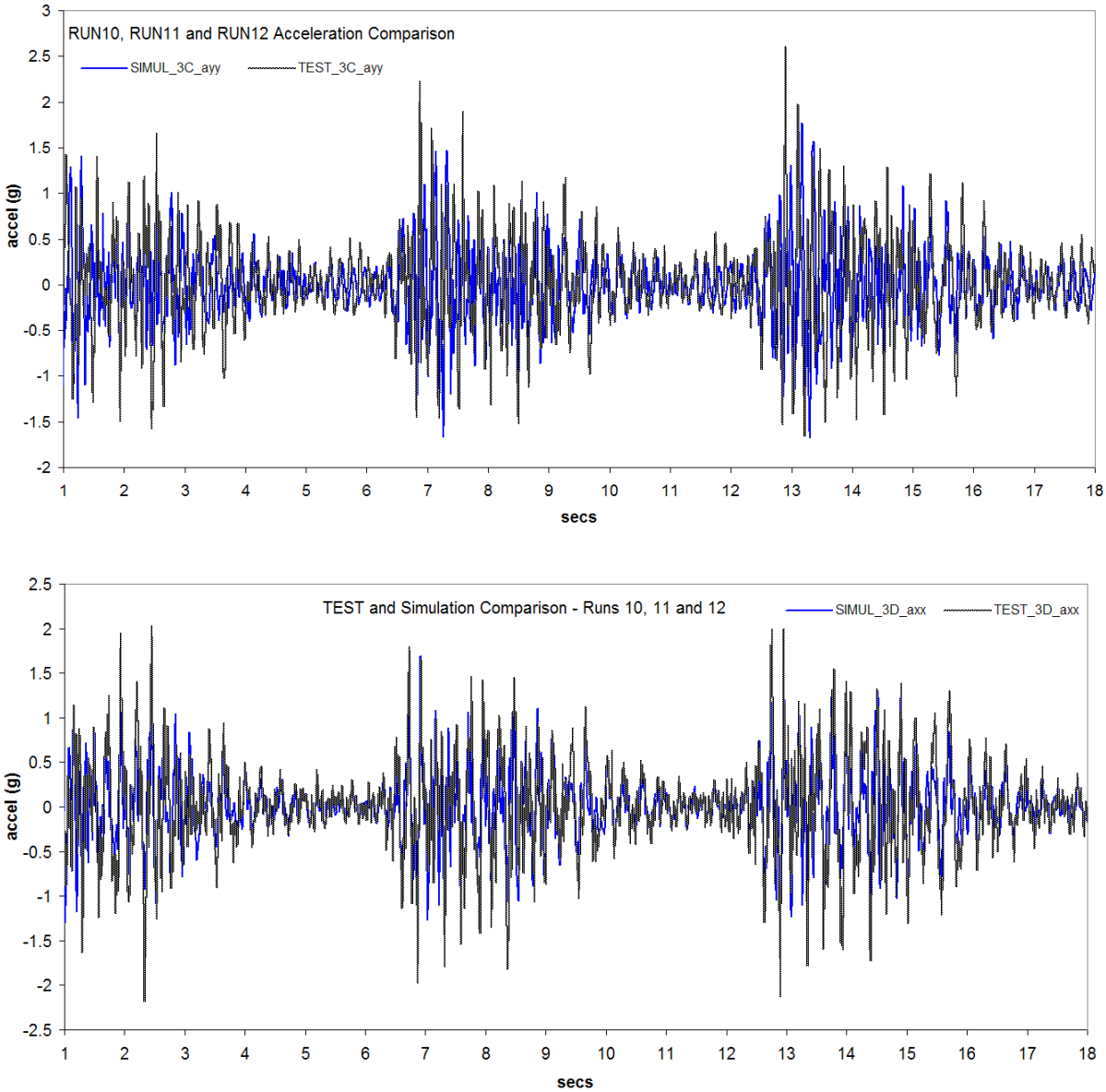

Figure 3-30 Comparison of predicted accelerations on the 3rd level of the structure (corners C and D) with recorded data during the shaking table tests RUN10, RUN11 and RUN12

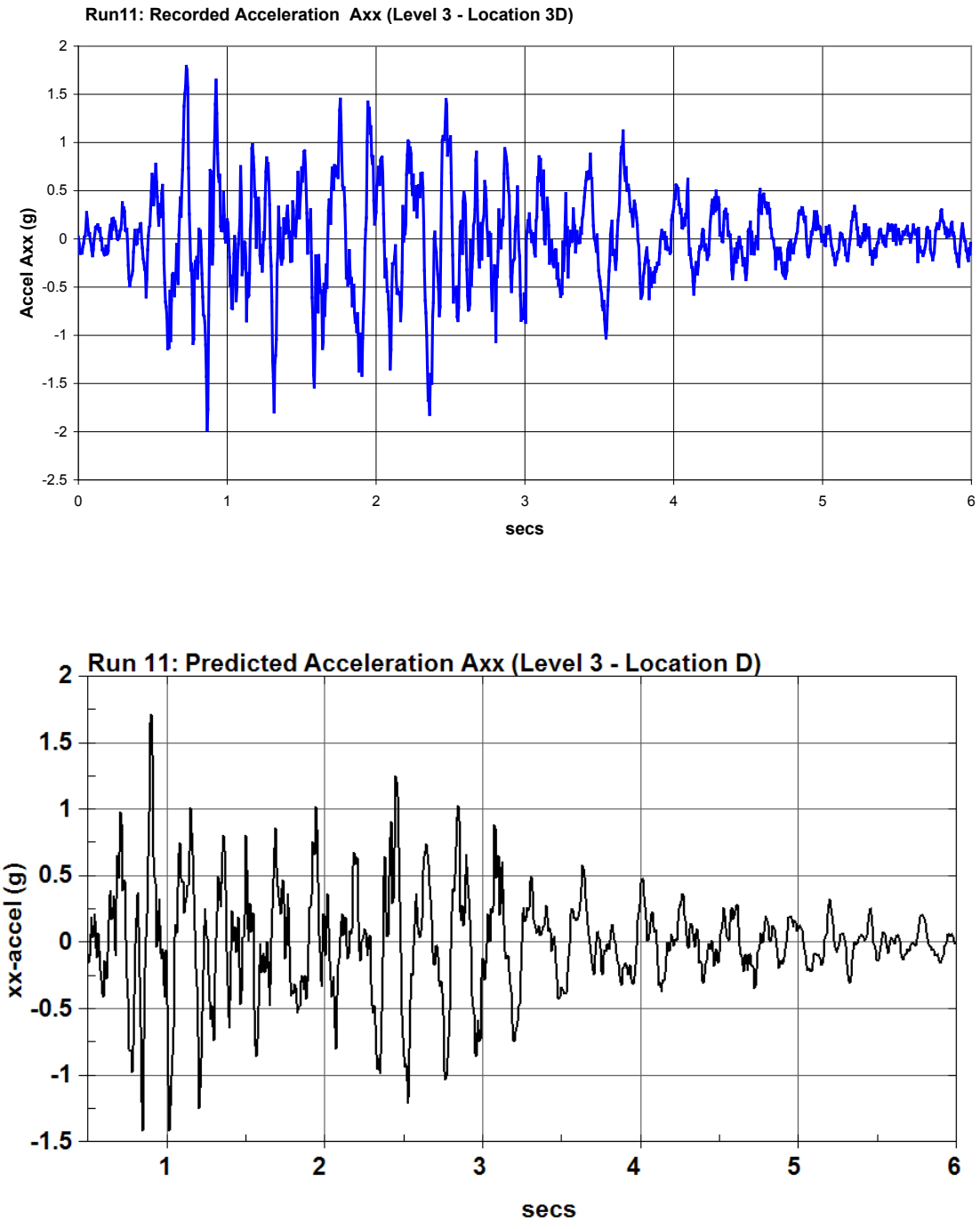

Figure 3-31 Comparison of accelerations on the 3rd level of the structure (corner D along the x-direction) with recorded data during the RUN11 test

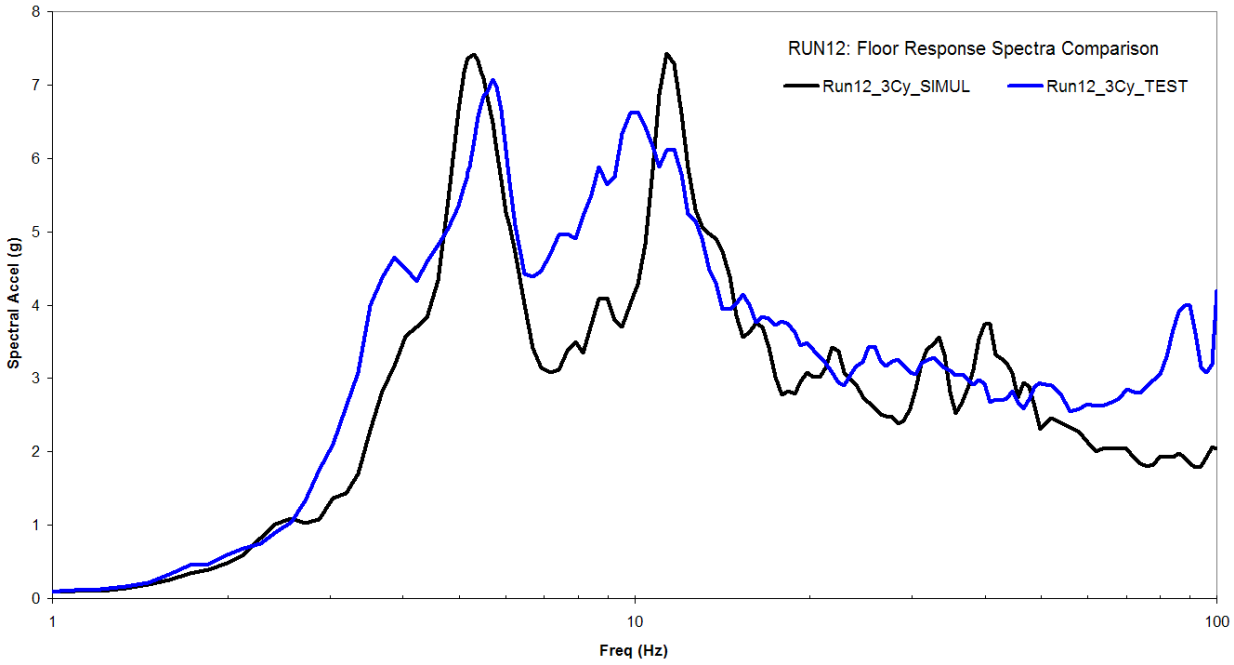

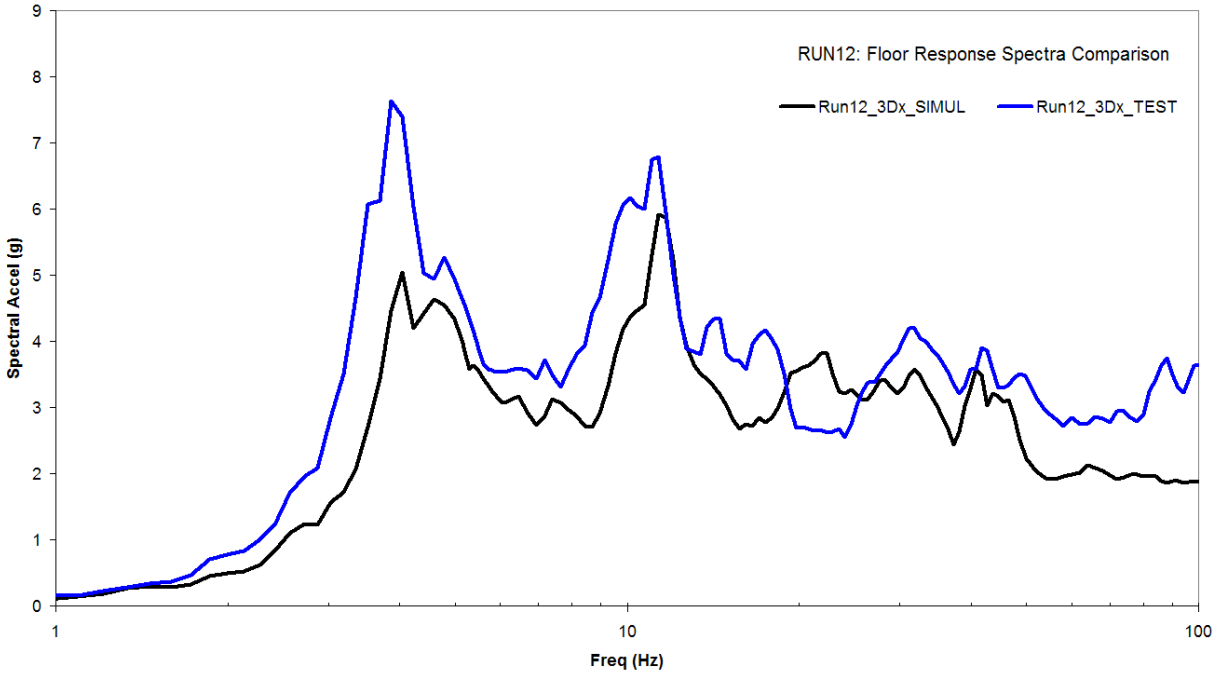

Figure 3-32 Floor response spectra comparison between predicted and recorded data during the RUN12 test

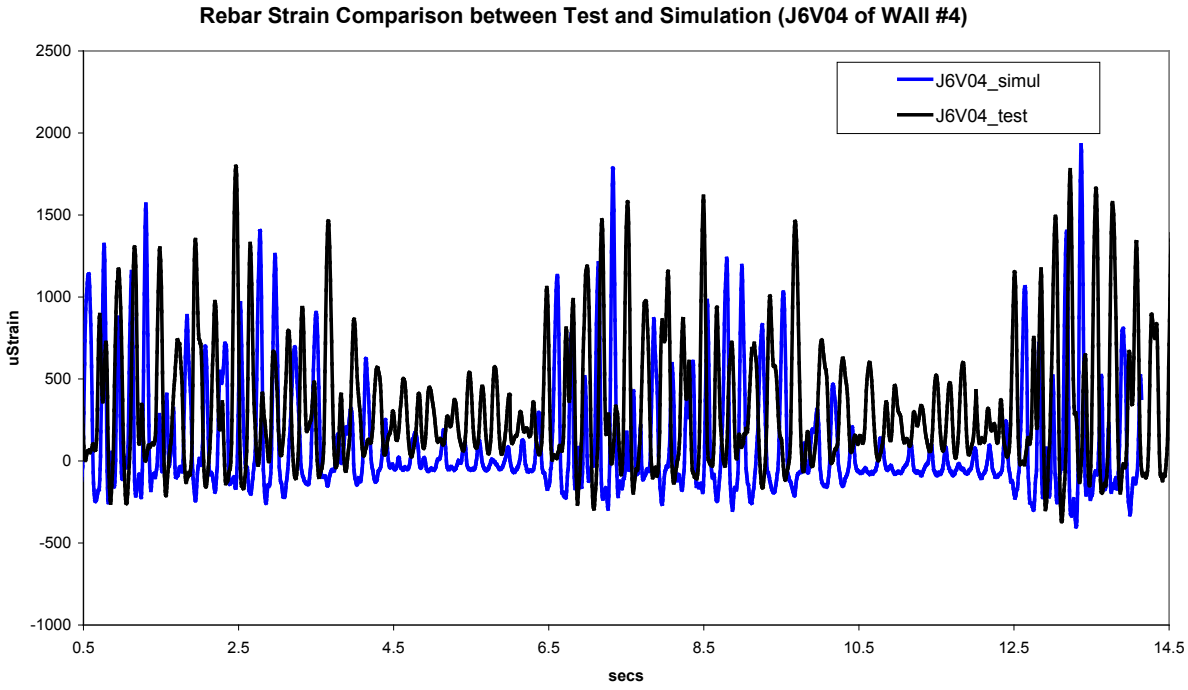

Figure 3-33 Comparison of rebar strain mid-height of Wall #4 (level 0 and level 1) at the edge C for tests RUN10, RUN11 and RUN12

RUN13 representing the last test in the 13-run sequence induced peak ground accelerations higher than originally planned for the test along the y-direction and lower in the x-direction. Specifically, in the planning of the benchmark, the PGA values for both directions were to be 1.0g. During the shaking table test, the PGA along the x-direction was only 0.75g and along the y-direction was 1.13g. The shaking table accelerations for the last test are shown in Figure 3.34.

The analysis for the RUN13 was performed without any further increase of the assumed damping of 4% used in RUN12. The analysis of RUN13 relied on the continuing concrete cracking to provide the potential increase in the 4% damping of the system assumed at the start of RUN13. Figure 3.35 depicts the comparison of structural accelerations between the test data and the non-linear analysis. Again, while the agreement is very good, the simulation under-predicts the experiment especially during the free-vibration tail. This is most likely the result of mismatch between the actual damping exhibited by the RC structure and the 4% assumed in the simulation. The under-prediction is also evident when the floor response spectra are compared (Figure 3.36). Also seen in the spectra comparison of Figure 3.36, where reflected are the accumulated damage and nonlinearities from the entire 13-test series (RUN1 through RUN13), is that the eigenfrequency drop in the test is slightly larger than what is predicted. This effect is more pronounced in the spectra along the x-direction. The non-linear analysis model reproduces the response spectra shape in the higher frequencies (~100 Hz) along the y-direction.

Excellent agreement in the structural displacements are seen in Figure 3.37 where relative displacements between the 3rd level and the level 0 (interface of vertical walls and foundation) at the corners C and D are presented.

Figure 3.38 depicts effective stress and damage state of the walls and column of the structure in the beginning of RUN13 (a) and at the end (b). Also shown in (c) are the crack patterns of the actual test structure. As seen in (a) the stress in Wall #4 is eventually relieved by the formation of cracks which reproduce quite well the patterns observed in the test specimen.

Figures 3.39 and 3.40 depict the evolution of the floor response spectra as a result of the cumulative damage experienced by the structure due to the 13-set sequence. As compared to similar spectra shown in Figures 2.31 and 2.32 for the actual test, one observes the similarity in the trend (lowering of eigenfrequencies) and also the difference in the level of damage or change in the dynamic properties of the reinforced concrete structure.

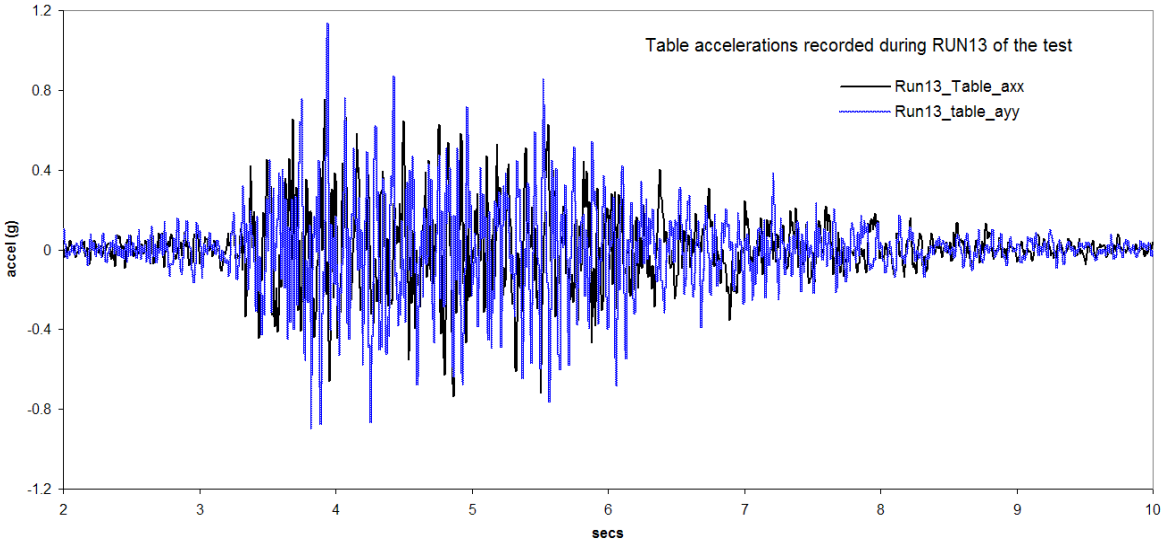

Figure 3-34 Acceleration pair recorded on the shaking table during the last test in series, RUN13, where PGA values were 0.75g in x and 1.13g in y

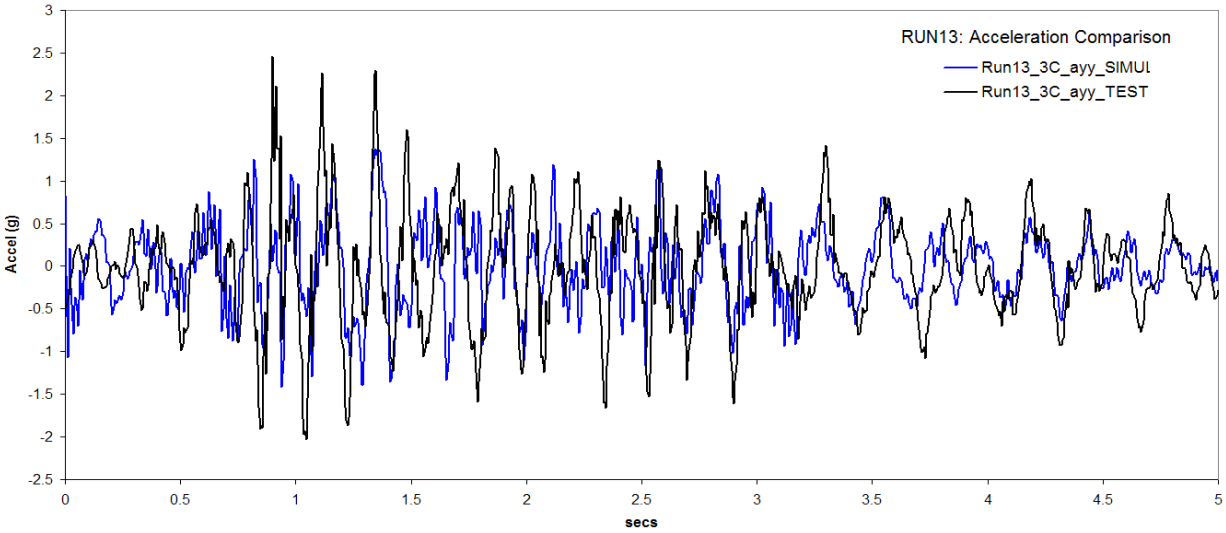

4

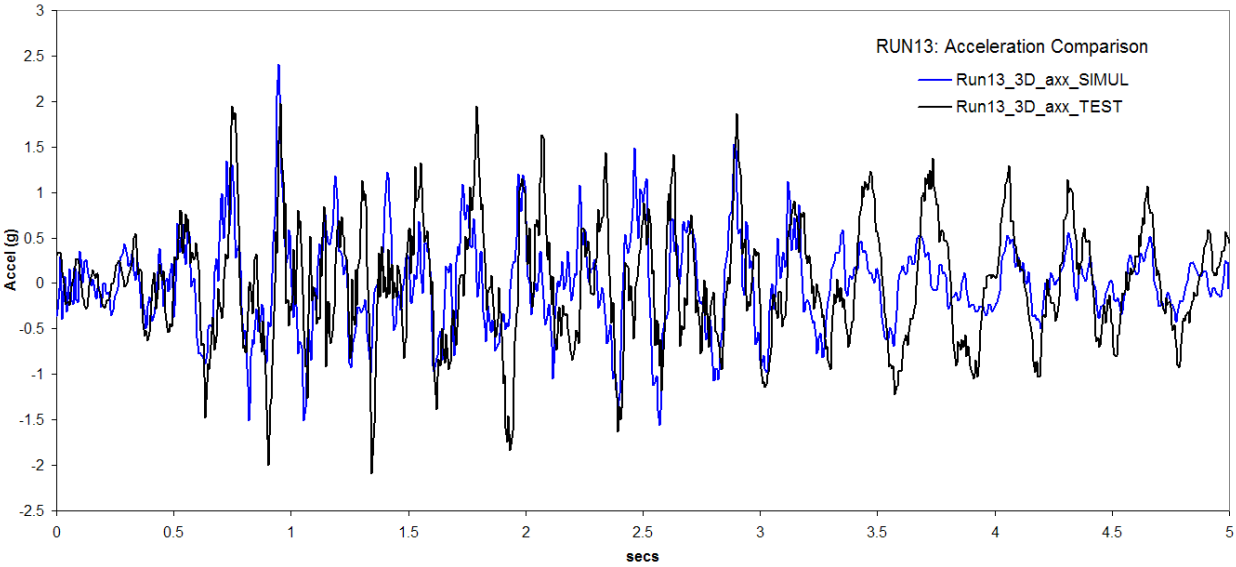

Figure 3-35 Comparison of structure accelerations at level 3 for the RUN13 test

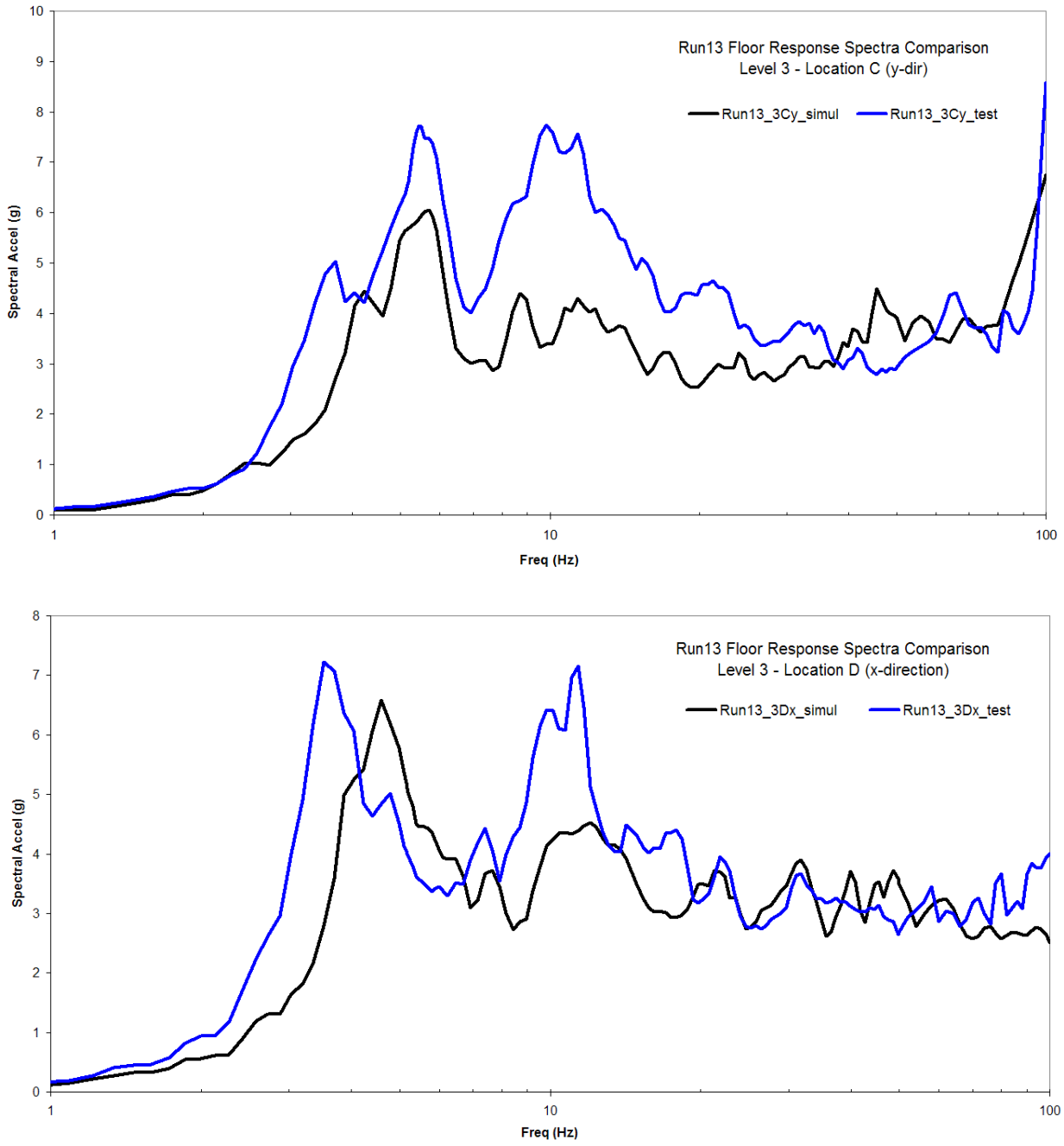

Figure 3-36 Acceleration floor response spectra comparison for the RUN13 test

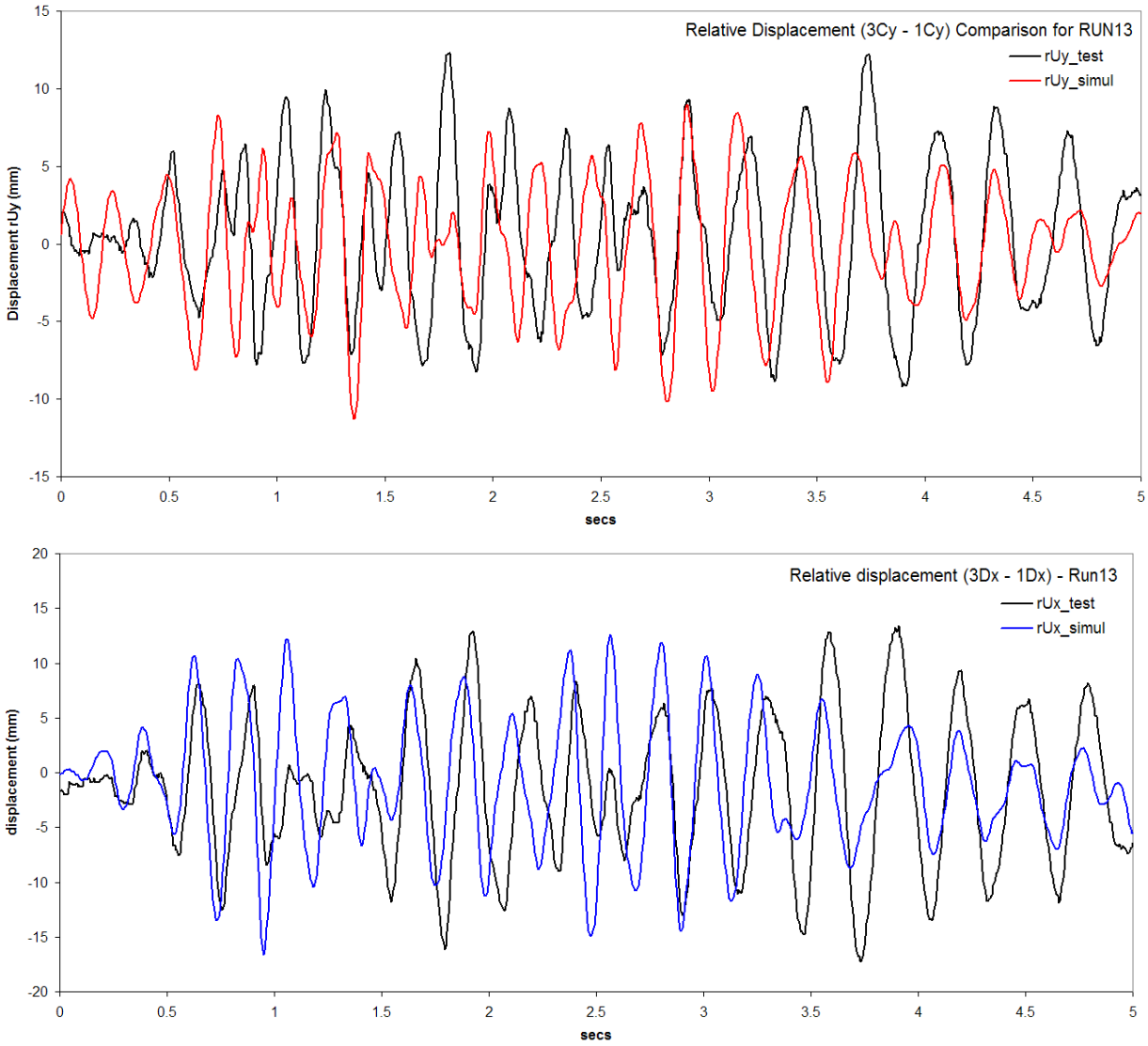

Figure 3-37 Comparison of relative displacements between level 3 and level 0(foundation/wall interface) for the RUN13 test

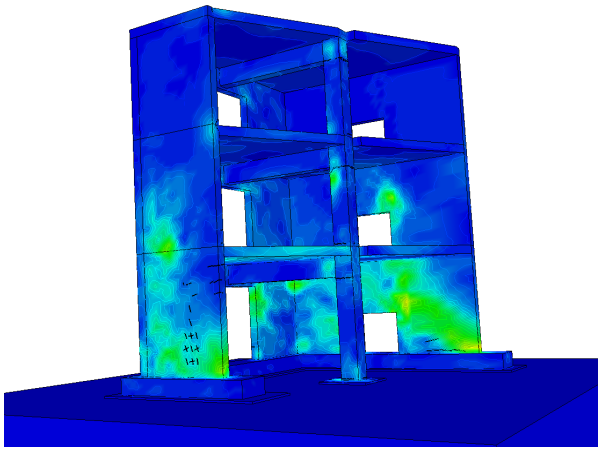

(a)

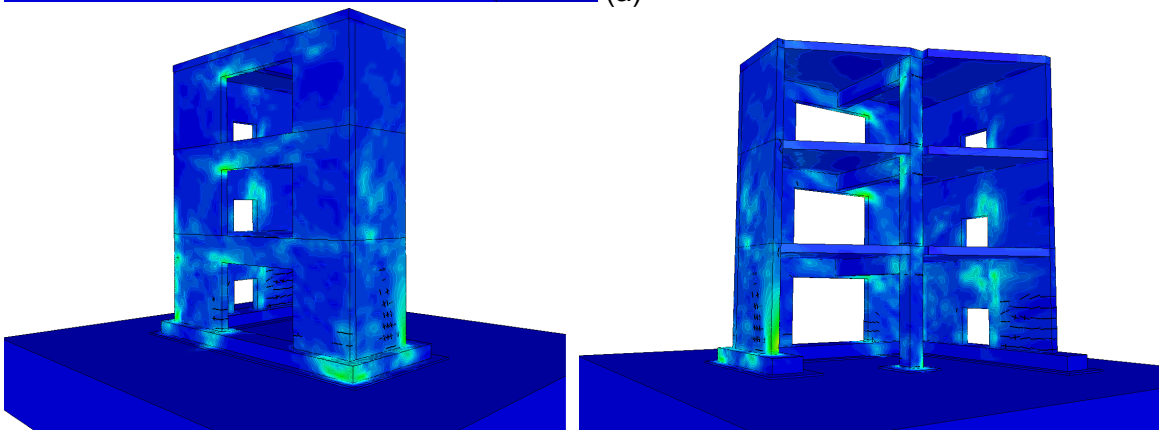

(b)

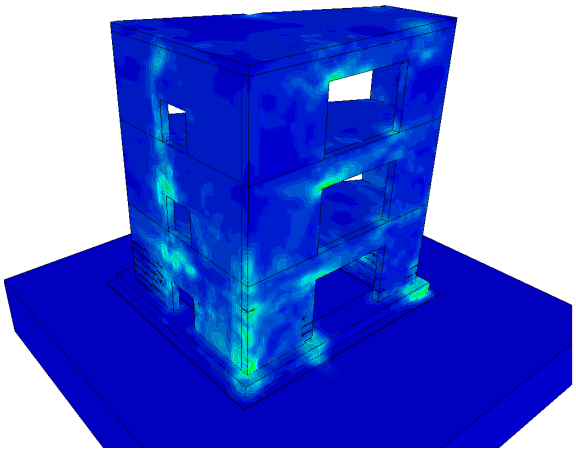

(c)

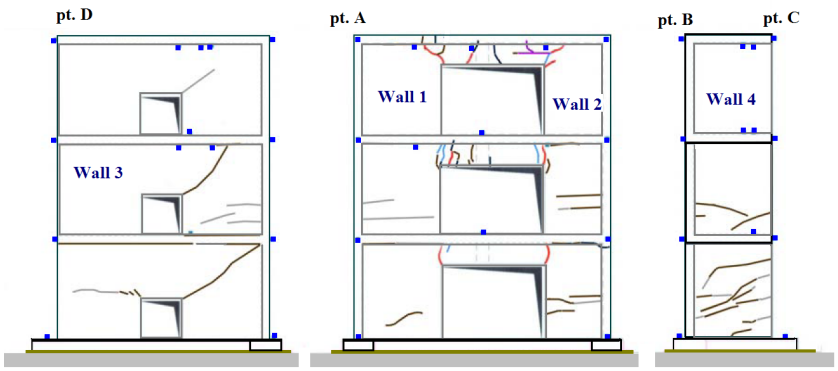

Figure 3-38 Predicted structural damage in the SMART structure at the end of the 13-run test

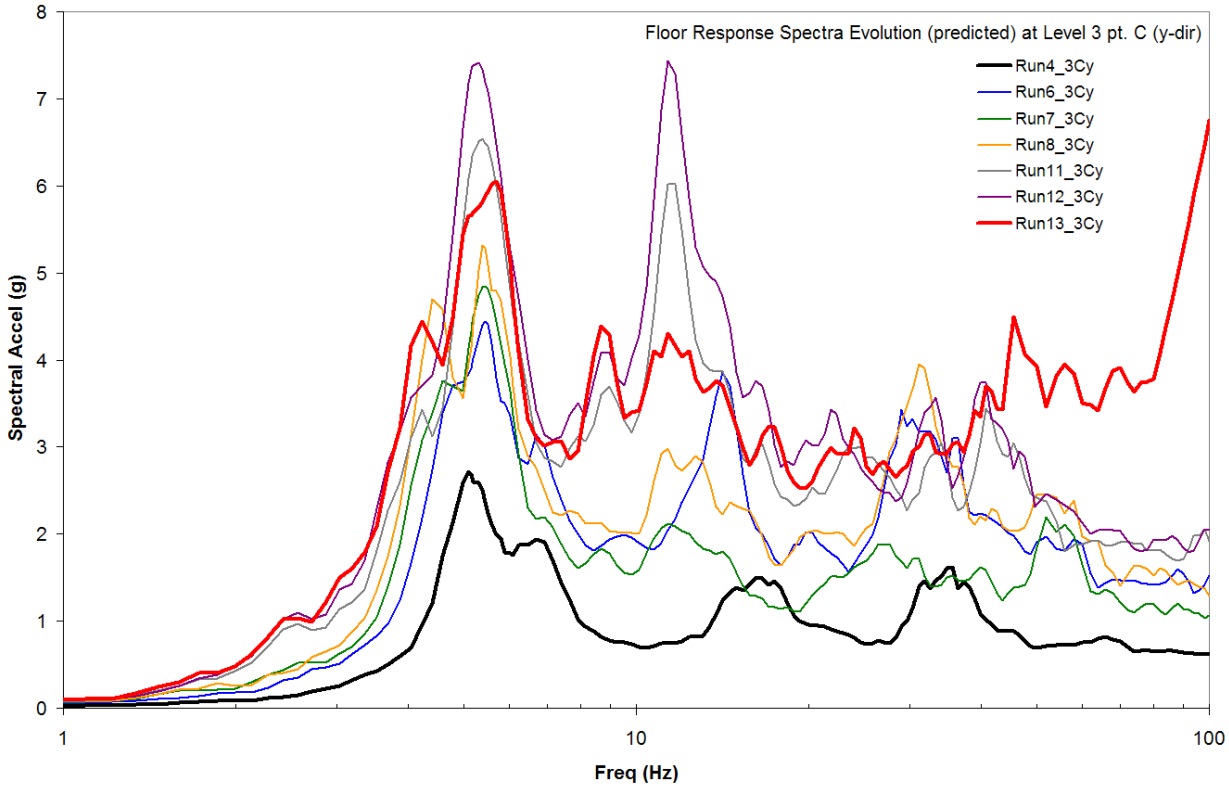

Figure 3-39 Predicted floor response spectra evolution during the application of the ten synthetic earthquake pairs along the y-direction

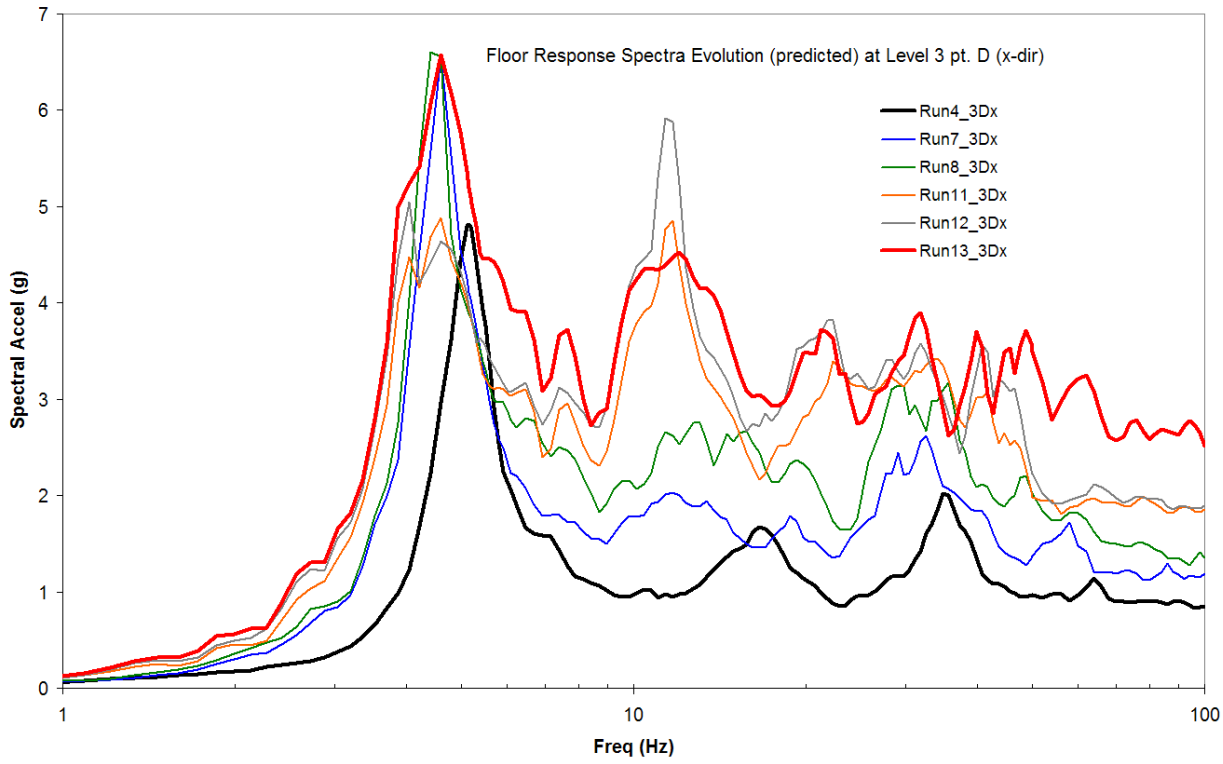

Figure 3-40 Predicted floor response spectra evolution during the application of the ten synthetic earthquake pairs along the x-direction

3.4. Overall Assessment of Prediction Phase

Based on the results of the non-linear analysis model, the general assessment is that the model predicted the experiment very well throughout. The numerical model was able to accurately predict the response of the structure on the shaking table under the action of a real earthquake (RUN3) which induced a very long free-vibration tail to the actual structure during the test. In addition, the analysis model was able to reproduce the response for structural accelerations, displacements and reinforcing bar strains when the structure behaved non-linearly and damage was accumulated in the concrete and the steel with localized yielding.

The agreement was good even though uncertainties regarding the test configuration and thus its numerical implementation exist. These uncertainties that have a profound effect on the structural response stem primarily from the shaking table whose boundary conditions and dynamic properties are not well understood and are still unavailable. It was indicated by the benchmark organizers during the close-out workshop that prior to the upcoming second phase of the benchmark efforts will be made to identify the dynamic properties of the shaking table/actuator system. Added to the shaking table uncertainties are lack of data regarding the concrete material and, in particular, the fracture energy that influences its cracking and/or crushing. Generic values were used in the non-linear analysis that may not be representative of the concrete used in constructing the test structure. Further, the need to “optimize” the size of the computational model such that the computational cost of the demanding analysis was manageable most-likely contributed to the small deviations observed between test data and prediction data.

3.4.1. Damping

The energy dissipation of the overall system (concrete structure, shaking table and its supports and of the interface conditions that exist between the bottom of the structure and the shaking table) is identified as the biggest uncertainty and the source of the deviations of the predicted data. The overall energy dissipation in the concrete structure, however, is a combination of the assumed initial damping and of the contribution by the progressing damage in the form of visible and permanent cracks. Given, however, that the accumulated damage in the concrete primarily takes place in micro-scale before it manifests itself into visible and permanent cracks, the non-linear analysis is unable to completely follow the constitutive and damage behaviour at this level.

As it was observed during the SMART2008 actual tests, damage below the threshold of cracking occurs even at very low earthquake intensities (RUN1 through RUN5). To account for that, better concrete damage accumulation models are needed to support the simulation and prediction analyses. In an effort to account for the increased energy dissipation within the concrete material due to micro-cracking (this happens at a scale that the numerical processes are unable to capture), the damping in the concrete was artificially increased during the 13-run analysis as the test progressed towards higher intensity levels. However, as the comparison of the test and predicted results show, these values may require further adjustment. To quantify the effect of the material damping ratio on the structural response using the design level earthquake input (RUN4), different levels of damping were introduced and the structural response was compared. Shown in Figure 3.41 are comparisons of structural accelerations in y- and x-directions for damping ratios of 1%, 1.5% and 2%. As seen from the comparison, the differences are relatively small.

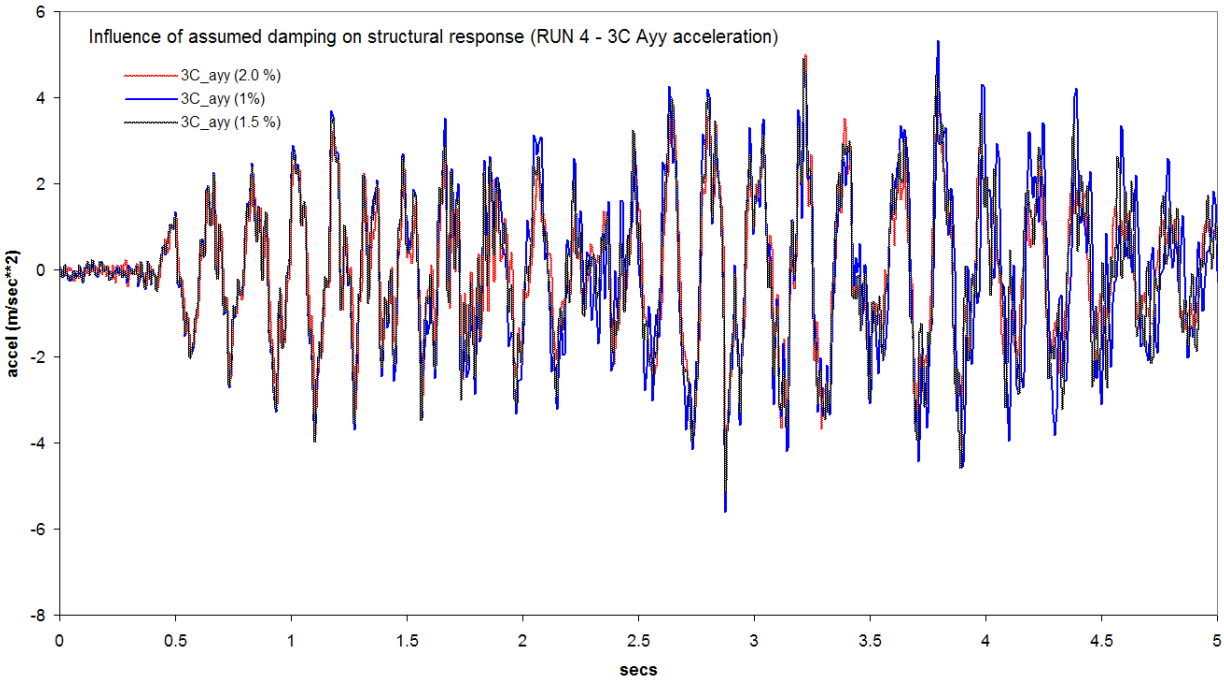

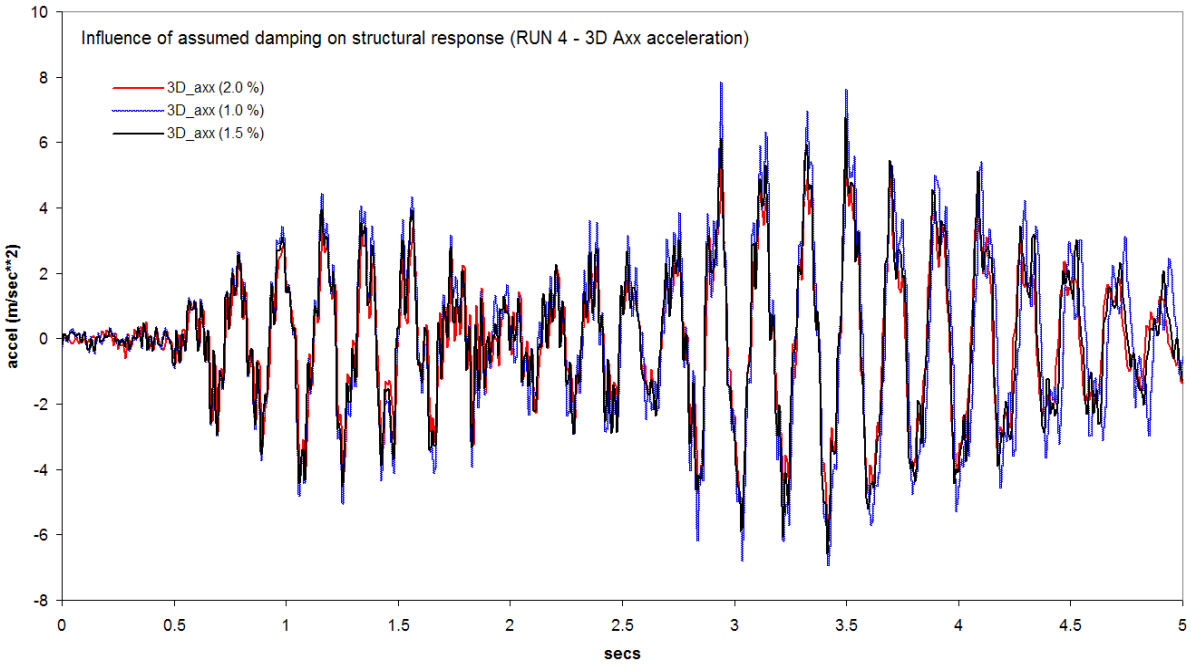

Figure 3-41 Effect of damping ratio on structural acceleration response

3.4.2. Torsional Effects

In an effort to address the torsional effects on the SMART2008 structure, a different model, shown in Figure 3.42 was generated and analysed under seismic loading. The structure depicted in Figure 3.42, has a rectangular, closed cross-section and it is made of the same materials as the actual SMART2008 structure. While the structure is not perfectly symmetric (different openings in the x- and y-walls as well as a floor support beam running only along the y-direction), it has eliminated the primary contributors to torsional behaviour.

In order to qualitatively assess the torsional effects the new, closed-section structure was analyzed for modes and frequencies and seismic excitations RUN3 and RUN6 and compared with the SMART2008 structural response and modal characteristics.

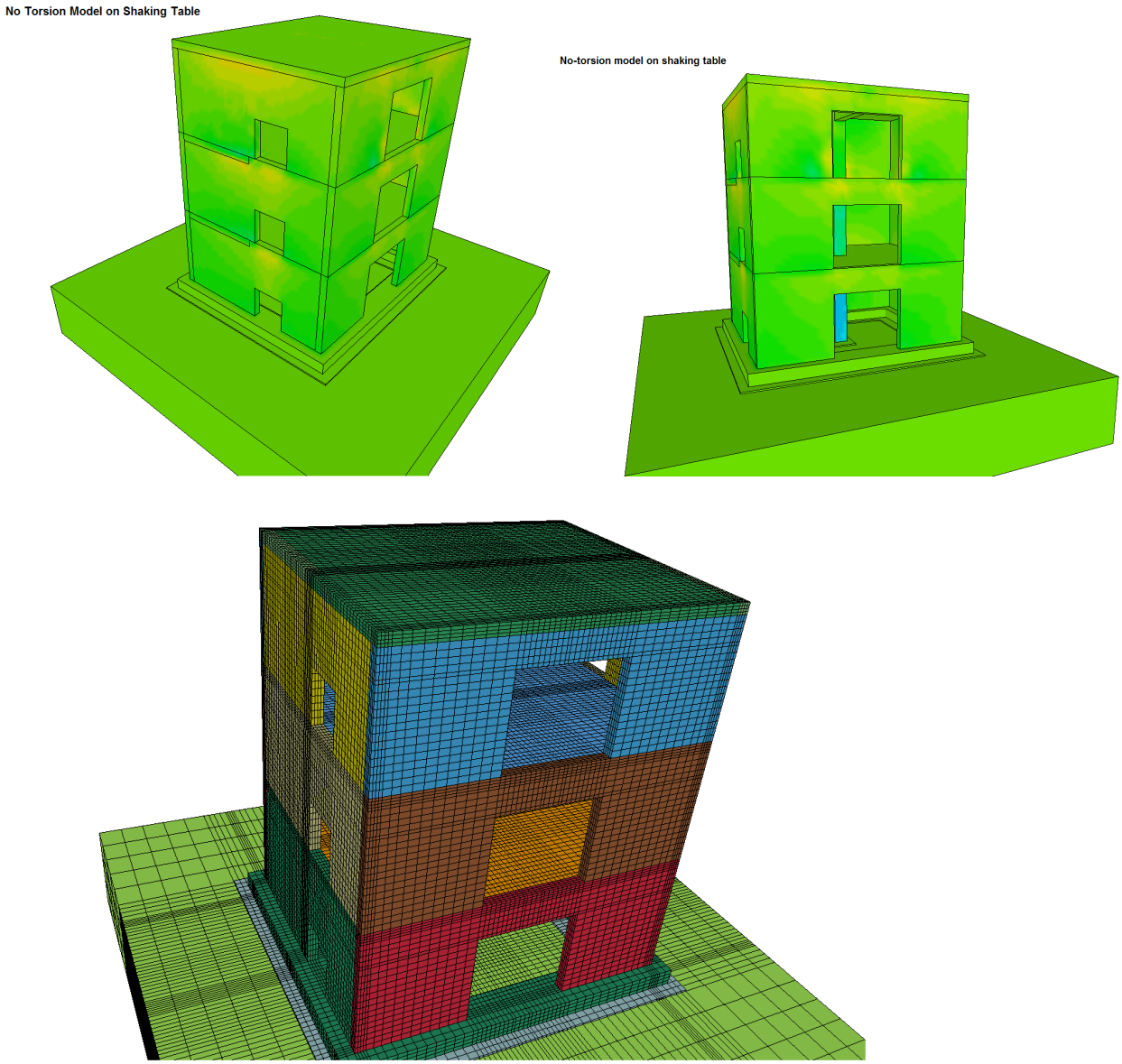

Figure 3-42 Model of a SMART2008-like structure on the shaking table with a rectangular instead of trapezoid cross section

Shown in Figures 3.43 are the fixed-base modes of the two structures. In the case of the SMART2008 structure the two first modes are not purely flexural but a combination of flexural and torsional. This, however, is not true for the rectangular, closed-section structure which exhibits pure flexural modes with higher eigenfrequencies indicating that the structure is stiffer.

The accelerations along the x- and the y-directions of the four corner locations of the third level of the rectangular structure are depicted in Figure 3.44. It is evident that there are minimal variations between the movements of the four corner locations implying the absence of torsional effects. For the actual SMART2008 structure, however, the accelerations at the extreme corners C and D shown in Figure 3.45 vary significantly indicating that the structure is experiencing torsion.

As shown in Figure 3.46 the actual SMART2008 structure experiences extensive cracking which is attributed to torsion exerted on the structure. This is evident from (a) the orientation of cracking in the central column (shear cracks), and (b) the cracking in the shear walls and the base. On the other hand, the rectangular, closed-section structure where the asymmetries are kept to a minimum experienced very little damage under the same loading. The slight damage observed is in the concrete beam which only runs along the y-direction.

Shown in Figure 3.47 are the acceleration response spectra at the shaking table level of input signals RUN3, RUN4 and RUN5 in the x and y directions. Also shown in the same figure is the torsional mode of the structure and the corresponding frequency f_t = 16.884 Hz. It can be observed that the torsional frequency of the structure on the shaking table coincides with a significant peak in the response spectrum of the input signals. This leads to the conclusion that the torsional effects are accentuated during the action of these signals. The effect was observed during the actual tests where the torsional frequency dropped significantly during RUN5 indicating that damage in the concrete was accumulated in the form of micro-cracks at a higher rate due to this “torsional” resonance.

Figure 3.48 compares the response spectra at the third level between the actual SMART2008 structure and the one of rectangular cross section where most of the asymmetries have been eliminated during RUN3. It can be observed that the spectral peak close to the torsional frequency of the structure (16.884 Hz) has disappeared for the rectangular structure which experiences no torsional effects. Similarly in Figure 3.49, response spectra comparison is depicted for RUN6.

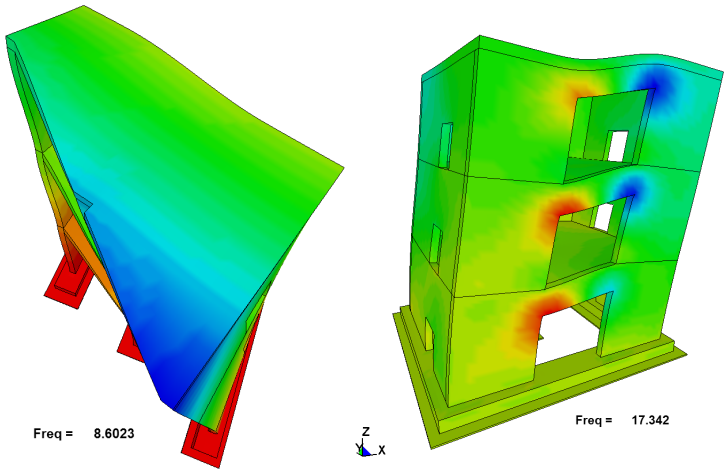

(a) “flexural” mode along x-axis (for the trapezoidal SMART2008 structure the mode is a combination of flexural and torsional)

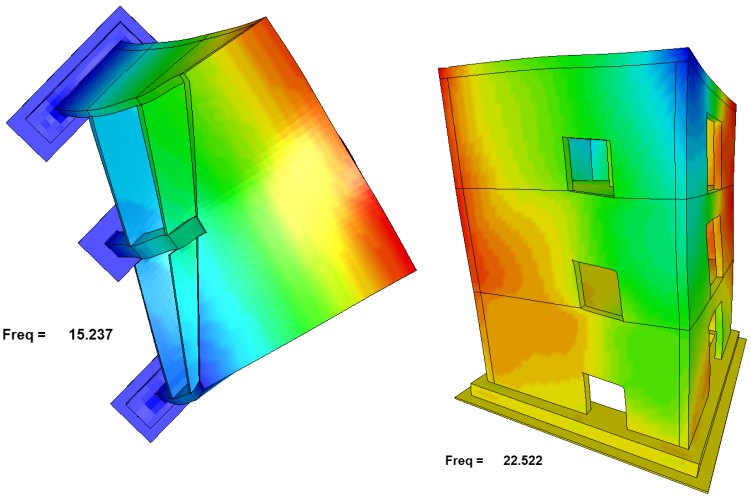

(b) “flexural” mode along y-axis (for SMART2008 structure the “flexural” mode is a combination of flexural and torsional)

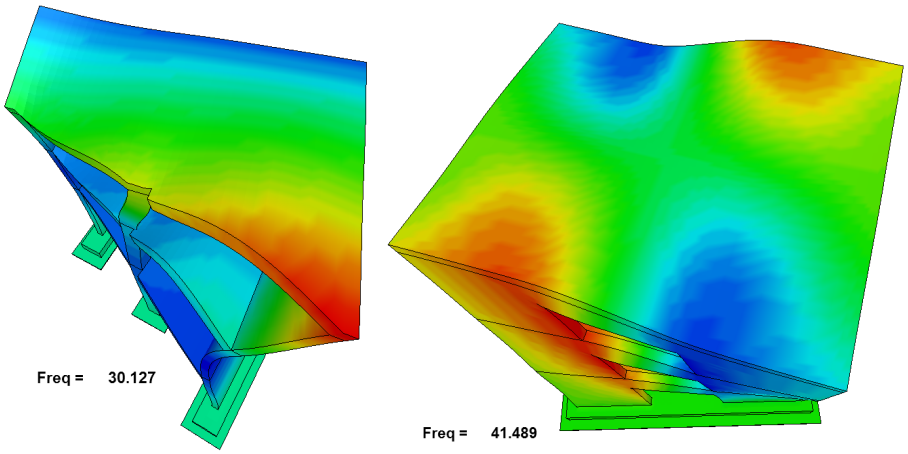

(c) torsional mode

Figure 3-43 Fixed-base mode comparisons between the trapezoidal SMART2008 structure and the one with rectangular cross section generated for comparison purposes

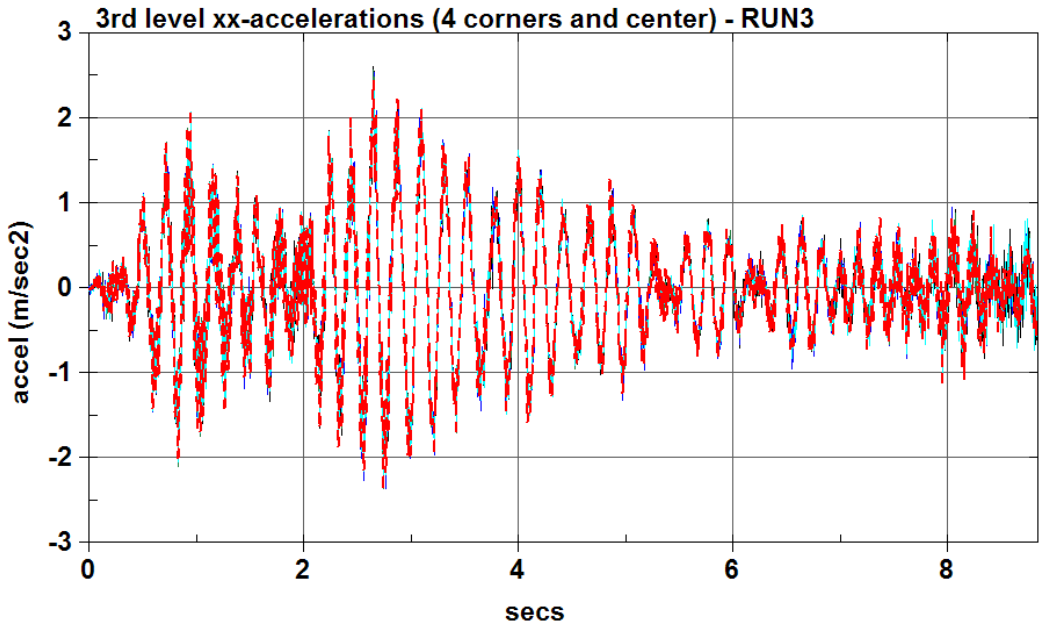

(a)

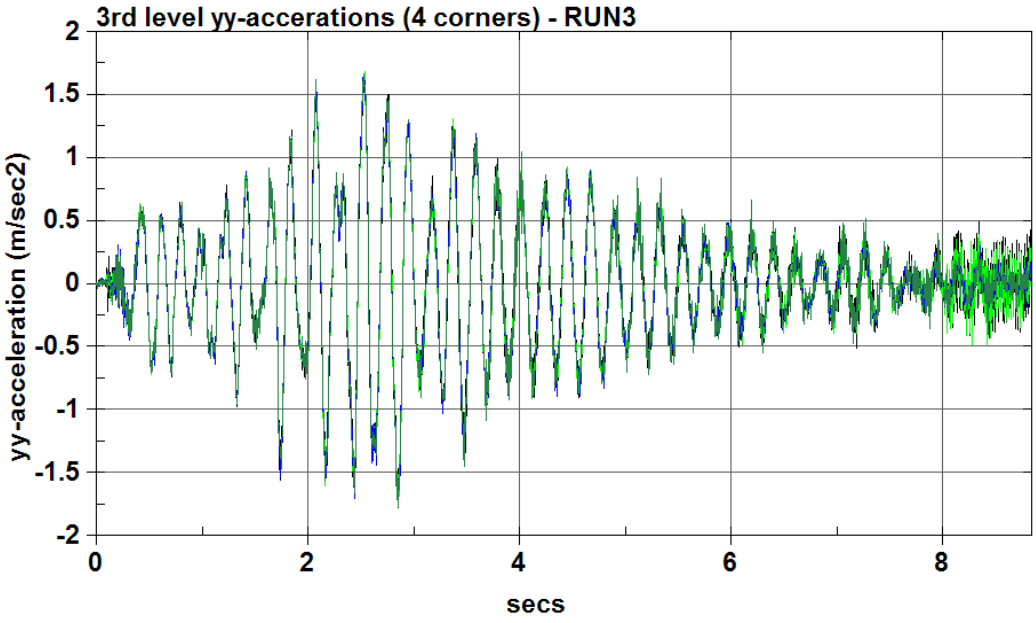

(b)

Figure 3-44 **Accelerations computed at the four corners of the rectangular cross section SMART2008-like structure for RUN3: (a) x-direction acceleration and (b) y-direction acceleration showing minimal variation between the acceleration traces and indicating that the structure is not exhibiting torsional behaviour**

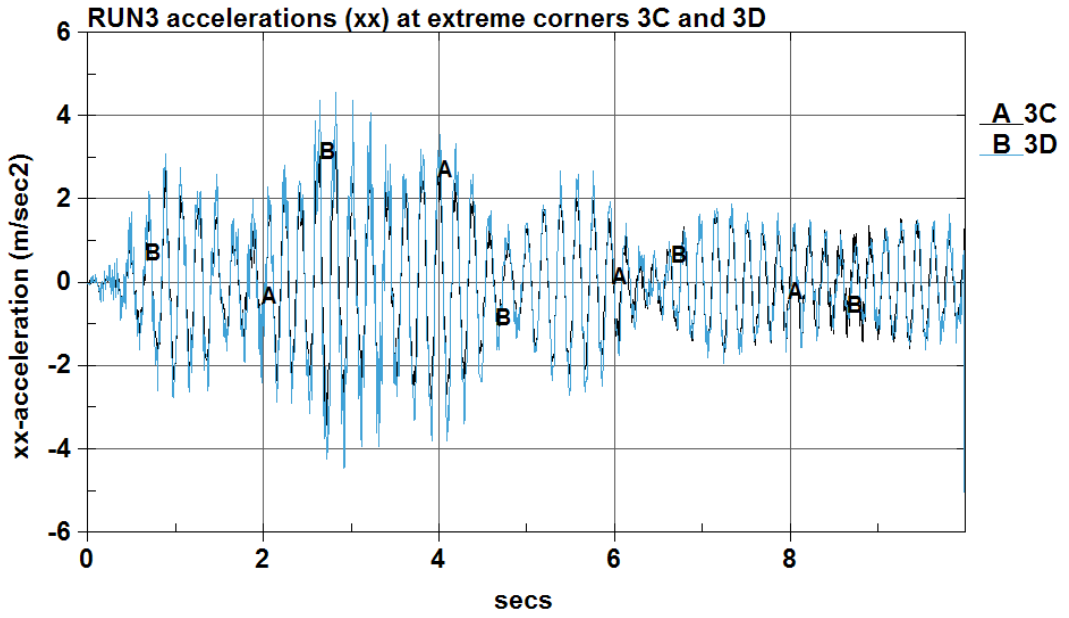

(a)

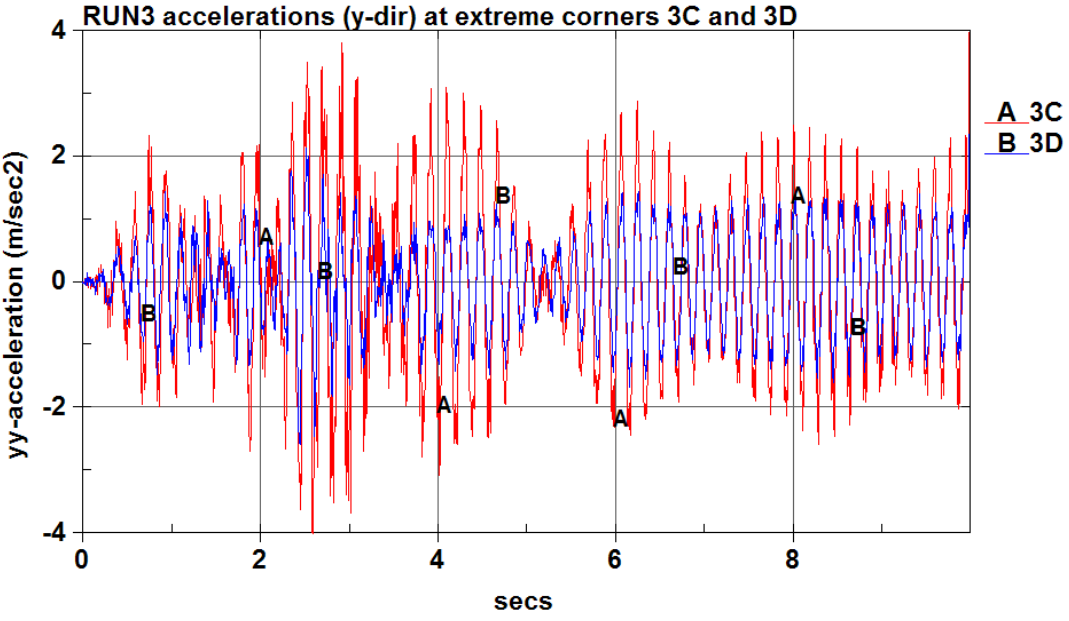

(b)

Figure 3-45 **Accelerations computed at two extreme locations of the trapezoidal SMART2008 structure (corners C and D) for RUN3: (a) x-direction acceleration and (b) y-direction acceleration. Depicted is the significant variation in acceleration amplitude indicating a torsional behaviour of the structure**

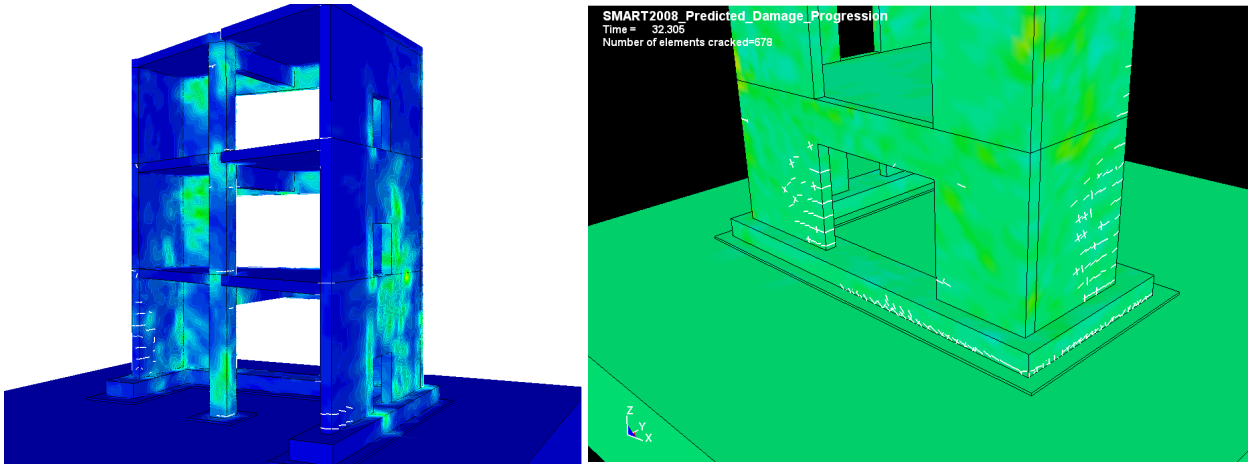

(a) SMART2008 structure

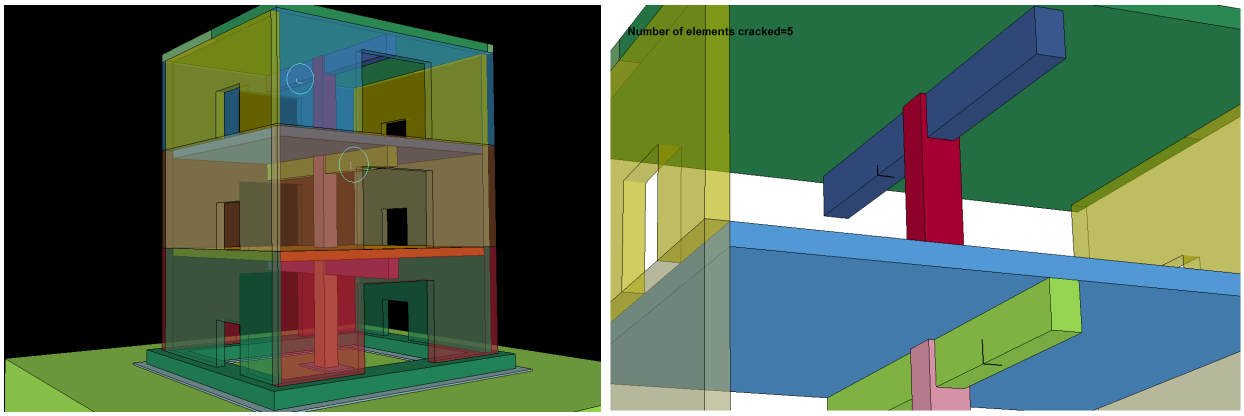

(b) Rectangular cross-section structure

Figure 3-46 Damage sustained by the two different structures under the sameseismic load: (a) actual SMART2008 structure, and (b) rectangular SMART2008-like structure with minimal asymmetries

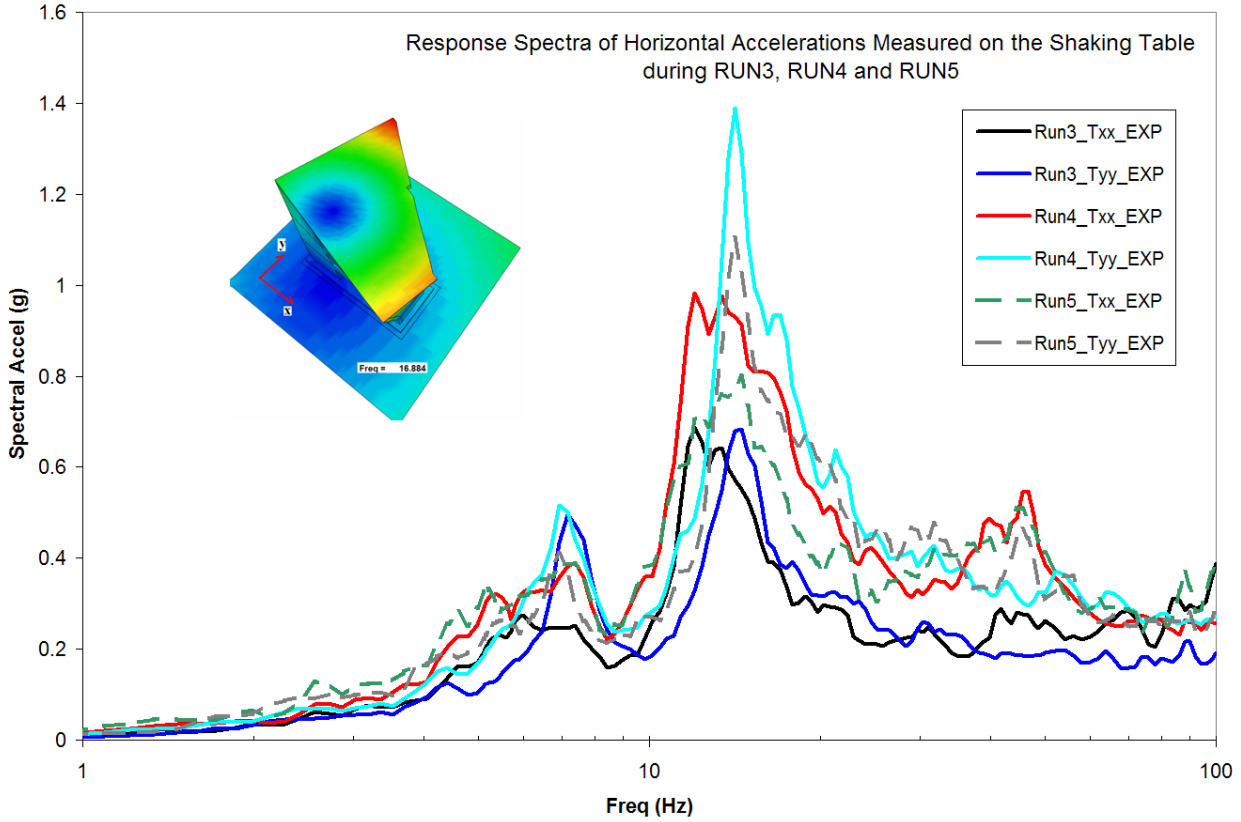

Figure 3-47 Response spectra of input accelerations signals RUN3, RUN4 and RUN5 along x and y directions and the torsional mode (insert) of the SMART2008 structure on the shaking table (ft = 16.884 Hz)

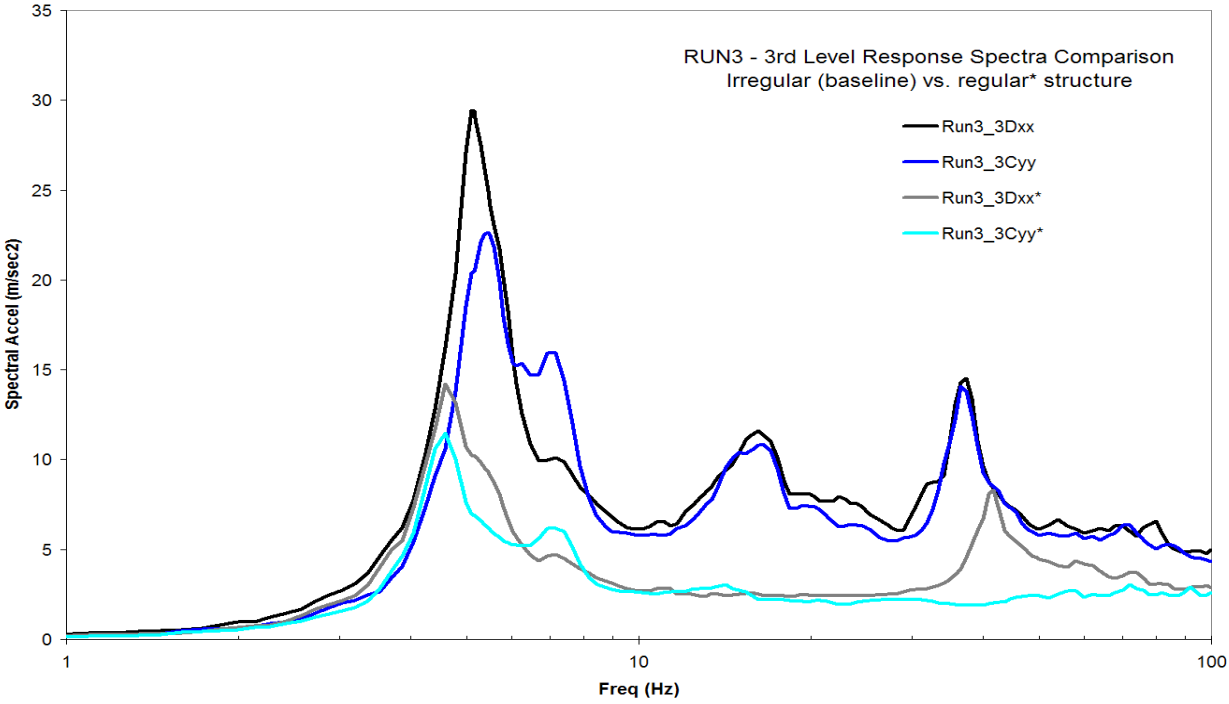

Figure 3-48 Third-level acceleration response spectra of the two structures (actual SMART2008 and rectangular version) for RUN3 input

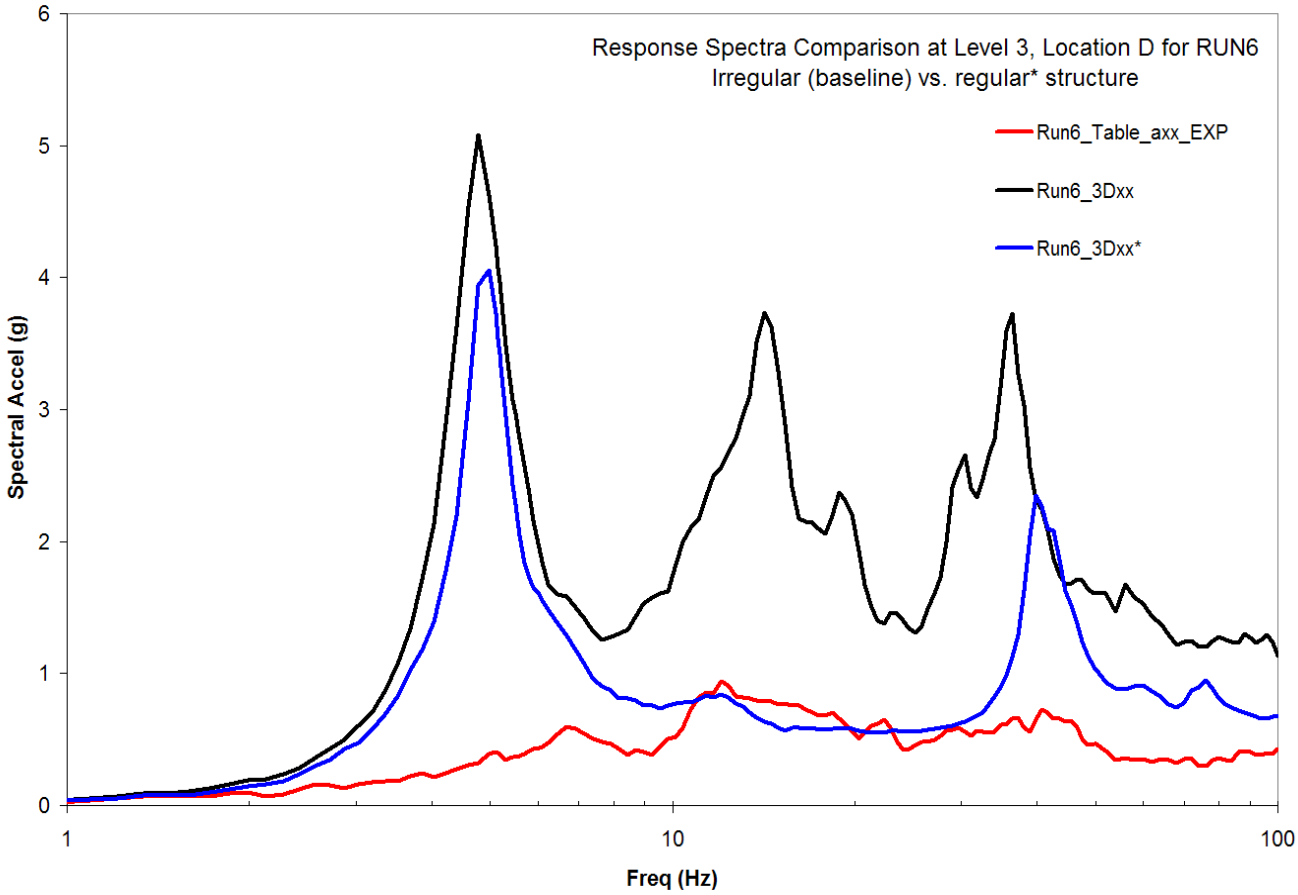

Figure 3-49 Third-level acceleration response spectra of the two structures (actual SMART2008 and rectangular version) for RUN6 input

4. VULNERABILITY ASSESSMENT OF 3-D NUCLEAR STRUCTURES

Following the shaking table test prediction effort of the SMART2008 benchmark, a 2nd phase of the activity was launched that was dedicated to variability, sensitivity and vulnerability analysis based on numerical models developed for the SMART test specimen. The objectives of the effort were to (a) quantify the influence of uncertainties that exist in the estimation of design parameters of the structure on the response and (b) investigate structural vulnerability methods and derive fragility curves for typical limit states. Uncertainties typically surround the generation of fragility curves for structural systems, where the variability of the structural demand is convoluted with the variability in the structural capacity. The resulting fragilities are compared with limit states that themselves exhibit uncertainties in their specification. Thus, the vulnerability part of the benchmark represented a serious attempt to streamline an important aspect of safety in structural design.

Given the significant uncertainties surrounding the interaction between the shaking table used in the experimental effort and the SMART structure, it was recommended by the benchmark organizers that a fixed-base representation of the SMART three-dimensional structure be adopted for both the sensitivity and the fragility analysis. Figure 4.1 depicts the numerical representation of the SMART structure used in the subsequent analyses where the shaking table was reduced to rigid plane and the structure is supported through the base steel plates as the appear in the design.

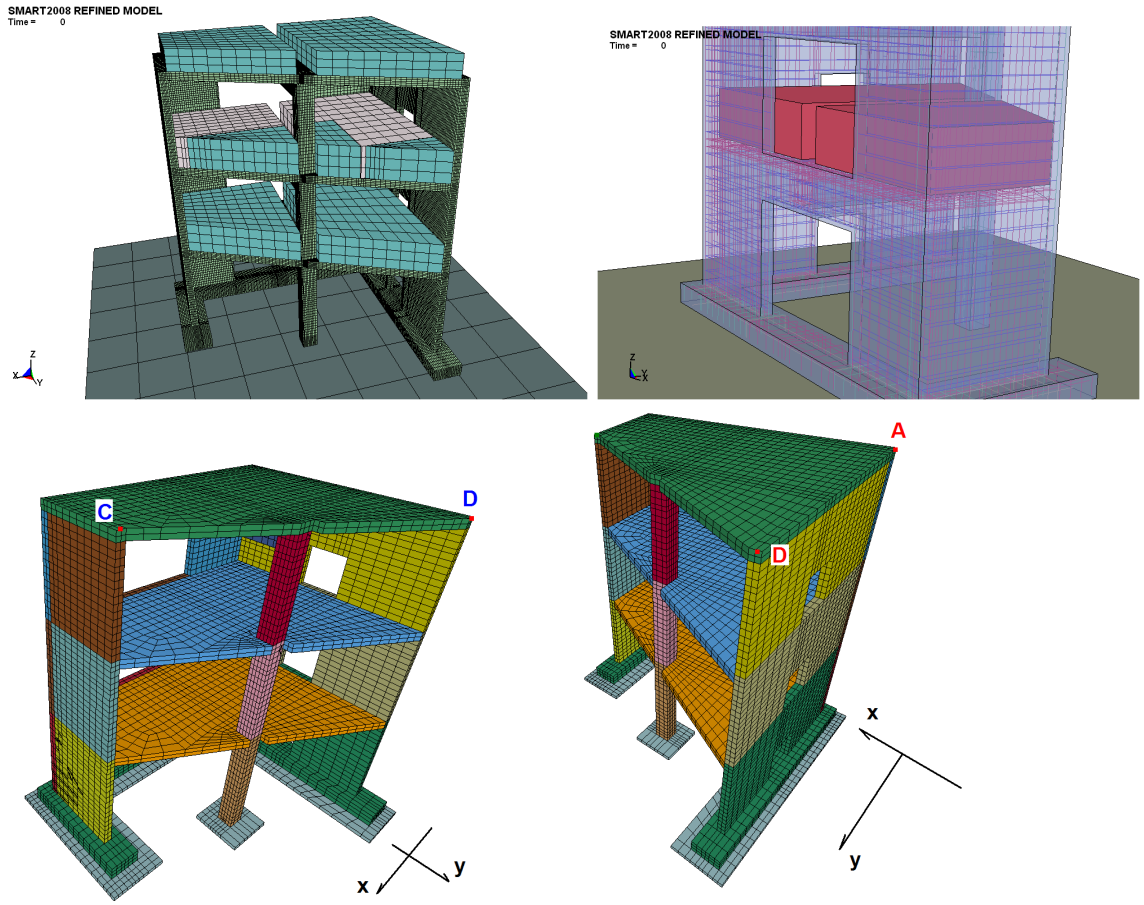

Figure 4-1 Numerical model used in the sensitivity analysis of the test structurealso depicting locations for floor response spectra generation

4.1. Sensitivity Studies

Though the sensitivity study, which aimed to quantify (a) the variability in the seismic response of the SMART2008 structure and (b) identify the contribution stemming from uncertainties in input design parameters such as material properties, the influence of nonlinearities was sought. Specifically, by establishing a range around the nominal value of structural properties that influence the design of the structure, the response of the structure was evaluated at (a) the seismic design level and (b) a seismic level significantly exceeding the design level earthquake.

Given that the design of the test structure followed a seismic code for nuclear structures which only allows for linear/elastic response, this phase of the study focused on quantifying the potential for the appearance of nonlinearities even at the design level earthquake. This was achieved by considering nonlinearities in the structural materials (i.e. bilinear stress-strain relations in the rebar and yielding uncertainty as well as non-linear behavior in the concrete beyond the allowable design stress by permitting cracking to appear) and by observing and analyzing floor response spectra generated by the nonlinear time history analyses. Appearance of nonlinearities in the structural response will impact the natural structural modes by (a) shifting the frequencies in the floor response spectra and (b) changing the displacement response or floor drifts anticipated in the structure for nominal or design values of the structural parameters.

It is also expected that even without the appearance of non-linear behaviour of the structure, the overall response will be influenced by the variability of the structural properties due to the changes in the fundamental modes of the overall structure. This in turn, when convoluted with the earthquake input frequency or period content, is expected to have a significant effect on the floor response spectra and consequently on the design of secondary systems.

The variability in material properties, the seismic input characteristics and the results of the nonlinear sensitivity analyses are described in the following subsections.

Variability Matrix of Structural Properties

In an effort to cover uncertainties in estimating influential design parameters such as concrete strength, rebar yield, structural damping and live loads, the variability matrix shown in Table 4.1 was established. The objective was to study and quantify the influence of each parameter on the structural response individually by studying its effect through the entire range of values while maintaining the nominal value for the remaining varying fields. Table 4.1 depicts the range of the four design parameters evaluated in this sensitivity study and the twelve distinct cases for each seismic input level used.

Each set of properties defines the dynamic characteristics of the structure prior to applying the base excitation. The choice of properties, regardless of the input, results in a variation of the eigenfrequencies of the fixed-base structure and in particular those cases where the concrete modulus E_c and the added mass are being varied. Therefore, even when the structure during the nonlinear analysis remains within the linear range, variation in the response is expected.

Seismic input

For this parametric study, two sets of horizontal synthetic accelerograms (one for each horizontal direction) were used to study the impact of parameter uncertainty. These accelerograms were derived from a white noise power spectrum, a process that prevented any bias towards a particular frequency band. Two seismic levels were selected to study the variability of the response; namely,

□
□□□□ at design level (with PGA equal to 0.2 g)
□□□□ at over design level (with PGA equal to 0.6g)

The acceleration time histories used in this parametric study were provided by the SMART200 benchmark organizers and had a duration of T_{dur} = 5 secs with a time step of Δ_t = 0.005 sec.

Figures 4.2a and 4.2b depict the pairs of horizontal accelerations used in the time integration analyses (nonlinear) and the response sensitivity assessment. Shown in Figure 4.3 are power spectral densities of the input accelerations for both the 0.2g and the 0.6g earthquake pairs. Based on the number of realizations per seismic level shown in Table 4.1, a total of twenty four (24) independent analyses were performed and post-processed.

Response Output

The parametric or sensitivity analysis was based on the following response variables:

(a) Maximum inter-story drifts (differential displacement between two floors) at each floor for the corner point A in the x and the y directions and point D in the x direction. The idea behind the selection is to compare the variability in the global response of the structure near the torsional center with that at a location at the extremity of the structure (as seen in Figure 4.1)

(b) Maximum absolute relative displacement experienced by the structure and expressed as the difference between the displacement at the base and any location over the vertical walls

(c) Floor response spectra at Level 3, and at locations D and C shown in Figure 4.1. Response spectra in the x-direction were to be evaluated at location D and along y-direction at location C.

Parametric Study Results

Shown in Figure 4.4 are the first three eigenmodes for the structure for five of the twelve parameter sets depicted in Table 4.1. The computed eigenfrequencies for the fixed-base SMART structure differ significantly from those of the actual structure that was tested on the shaking table. In particular, the eigenfrequencies for the second mode (flexural mode along the y-direction) and the third mode (twisting about the vertical axis) are much higher than the counterparts of the actual structure on the shaking table. As discussed previously, this is attributed to the interaction of the structure with the massive table.

Figures 4.5 through 4.9 depict response spectra computed on level 3 of the structure under different realizations of the structural parameters and seismic input pairs. Evident are the "nonlinear" effects on the response spectra that are induced by the 0.6g seismic input.

Shown in Figure 4.10 are inter-story drift transients between floors of the test structure for the 0.6g seismic input pair. The results depicted compare the nominal concrete modulus with the case of the lowest concrete modulus value expected within the parametric space.

Tables 4.2 and 4.3 are summaries of computed inter-story drifts at selected locations (corners A and D of wall #3) on the structure for 0.2g and 0.6g PGA respectively. Table 4.4 lists the maximum relative displacements observed in the fixed-base SMART structure under the action of the two seismic pairs corresponding to 0.2g and 0.6g PGA respectively.

Table 4.1 Structural properties variability matrix used in the sensitivity analysis of the SMART test structure

Case	E (MPa)	Fy (MPa)	Damping (%)	Added Mass (T)
1 - Reference	32 000	500	2	33.85
2	**25 600**	500	2	33.85
3	**28 800**	500	2	33.85
4	**35 200**	500	2	33.85
5	**38 400**	500	2	33.85
6	32 000	**425**	2	33.85
7	32 000	**575**	2	33.85
8	32 000	**650**	2	33.85
9	32 000	500	**0.5**	33.85
10	32 000	500	5	33.85
11	32 000	500	2	**30.46**
12	32 000	500	2	**37.23**

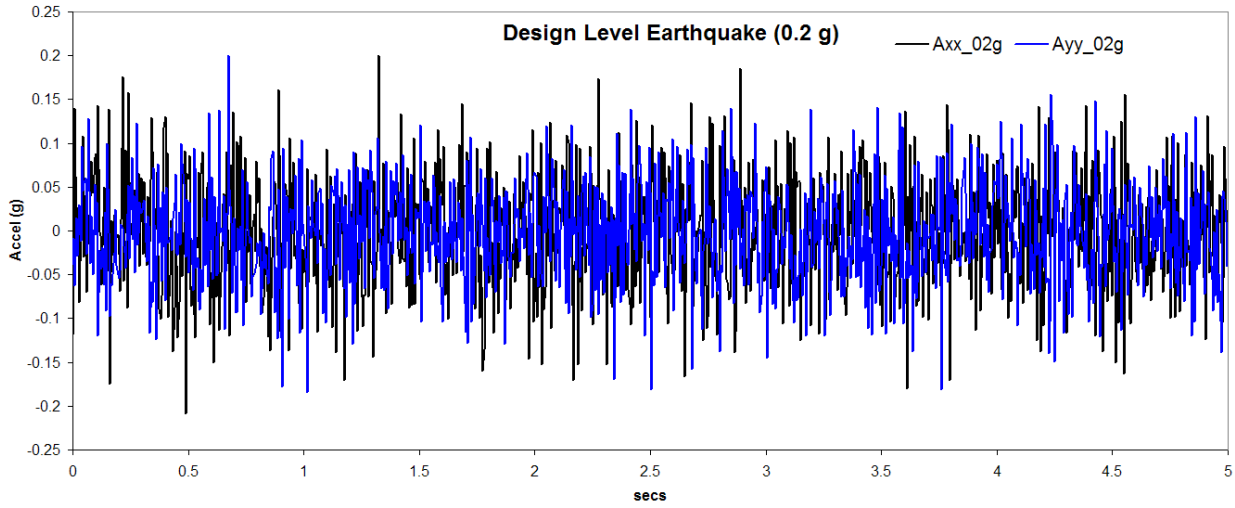

(a)

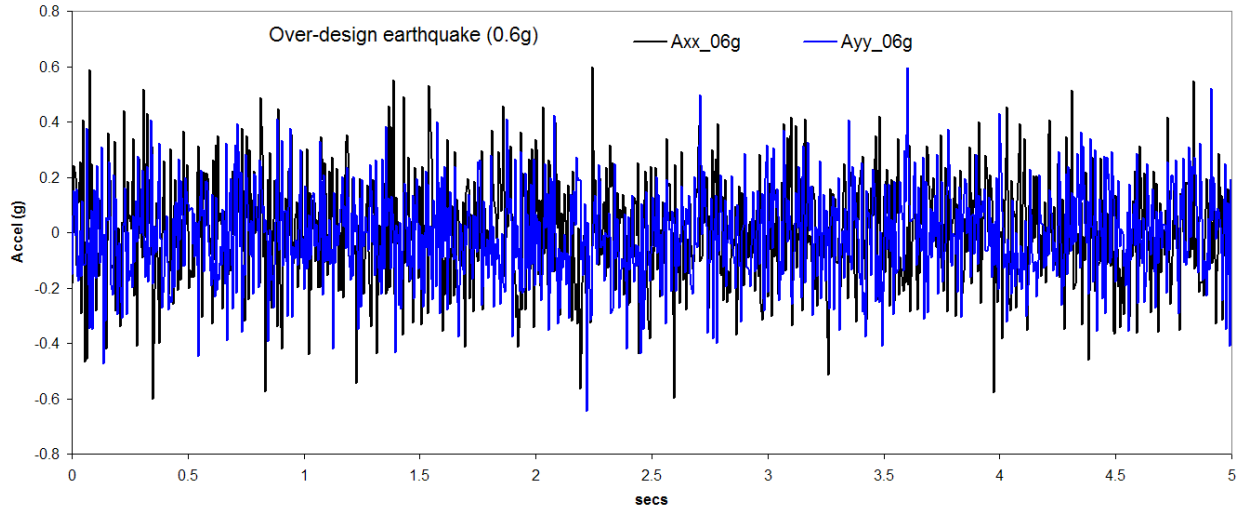

(b)

Figure 4-2 **Bi-directional base input acceleration time histories (synthetic) generated from a white noise power spectrum and used simultaneously in the sensitivity analyses for the 0.2g and 0.4g PGA earthquakes**

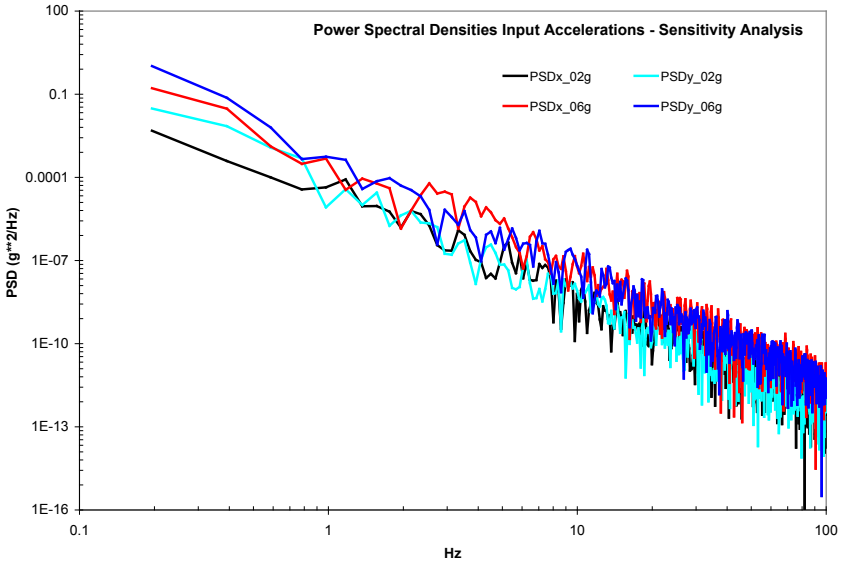

Figure 4-3 Power spectral densities (PSD) of the input accelerations used in thesensitivity analysis

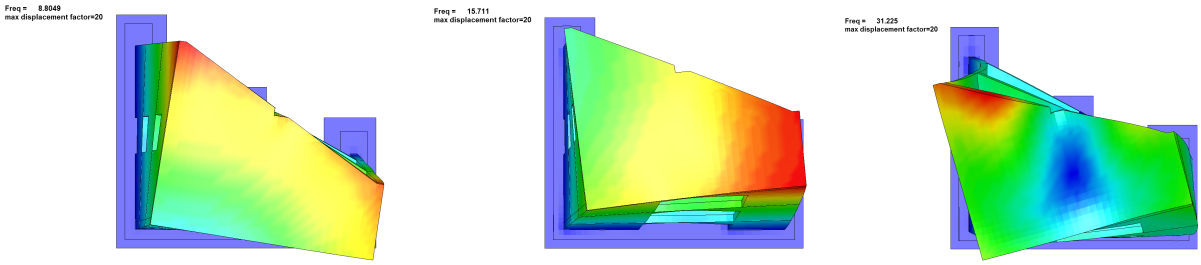

(a) Reference (E_c = 32 GPa; F_y= 500 MPa; M = 33.85 T)

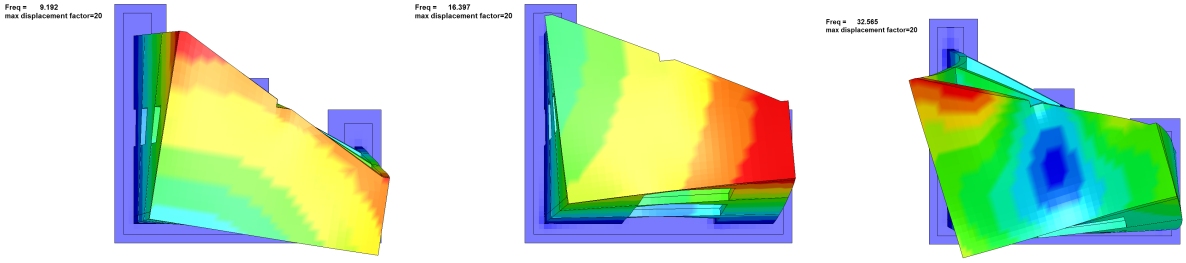

(b) Case 2 (E_c = 25.6 GPa; F_y= 500 MPa; M = 33.85 T)

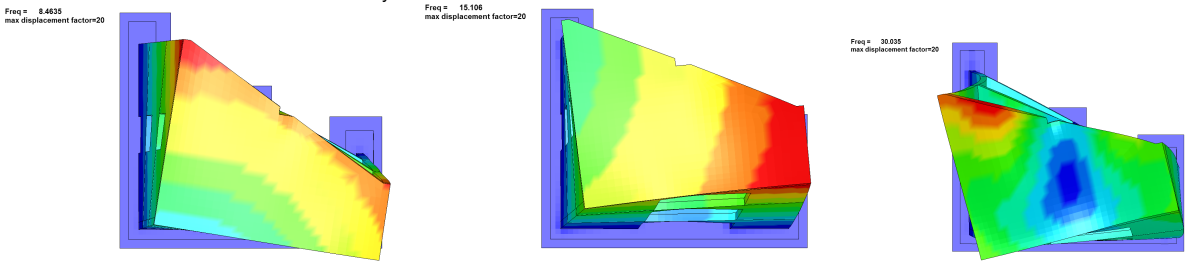

(c) Case 6 (E_c = 38.4 GPa; F_y= 500 MPa; M = 33.85 T)

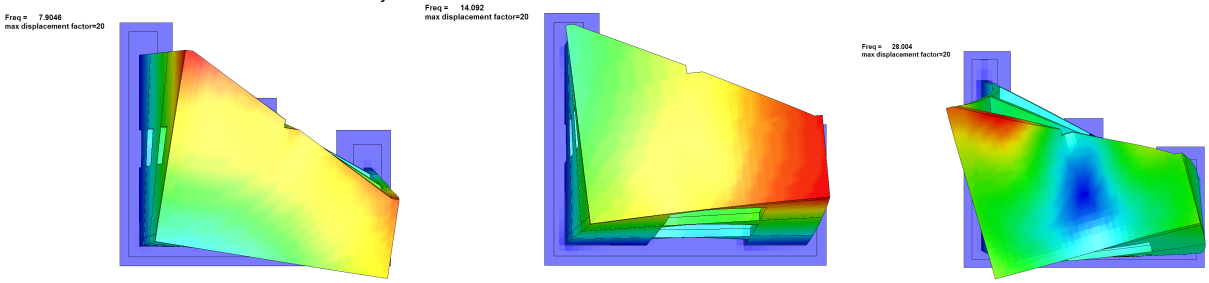

(d) Case 12 (E_c = 32 GPa; F_y= 500 MPa; M = 37.23 T)

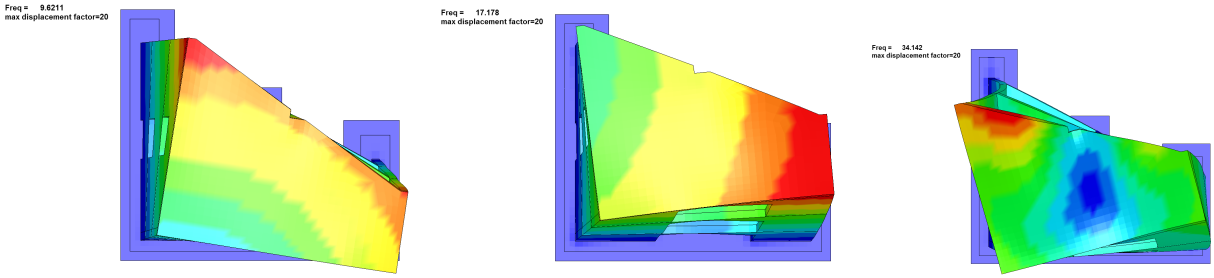

(e) Case 11 (E_c = 32 GPa; F_y= 500 MPa; M = 30.46 T)

Figure 4-4 Influence of the varying structural parameters on the first three eigenfrequencies and modal shapes of the fixed base structure used in the sensitivity study

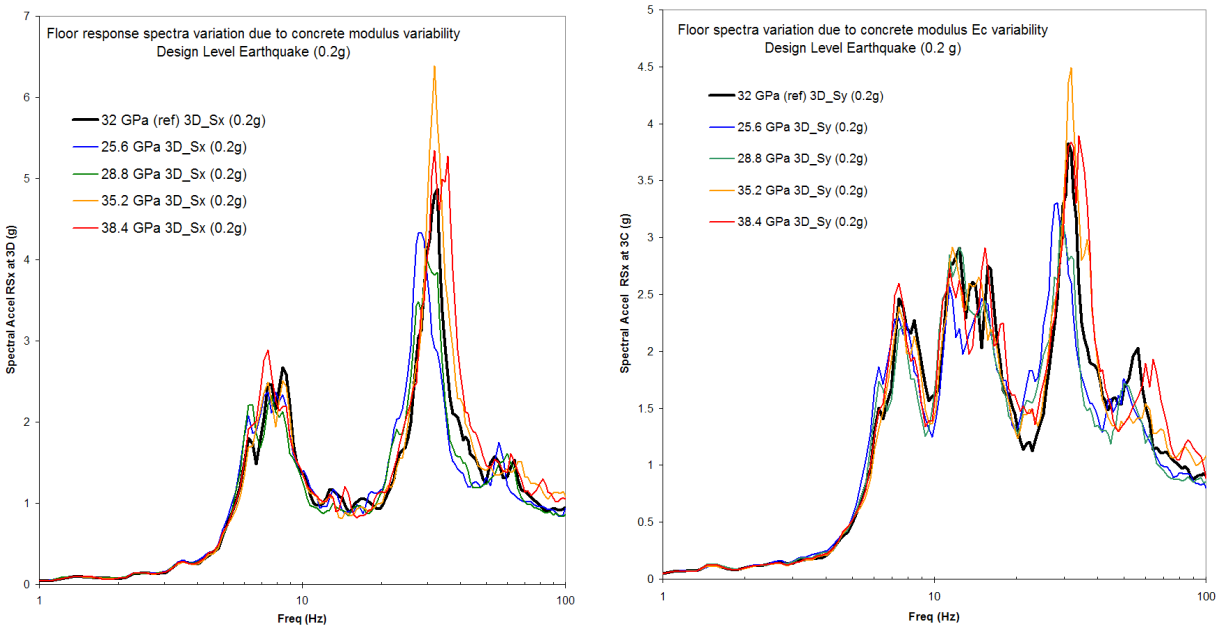

Figure 4-5 **Floor response spectra variability due to uncertainties in the concrete modulus computed on Level 3 (x-direction at D and y-direction at C) for the 0.2g earthquake input pair**

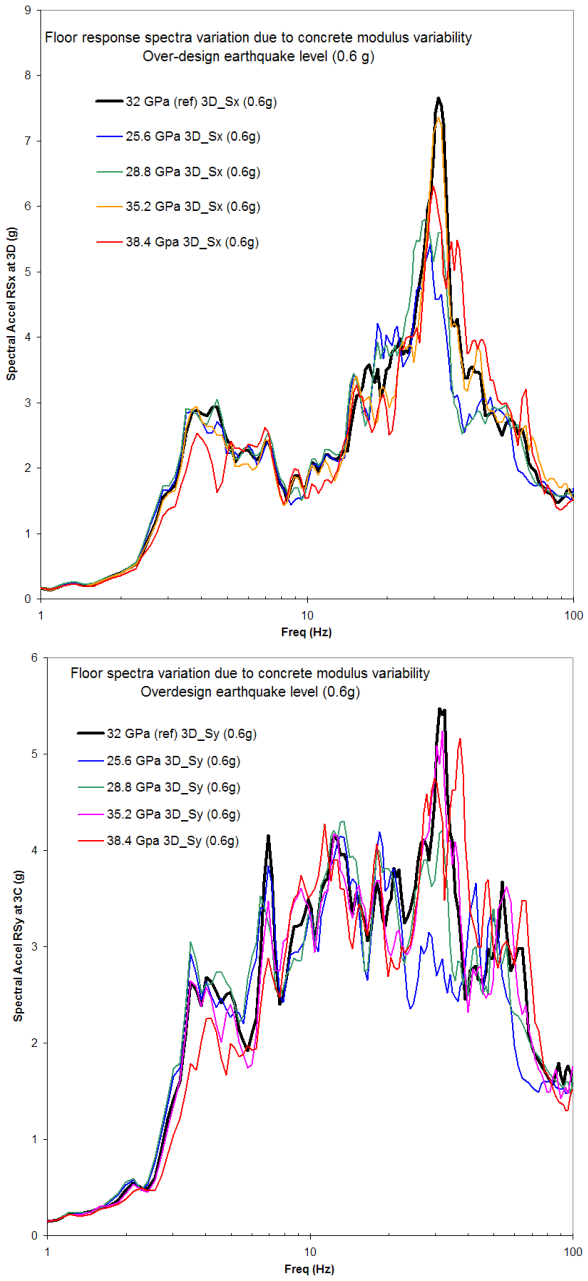

Figure 4-6 **Floor response spectra variability due to uncertainties in the concrete modulus computed on Level 3 (x-direction at D and y-direction at C) for the 0.6g earthquake input pair**

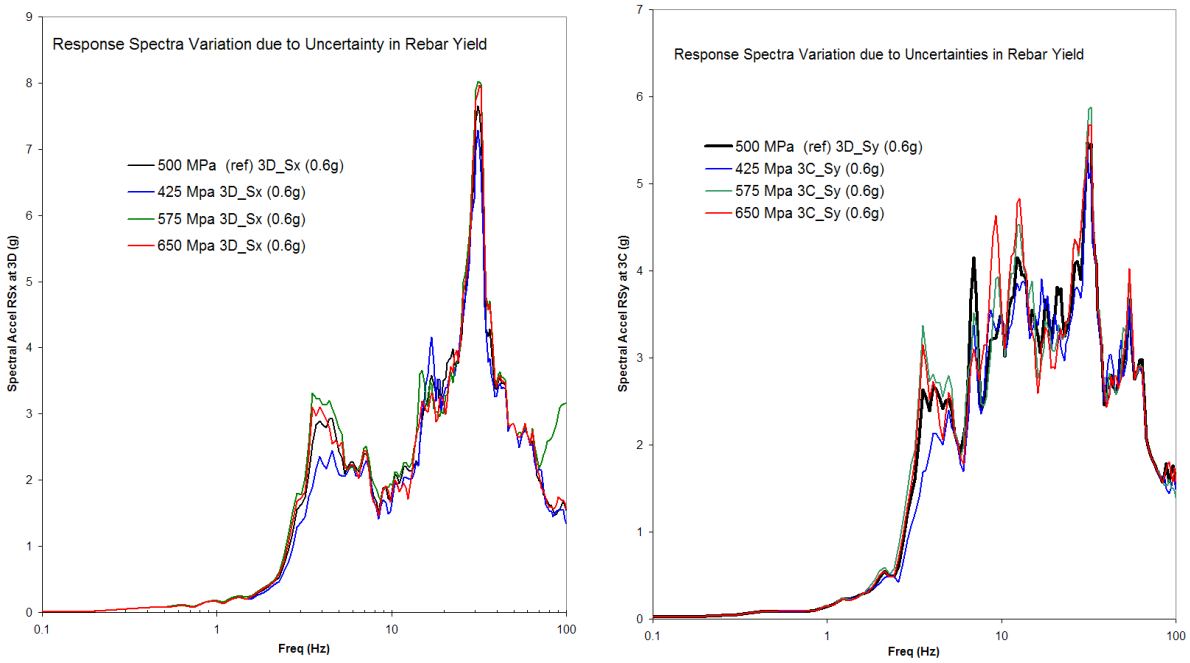

Figure 4-7 **Floor response spectra variability due to uncertainties in rebar yield strength computed on Level 3 (x-direction at D and y-direction at C) for the 0.6g earthquake input pair**

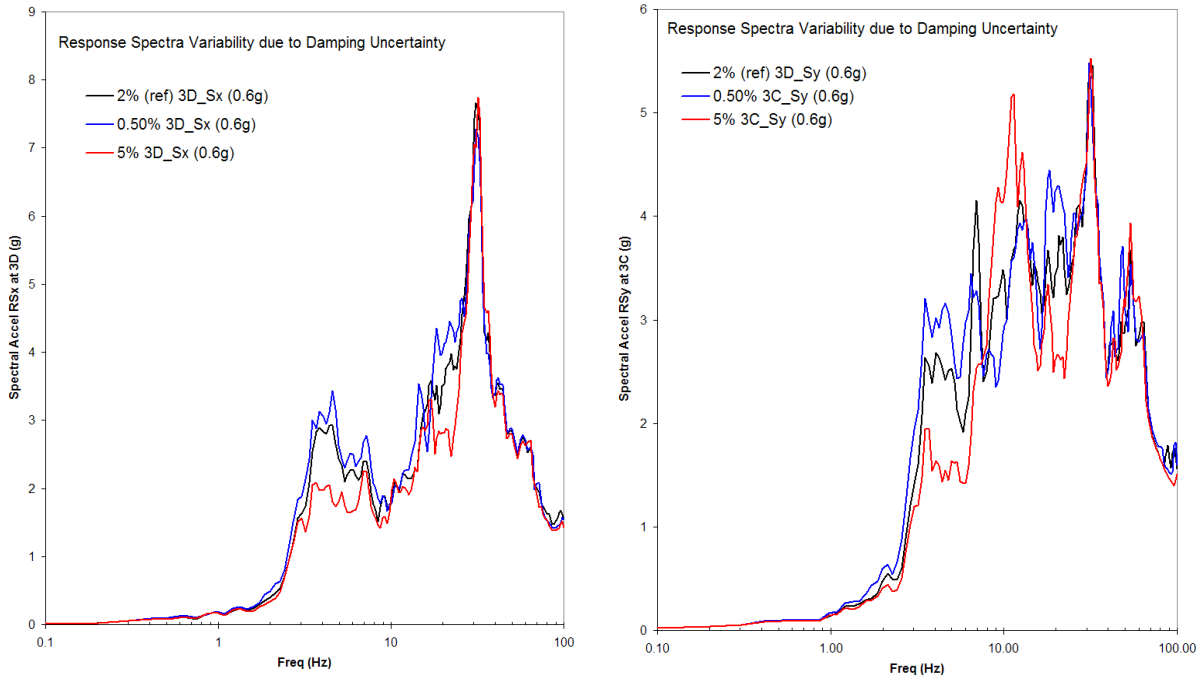

Figure 4-8 **Floor response spectra variability due to uncertainties in structural damping computed on Level 3 for the 0.6g earthquake input pair**

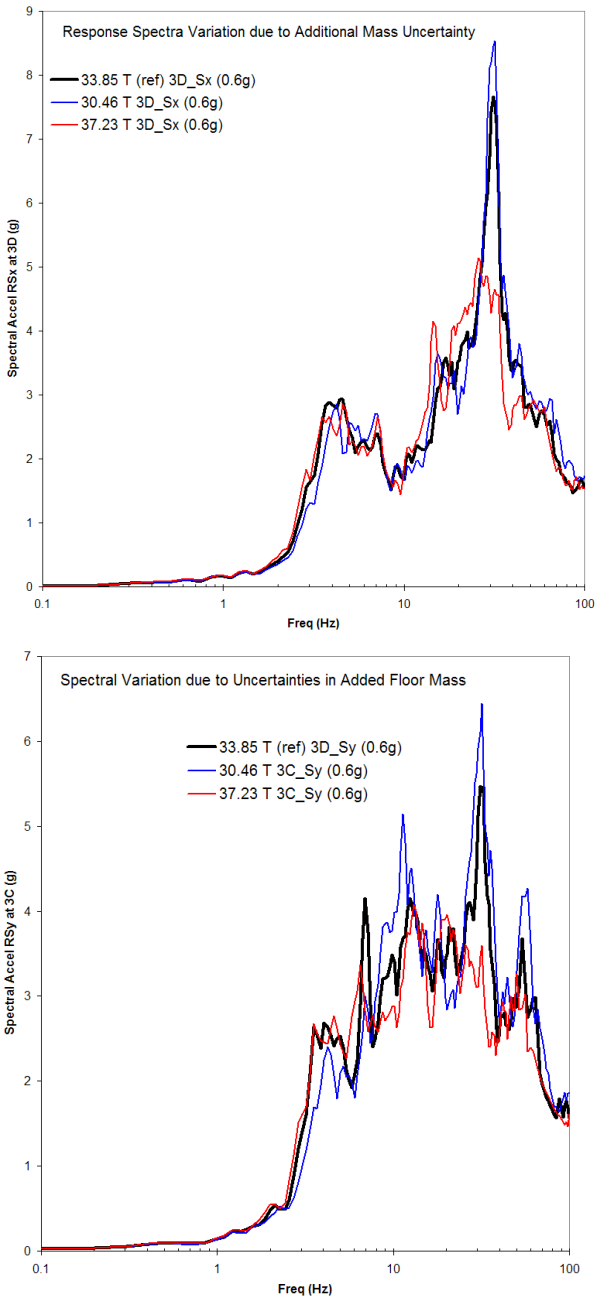

Figure 4-9 **Floor response spectra variability due to uncertainties in added floor mass computed on Level 3 for the 0.6g earthquake input pair**

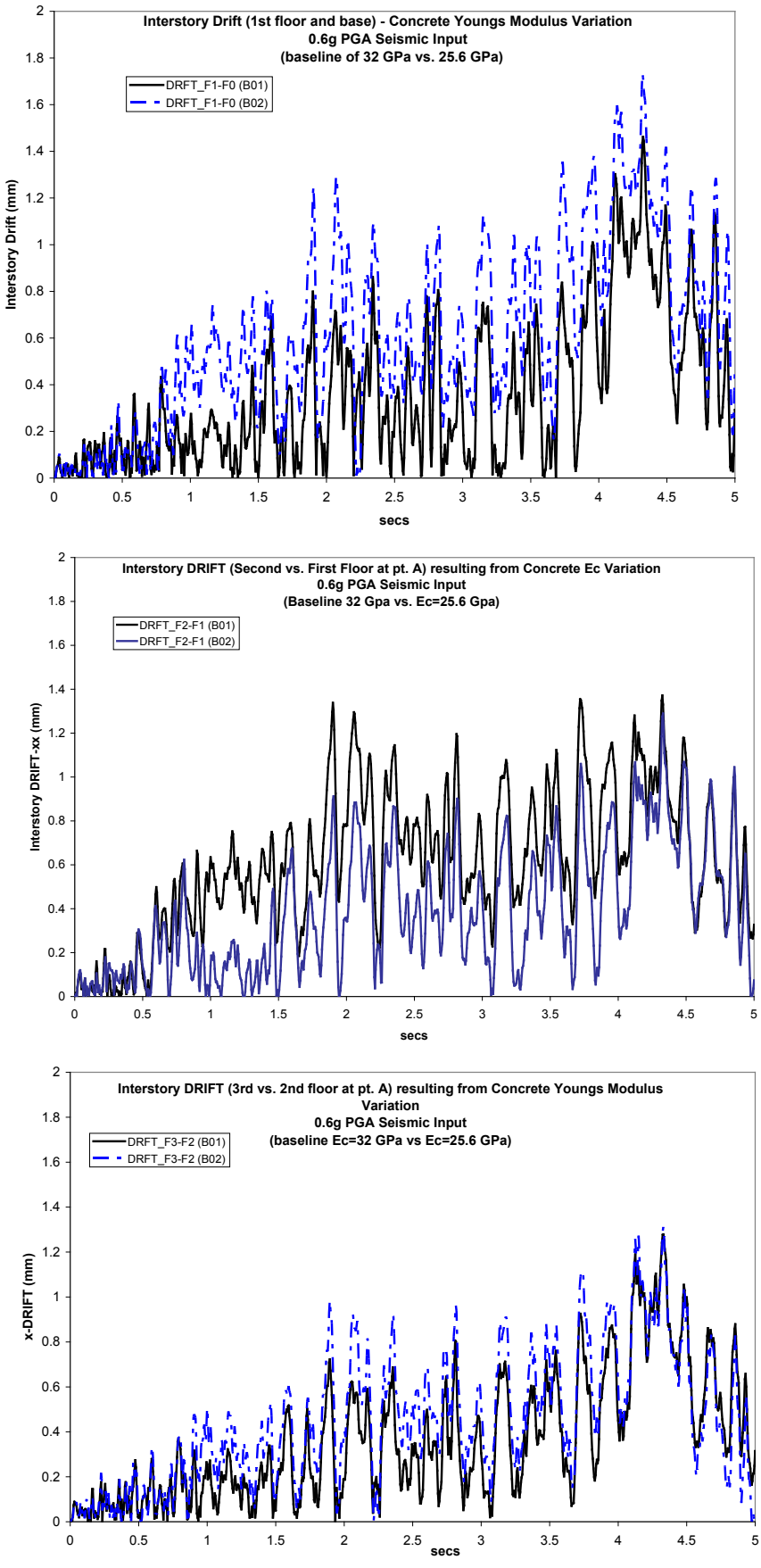

Figure 4-10 Inter-story drift transients for the 0.6g seismic input pair comparing the nominal concrete modulus with the lowest value in the parametric space

Table 4.2 Summary of computed inter-story drifts between structural levels at corner locations A and D for the 0.2g seismic input pair.

	LEVEL 1			LEVEL 2			LEVEL 3		
	pt. A	pt. A	pt. D	pt. A	pt. A	pt. D	pt. A	pt. A	pt. D
Case	x-dir	y-dir	x-dir	x-dir	y-dir	x-dir	x-dir	y-dir	x-dir
1-Ref	0.28	0.187	0.66	0.295	0.2	0.73	0.302	0.181	0.741
2	0.288	0.125	0.68	0.267	0.147	0.774	0.258	0.141	0.831
3	0.35	0.17	0.794	0.33	0.186	0.826	0.3	0.176	0.828
4	0.332	0.195	0.693	0.31	0.191	0.722	0.318	0.154	0.69
5	0.326	0.18	0.78	0.326	0.177	0.764	0.322	0.166	0.78
6	0.28	0.187	0.66	0.295	0.2	0.73	0.302	0.181	0.741
7	0.28	0.187	0.66	0.295	0.2	0.73	0.302	0.181	0.741
8	0.28	0.187	0.66	0.295	0.2	0.73	0.302	0.181	0.741
9	0.4	0.2	0.9	0.392	0.192	0.88	0.34	0.174	0.853
10	0.23	0.13	0.5	0.241	0.151	0.59	0.226	0.151	0.562
11	0.3	0.2	0.69	0.303	0.196	0.82	0.297	0.178	0.827
12	0.315	0.181	0.736	0.284	0.191	0.83	0.28	0.185	0.838

Table 4.3 Summary of computed inter-story drifts between structural levels at corner locations A and D for the 0.6g seismic input pair.

	LEVEL 1			LEVEL 2			LEVEL 3		
	pt. A	pt. A	pt. D	pt. A	pt. A	pt. D	pt. A	pt. A	pt. D
Case	x-dir	y-dir	x-dir	x-dir	y-dir	x-dir	x-dir	y-dir	x-dir
1-Ref.	1.62	0.8	4.62	1.35	0.57	4.26	1.29	0.552	3.94
2	1.85	0.74	4.8	1.432	0.61	4.32	1.38	0.6	3.944
3	1.817	0.77	4.93	1.41	0.595	4.454	1.38	0.568	3.94
4	1.64	0.753	4.18	1.48	0.49	3.9	1.41	0.478	3.5
5	1.47	0.8	3.14	1.1	0.53	2.93	1.12	0.5	2.7
6	1.373	0.826	4.135	1.147	0.616	3.57	1.076	0.6	3.25
7	1.908	0.785	5.16	1.516	0.604	4.6	1.486	0.58	4.24
8	1.955	0.534	4.816	1.543	0.42	4.444	1.442	0.41	4.01
9	1.333	0.78	4.33	1.165	0.736	4.25	1.128	0.716	4.06
10	2.32	0.766	5.914	1.767	0.585	5.331	1.85	0.581	4.824
11	1.533	0.74	3.51	1.124	0.488	3.17	1.035	0.461	2.986
12	2.1	0.772	5.778	1.49	0.704	5.01	1.467	0.668	4.71

Table 4.4 Maximum relative displacements computed for the fixed-base SMART structure and the two seismic pairs (0.2g and 0.6g)

	0.2 g			0.6 g	
	Δx (mm)	Δy (mm)		Δx (mm)	Δy (mm)
	x-dir	y-dir		x-dir	y-dir
1 –Ref.	1.96	2.1		12.7	11.13
2	2.18	2.4		12.85	11
3	2.3	1.91		13.27	11.34
4	1.984	1.93		11.24	9.75
5	2.146	2.018		8.42	7.65
6	1.96	2.1		10.95	10.08
7	1.96	2.1		13.8	11.45
8	1.96	2.1		13.01	10.17
9	2.5	2.245		12.57	14.36
10	1.574	1.25		15.87	12.7
11	2.264	2.06		9.17	7.88
12	2.35	1.86		15.25	12.46

4.2. Vulnerability Study – Seismic Fragility Assessment

An integral part of the SMART2008 benchmark was the utilization of the test structure numerical model to develop fragility curves in an effort to convolute uncertainties in the seismic input with uncertainties in the structural capacity. In the parametric study of the previous section, the influence of the variation of individual design or structural properties on the response of the global structure was quantified according to ranges that are typically introduced in design. In the vulnerability aspect of uncertainty treatment described in this section, a multi-dimensional uncertainty matrix describing the structural capacity is convoluted with uncertainties regarding the seismic excitation. Thus, the combined effect can be compared to the anticipated limit state or capacity of the structure.

Structural capacity ***A*** is defined as the limit seismic load before a pre-defined performance limit state (or damage state) is reached by the structure. Due to the fact that capacity is influenced by uncertainties surrounding structural properties that can be characterized as random, capacity itself can be considered and treated as a random variable. The limit seismic load is a function of a parameter characterizing ground motion such as PGA, PGD, PGV or CAV. If PGA is selected as the seismic ground motion level indicator, for example, then capacity can also be expressed in terms of PGA. As a result, the probability of failure (or exceedance of the performance limit state) of the structure due to seismic ground motion level α is expressed by fragility curves which represent the following relation

$$P_f(\alpha) \equiv P(failure \mid \alpha) = P(A < \alpha) \qquad (4.1)$$

Failure or exceedance of the performance state at a ground motion level α occurs when the actual capacity of the structure is inferior to the seismic demand at the level α. Exceedance of a limit state could be expressed in a variety of ways using terms such as inter-story drift, structure yielding, reduction of fundamental modes, etc.. To establish the relation between the demand and capacity, typically a computationally intensive non-linear analysis is required in which a randomized structure is subjected to increasing seismic input which is also random in nature.

For the SMART structure shown in Figure 4.11, the structural elements above the shaking table are considered including the steel plate at the structure/table interface. The structure is

subjected to horizontal pairs of earthquakes at the base and all the structural elements are governed by non-linear constitutive relations (i.e. concrete can crack and crush and rebar can yield and fail).

In order for the probability of failure or exceedance to be quantified, given that both the capacity and the exciting earthquake are random variables, a significant number of convolutions at any given seismic level ***α*** will normally be required to increase the confidence in the estimation of probability. Capacity is treated as a random variable due to the uncertainties surrounding its structural properties while the seismic input, despite specifying its ground motion level ***α***, is still a random process of duration, frequency content, significant number of cycles, etc. This "complete" approach can be expressed according to the relation below

$$P(d \geq C) \mid a = \frac{N_{fail} \mid_a}{N_{total} \mid_a} \tag{4.2}$$

where N_{total} represents the total number of random realizations/input pairs and N_{fail} is the number of realizations during which failure has been reached. When utilizing (4.2) to derive the fragility of a structure, the number of seismic inputs can be very large as one attempts to saturate the earthquake ensemble with duration, frequency content, magnitude, hypo-central distance, etc.

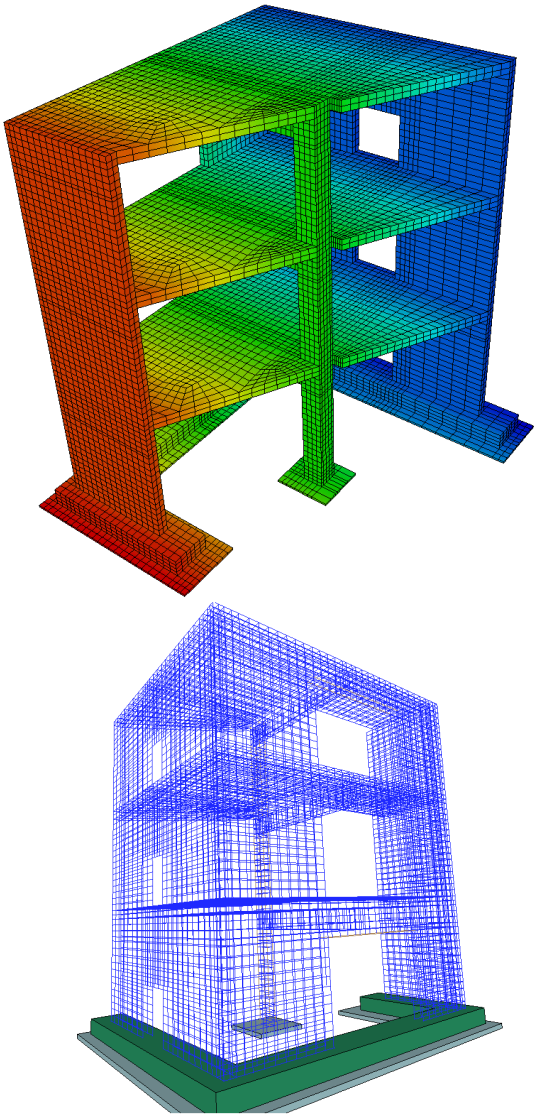

Figure 4-11 Fixed-base model used for the nonlinear analyses in fragility assessment depicting the discretization of the concrete structure and the steel rebar distribution

The randomization of the SMART structure used in the fragility phase of the benchmark was achieved by assuming that four (4) key structural properties have a degree of uncertainty around a nominal or design value. Specifically, the following randomization is introduced:

- *Secant concrete Young's modulus described by a mean value of E_c=32,000 MPA and a standard deviation of 2,200 MPa,*
- *Rebar yielding stress with mean Fy = 500 MPa and standard deviation of 30 MPa,*
- *Structural damping with nominal (mean) value of 2% and standard deviation of 1%,*
- *Added floor masses with mean total of 33.85 T and standard deviation of 5%.of the mean value*

However, while these structural parameters are expected to follow a certain distribution around the mean value (uniform, normal, log-normal, etc.) there is no provision for spatial variation or

spatial correlation between locations around the structure. Such an added requirement will add additional variation in the process and result in additional computational cost. A procedure that may be adopted in an effort to account for the spatial variability around the structure of the key structural properties is discussed in the report in a later section.

As noted previously, the randomization of the four key structural properties listed above occurs simultaneously rather than isolating one varying parameter at a time. This process leads to distinct “multi-dimensional random realizations” of the structural capacity that are in accordance to the adopted distribution.

Traditionally in vulnerability analysis of structures, limit or damage states have been defined qualitatively as light, moderate, extensive and complete. In developing fragility curves, however, in addition to the qualitative damage states, quantitative limit states must be established so that they can be compared with the seismic demand at a given intensity level. Different measures or indicators are used to describe the maximum state that the structure reaches as a result of a seismic load. The selection of these indicators may be influenced by the type of structure, empirical observations of performance of similar structure under real seismic loads, etc.

No exact formulation exists in establishing limit states for a structure. Such states may be specified or derived using either physics-based models or judgment stemming from experience and observations. A physics-based approach defines some functional level to be assigned to the structure for various levels of damage and is based on engineering analysis. Using judgment to define the limit states, the goal is to define functionality levels which would be assigned to the structure by decision makers for different levels of observed damage.

For the fragility analysis of the SMART structure inter-story drifts and eigenfrequency degradation were adopted as damage indicators. The qualitative and quantitative definition of the damage indicators and limit states are listed below:

Maximum inter-story drift at location A (x and y directions) and location D (x direction). The objective of linking the maximum drifts at the selected locations of the SMART structure is to evaluate the local damage effects.

Three limit states are being considered and expressed in terms of the structure story height *h* (*h* = 1.2 m)

- *Light damage (h/400)*
- *Controlled damage (h/200)*
- *Extensive damage (h/100).*

Degradation of structural eigenfrequencies (first two modes) in order to account for the overall structural behavior and evolution of its dynamic characteristics.

Similarly, three damage levels are considered that have been quantified as follows:

- *Light damage (frequency drop of 15%)*
- *Controlled damage (frequency drop of 30%)*
- *Extensive damage (frequency drop of 50%)*

The degradation of eigen-frequencies is deduced by comparing the estimated eigenfrequency of the structure at the end of the seismic load to the initial frequency estimated based on the corresponding realization of the randomized structural properties.

While additional uncertainty can be introduced in the damage criteria, which in turn will add further computational burden in an effort to capture the influence on the vulnerability assessment, no variability in the defined limit states have been assumed in this analysis.

Generation of Fragility Curves

Fragility curves are continuous functions reflecting the conditional probability that the response of a structure to increasing seismic excitations represented by a random process exceeds a given performance limit state defined both qualitatively and qualitatively. The structural response is typically defined by a pre-selected variable such as inter-story drift, frequency drop, yielding, etc. Theoretically, fragility represents the probability that the response of the structure exceeds a given threshold conditional on an earthquake intensity parameter (see Equations 4.1 and 4.2). The conditional probability of failure of a structure can be linked to a seismic input motion indicator, such as PGA, CAV or PGD. This is due to the fact that both the seismic demand and the capacity can be expressed in terms of the selected seismic input indicator.

For a given structure, such as the SMART test structure used in the benchmark, fragility curves are developed from a number of seismic response data obtained using simulated ground motions and through a nonlinear time history analysis. Fragility curves will be affected by several parameters such as (a) performance limit criteria which can be both random and multidimensional (where a correlation of more than one damage indicator is used), (b) input ground motion random character, (c) uncertainties in structural properties and their proper randomization, and (d) appropriate modeling of the structure which captures the damage indicators. To establish fragility curves that incorporate uncertainties in all four groups of parameters, an extensive computational effort is required given that each participating parameter is treated as random thus requiring convolution with the remaining three groups over their range of uncertainty. In order to reduce the computational effort while maintaining high confidence levels, certain assumptions have been introduced in randomization of the influential parameters. These assumptions permitted the description of uncertainty in closed-form expressions which resulted in closed-form solutions of the fragility curves.

For example, a two parameter lognormal distribution function has been used extensively for the construction of fragility curves. This was made possible by assuming that the structural properties defining capacity in the structure are log-normally distributed and so is capacity itself.

The assumption of a lognormal capacity distribution was introduced during the development of probabilistic risk assessment methodologies for nuclear power plants in the 1970's and 1980's. It was prompted by observations that the actual structural strength and the design strength are related through a multiplicative safety factor resulting from a multitude of factors each of which is associated with a specific source of uncertainty in the structure. Based on the assumption of lognormal distribution for each of these factors, the overall safety factor is also distributed log-normally due to the multiplicative nature of variables defined by a lognormal distribution. Therefore, by assuming that uncertainties in key parameters influencing capacity (i.e. strength, damping, etc.) are log-normally distributed, the capacity is log-normally distributed as well. This assumption has significant implications in that it enables the capturing of uncertainty in the structural capacity into a single, analytical expression in terms of either a response value (deformation, ductility, etc.), or better yet, a seismic input indicator, such as peak ground acceleration (PGA), peak ground velocity or cumulative absolute velocity (CAV).

Evaluation of fragilities can be further simplified by developing a probability distribution for the demand conditioned on the seismic input indicator (i.e. PGA, PGD, CAV) and convolving it with the capacity distribution. If the seismic demand is assumed to also follow a log-normal distribution then fragilities can be deduced from the following relation

$$P[D > C_{|\alpha}] = \Phi[\frac{\ln(S_d / S_c)}{\sqrt{\beta^2{}_{D|\alpha} + \beta^2{}_C}}] \quad (4.3)$$

where S_d is the median estimate of the demand, S_C is the median estimate of the capacity, $\beta_{D|\alpha}$ is the dispersion or logarithmic standard deviation of the demand conditioned on the intensity measure α and β_C is the dispersion of the capacity. Written in a different form, when the lognormal fragility model is chosen, the fragility curves can be defined from the relation

$$P_f(\alpha) = \Phi[\frac{\ln(\alpha / A_m)}{\beta}] \quad (4.4)$$

where Φ(•) is the standard Gaussian cumulative distribution function and fragility curves, are entirely determined by only two parameters, which are median capacity Am and lognormal standard deviation β. These parameters can be evaluated by means of regression analysis.

Fragility curves based on relation (4.4) were developed in this benchmark according to the following procedure:

- A suite of ***N=50*** ground motions are selected that contain characteristics of earthquakes that are relevant to the location of the structure in question. While typically the ensemble consists of real earthquakes and/or a combination of real and synthetic ground motions, fifty synthetic records were utilized in the analysis.

- ***N=50*** realizations of the structure were generated by considering the four random distributions of the structural parameters (E_c, F_y, damping and added floor mass). This resulted in 50 independent structural variations of the model shown in Figure 4.11.

- The 50 seismic bi-directional synthetic earthquakes were randomly paired with the 50 structural realizations and through a full non-linear time history analysis for each pair, various responses were monitored and recorded (displacements, floor accelerations, structural frequency evolution, etc.)

- A regression analysis between responses and seismic input indicators were performed to derive the median capacity and the dispersion which are then used to develop the corresponding fragility curves.

In the following sections the details of the above adopted generic process leading to fragility curves is presented in more detail.

Ground Motion Suite

An ensemble of 50 bi-directional horizontal accelerograms provided by the SMART benchmark organizers were used in the fragility analysis. All 50 accelerograms are synthetic and have been derived from a spectrum similar in shape with the one used to design the SMART2008 specimen. Effort was made to ensure that the frequency range is saturated and that the duration of the strong motion in the records covers a wide range. By selecting a large ensemble of earthquakes, which cover the range of interest for both frequency content and duration, one avoids the possibility of excluding probable scenarios near the tails of the distributions characterizing the seismic demand and the structural capacity.

Indicators such as peak ground acceleration, displacement and velocity as well as cumulative absolute velocity (CAV), were provided for each of the bi-directional records. Figure 4.12 depicts the distribution of peak ground accelerations characterizing the 50-member ensemble.

Figure 4.13 depicts the regression between indicators such as PGA, PGD and CAV. It is observed that the PGA has stronger correlation with CAV than PGD. Figure 4.14 depicts acceleration time histories and response spectra for a subset of the 50 earthquake pairs.

Structural Realizations

In order to perform a convolution with the N number of earthquakes selected to represent the demand, an equal number of structural capacity realizations need to be generated according to a statistical model. Having accepted the fact that uncertainties surrounding the structural properties follow the log-normal distribution, the main task is to enable the propagation of the uncertainty throughout the model. As noted earlier, the structural properties that exhibit uncertainty are the secant concrete modulus E_c, the yield stress in the rebar F_y, the structural damping and the added live load. Their distribution is defined by their mean value and the standard deviation. In order to propagate the uncertainty through the model without being biased towards the mean value of the structural parameters, the stratified Latin Hypercube sampling approach was employed. Figure 4.15 depicts the sampling approach used to construct the N=50 realizations which is based on the principle that the entire range (i.e. mean-3σ – mean+3σ) is represented in the sample. This is done by selecting the random values of the structural property on the basis of the cumulative distribution function which is divided in equal intervals of cumulative probability.

Figure 4.16 depicts two of the four randomized parameters following a log-normal distribution. As shown, the entire range is represented. The non-uniform distribution shown in the two traces is the result of the distribution of the uncertainty in two groups of 30 and 20, respectively. The first 30 realizations were constructed to satisfy the requirements of the benchmark, while added to the distribution were 20 additional earthquake-realization pairs.

Non-Linear Analysis

The 50 realizations of the structure properties were introduced into the numerical model shown in Figure 4.11 and were paired with the 50 synthetic ground motions (x and y directions acting simultaneously at the base of the structure) leading to 50 non-linear analyses of the structure. Eigenfrequencies of the structure for each of the realizations were extracted prior to the applications of the earthquake pair, mid-way of the transient analysis, and at the end of the record, in an effort to observe the degradation in the structural modes resulting from damage in the concrete and yielding or failure in the rebars. In addition, acceleration responses were monitored through-out the structure and response spectra were generated. Shifting of response spectra peaks were monitored and were correlated with the shifting of frequencies derived directly from the analysis. Displacements at selected locations in the structure were also monitored and maximum inter-story drifts were deduced and recorded.

Figure 4.17 depicts the condition of the structure at the end of four out of the fifty analyses performed indicating variability in the level of damage experienced. Shown in Figure 4.18 is the state of the structure where reinforcing steel bars failed near the foundation. As compared to the shaking table test where input PGA values in excess of 1.0g were achieved leading to minimal progressive cracking and no rebar failure, it is evident that the convolution of seismic inputs with randomized structural properties has the potential of inducing higher levels of damage in the same structure although the fixed-base conditions may have contributed to the increased damage state.

Figure 4.19 depicts trends between the different seismic input indicators and the structural response while Fig. 4.20 shows the regression between the different response variables.

Figures 4.21 and 4.22 illustrate the variability in the response spectra observed on the 3rd level of the structure.

Estimation of Fragility Curve Parameters

Following the N=50 deterministic analyses which randomly paired the 50 seismic inputs with the 50 property uncertainty realizations and the monitoring/estimation of the structural responses, the two parameters shown in equation 4.4 (median capacity A_m and the dispersion β) can be deduced from regression analysis.

Specifically, by denoting the numerical analysis output as Ψ (drift, displacement, frequency drop, etc.) and the ground motion indicator (PGA, PGD, CAV, etc.) as **ς,** upon completion of the deterministic analyses there exist N = 50 structure response outputs **Ψ** (Ψ_1, Ψ_2,,, Ψ_N) corresponding to ground motion indicator levels **ς** (ς_1, ς_2, ,, ς_N). Given that **Ψ** is assumed to be log-normally distributed it implies that ln(**Ψ**) is a normally distributed random variable. By performing linear regression on ln(**Ψ**) and ln(**ς**) according to the relation

$$\ln(\Psi) = \alpha + b\ln(\varsigma) + \varepsilon \qquad (4.5)$$

parameters *α* and *b* can be determined. ε represents the uncertainty of the regression relation and is a normally distributed random variable with median = 1 and logarithmic standard deviation $\sigma_{\ln\varepsilon}$, which is also equal to dispersion or log-standard deviation β. Figure 4.23 depicts one of the regression relations used to estimate the parameters of equation 4.5.

Following the estimation of parameters *α* and *b* in (4.5) the **median seismic capacity A_m** can be evaluated from the following relation

$$\ln(\Psi_{\lim itSTATE}) = a + b\ln(A_m) \qquad (4.6)$$

Where $\Psi_{limitSTATE}$ is the response corresponding to the limit state (light, controlled, and extensive damage). Table 4.4 summarizes the median seismic capacity and the corresponding dispersion for the three damage states, damage indicators and various seismic input indicators (PGA, CAV, etc.). Having established the median capacity and dispersion for all cases as depicted in Table 4.5 fragility curves using equation 4.4 are generated.

Figures 4.24 - 4.29 depict fragility curves for three different motion indicators (PGA, PGD and CAV) and the three damage states based on various damage indicators (floor drift at different locations and degradation of first and second eigenfrequencies). As seen from the generated fragility curves there exists significant variability between the different input and damage indicators. The correlation between the structural responses seen in Figures 4.19 and 4.20 are a pre-cursor of the variability that would be expected in deriving the fragilities.

To address the variation observed in fragilities when different metrics are used (either seismic input indicators or damage indicators) methodologies have been proposed that introduce multi-dimensional fragility surfaces where limit states are correlated, for instance, displacements and accelerations observed in a structure. For such approach, the response can be represented by a “bell surface” in, say, the spectral acceleration – spectral displacement plane and the limit states in terms of accelerations, displacements, or velocities.

While fragility curves are difficult to defend regarding their accuracy in representing the damage or failure probability of a given structure, given the uncertainties in establishing limit states and their definition, it is important, however, for the variability between different metrics to be minimized. While confidence levels can be increased by increasing the number of realizations with a corresponding computational cost, it is the quantification of the limit states that will remain as the biggest challenge. Recommendations on ways to improve confidence levels in fragility estimates are included in the summary chapter.

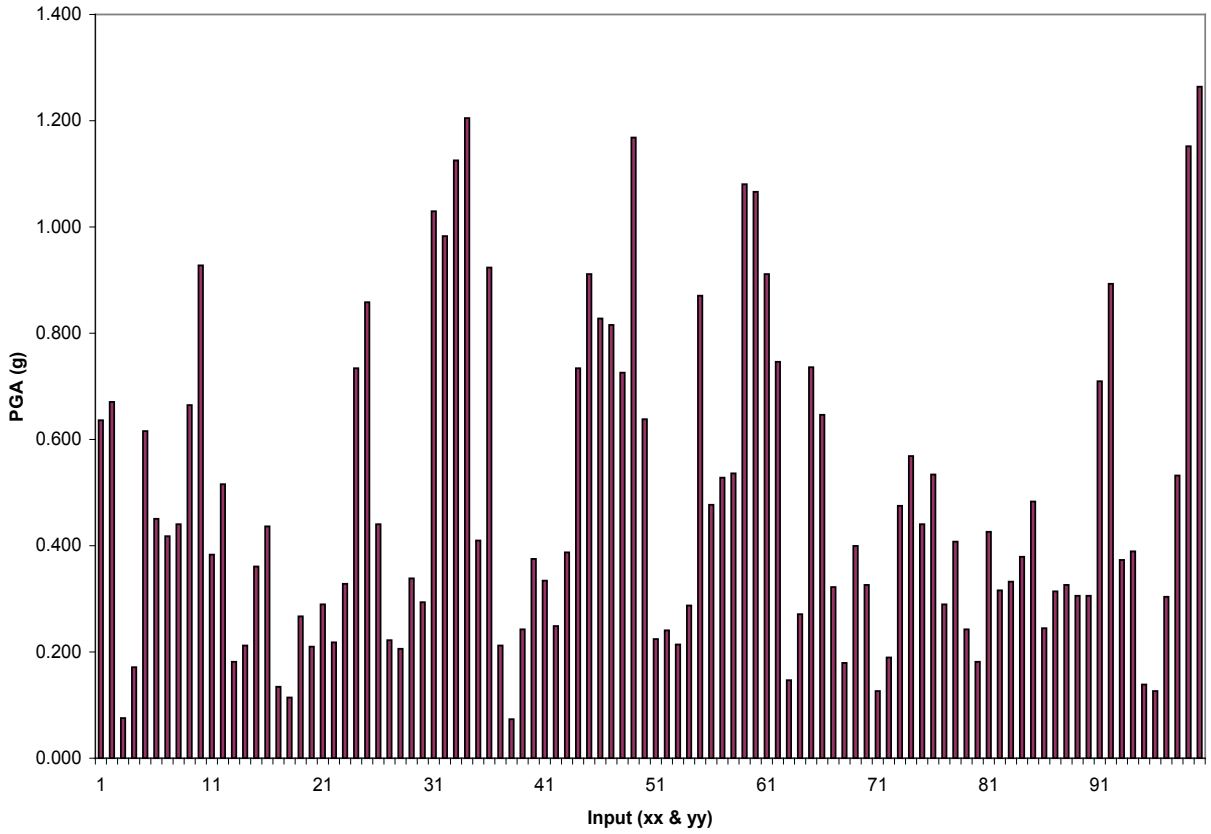

Figure 4-12 Peak ground accelerations histogram of the 50 earthquake sets (x and y directions) used in fragility analysis

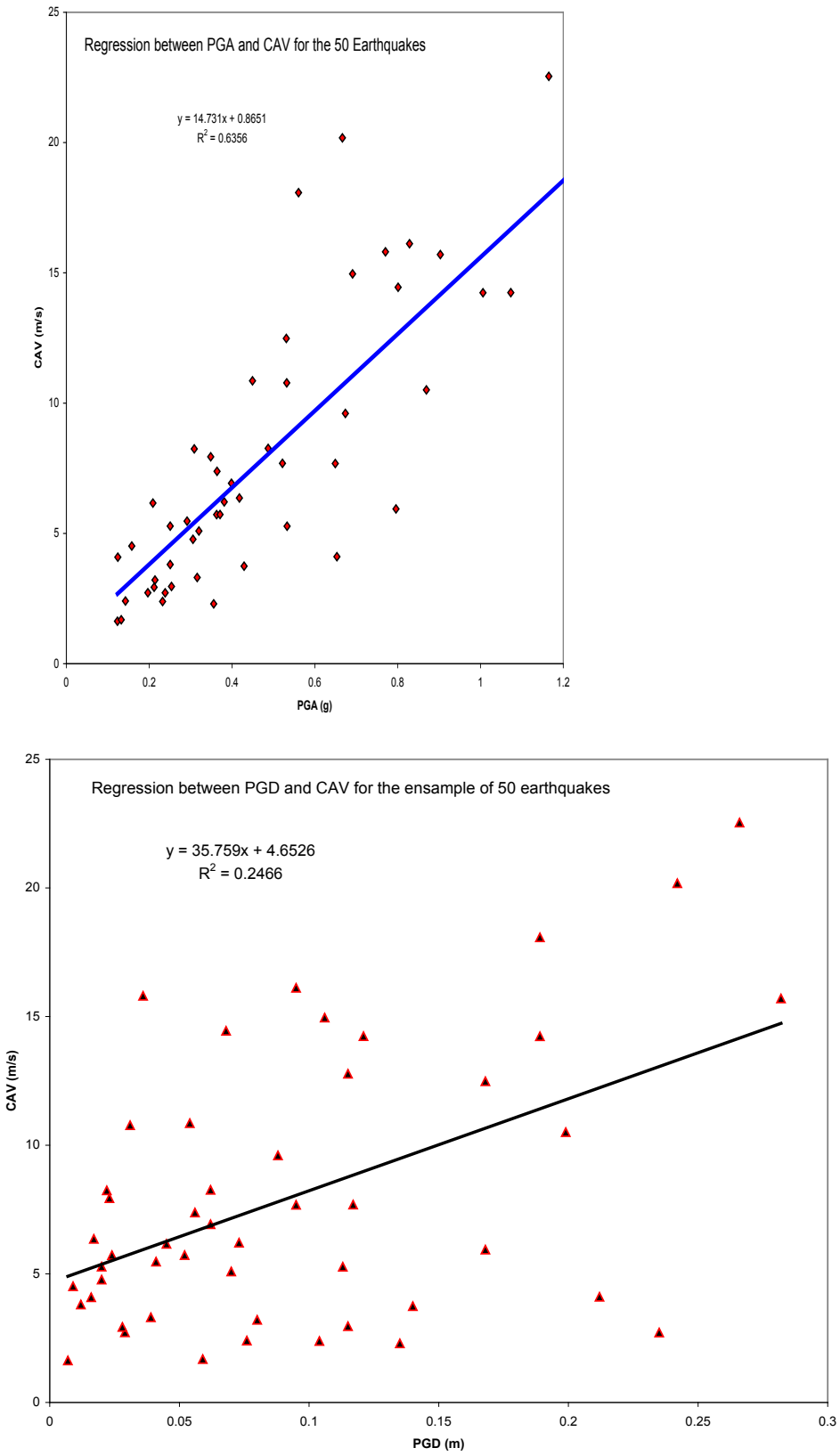

Figure 4-13 Regression between different indicators of the 50 bi-directional synthetic records used in the fragility analysis

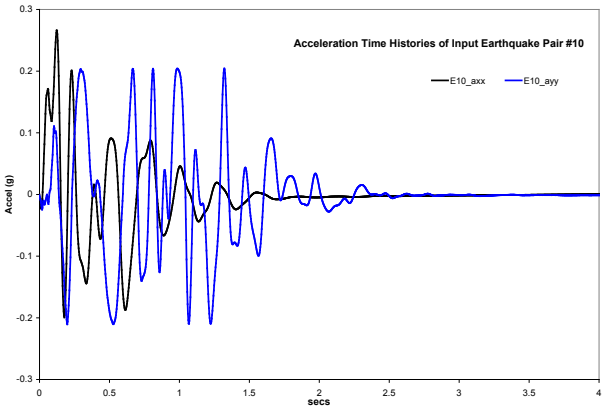
Acceleration Time Histories of Input Earthquake Pair #10
E10_axx
E10_ayy
Accel (g)
secs

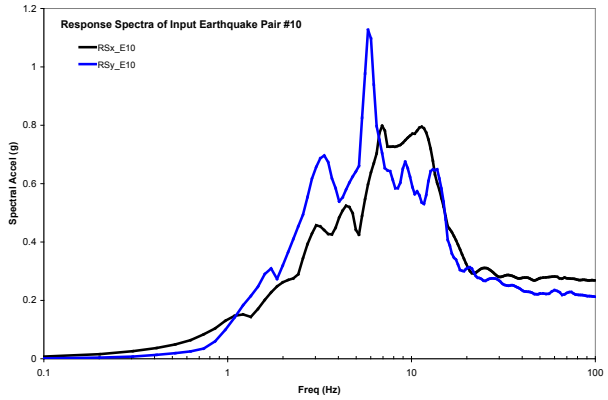
Response Spectra of Input Earthquake Pair #10
RSx_E10
RSy_E10
Spectral Accel (g)
Freq (Hz)

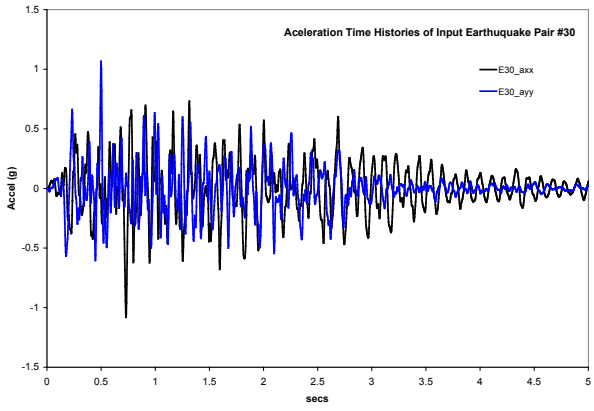
Aceleration Time Histories of Input Earthuquake Pair #30
E30_axx
E30_ayy
Accel (g)
secs

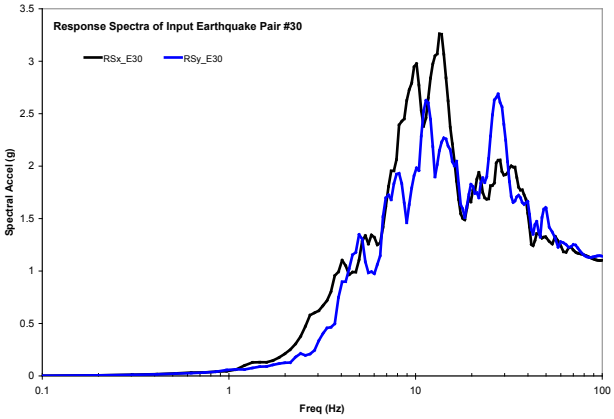
Response Spectra of Input Earthquake Pair #30
RSx_E30
RSy_E30
Spectral Accel (g)
Freq (Hz)

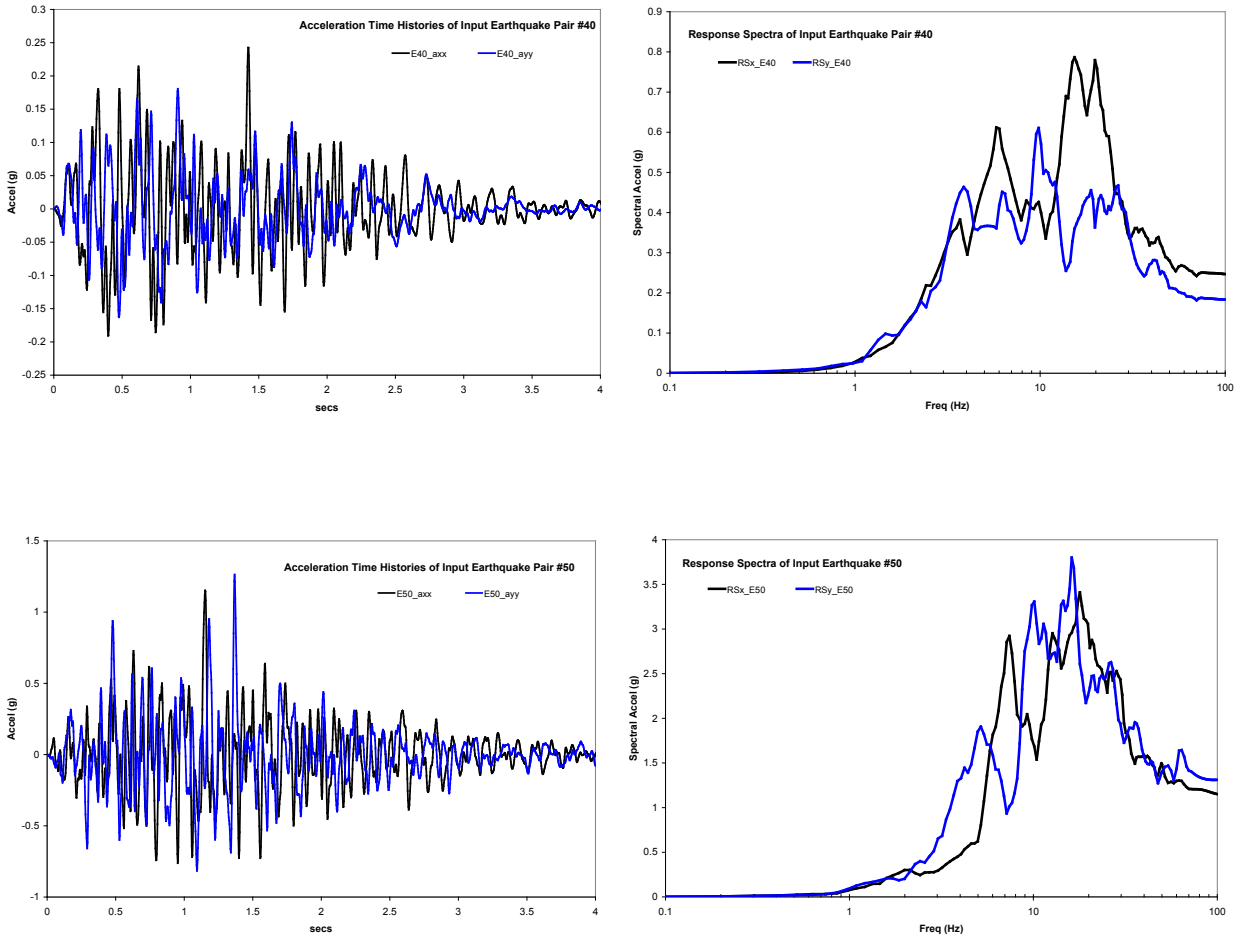

Figure 4-14 Four acceleration time histories and four response spectra of a sub-set of the 50 synthetic records used in the fragility analysis (First two pairs of time histories and response spectra are on previous page – 116)

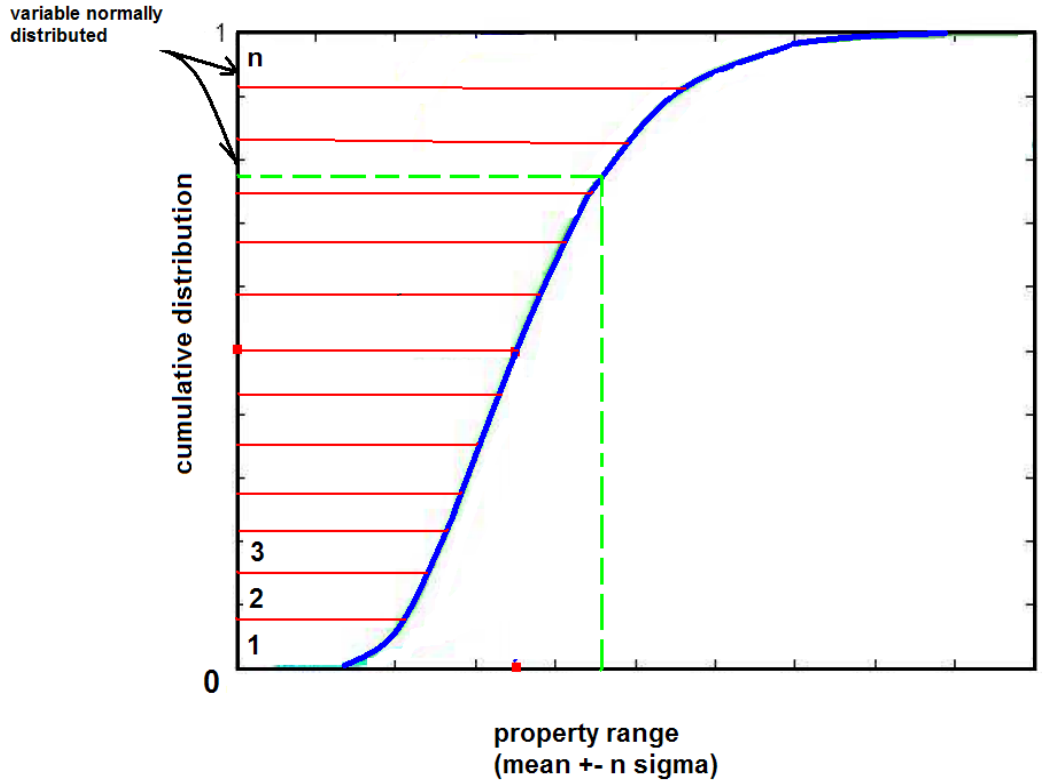

Figure 4-15 Stratified sampling Latin Hypercube used for uncertainty distribution of the structural properties

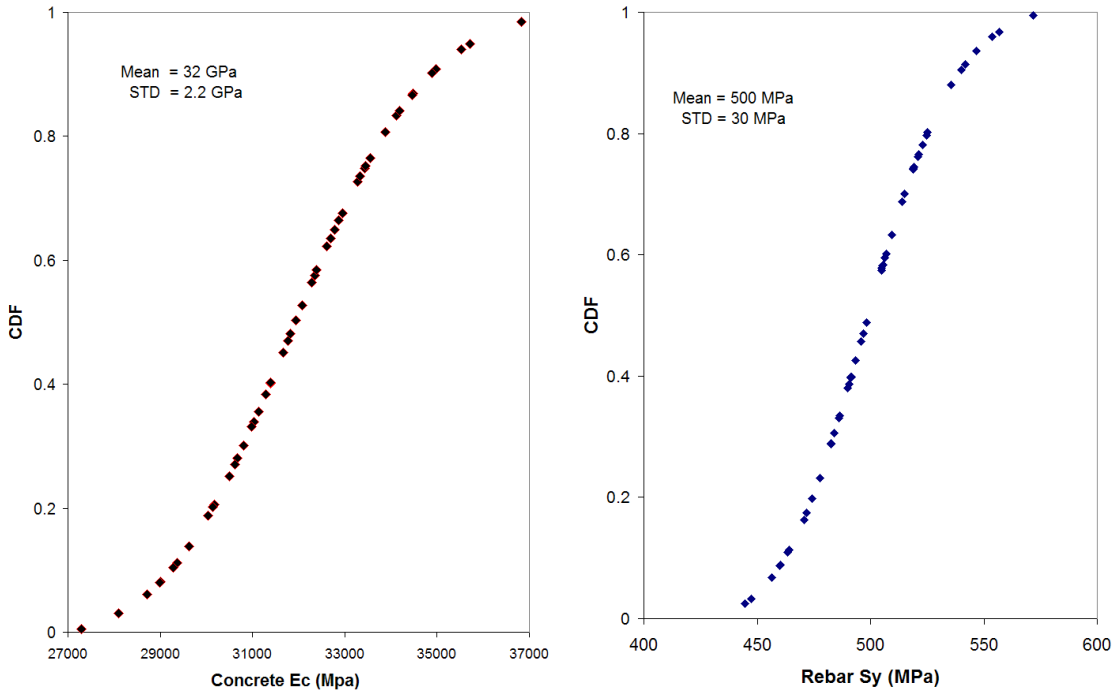

Figure 4-16 Cumulative distribution function of structural properties (concrete Ec and rebar Fy) of the 50 realizations used to log-normally distribute uncertainty

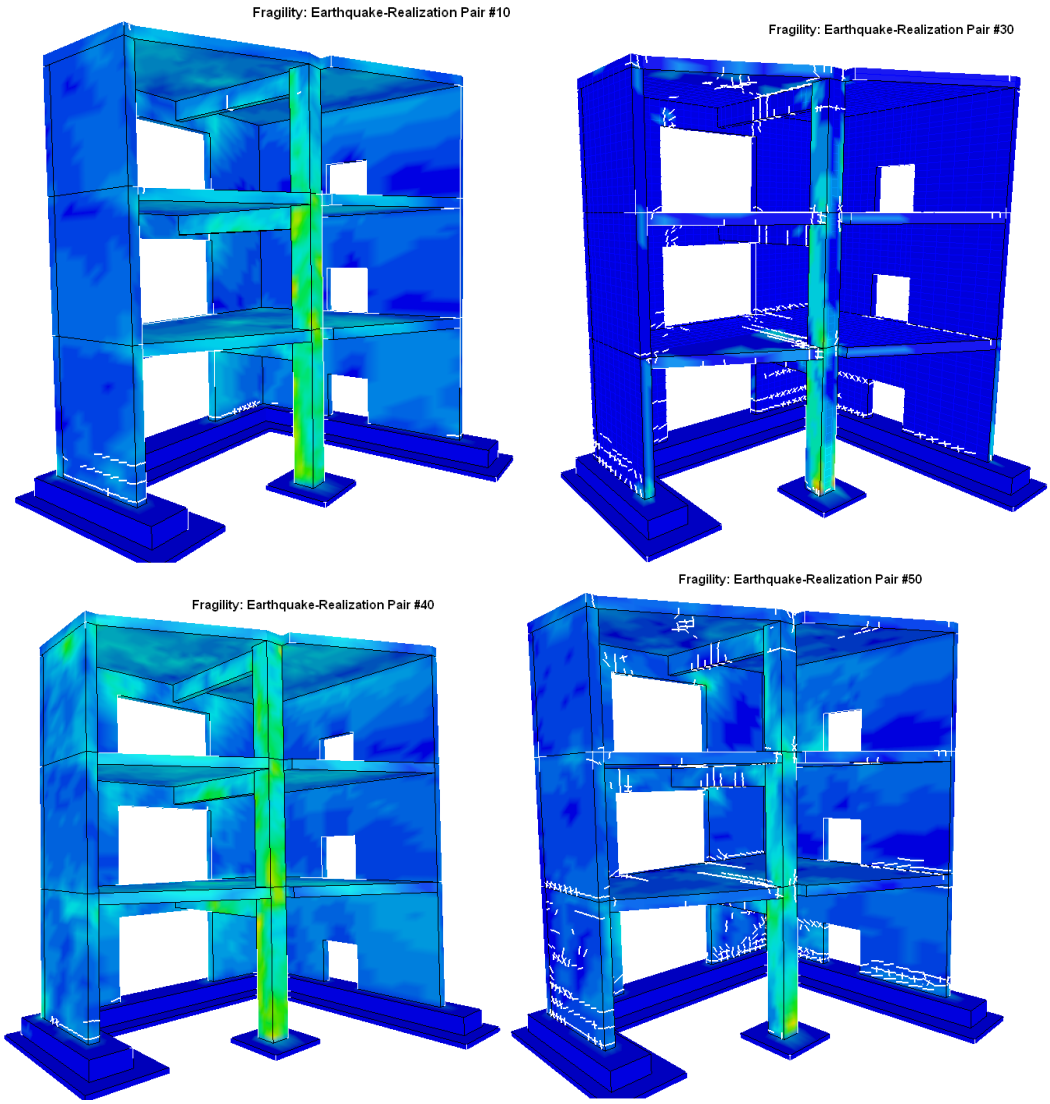

Figure 4-17 Damage conditions (crack extend and pattern) reached in the structure at the end of four seismic inputs out of the 50 randomly selected earthquake-realization pairs

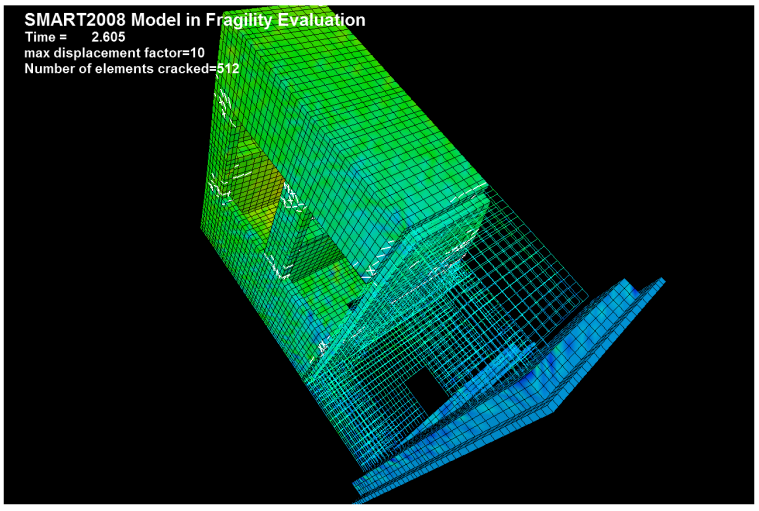

Figure 4-18 Damage conditions (reinforcement failure near the base of the structure) reached during one of the randomly selected earthquake-realization pairs

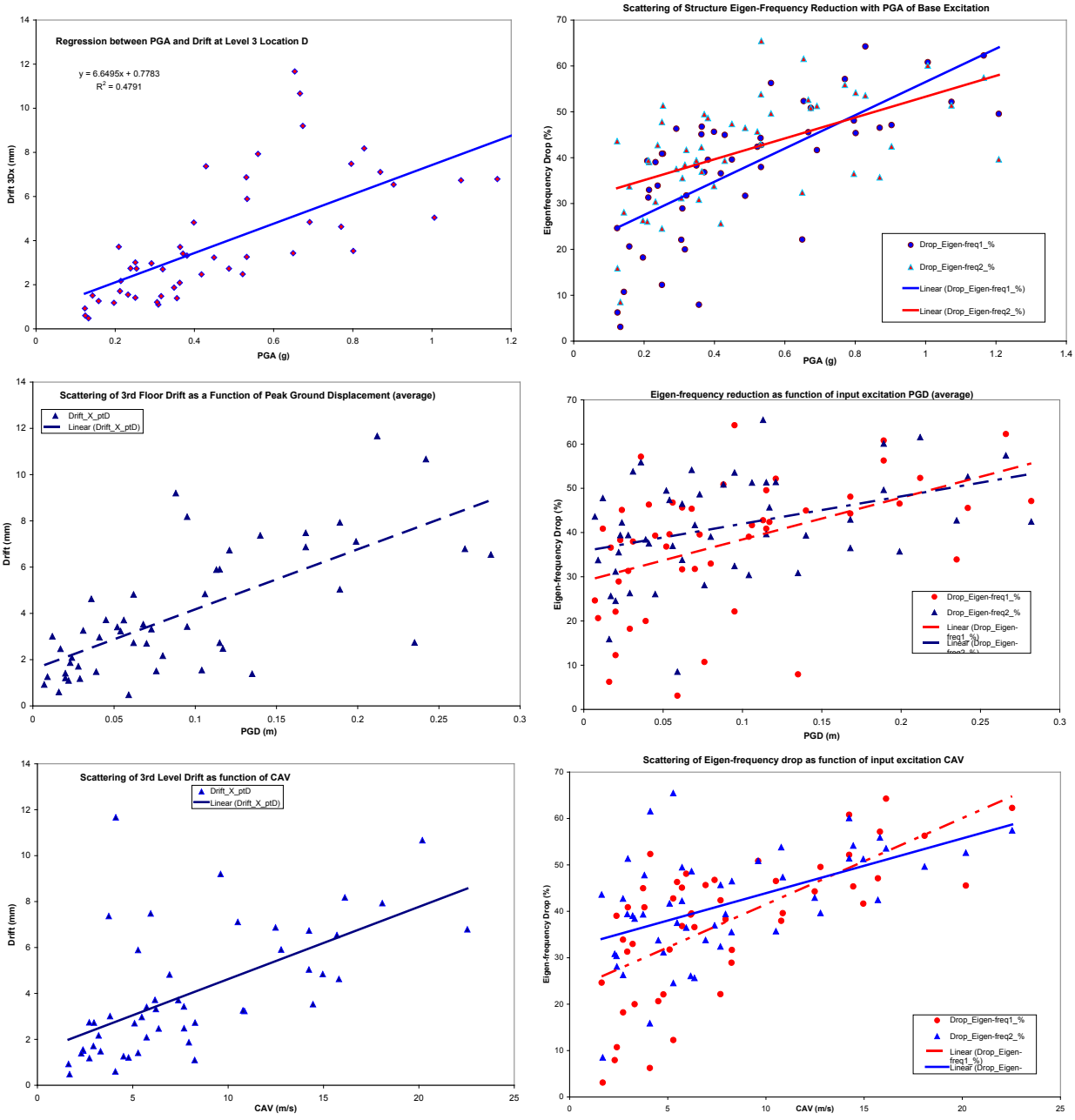

Figure 4-19 Regression between seismic input indicators of the 50-earthquake ensemble and structure response in terms of floor drifts and eigenfrequency degradation

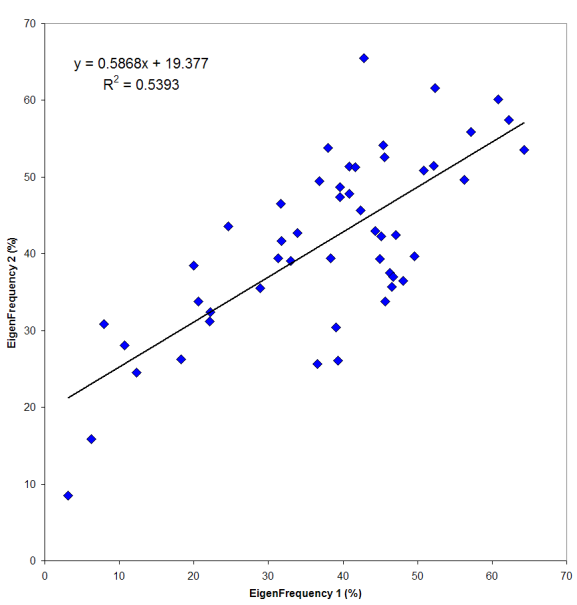

(a)

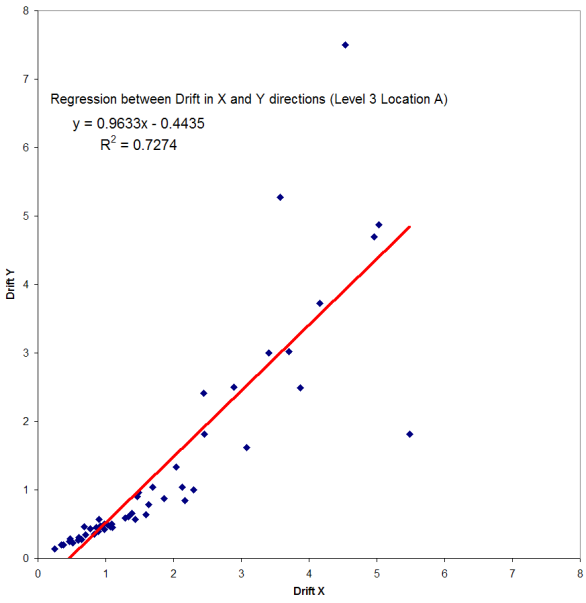

(b)

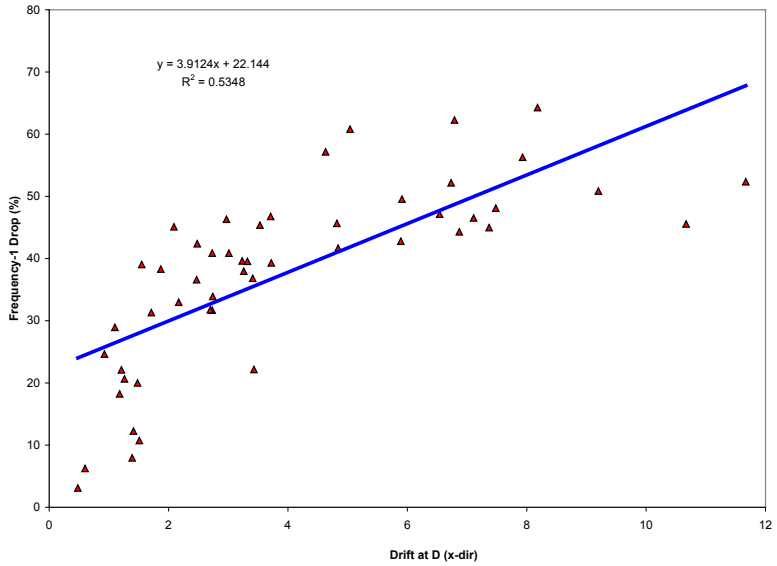

(c)

Figure 4-20 Regression between non-linear analysis output variables monitored on the test structure for the 50 pairs of structural property realizations and the seismic inputs. (a) Regression between 1st and 2nd structural frequency drop, (b) regression between drifts along x and y at the same structural location and (c) regression between drift at a structural extremity (location D) and drop in 1st frequency

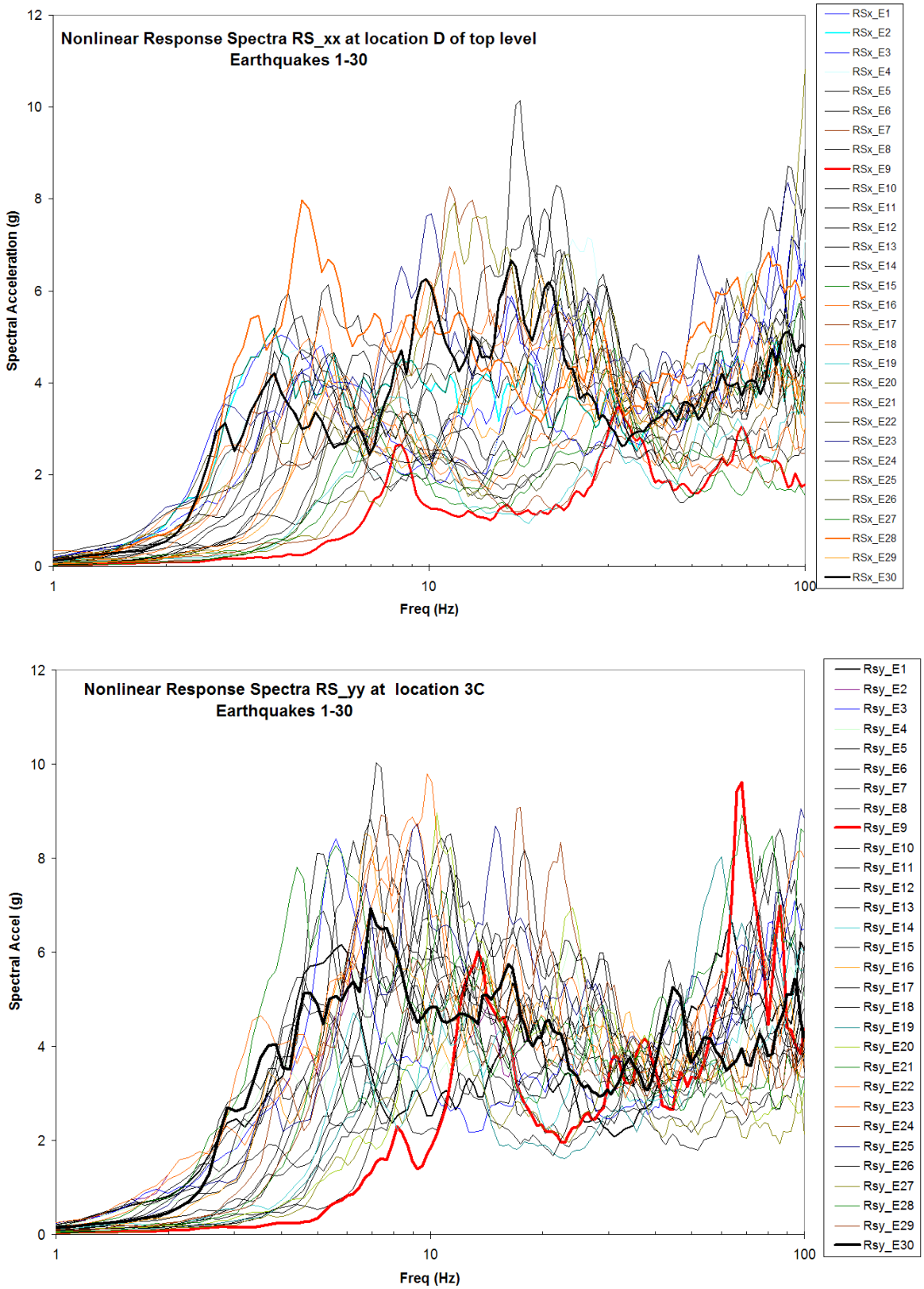

Figure 4-21 Non-linear response spectra generated on level 3 of the structure at location D (x-direction) and location C (y-direction) from the analysis of the 30-set earthquake pairs

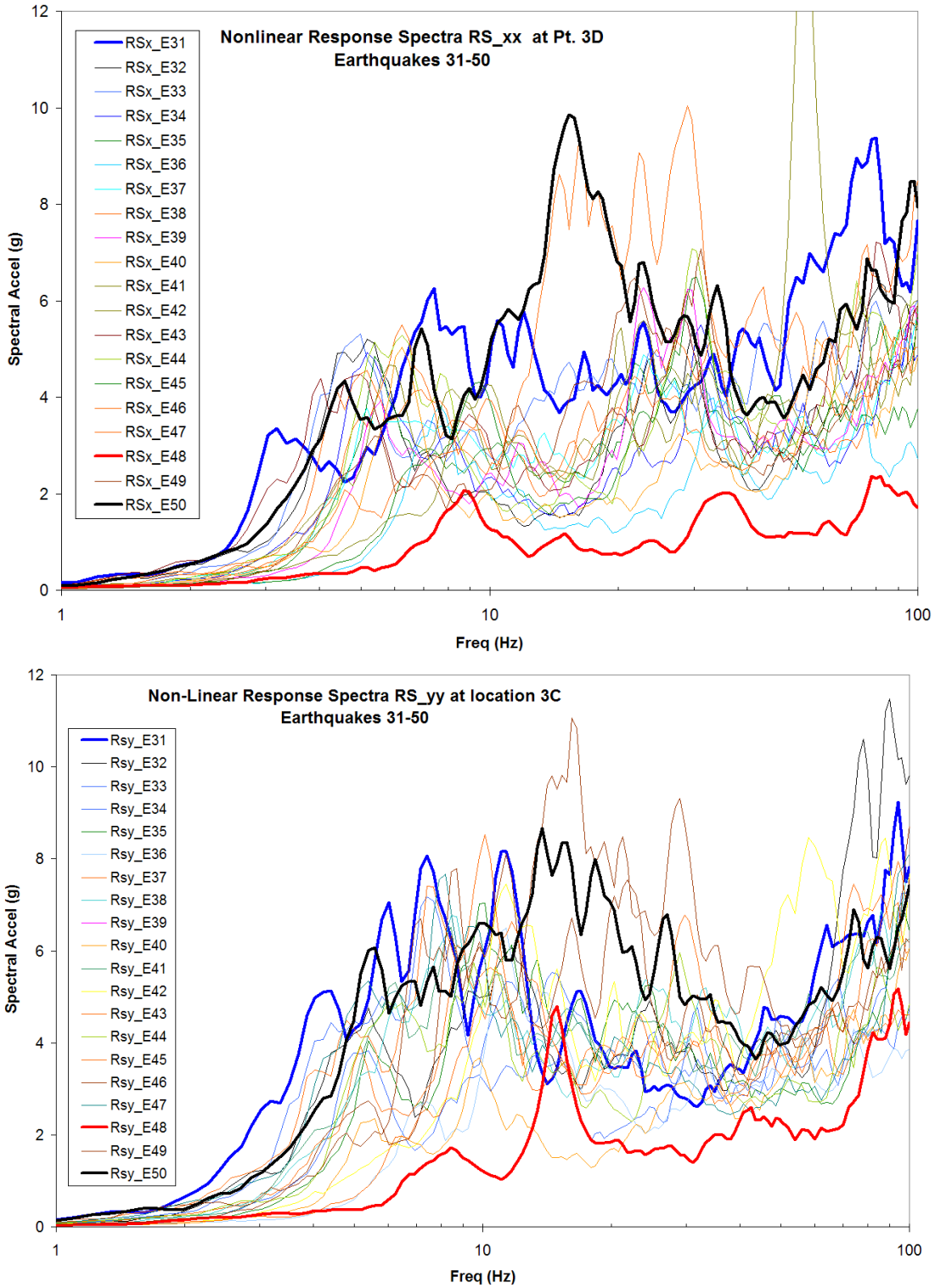

Figure 4-22 Non-linear response spectra generated on level 3 of the structure at location D (x-direction) and location C (y-direction) from the analysis of the extra 20-set earthquake pairs

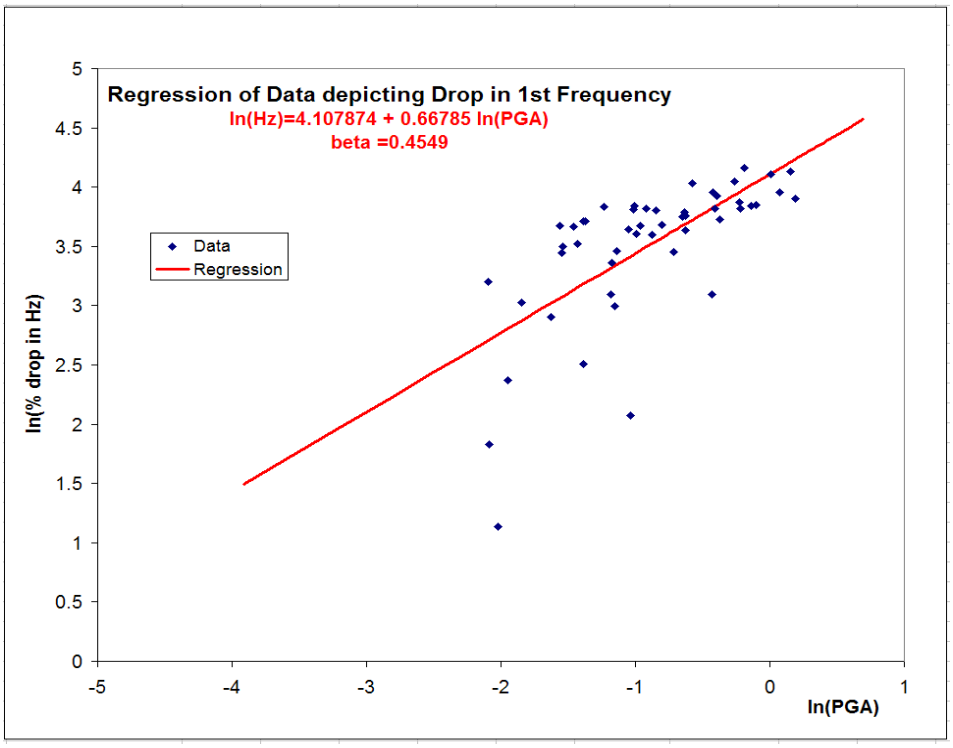

Figure 4-23 **Regression analysis between the logarithms of the PGA and eigenfrequency drop used to estimate median capacity and log-standard deviation**

Table 4.5 **Summary of estimates of median capacity A_m and log-normal deviation β.**

			Light damage		*Controlled damage*		*Extensive damage*	
	metric	**response**	**Am**	**Beta**	**Am**	**Beta**	**Am**	**Beta**
1	PGA	max drift pt A x	0.833777	0.46724	1.581545	0.562	2.999942	0.7182
2	PGD	max drift pt A x	0.264676	0.6279	0.921997	0.7013	3.211765	0.83172
3	CAV	max drift pt A x	16.28560	0.57628	37.18083	0.6554	84.88570	0.79347
4	PGA	max drift pt A y	1.081667	0.56126	1.792055	0.6423	2.968993	0.78263
5	PGD	max drift pt A y	0.460597	0.78644	1.262226	0.8462	3.459016	0.95707
6	CAV	max drift pt A y	21.74134	0.67528	40.70131	0.744	76.19571	0.86804
7	PGA	max drift pt D x	0.391637	0.50586	0.780536	0.5945	1.555614	0.74391
8	PGD	max drift pt D x	0.060917	0.61079	0.213835	0.686	0.750618	0.81888
9	CAV	max drift pt D x	6.138204	0.61029	15.39055	0.6855	38.58932	0.81851
10	PGA	1st freq drop	0.122945	0.51906	0.347101	0.6057	0.745831	0.75294
11	PGD	1st freq drop	0.002231	0.62518	0.041942	0.6988	0.364468	0.82967
12	CAV	1st freq drop	1.532403	0.54159	5.331796	0.6252	13.36413	0.76865
13	PGA	2nd freq drop	0.026502	0.37838	0.186933	0.4906	0.788738	0.66383
14	PGD	2nd freq drop	3.678E-0	0.42019	0.007789	0.5235	0.403240	0.68852
15	CAV	2nd freq drop	0.177176	0.39605	2.319474	0.5043	15.43719	0.67406

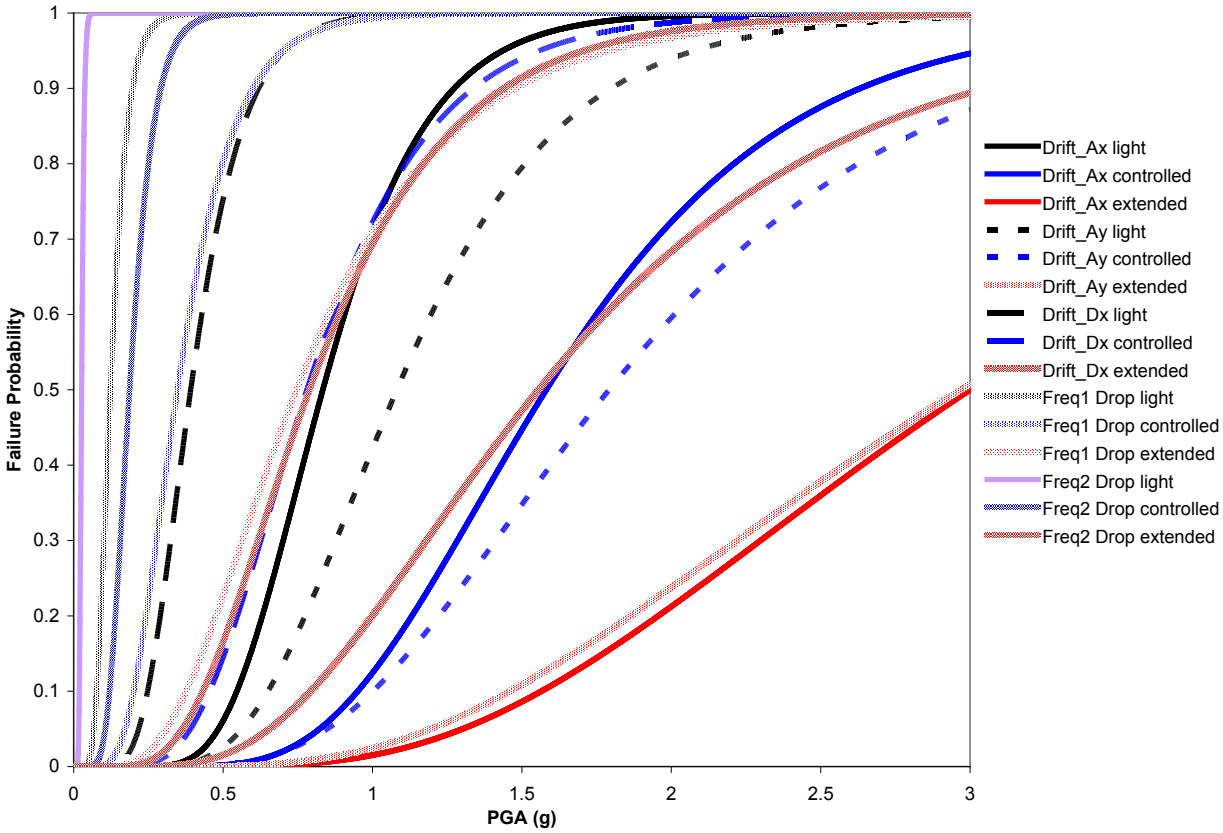

Figure 4-24 Fragility curves for all three damage states and all capacity measures using PGA as the demand indicator

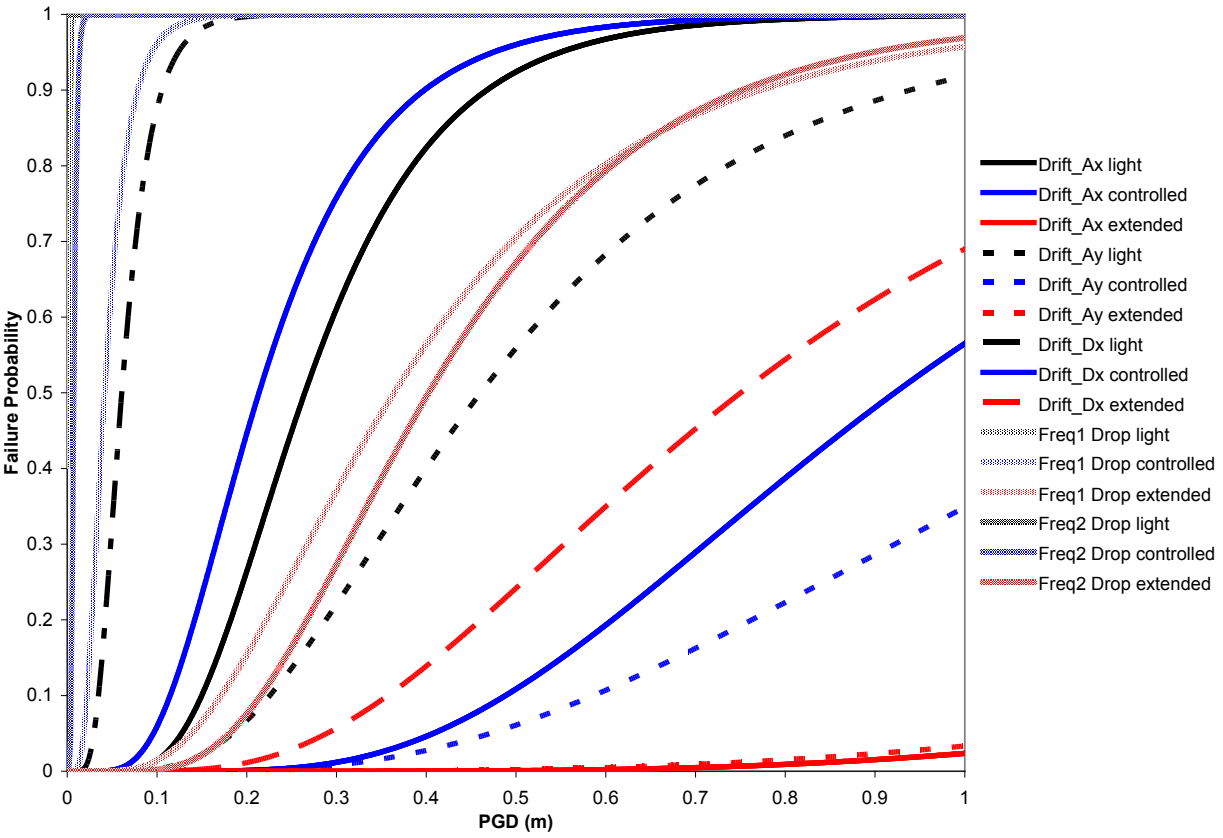

Figure 4-25 Fragility curves for all three damage states and all capacity measures using PGD as the demand indicator

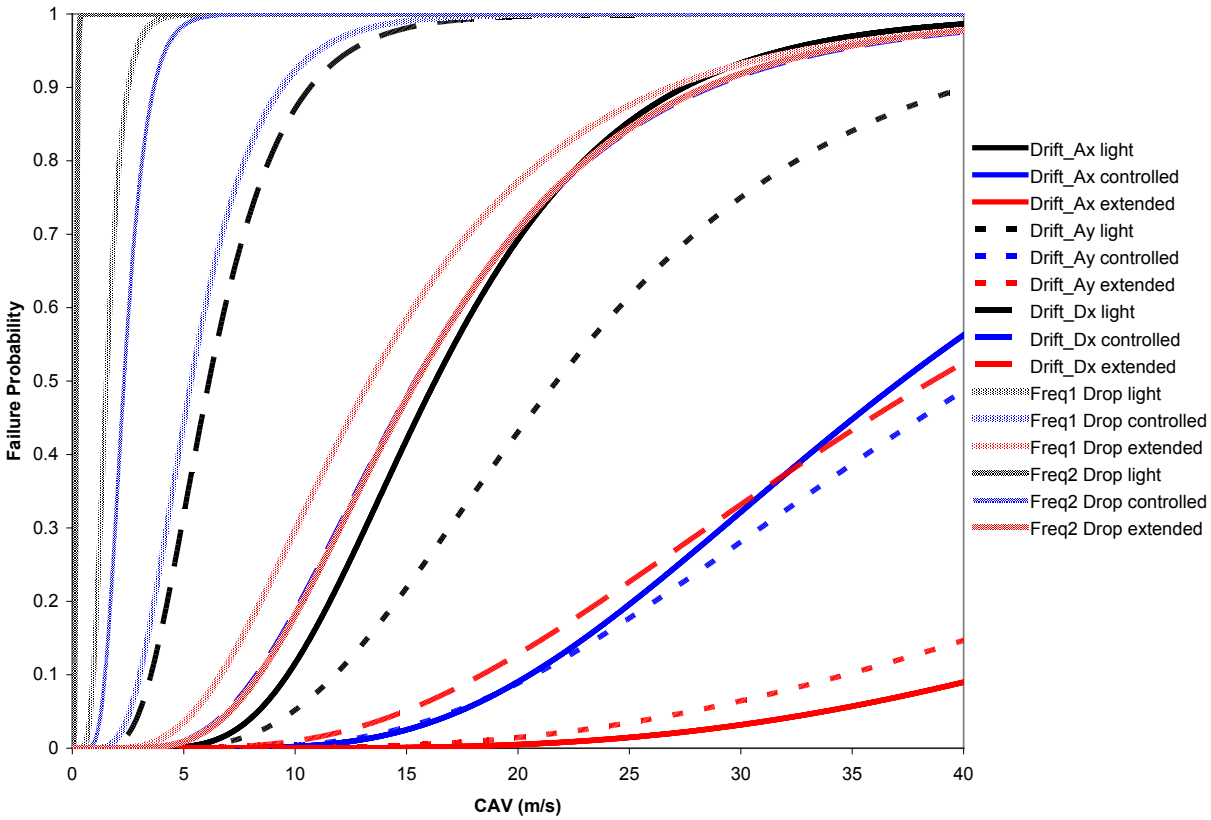

Figure 4-26 Fragility curves for all three damage states and all capacity measures using CAV as the demand indicator

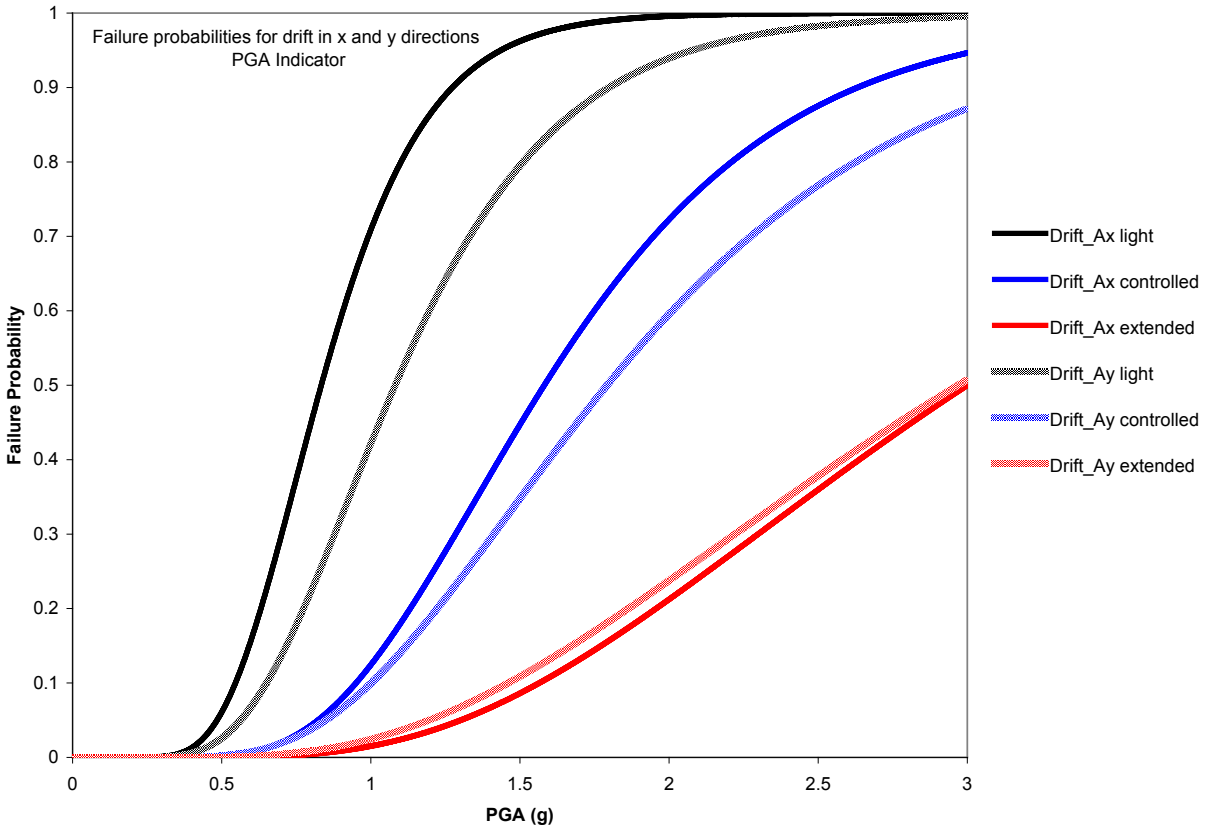

Figure 4-27 Fragility curve comparison for different drift measures - PGA

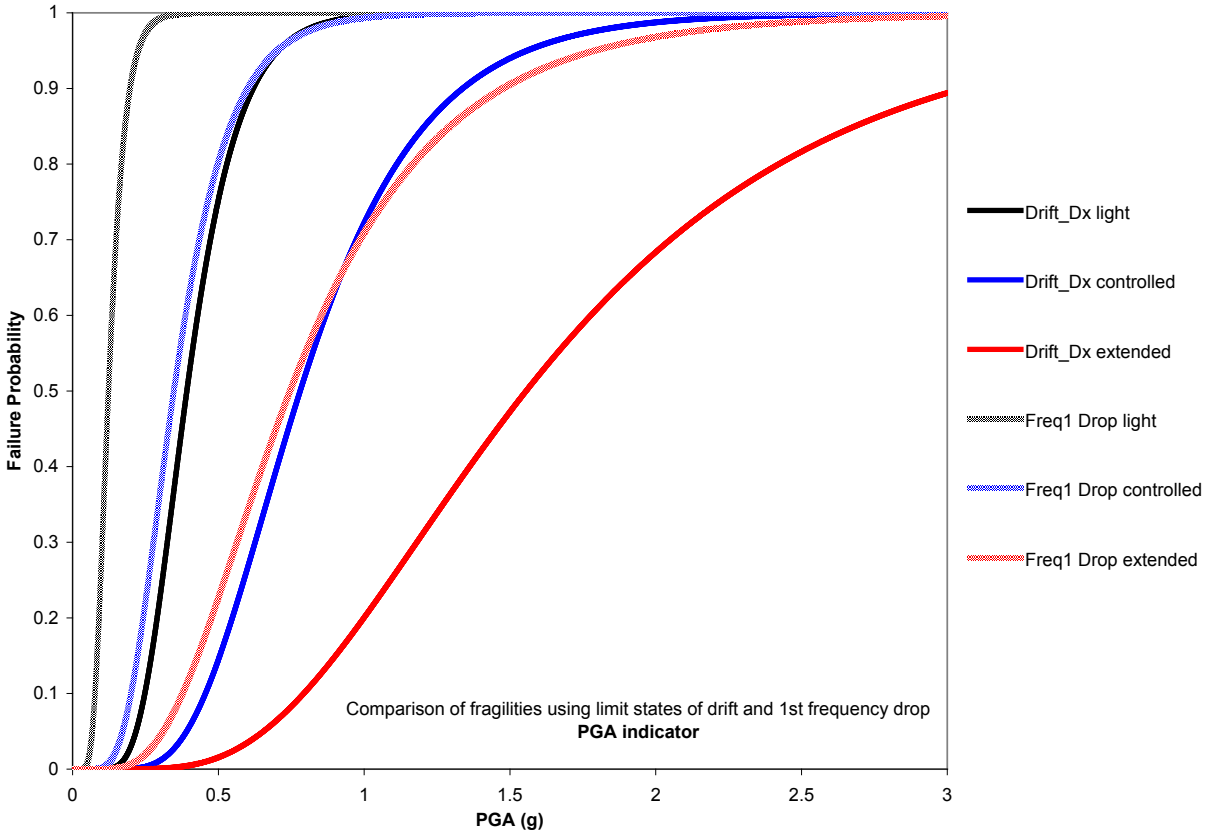

Figure 4-28 Fragility curve comparison between drift and frequency drop - PGA

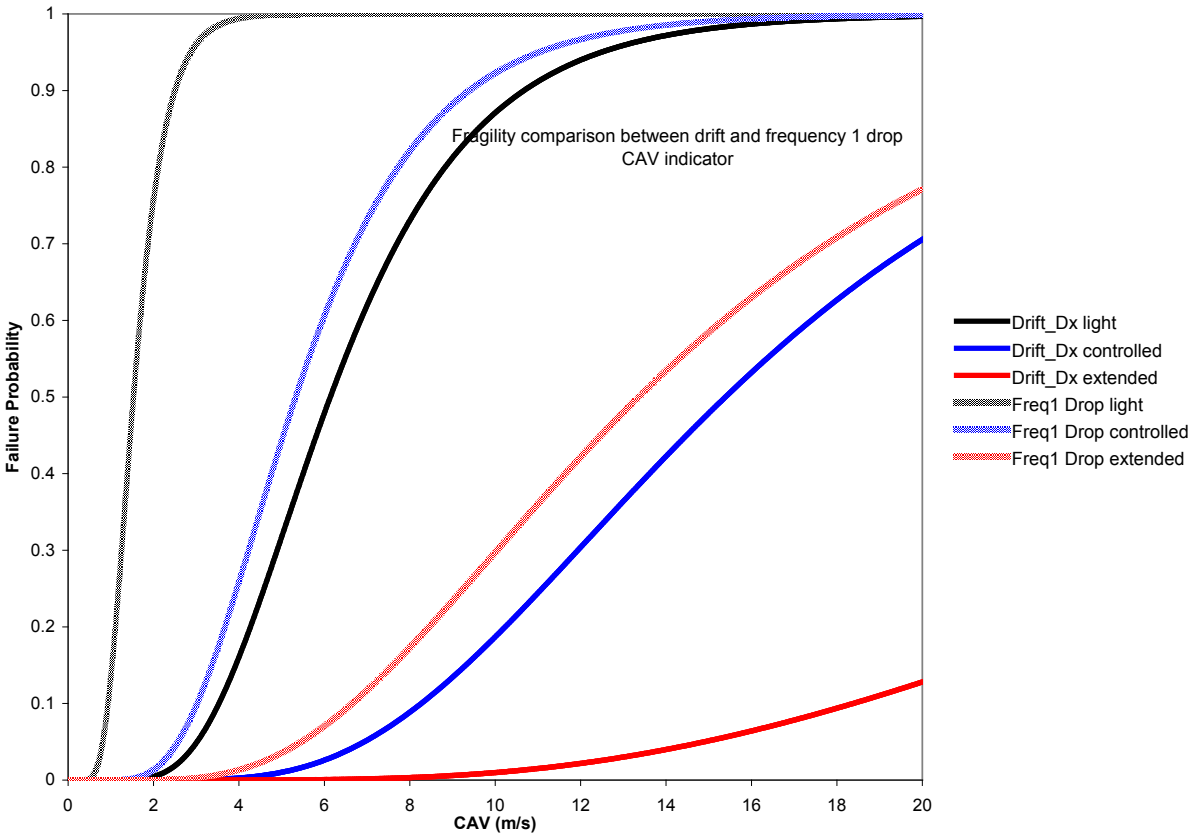

Figure 4-29 Fragility curve comparison between drift and frequency drop - CAV

5. SUMMARY

The SMART2008 benchmark addressed the complex issue of multi-directional seismic loading on reinforced concrete nuclear structures when subjected to torsion and nonlinearities. The benchmark, officially initiated in 2008, was coordinated by CEA Saclay, France and supported by Electricite de France (EDF). The benchmark used a quarter-scale nuclear structure designed according to the French nuclear code. The test structure was used as the basis for a series of independent numerical studies and was eventually tested on the shaking table at CEA, Saclay under a series of multi-directional seismic loadings.

An international numerical prediction contest that accompanied the shaking table tests aimed to (a) assess the state-of-the-art of numerical capabilities to analyze non-linear structures and compare the different best-estimate methods for floor response spectra generation and (b) evaluate the different methodologies and guidelines on nuclear design.

Upon completion of the shaking table tests and the best-estimate predictions of the response, a vulnerability study was undertaken where seismic fragility curves were generated. The vulnerability study considered the variability in the response of structures stemming from (a) structural property uncertainties, (b) random character of the seismic input and (c) numerical representation of the structural systems.

This section summarizes the findings/assessments that were drawn from the shaking table tests and the accompanying numerical analyses. Further, based on findings that may have structural design implications, discussions on specific approaches that address identified outstanding issues are presented.

5.1. SMART2008 Shaking Table Test Assessment

A series of shaking table tests of the SMART2008 structure were performed where real, low intensity earthquake signals were applied followed by a series of synthetic earthquakes increasing in intensity for up to 1.13g horizontal PGA in the last test. Upon completion of the +tests, the following observations were made:

- The SMART reinforced concrete structure was designed by precisely following the guidelines of the French nuclear design code with a design level earthquake of 0.2g PGA. In the course of the shaking table tests peak accelerations at the base of the structure reached PGA levels of 1.13g (a factor greater than 5 times the design level). Examination of the structure at the end of the tests revealed that the structure resisted the excessive seismic loads and suffered only minor damage. The observed damage was in the form of concrete cracking and minor, localized rebar yielding (observed in rebar recorded strain).

- Reinforced concrete under seismic loads that are much lower than the design earthquake level appear to undergo stiffness changes due to micro-cracking or adjustment in the concrete-rebar interface. The SMART2008 tests confirmed observations made in a previous study of seismic behavior of reinforced concrete shear walls (i.e. CAMUS benchmark, D. Combescure, et al.). The common observation in the two shaking table experiments is that the eigenfrequencies of the structure are reduced following seismic loads with intensities as low as 0.1g that are attributed to a reduction in the reinforced concrete stiffness. As a result, floor response spectra generated from actual in-structure recordings undergo a shift of their peaks towards lower frequency values, a feature that may have implications to the design of equipment supported on floors.

- The influence of the shaking table on the dynamic response of the structure was assessed to be significant in that it (a) lowers the eigenfrequencies of the combined system and thus the response of the structure relative to the frequency content of the input excitation and (b) alters the shape of the floor response spectra. The role and participation of the shaking table can be viewed as similar to SSI where the role of the soil supporting the structure is significant.

- The inability to fully control the shaking table motions, and in particular its vertical motion and the rotational or rocking response during the tests, introduced uncertainties regarding the anticipated and observed structural responses. Added to the controllability issue was the fact that the dynamic properties of the table supports (actuators) are not well understood or established, so best-estimates were introduced to explain the observed response. As a result, the observed motions on the table deviated from the excitations intended to be introduced at the different stages of the 13-run test series. The uncertainties surrounding the role of the shaking table (dynamic properties, stiffness, and interface conditions with the structure) can be said to resemble those associated with the interface of real structures with the supporting soil and the assumptions that are made to account for the SSI.

- An extensive instrumentation array was implemented during the SMART2008 tests that captured a multitude of in-structure response data (multi-directional accelerations throughout the structure, absolute displacements, steel reinforcement strain) and monitored concrete damage. The collected test data (a) provide the basis for assessing the numerical models and their capability to predict non-linear structural response and (b) contain a wealth of information that can lead to important insights for the seismic response and capacity of reinforced concrete structures and the potential use of such structures in nuclear design.

5.2. Numerical Prediction Assessment

A series of numerical analyses were conducted as an integral part of the SMART2008 benchmark. In the first phase, prior to the construction of the test structure, a blind prediction of the seismic response of the structure to synthetic seismic loads generated from the same design spectrum was performed by 35 research teams. In addition, static and modal analyses were performed under different loading and boundary conditions. The primary goal was for the benchmark to assess the different methodologies (linear and/or nonlinear time history analyses, modal or spectral analyses, linear static or non-linear static or push-over analyses, etc.) used in different parts of the world to design reinforced concrete structures when subjected to 3-D effects and non-linear behavior. The summary assessment of (a) the methodologies, (b) types of analyses and (c) result correlation or scattering was presented by the SMART2008 organizers during the proceedings of a dedicated workshop organized in December 2010 at CEA, Saclay. According to the summary, the variation in the structural response using the different methodologies was significant and stemmed primarily from (a) assumed properties of materials involved such as concrete moduli and damping, and (b) the level of simplicity introduced in the numerical model adopted to describe the structure. Based on the identified sources for the wide variability, it was concluded that better guidance in the design codes is needed regarding the adoption of design parameters which are meant to compensate for the non-linear behavior (i.e. damping specification).

During the second phase which was launched after the construction and preliminary testing on the shaking table of the structure, predictions of its non-linear, 3D response resulting from the sequence of seismic loads were made and compared to the actual test data.

The integrated assessment conducted by the SMART2008 benchmark organizers regarding the best-estimate prediction of the shaking table tests by the participants is the following:

- Numerical prediction models generally over-predict the in-structure accelerations while under-predict the displacements. This is primarily attributed to the lack of understanding of the evolution of damping in the reinforced concrete structure. An important parameter is the often arbitrary selection of initial structural damping ratio for the structure under seismic load. Observed in the seismic tests is a reduction of stiffness in the reinforced concrete even at low intensity seismic loads leading to shifting of eigen-frequencies and increased damping. In analytical models, capturing the progression of damping or damage at low intensity levels is difficult and as a result the estimated stiffness of the structure remains high thus leading to predictions with higher accelerations and lower displacements as compared to the actual response. The implementation of a progressive increase in structural damping may help in accounting for these nonlinearities but the quantification is not easy and the selection may not be appropriate.

- The ability of the numerical models to predict the shaking table tests correlated with the type of analysis and the complexity of the model used to represent the structure. Non-linear analyses based on models with nonlinearities in the constitutive models proved to be best suited in capturing the structural response when the structure entered the nonlinear regime. Numerical models which adopted an “exact” representation of the actual structure (concrete, rebars, shaking table, etc.) were able to capture, in spite of uncertainties surrounding the actual test set-up, the general behavior of the structure through the sequence of tests. This implies than non-linear analyses have the best chance in capturing the complex behavior of structures which are allowed to experience non-linear behavior.

As presented in the previous chapter, the BNL numerical effort was based on a three-dimensional representation of the structure that included all elements of the combined system. This included the shaking table, the actuators and support springs (with best-estimate spring constant values), the concrete and its constitutive relations, and the rebars in discrete form. Optimization of the steel reinforcement distributions was implemented to reduce the computational burden. A fully non-linear scheme was adopted and used for all phases of the prediction (blind and best-estimate) as well as for the preliminary push-over analyses. Based on the comparison between the predictions made with the BNL 3-D, non-linear numerical model and the actual shaking table test results the following assessment is made:

- Excellent agreement, in general, with the shaking table test was obtained using the elaborate non-linear model developed. In particular, the model was able to reproduce the accelerations, displacements, and rebar strains both in terms of peak values and shape of the transients.

- The adoption of (a) best estimates of fracture energy in the concrete (fracture energy properties of normal density concrete were used) and (b) the progressive increase in structural damping as the concrete structure was being damaged with the seismic excitation sequence, resulted in often slightly under predicting both the displacements and the accelerations. This is attributed to the role of cracks that develop as a result of the fracture energy assumed and the value of structural damping assumed for the damaged concrete. Another potential source is the fact that no effort was made to adjust or update the concrete moduli (tangent and secant) with the progression of damage.

- The model predicted the locations where damage was observed in the test structure quite accurately. Deviations that exist between the predictions and the test stem from the fracture energy assumed and from the simplification/optimization of the steel rebar distribution and layout.

- The model was able to accurately predict the response of the test structure under real earthquake signals when long-duration free-vibration tails in the resulting transients were observed in the test. This is important because of the damageability potential of such earthquakes due to the multiple significant stress cycles they induce in the structure even when their intensity is below the design earthquake level. Having available a numerical model that can predict such response induced by real earthquake signals can provide insights to the initiation of structural damage.

- As with all other prediction models, the BNL model/process was also influenced by the role of the shaking table and its dynamic properties. While sensitivity studies were performed regarding the modal characteristics of the combined system, research on quantifying the interaction between table and structure, which in turn resembles SSI, may provide important insights and quantification of these effects.

5.3. Sensitivity and Fragility Studies

The large variability in the predicted SMART structure response observed during the numerical prediction phases of the benchmark, reinforced the need for a sensitivity study to quantify the effect of uncertainties in the structural parameters. By following a widely used approach in structural design where a range of values of key parameters is established, typically arbitrarily, the effect of individual parameters such concrete modulus, damping, steel yield stress and added live loads was evaluated through a multitude of analyses. The objective was to observe the variability of the response of the structure in terms of floor response spectra and floor drifts, two response parameters of importance in the design of reinforced concrete structures. The variability was attributed to (a) the epistemic uncertainty of structural parameters and (b) the sensitivity of the response to the modeling adopted and the analysis approach. To minimize the pool of uncertainty sources, the shaking table was eliminated, resulting in a fixed base structure. The variability in the input was also minimized (only two specific, white noise based excitations were used). Results from the study indicate that the uncertainties in the structural damping have the greatest influence on the response and in particular floor response spectra.

In addition to the structural parameter sensitivity studies, a vulnerability assessment was performed and seismic fragility curves were generated. This was accomplished by introducing probabilistic measures in both the seismic input and in the structural parameters, and by evaluating exceedance probabilities of limit states through convolution of randomized excitation with randomized properties. To explore the influence that the choice of demand and capacity indicators may have on the exceedance of pre-defined limit states, fragilities that covered the different demand-capacity combinations were derived. Based on the assessment of the BNL vulnerability study where a random earthquake family of fifty (50) records was convoluted with fifty (50) random realizations of the structural parameters, the following observations and recommendations are deduced:

- Since fragility curves are used as a tool in decision making, adopting procedures that do not account for uncertainties in establishing the limit states of a given structure which consequently deduce estimates that are non-conservative may lead to wrong decisions. One possible approach is to treat performance limit states as random variables instead of deterministic quantities, ensuring that uncertainties are accounted for and that the level of conservatism can be decided upon based on the sensitivity analysis results.

- The definition of the limit threshold or limit state has a significant effect on fragility curves, so a parametric analysis may be needed to understand the sensitivity of different elements such as non-linear treatment, variations in the structural model**,** number of earthquakes, etc.

- Multi-dimensional performance limit states need to be explored so they can eliminate the large deviations that exist between fragilities derived using different demand and capacity indicators. As observed in the analysis, large differences exist between fragility curves which were established using the same demand indicator (i.e. PGA) and different capacity threshold (i.e. floor drift vs. frequency drop). For example, for a multi-dimensional performance limit state based on displacements and accelerations of a building story, the fragility can be derived as a convolution of the two single-threshold fragilities.

- Structure capacity realizations, where the distribution of strength (or its uncertainty) is influenced by spatial correlation conditions (rather than being described by a pre-defined distribution of uncertainty, i.e. log-normal), should be studied in more detail. Specifically, when, for the purpose of simplicity which allows fragilities to be derived in the form of analytical expressions, one accepts a given distribution of the uncertainty as a priori, influential parameters defining capacity or lack-of could be inadvertently omitted. Accepting, for example that the uncertainty in structural capacity is expressed in terms of a lognormal distribution constitutes such a simplified approach. In 3-D structures, however, the spatial variability or uncertainty of key structural parameters may be more important than the distribution governing the fluctuation of the property around the nominal value and so it must be captured in the fragility evaluation. Spatial variability in soil properties and their effect on the dynamic response of the structure they support has been explored in Simos et al. (2004) along with procedures through which spatial correlation based on limited field data can be introduced in the randomized model.

- The number of earthquakes that form the randomized suite used to integrate with the random realizations of the capacity may need to be optimized both in the number of earthquakes and the type. In particular, the selection of the earthquake suite to reflect ground motions characteristic of the local site where fragilities for a structure are being generated should be favored over a pool of earthquakes that tend to saturate the range of frequencies and peak ground accelerations. Synthetic earthquakes based on power spectra reflecting the energy content in a given area may form a most appropriate suite.

- Efforts should be dedicated towards the development of fragilities based on static non-linear (push-over) analyses. By relying on the demonstrated capabilities of such non-linear methods to predict large deformations and failure in reinforced concrete structures, higher-confidence fragilities (in terms of the actual capacity and the quantification of the performance limit states) can be deduced and utilized in decision-making for the performance of existing structures

5.4. Impact on Design Approaches and Implications

The multi-directional shaking table tests of the 3-D SMART2008 reinforced concrete structure succeeded in inducing both torsion and non-linear behavior as they were intended when the benchmark was conceptualized. Based on the recorded test data and their assessment, as well as the results of the numerical analyses that accompanied the experiment, the following observations with potential impact on design approaches are deduced:

- The inherent capacity of the reinforced concrete structure is much higher than the “per-design” capacity. Specifically, the SMART2008 structure was designed and constructed according to the French seismic design code for 0.2 PGA design level earthquake. Peak ground accelerations in one of the tests exceeded 1.0 g. The structure, which had been progressively damaged by a series of seismic loads exceeding the design level, suffered only minor additional damage at approximately five (5) times the input intensity. The available excess capacity is attributed to the fact that the design is based on linear-elastic behavior of the structural materials (concrete and reinforcing steel) and does not

account for stiffness reduction which in turn reduces the acceleration demand on the structure.

- Reinforced concrete structures are observed to undergo stiffness reduction at lower seismic intensities than the design level. Such observations were made in a shear wall test on the same shaking table (CAMUS Shear Wall Experiment, D. Combescure, et al.) and were reconfirmed during the SMART2008 experiment. The reduction in stiffness is attributed to micro-cracking that takes place within the concrete. As the test results indicated, changes in the dynamic properties of the reinforced concrete structure were noticeable even after subjecting the structure to seismic loads of 0.05g PGA. This observation has significant implications in the seismic design of reinforced concrete nuclear structures in that (a) the response of the structure could be significantly altered as a result of the dynamic property changes (shifting of eigenfrequencies towards lower values) and their correspondence to the frequency band of the input acceleration energy and (b) the floor response spectra estimated for the structure based on the design stiffness can experience large variations both in terms of spectral accelerations and frequency content.

- To fully understand and quantify the stiffness reduction that takes place at low seismic intensities, dedicated research in this area remains. Such effort could be based on experimental studies which will explore the accumulated damage and its effect on the concrete stiffness and its implementation into the constitutive concrete models. Subsequently, and via the enhancement of numerical models that already account for damage in materials such as concrete, guidelines on concrete stiffness reduction can be deduced. Further, the existing guidelines on design floor response spectra (i.e., generation of envelope floor spectra) could be revisited to assess if the drop in spectral frequencies due to stiffness reduction is adequately accounted for.

- Observed in the shaking table tests below or at design level are low energy dissipation characteristics of the overall system (RC structure, shaking table and mounting conditions). It is assumed, based on these low intensity tests, that the damping exhibited by the RC structure alone is still quite low. This finding is in fact in line with the generally accepted notion that at seismic intensity levels well below the design level (i.e., well below the OBE level) the damping in the concrete is typically between 1%-2%. Specifically, damping values as low as 1% of critical have been observed as compared to the 4%-7% recommended by regulatory bodies on reinforced concrete structures for OBE and SSE. Because the test structure and its support conditions are not typical of a nuclear RC structure, extrapolation of the observations on damping values from the SMART2008 to nuclear RC design and practice should be avoided.

- Based on the comparison of the test data with the predicted data using a fully non-linear, 3-D analysis of the SMART structure that was implemented by BNL, it can be concluded that such analyses, in spite of the high computational burden, can quite accurately reproduce the response and the damage experienced by the structure even when multi-directional loads are applied on an asymmetric structure.

- The SMART2008 benchmark organizers, who evaluated the different analyses approaches used by the participants to derive best-estimates of the response, concluded that non-linear approaches with exact representation of the geometry, including the shaking table which introduces SSI-like effects, were able to derive the most accurate estimates of the actual test accelerations and deformations. In spite of the computational cost, which rapidly diminishes due to parallel processing in the computational space, the use of non-linear treatment of a real nuclear concrete structure should be considered by the regulatory authorities and be allowed to influence the design. Confirmation of the SMART seismic tests and of other similar tests such as

the CAMUS shear wall tests demonstrate that non-linear methods have matured since the early days of nuclear structural design. A number of other benchmarks on reinforced concrete under high strain loading (i.e. high velocity impact) have also shown that the ability of the current non-linear numerical techniques to predict the response and damage has improved in recent years.

- Using the non-linear methodology that was developed and used by BNL to predict the seismic response of the asymmetric 3-D structure under multi-directional loading, conventional methods widely used in the industry can be qualified and augmented to include effects stemming from nonlinearities. Figure 5.1 shows a verification of the SRSS method using the SMART structure and a bi-directional seismic input of 0.2g PGA (design level). As seen in the generated floor response spectra the SRSS method, which was primarily applied to structures idealized as stick models, is reproducing the floor spectrum generated by the simultaneous action of the two-directional input. Further, generation of design floor spectra based on existing guidelines can be developed and the adequacy of the enveloping provisions can be evaluated for the conditions where the structure exhibits non-linear response. Figure 5.2 shows the deduction of "design" floor response spectra for the 3rd floor of the SMART2008 structure using US NRC guidelines on enveloping procedures over computed spectra at various floor locations. Figure 5.2 also includes spectra comparison at the structural extremity D between the SRSS and the direct methods.

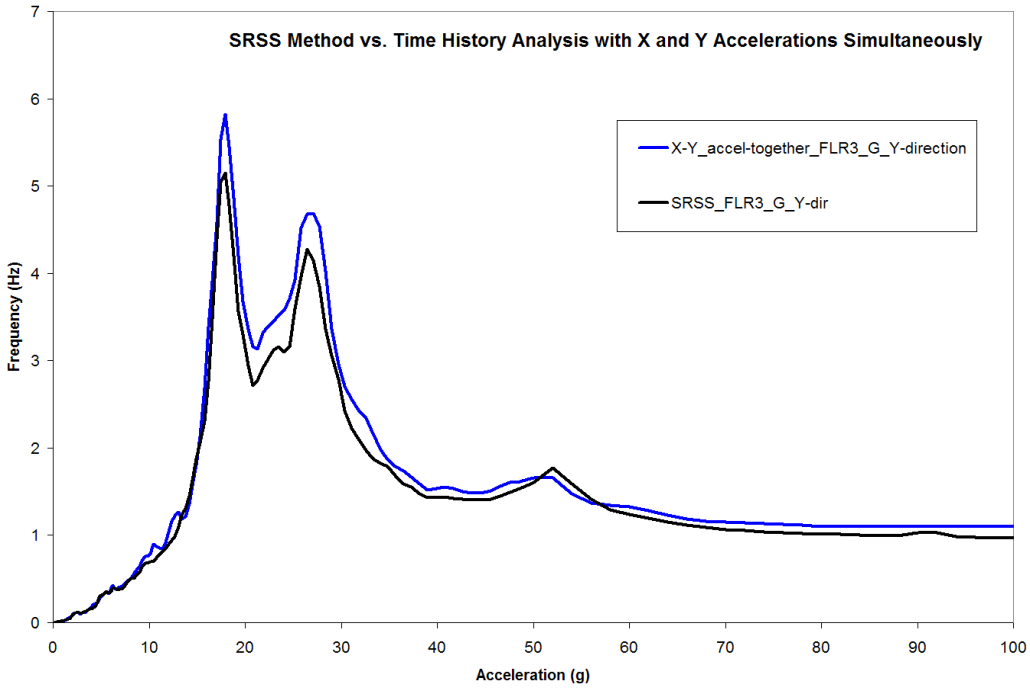

Figure 5-1 Comparison of acceleration spectra between the direct method (i.e., both orthogonal excitations acting on the structure simultaneously) and the SRSS method where the two responses were computed independently

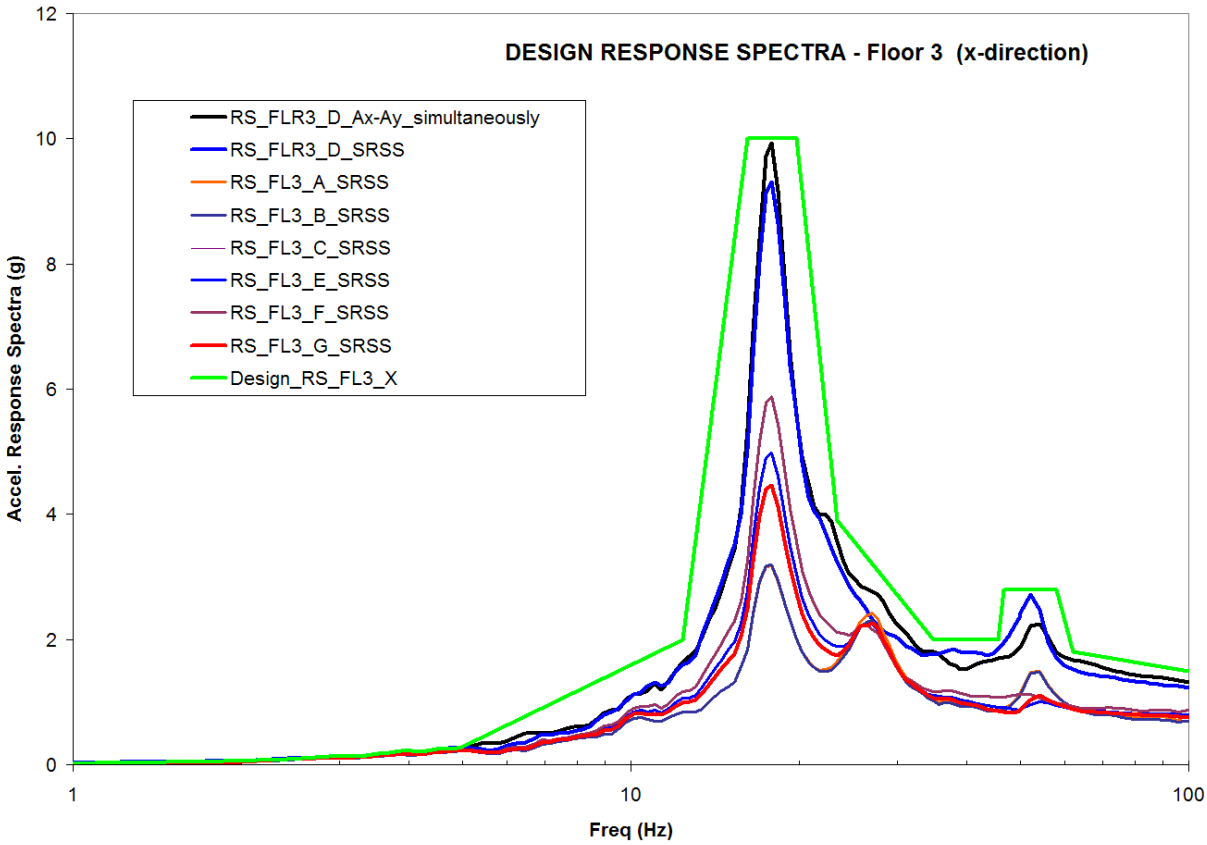

Figure 5-2 Generation of design response spectra by enveloping proceduresusing US NRC guidelines

Summarized below is the overall assessment based on the comprehensive SMART benchmark (shaking table tests and independent analyses that were performed) drawn by the organizing committee and concurred by the participating teams during the closing workshop:

- There exists great variability and scattering in the results produced by the different approaches attempting to analyze the same structure under generally the same conditions (i.e. boundary conditions in the case of SMART varied depending on the participation of the shaking table). This prompts the question whether some of the conventional practice in seismically analyzing structures should be re-considered.

- While good agreement may be observed using similar hypotheses and similar types of dynamic analysis, variations in the development of floor response spectra were still observed. These variations may have implications in design. Therefore, guidelines and a simplified methodology should be derived for developing floor response spectra along with provisions for minimum spectral values regardless of the complexity of the approach employed.

- More precise guidelines should be developed regarding the numerical modeling and the level of simplification allowed for structures using conventional analyses (i.e. equivalent static, response spectrum, non-linear static, linear dynamic and even non-linear dynamic).

- Better guidelines should be developed regarding the damping values according to the type of analysis that is adopted. Further research can enable a better understanding of the damping parameter and, in particular, its evolution which greatly influences the structural response.

- Guidelines, under say the auspices of ASCE or RFS (French Fundamental Safety Rules RFS2001-01), should be developed in order to better account for the concrete Young's modulus and how it is modified depending on the type of analysis to be performed. As with structural damping, further work could help to identify the degradation and thus the need for updating of the modulus as a function of the loading history and the structural damage.

- The assessment results should be considered at the industry updated related consensus codes and the NRC considers them for regulatory endorsement.

6. REFERENCES

[1] Kinali K. and Ellingwood B.R., 2007. “Seismic fragility assessment of steel frames for consequence-based engineering: A case study for Memphis TN.” *Eng. Structures* 29, 1115-1127.

[2] Hamburger R.O., Foutch D.A. and Cornell C.A., 2003. Translating Research to Practice: FEMA/SAC Performance-based Design Procedures. *Earthquake Spectra* 19 (2), 255-267.

[3] Shinozuka M., Feng, Q., Lee, J. and Naganuma T., 2000, “Statistical analysis of fragility curves.” *J. Eng. Mech. ASCE* 126 (12), 1224-1231.

[4] Shinozuka, M., Feng, M. Q., Kim, H., and Kim, S. (2000a). "Non linear static procedure for fragility curve development." *Journal of Engineering Mechanics, ASCE*, 126(12), 1287-95.

[5] G. P. Cimellaro, A. M. Reinhorn, M. Bruneau and A. Rutenberg, “Multi-Dimensional Fragility of Structures: Formulation and Evaluation,” Technical Report MCEER-06-0002, 2006.

[6] B. G. Nielson and R. DesRoches, “Seismic fragility methodology for highway bridges using a component level approach,” *Earthquake Engng Struct. Dyn.* 2007; **36**:823–839.

[7] *N. Simos and C. Costantino, “*Soil Spatial Variability Effects on Soil-Structure Interaction Studies. Enveloping Uncertainties in Structural Response,” *Proceedings of Third UJPN Workshop on Soil-Structure Interaction*, Menlo Park, CA, 2004.

[8] D. Combescure, et al. “CAMUS 2000 Benchmark. Experimental Results and Specifications to the Participants,” SEMT/EMS/RT/02-067/A, 2002.

[9] *J. Mazars*, French Advanced Research on Structural Walls: An Overview on Recent Seismic Programs, Proceedings of the 11th European Conference on Earthquake Engineering, Invited Lectures Volume, pp. 21-41, Paris, France, 1999.

[10] *M.J.N. Priestley*, Displacement Based Approaches to Rational Limit States Design of New Structures, Proceedings of the 11th European Conference on Earthquake Engineering, Invited Lectures Volume, pp. 317-335, Paris, France, 1999.

[11] B.J. Broadhouse, “The Winfrith Concrete Model in LS-DYNA3D,” SPD/D(95)363, Winfrith Technology Center, 1995.

[12] S. Limkatanyu, E. Spacone, “Reinforced Concrete Frame Element with Bond Interfaces. I. Displacement-Based, Forced-Based, and Mixed Formulations,” Journal of Structural Engineering, Vol. 128, No. 3, March 2002.

[13] Y.K. Wang, et al, “Assessment of the Relevance of Displacement Based Design Methods/Criteria to Nuclear Plant Structures,” NUREG/CR-6719, 2001.

[14] Y. Kitada, et al, Near-Field Earthquakes Observed Recently in Japan, Private Communication.

[15] M. Brun, et al, “New Needs for Seismic Design: Near Field Earthquake Specific Studies and Site Effects Evaluations,” Proceedings of OECD/NEA Brookhaven National Laboratory Meeting, November, 1999.

[16] R.W. Clough, J. Penzien, *Dynamics of Structures*, McGraw Hill, 1975.

[17] B. Li, F.G. A Al-Bermani and Kitipornchai, *Maximum Response of Asymmetric Structures Subject to a Multi-component Earthquake*, Earthquake and Structural Dynamics, Vol. 22, pp. 1047-1066, 1993.

[18] R.P. Kennedy, S.A. Short, *Effective Ground Motion Considerations for Nuclear Power Plant Design*, Transactions of 8th SMiRT, Vol. K, pp. 127-134, 1985.

[19] ANSYS, Swanson Analysis Systems, Version 6.1, 2001.

[20] LS-DYNA, Version 9.70, LSTC, Livermore, CA.

[21] Truegrid Software, XYZ Scientific Applications, Livermore, CA.

[22] N. Simos, A. J. Philippacopoulos "*Fundamentals of Direct Generation of Spectra (DIGES) Code,*" BNL-NUREG-60612, 1994.

NRC FORM 335
(12-2010)
NRCMD 3.7

U.S. NUCLEAR REGULATORY COMMISSION

BIBLIOGRAPHIC DATA SHEET

(See instructions on the reverse)

1. REPORT NUMBER
(Assigned by NRC, Add Vol., Supp., Rev., and Addendum Numbers, if any.)

NUREG/CR-7119

2. TITLE AND SUBTITLE

Experimental Studies of Reinforced Concrete Structures under Multi-Directional Earthquakes and Design Implications

3. DATE REPORT PUBLISHED

MONTH	YEAR
July	2013

4. FIN OR GRANT NUMBER

N-6510

5. AUTHOR(S)

N. Simos

C.H. Hofmayer

6. TYPE OF REPORT

Final Technical

7. PERIOD COVERED (Inclusive Dates)

8/1/2007 to 6/30/2012

8. PERFORMING ORGANIZATION - NAME AND ADDRESS (If NRC, provide Division, Office or Region, U. S. Nuclear Regulatory Commission, and mailing address; if contractor, provide name and mailing address.)

Brookhaven National Laboratory
P.O. Box 5000
Upton, New York 11973-5000

9. SPONSORING ORGANIZATION - NAME AND ADDRESS (If NRC, type "Same as above", if contractor, provide NRC Division, Office or Region, U. S. Nuclear Regulatory Commission, and mailing address.)

Division of Engineering
Office of Nuclear Regulatory Research
U.S. Nuclear Regulatory Commission
Washington, D.C. 20555-0001

10. SUPPLEMENTARY NOTES

11. ABSTRACT (200 words or less)

This report describes the results of a multi-phase study focusing on the SMART2008 (Seismic design and best-estimate Methods Assessment for Reinforced concrete buildings subjected to Torsion and non-linear effects) shaking table experiment. The aim of the project that was launched in 2008 was to, in addition to the shaking table experiments, enable an international benchmarking study to take place where different methodologies, modeling and numerical approaches are used to study and predict the non-linear behavior and damage of reinforced concrete structures. Specifically, a 1/4th scale model of a nuclear reinforced concrete structure designed according to the French nuclear practices was tested on the shaking table at CEA Saclay, France using thirteen multi-dimensional earthquakes ranging from low seismic intensities to five times the design level. Leading up to the shaking table experiments and following some of the initial test results, three numerical prediction phases were executed which included (a) a "blind" prediction phase based on using best-estimate data for the structural properties and the induced seismic loads, (b) an "updated" prediction phase where best estimates were improved using some of the initial shaking table test results enabling the studies of higher loadings, and (c) a sensitivity and vulnerability analysis phase based on the SMART2008 specimen numerical model used in the prediction phase enabling the generation of damage fragility curves for the structure.

The report provides a detailed description of the SMART2008 experiments and of the assessment of the test results, the structural response predictions using modeling and numerical techniques, as well as the damage fragility assessment.

12. KEY WORDS/DESCRIPTORS (List words or phrases that will assist researchers in locating the report.)

Structural Analysis Reinforced Concrete Nonlinear Motion
Torsional Analysis Earthquake Multi-directional Loading

13. AVAILABILITY STATEMENT

unlimited

14. SECURITY CLASSIFICATION

(This Page)
unclassified

(This Report)
unclassified

15. NUMBER OF PAGES

16. PRICE

Federal Recycling Program

UNITED STATES
NUCLEAR REGULATORY COMMISSION
WASHINGTON, DC 20555-0001

OFFICIAL BUSINESS

NUREG/CR-7119

Experimental Studies of Reinforced Concrete Structures Under Multi-Directional Earthquakes and Design Implications

July 2013